

Antimicrobial Carbohydrate Vaccines:

Development of *Burkholderia pseudomallei* immunogens

Matthew Ian Donaldson

This thesis is submitted in fulfilment of the requirements of the degree of Doctor of Philosophy at the University of East Anglia

Department of Biological Chemistry

John Innes Centre

Norwich

September 2013

© This copy of the thesis has been supplied on condition that anyone who consults it is understood to recognise that its copyright rests with the author and that no quotation from the thesis, or information derived therefore, may be published with the author's prior written consent.

Date

24/09/2013

I declare that the work contained in this thesis, submitted by me for the degree of Doctor of Philosophy, is to the best of my knowledge my own original work, except where due reference is made.

Signed

Matthew I. Donaldson

Acknowledgements

First and foremost I would like to thank Rob for all his help and support over the last four years, without which I am sure that this thesis would not have been written. I would also like to thank both Sergey and Martin for their guidance and advice on all aspects of chemistry and biochemistry. The Field group was a fantastic environment to complete a PhD, not only for the breadth and quality of the science, but also as a result of the fantastic people in the lab. You have all contributed to my work and education as a scientist, provided me with some great memories and were instrumental in getting me through my PhD. A special mention must go again to Sergey, Mike P and Giulia for all their help with this research as part of the DSTL project. Ellis, Mike R and Steph have really helped me to see a different side of science with their own unique and drastically different takes on Biology. I must also thank those at JIC who provide such fantastic services, in particular Gerhard and Lionel for all their help with mass-spectrometry. I would also like to thank Hadrien and George for all their help; opening my eyes to the wonders of VLPs and plants.

Due to the nature of my research I was fortunate enough to be part of a larger industrial collaboration involving DSTL – Porton Down, iQur and Mologic. I am grateful to these collaborators for all the help with the different aspects of my project. I am especially thankful to all those at Mologic for their generous support of my PhD as my industrial sponsors; in particular I must extend my thanks to Mark and Paul Davis for their infectious enthusiasm for science and continued guidance throughout this work.

A very special thanks must go to my family who have provided me with such fantastic encouragement over the years and they have got me through all the ups and downs associated with a PhD. It is impossible for me to conceive completing this PhD without the love and support of my parents, sister and grand-parents.

I have made some great friends in Norwich, with whom I have shared many great times ranging from the many evenings spent in Norwich's pubs and clubs, to trips to New

York, Berlin, Prague and even as far afield as Devon. I am lucky enough to also have an unbelievable group of friends from Ipswich, despite not fully appreciating the outrageous demands made of the perpetual student they were a truly great support network and always there to provide a welcome distraction. Last, but by no means least Ana, simply put the best thing about my time in Norwich.

Abstract

The potential bio-terror threat posed by *Burkholderia pseudomallei* highlights the need for an effective vaccine. Immunisation and challenge experiments in mice have demonstrated that the capsular polysaccharide (CPS-1) of *B. pseudomallei*, which is composed of β -1,3-linked 6-deoxy-D-*manno*-heptopyranose residues, is a promising candidate for vaccine development. This thesis set out to explore routes to potential vaccine candidates for *Burkholderia pseudomallei* infection based on both bottom-up synthetic monosaccharide constructs and top-down CPS-1 conjugates.

Initially this thesis focused on the development of a monosaccharide antigen based on the 6-deoxy-D-*manno*-heptose building block of CPS-1. The antigens were conjugated to TetHc carrier protein via an 8-(methoxycarbonyl)octyl linker using traditional acyl hydrazide conjugation chemistry. The TetHc monosaccharide conjugates were analysed by SDS-PAGE and MALDI-ToF mass spectrometry before undergoing immunisation trials in sheep. Immunological assessment of the resulting polyclonal antisera was conducted by ELISA, slot-blot and the Octet biosensor system. These studies demonstrated the generation of antibodies that were specific for the cognate monosaccharide. Preliminary investigations showed that the 6-deoxy-D-*manno*-heptose-derived antibodies reacted positively with the natural CPS-1. The linker was shown to be important in the specificity of the polyclonal sera, leading to cross reactivity with non-parent monosaccharide antigens. A second generation of antigens was developed using a short linker, 3-(methyl mercaptopropionate).

The expression and purification of the natural *B. pseudomallei* CPS-1 was achieved in an avirulent strain of *Burkholderia*, *B. thailandensis* E555. Characterisation of the capsular polysaccharide highlighted the co-expression of an α -1,3-mannan polysaccharide. Mild acid hydrolysis of the CPS-1 preparation, combined with capillary electrophoresis was trialled with a view to the generation of oligosaccharide fragments of CPS-1 for conjugation and immunisation studies. While initial carbohydrate conjugates were prepared with a previously described tetanus toxoid Hc fragment, the development and *in planta* expression of a chemically conjugatable Hepatitis B core virus-like particle system was also achieved.

List of Abbreviations

[α]_D	specific optical rotation at 20°C
α	alpha configuration
abs	absolute
Ac	acetyl
Ac₂O	acetic anhydride
AcOH	acetic acid
<i>A. tumifaciens</i>	<i>Agrobacterium tumifaciens</i>
AmBic	ammonium bicarbonate
aq.	aqueous
ar	aromatic
asp	Aspartic acid
ATP	adenosine 5'-triphosphate
β	beta configuration
Bn	benzyl
bp	base pair
BSA	bovine serum albumin
Bth-CPS-1	capsular polysaccharide extracted from <i>B. thailandensis</i> E555 $\Delta wbiI$
Bz	benzoyl
CD₃OD	d ₃ -methanol
CDCl₃	d ₁ -chloroform
CHCl₃	chloroform
ConA	Concanavalin A
conc.	concentrated
COSY	correlation spectroscopy
CPMV	Cowpea Mosaic Virus
CPS-1	capsular polysaccharide
d	doublet
D₂O	d ₂ -water
D3K6D3	(asp) ₃ -(lys) ₆ -(asp) ₃
Da	dalton
DAST	dimethylaminosulphur trifluoride
DCM	dichloromethane
dd	doublet of doublets
DDQ	2,3-dichloro-5,6-dicyano-1,4-benzoquinone
DMAP	dimethyl-4-aminopyridine
DMF	<i>N,N</i> -dimethyl formamide

DMSO	dimethyl sulfoxide
DNA	deoxyribonucleic acid
DP	degree of polymerisation
dpi	days post infiltration
DT	diphtheria toxin
DT_{CRM197}	diphtheria toxin CRM197 mutant
DTT	dithiothreitol
<i>E. coli</i>	<i>Escherichia coli</i>
EDTA	ethylenediaminetetraacetic acid
ELISA	enzyme-linked immunosorbent assay
equiv.	equivalent(s)
EtOAc	ethyl acetate
EtOH	ethanol
FITC	fluorescein isothiocyanate
Glc	D-glucose
Glc-BSA	D-glucose-BSA glycoconjugate
GlcOMe	methyl- β -D-glucopyranoside
Glc-TetHc	D-glucose-TetHc glycoconjugate
6D6FGlc-BSA	6-deoxy-6-fluoro-D-glucopyranose-BSA glycoconjugate
6D6FGlc-TetHc	6-deoxy-6-fluoro-D-glucopyranose-TetHc glycoconjugate
gly	glycine
h	hours
HBcAg	hepatitis B core antigen
HBcAg	extracellular form of hepatitis B core antigen
HBex	hepatitis B extraction buffer
HBsAg	hepatitis B surface antigen
Hep-BSA	6-deoxy-D-manno-heptopyranose BSA glycoconjugate
Hep-TetHc	6-deoxy-D-manno-heptopyranose TetHc glycoconjugate
6dHepp	6-deoxy-D-manno-heptopyranose
Hex	hexane
HPAEC-PAD	high performance anion chromatography with pulsed amperometric detection
HR ESI-MS	high resolution electrospray ionisation mass spectrometry
HSQC	heteronuclear single quantum coherence
Hz	Hertz
<i>J</i>	coupling constant (Hz)
KLH	Keyhole Limpet Hemocyanin
<i>kmR</i>	kanamycin resistance

kDa	kilodalton
LB	Luria-Bertani
LB-L	Luria-Bertani-Lennox
LIF	laser induced fluorescence
lys	lysine
m	multiplet
M	molar [mol/L]
<i>m/z</i>	mass/charge ratio
mAb	monoclonal antibody
MAC	membrane attack complex
MALDI-ToF	matrix assisted laser desorption ionisation-time of flight
Man	D-mannopyranose
Man-BSA	D-mannopyranose-BSA glycoconjugate
Man-TetHc	D-mannopyranose-TetHc glycoconjugate
mDa	megadalton
MeCN	acetonitrile
MeOH	methanol
MHz	megahertz
min	minute
MIR	major immunodominant region
MMA	MES, MgCl ₂ and acetosyringone buffer
MQ-H₂O	Milli-Q water (Millipore; ≥ 18 Ω)
MS	mass spectrometry
MWCO	molecular weight cut off
μ-wave	microwave
<i>N. benthamiana</i>	<i>Nicotiana benthamiana</i>
NaOMe	sodium methoxide
NMR	nuclear magnetic resonance spectroscopy
NOESY	nuclear overhauser effect spectroscopy
O/N	overnight (16 h)
OD	optical density
PBS	phosphate-buffered saline
PCR	polymerase chain reaction
Ph	phenyl
ppm	parts per million
R	organic group
<i>rcf</i>	relative centrifugal force

rt	room temperature
s	singlet
sat.	saturated
SDS-PAGE	sodium dodecyl sulphate polyacrylamide gel electrophoresis
S_N2	bimolecular nucleophilic substitution
t	triplet
TACA	tumour associated carbohydrate antigen
TBE	tris-borate EDTA
TEM	transmission electron microscopy
TetHc	tetanus toxoid Hc fragment
TFA	tetrafluoroacetic acid
t-HBcAg	tandem-hepatitis B core antigen
THF	tetrahydrofuran
TLC	thin layer chromatography
TLC	thin layer chromatography
ToF	time of flight
Tris-HCl	tris(hydroxymethyl) aminomethane, hydrochloride
TTSS	type three secretion system
UV	ultraviolet
VLP	virus-like particle
w/v	weight per volume
wt-HBcAg	wild type-hepatitis B core antigen

Table of Contents

1	Introduction.....	1
1.1	Carbohydrates and bacterial infection.....	3
1.1.1	Bacterial adhesion.....	3
1.1.2	Bacterial polysaccharide virulence factors.....	4
1.1.2.1	The complement system.....	6
1.1.3	Carbohydrate-based vaccines.....	10
1.2	<i>Burkholderia pseudomallei</i>	13
1.2.1	Vaccination of <i>B. pseudomallei</i>	15
1.2.2	Virulence factors and pathogenicity of <i>B. pseudomallei</i>	18
1.2.3	Polysaccharides of <i>B. pseudomallei</i>	18
1.2.3.1	The capsular polysaccharide of <i>B. pseudomallei</i>	19
1.3	Synthetic strategy.....	22
1.3.1	Synthesis of β -mannosides.....	22
1.3.2	Synthesis of 6-deoxy-D- <i>manno</i> -heptose.....	27
1.4	General aims of the study.....	34
1.5	References.....	35
2	Chapter 2: Synthesis of monosaccharide antigens.....	44
2.1	Introduction.....	44
2.1.1	The monosaccharide antigens.....	44
2.1.1.1	Carrier proteins.....	45
2.2	Results and discussion.....	48
2.2.1	Synthesis of 8-methoxycarbonyl octanol (58).....	48
2.2.2	Synthesis of 8-(hydrazinocarbonyl)octyl α -D-mannopyranoside (64).....	49

2.2.3	Synthesis of 8-(hydrazinocarbonyl)octyl β -D-glucopyranoside (69) ...	50
2.2.4	Synthesis of methyl 2,3,4-tri- <i>O</i> -benzyl 6-deoxy- α -D- <i>manno</i> -heptopyranoside (30).....	51
2.2.5	Improvements to the synthetic route for 6-deoxy-D- <i>manno</i> -heptopyranose (32).....	54
2.2.5.1	The use of polymer bound triphenylphosphine	54
2.2.5.2	Nitrile reduction	55
2.2.5.3	Protecting group-free synthesis of nitrile (78)	58
2.2.5.3.1	Direct synthesis of nitrile (78).....	58
2.2.5.3.2	Indirect synthesis of nitrile (78) via the iodide (77)	59
2.2.6	Synthesis of 8-(hydrazinocarbonyl)octyl 6-deoxy- α -D- <i>manno</i> -heptopyranoside (91).....	60
2.3	Conjugation of monosaccharide haptens to carrier protein	61
2.3.1	Expression of TetHc fragment in <i>E. coli</i>	61
2.3.2	Conjugation of haptens.....	63
2.3.2.1	Mannose-TetHc (Man-TetHc) glycoconjugate (92)	66
2.3.2.2	Mannose-BSA (Man-BSA) glycoconjugate (93).....	68
2.3.2.3	Glucose and Heptose glyconjugates	68
2.3.2.4	Summary of the monosaccharide hapten conjugation to TetHc and BSA	69
2.4	Conclusions	69
2.5	References	71
3	Production and characterisation of capsular polysaccharide from <i>Burkholderia thailandensis</i>	75
3.1	<i>Burkholderia thailandensis</i>	75

3.2	Results and discussion	77
3.2.1	NMR characterisation of CPS-1 (4) from <i>B. pseudomallei</i>	77
3.2.1	Monosaccharide analysis of <i>B. pseudomallei</i> polysaccharide extracts.....	80
3.2.2	Extraction of CPS-1 from <i>B. thailandensis</i>	82
3.2.3	NMR characterisation of CPS-1 extract from <i>B. thailandensis</i> E555 <i>ΔwbiI</i>	89
3.2.4	Monosaccharide analysis of CPS-1 extracted from <i>B. thailandensis</i> E555 (<i>ΔwbiI</i> pKNOCK-KmR mutant).....	93
3.2.5	Partial acid hydrolysis and capillary electrophoresis experiments	96
3.3	Conclusions	98
3.4	References	102
4	Chapter 4: Immunological assessment of anti-monosaccharide antibodies.....	105
4.1	Generation of polyclonal antibodies	105
4.1.1	Kinetics of the immune response	106
4.2	Results and discussion.....	109
4.2.1	ELISA analysis of glucose derived antibodies.....	109
4.2.1.1	Competition ELISAs with Glc-TetHc polyclonal sera	113
4.2.2	ELISA analysis of heptose derived antibodies	117
4.2.3	Slot-blot analysis of monosaccharide derived antibodies	119
4.3	Enhancement of the antigenicity of the monosaccharide antigens.....	120
4.3.1	Synthesis of 6-deoxy-6-fluoro-D-glucose TetHc antigen (112)	121
4.3.1.1	Immunological assessment of the 6D6FGlc-TetHc sera.....	125
4.3.2	Synthesis of short linker haptens	127

4.4	Immunological assessment of anti-CPS-1 monoclonal antibody	128
4.4.1	Conjugation of CPS-1 to cBSA carrier protein	128
4.4.2	Biotinylation of CPS-1	134
4.4.3	ELISA assessment of monoclonal antibody against CPS-1	137
4.5	Octet analysis	139
4.6	Conclusions and future directions	143
4.7	References	145
5	Hepatitis B core Antigen Virus-like Particle carrier protein	147
5.1	Introduction	147
5.1.1	Hepatitis B virus	149
5.1.2	HBcAg tandem core	152
5.1.2.1	The peptide insert	154
5.1.3	VLP production	156
5.1.3.1	The pEAQ-HT expression system	156
5.2	Results and discussion	157
5.2.1	Production of the D3K6D3 plasmids	157
5.2.2	<i>In planta</i> expression of the VLPs	158
5.2.3	Conjugation with FITC	162
5.2.4	Purification of VLPs by size exclusion chromatography	164
5.3	Conclusions	171
5.3.1	Future directions	171
5.4	References	173
6	Conclusions and outlook	176
6.1	Monosaccharide antigens	176

6.2	Natural polysaccharide	179
6.3	D3K6D3 t-HBc-Ag virus-like particle	180
6.4	Summary	181
6.5	References	182
7	Experimental.....	183
7.1	General experimental	183
7.2	Chapter 2 experimental	187
7.3	Chapter 3 experimental	209
7.4	Chapter 4 experimental	213
7.5	Chapter 5 experimental	226
7.6	References	234
8	Appendix	236
8.1	Glycoconjugate MALDIs	236
8.2	NMR overlay of crude <i>B. thailandensis</i> CPS-1 preparation and authentic <i>B. pseudomallei</i> CPS-1 sample	238
8.3	¹³ C NMR of <i>B. thailandensis</i> CPS-1 prep.....	239
8.4	NMR integration of H-1 and H-2 of CPS-1 preparations from <i>B. pseudomallei</i> and <i>B. thailandensis</i>	240
8.5	ELISA of separate sera samples CF1497 and CF1498.....	241
8.6	MALDI-ToF of 6D6FGlc-TetHc glycoconjugate (112).....	242
8.7	¹³ C NMR data for 8-(methoxycarbonyl)octyl 6-deoxy-6-fluoro- β-D-glucopyranose (107) and 8-(methoxycarbonyl)octyl 2,4-di-O- acety-β-D-allopyranoside(109)	243
8.8	pEAQ- <i>HT</i> wtHBcAg plasmid	245

8.9 References.....247

1 Introduction

Glycobiology is the study of the structure, biosynthesis and biology of carbohydrates that are ever present throughout nature in a variety of glycoconjugates¹. Polysaccharides are one of the three major classes of biopolymers, along with polypeptides and polynucleotides, which are responsible for the majority of information transfer in biological systems. Carbohydrates are the most abundant and structurally diverse organic molecules in nature². Part of this structural diversity can be attributed to the inherent variability of the structure of the monosaccharide building blocks. However, it is the formation of glycosidic linkages which is primarily responsible for the variety seen in glycan structures. When compared to polynucleotides and polypeptides the number of different theoretical oligomers that can be derived from a set number of monomers is dramatically increased (Table 1.1)³.

Oligomer Size	Polynucleotide	Polypeptide	Polysaccharide
1	4	20	20
2	16	400	1,360
3	64	8,000	126,080
4	256	160,000	13,495,040
5	102	3,200,000	1,569,745,920
6	4,096	64,000,000	192,780,943,360

Table 1.1: Table summarising the potential oligomer variations of the three major biopolymers. Data taken from Werz *et al.*³. Data for polypeptides derived from the 4 nucleotide bases and polypeptide data derived from the 20 amino acids. Data for polysaccharides was derived from calculations using the alpha and beta form of the 10 most abundant mammalian monosaccharides: D-glucose, D-galactose, D-mannose, D-sialic acid, N-acetyl-D-glucosamine, N-acetyl-D-galactosamine, L-fucose, D-xylose, D-glucuronic acid and L-iduronic acid

The data for the polysaccharide complexity in Table 1.1 is based on theoretical calculations using both the alpha and beta form of the 10 most abundant mammalian monosaccharides³. The high number of theoretical polysaccharides arises from the fact that each monosaccharide has multiple sites for attachment. The formation of a glycosidic linkage also generates a new stereocentre in the extending oligomer which gives rise to yet more configurations for each bond. This is represented in Figure 1.1

which looks at glycosidic bond formation in its simplest form, between two D-glucose residues.

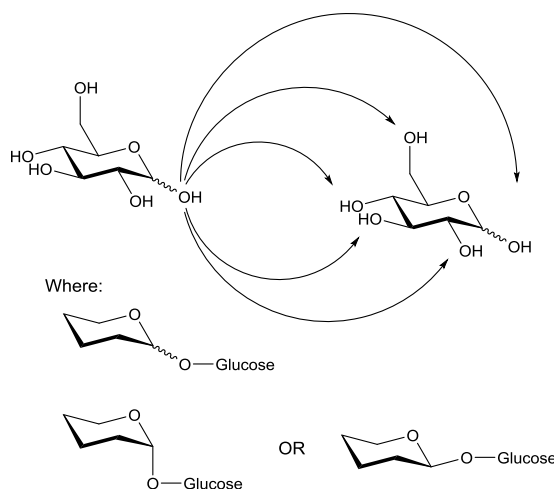


Figure 1.1: Schematic representation of possible sites for formation of a glycosidic bond between two D-glucose residues highlighting the ten possible combinations between two identical monosaccharides.

Beyond the complexity of the glycosidic linkages, carbohydrates are subject to an array of post-synthetic modifications, such as methylation, acetylation, phosphorylation and sulfation further increasing their structural diversity^{3,4}. It is the structural variety found in carbohydrates that facilitates the many roles which they play in nature.

Carbohydrates are a ubiquitous energy source, as well as structural components of a number of natural materials such as plant tissue and the shells of many insects and crustaceans. It is estimated that 4×10^{11} tonnes of carbohydrates are produced per annum by plants and photosynthesising bacteria, the majority of which are produced as polysaccharides¹. However, by far the most extensive role of glycans in nature is their presence on cell surfaces². The interaction of glycans with carbohydrate-binding proteins mediates a vast number of intra- and extra-cellular processes, for example, fertilisation⁵ in mammals, oligosaccharide signalling in plants⁶ and invasion and infection of micro-organisms⁷⁻⁹. The prominence of carbohydrates in the infection and pathogenesis of micro-organisms results in glycans playing an integral role in the immune response of both mammals^{2, 4,10} and plants¹¹. The subject of Glycobiology and

Immunology is vast and has been studied since the identification of the ABO(H) blood groups over a century ago¹². The focus of this thesis is the development of a carbohydrate-based vaccine for the bacterial pathogen *Burkholderia pseudomallei* and as a result this introduction will only focus on the role of glycans in bacterial infection, and subsequent potential for development of carbohydrate vaccines.

1.1 Carbohydrates and bacterial infection

1.1.1 Bacterial adhesion

Cell-surface carbohydrates are readily accessible and represent ideal binding sites for opportunistic pathogens such as viruses¹³, bacteria^{14,15,16}, parasites^{17, 18}, yeast¹⁹ and other fungi²⁰. The adhesion to mammalian cells, through adherence factors (adhesins), is an essential first step in the pathogenesis of many infectious diseases. The attachment of bacteria facilitate the site specific colonisation and subsequent development of disease-states in the host²¹. Attachment to cell membranes also prevents the removal of bacteria through normal process such as urination or vomiting. For example, certain strains of *E. coli*²² (bladder – urinary tract infection) and *Salmonella*²³ (intestinal cell mucosa – infectious diarrhoea) express adhesins known as pili of fimbriae which protrude from the cell surface and bind to specific carbohydrate receptor sites on target cells²⁴. The role of adhesins in the bacterial colonisation (pathogenic, commensal and probiotic bacteria) of the gastrointestinal tract is currently subject of much research^{25, 26}. The gastrointestinal tract is covered in a mucosal layer, of which mucins are the major structural component²⁵. Mucins are highly O-glycosylated proteins with tandem repeat domains rich in proline, threonine and serine²⁶. Although not fully understood, interference of the interaction between bacterial adhesins and mucins in the gastrointestinal tract is believed to offer a route to limit the infection by pathogenic bacteria²⁵. Another examples of the role of carbohydrates in colonisation of bacteria is the expression of surface-anchored proteins or afimbrial adhesins, which bind to host cell carbohydrate receptors and establish colonisation. The attachment of adhesion proteins to cell surface glycans is depicted in Figure 1.2.

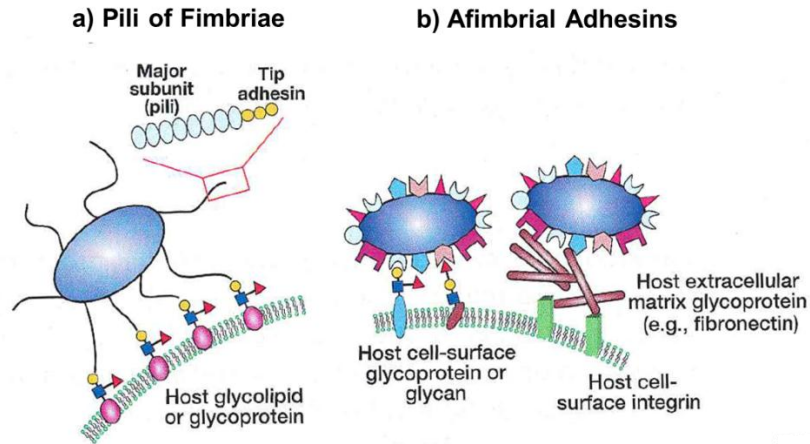


Figure 1.2: Schematic representation of the binding of bacterial cells to host cell glycans through a) pili or fimbriae and b) afimbrial adhesins. Image reproduced from Essentials of Glycobiology with permissions copyright Cold Spring Harbor Laboratory Press 2008.

1.1.2 Bacterial Polysaccharide Virulence Factors

Polysaccharide virulence factors play an essential role in the survival and virulence of many bacteria²⁷. Virulence factors are molecules which are produced by pathogens (bacteria, viruses, fungi and protozoa) that allow them to establish and maintain disease states in a host²⁸⁻³³. For example, it has been shown that removal of key carbohydrate moieties from the outer core polysaccharide of *S. enterica* leads to attenuation of the bacteria¹⁵.

Toxins are a good example of bacterial virulence factors and can be divided into two sub-groups: endotoxins which remain 'within' the cell, and exotoxins which are released into the host environment³⁴. The lipopolysaccharide (LPS) of Gram-negative bacteria is a typical example of an endotoxin. LPS accounts for around 30% of the total outer cell membrane weight (of Gram negative bacteria) and elicits a strong immune response in mammals as a result of activation of the Toll-like receptor-4. LPS (Figure 1.3) is comprised of a polysaccharide (O-antigen) attached to a lipid (Lipid A) through core oligosaccharide residues (Outer and Inner Core)³⁵. The O-antigen region of LPS consists of repeating oligosaccharide units. Variability in the O-antigen region is responsible for much of the antigenic variation between different Gram-negative species. The role of the O-antigen in the virulence of bacteria is elegantly

demonstrated by the K-12 strain of *E. coli*. K-12 is a widely used laboratory strain, which is known to have mutations in the O-antigen gene cluster resulting in the abrogation of O-antigen biosynthesis. These mutations prevent the K-12 *E. coli* strain from surviving outside of laboratory conditions, indicating that the O-antigen is essential for bacterial survival in the normal environment³⁶. The core region can be divided into two sections, the inner core which attaches the oligosaccharide region to Lipid A through an acid-labile ketosidic linkage,³⁶ and the outer core which links the inner core to the O-antigen. Lipid A anchors LPS into the cell membrane and is the bioactive region responsible for the over stimulation of the immune system and subsequent toxic effects. As a result of this over stimulation of the immune system, septic shock syndrome can occur, which often requires urgent medical attention³⁷.

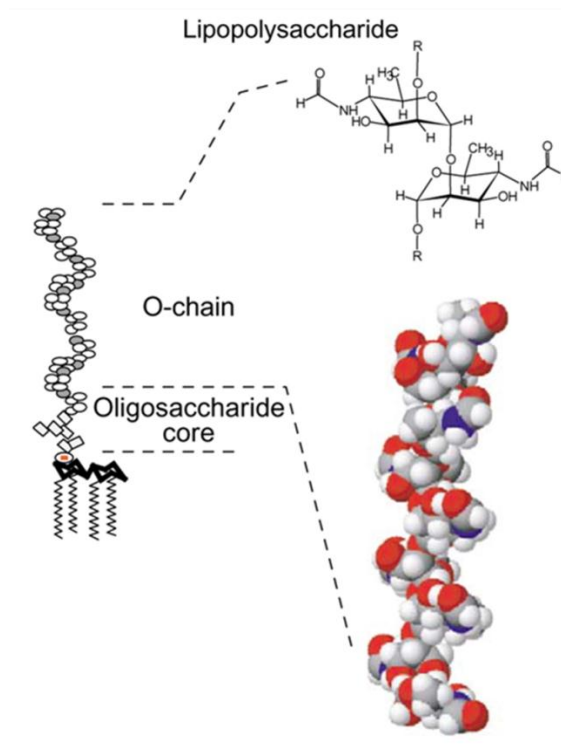


Figure 1.3: Schematic representation of lipopolysaccharide structure of Gram-negative bacteria. Picture reproduced with permissions from Lapaque *et al*³⁵ copyright Elsevier 2005.

Other polysaccharides which play a vital role in the virulence of bacteria are exopolysaccharides (EPS) and capsular polysaccharides (CPS). Dental plaque is a biofilm and is primarily comprised of EPS from *Streptococcus mutans* bacteria³⁸. Glucan-mediated binding of bacteria to the EPS produced by *S. mutans* facilitates the

colonisation by bacteria in the mouth³⁹. Within biofilms bacteria exist in polymicrobial communities in which they live in a dormant state surviving on low nutrient levels. In this state the bacteria are less susceptible to anti-bacterial treatments and host immune defence mechanisms.

Capsular polysaccharides are high molecular weight polysaccharides which form a matrix layer around the bacterial cell encapsulating it. Unlike EPS, capsules are tethered to the cell membrane, typically through a lipid moiety⁴⁰. The encapsulation of bacteria by capsules makes these polysaccharides ideal antigens for use in vaccines (Section 1.1.3). There have been a number of functions of capsules postulated over the years including desiccation prevention, adherence and resistance to host immunity⁴¹. The encapsulation of bacteria by polysaccharides prevents the normal activation of the Complement System, a major feature of innate immunity, resulting in the increased virulence of the bacterium⁴⁰.

1.1.2.1 *The complement system*

The complement system consists of a number of glycoproteins which react in a series of cascade reactions to facilitate the destruction of a pathogen (Figure 1.4). These glycoproteins (approximately 30 in total) circulate the body in the blood plasma. The proteins are generally in an inactive state until they are activated by a protease, which in turn converts the cleaved protein into a protease in a specific sequence. There are two pathways in which the complement system can contribute to the innate immunity of a host, the Classical pathway and the Alternative pathway⁴².

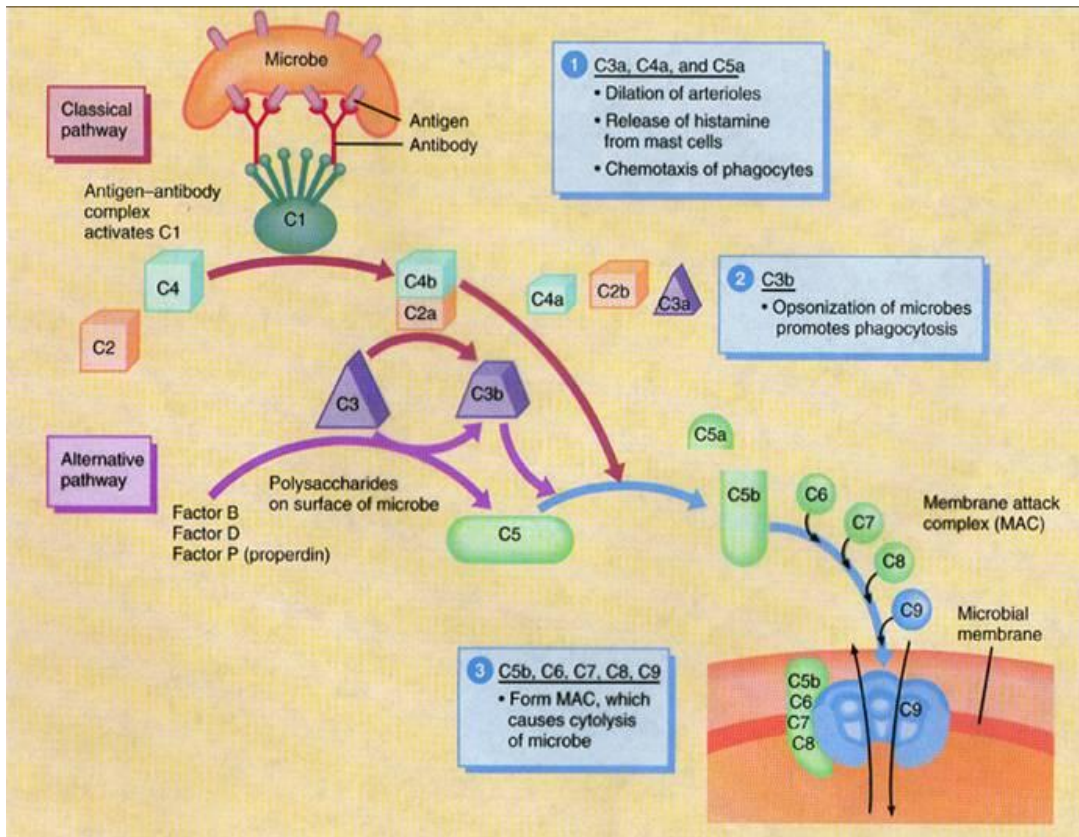


Figure 1.4: Schematic representation of the Classical and Alternative pathways of the complement system adapted from Austin Peay State University website, J. Thompson lecture notes⁴³.

The Classical Pathway

In the Classical Pathway the initial step in the complement cascade is the binding of the **C1** protein complex to antibodies bound to antigens on the surface of a pathogen. The **C1** complex is activated and a serine protease cleaves the next glycoprotein in the cascade **C4** into a small (**a**) and large (**b**) fragment. Upon cleavage **C4b** binds to carbohydrate residues on the cell surface and **C4a** diffuses away from the cell. The activated **C4b** cleaves **C2**, again into two fragments, **C2a** binds to surface bound **C4b** and **C2b** diffuses away. The **C4b.C2a** complex, or **C3** convertase, catalyses the cleavage of the **C3** glycoprotein into two fragments **a** and **b**. **C3** is the most abundant of all the complement factors and is vital in the amplification of the innate immune response. Numerous copies of **C3b**, an opsonin, bind to glycoproteins scattered on the cell surface and facilitate phagocytosis of the pathogen by macrophages and neutrophils. **C3b** proteins also bind to protein **C5** instigating an allosteric change making **C5** susceptible to cleavage (again into **C5a** and **C5b**) by the **C4b.C2a** complex. **C3a**, **C4a** and **C5a** are classed as anaphylatoxins, which stimulate the release of histamine and other compounds from immune cells resulting in a localised inflammatory response. **C5b** triggers the assembly of the membrane attack complex (MAC) on the surface of the cell. The **C5b.6.7.8.9** (up to 18 copies of **C9**) complex forms a pore in the surface of the cell membrane which allows the diffusion of ions, small molecules and water resulting in cell lysis^{42, 44, 45}.

The Alternative Pathway

The alternative pathway does not require initial activation of the complement system by antibody-antigen interactions. In normal serum, **C3b** exists in trace amounts and can be activated by polysaccharides (eg. LPS) and other endotoxins. Activated **C3b** combines with complement factor **B**, a single polypeptide chain which is present in blood serum to form the **C3b.B** complex⁴². Cleavage of the **C3b.B** complex by complement factor **D** generates the **C3** convertase complex **C3b.Bb**. The generation of a separate **C3** convertase complex in the Alternative pathway, is the basis of the amplification of the complement system as more **C3b** is generated, which in turn binds with complement factor **B** to continue the cycle as shown by Figure 1.5⁴⁴.

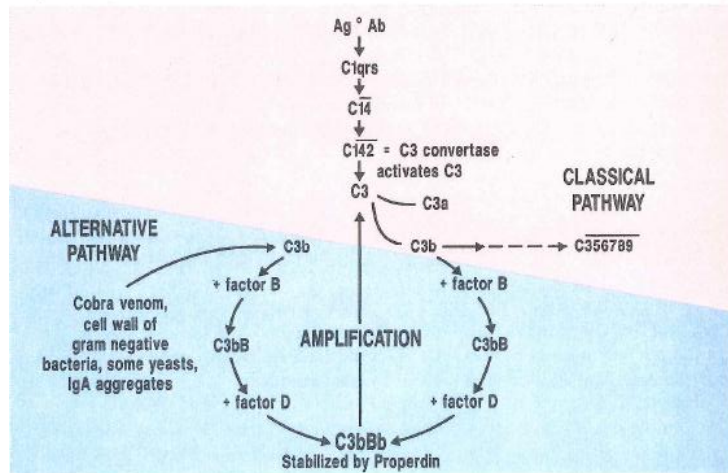


Figure 1.5: Amplification of the complement system cascade by the Alternative Pathway. Picture reproduced with permissions from Immunology A Short Course Copyright John Wiley and Sons 2009⁴².

Capsular polysaccharides interfere with the complement system by blocking the deposition of sub-unit **C3b** onto the surface of bacterial cells, thus preventing the opsonisation of the bacteria⁴⁰. The interference of the complement system by the capsular polysaccharide of *B. pseudomallei*, the target pathogen of this research, was demonstrated by a series of immunofluorescence experiments carried out by Reckseidler-Zenteno and co-workers (Figure 1.6)⁴⁶. Figure 1.6 demonstrates the prevention of **C3b** deposition (no red staining) on the surface of *B. pseudomallei* cells which produce the capsular polysaccharide (Figure 1.6 B and C). The capsule masks the **C3b** binding receptors on the surface of the cell and helps the bacteria to avoid opsonisation and subsequent phagocytosis. Mutant CPS negative *B. pseudomallei* strains have been shown to be 1,000 fold times less virulent than the wild-type, CPS positive strain, demonstrating the importance of CPS for the virulence of *B. pseudomallei*⁴⁶.

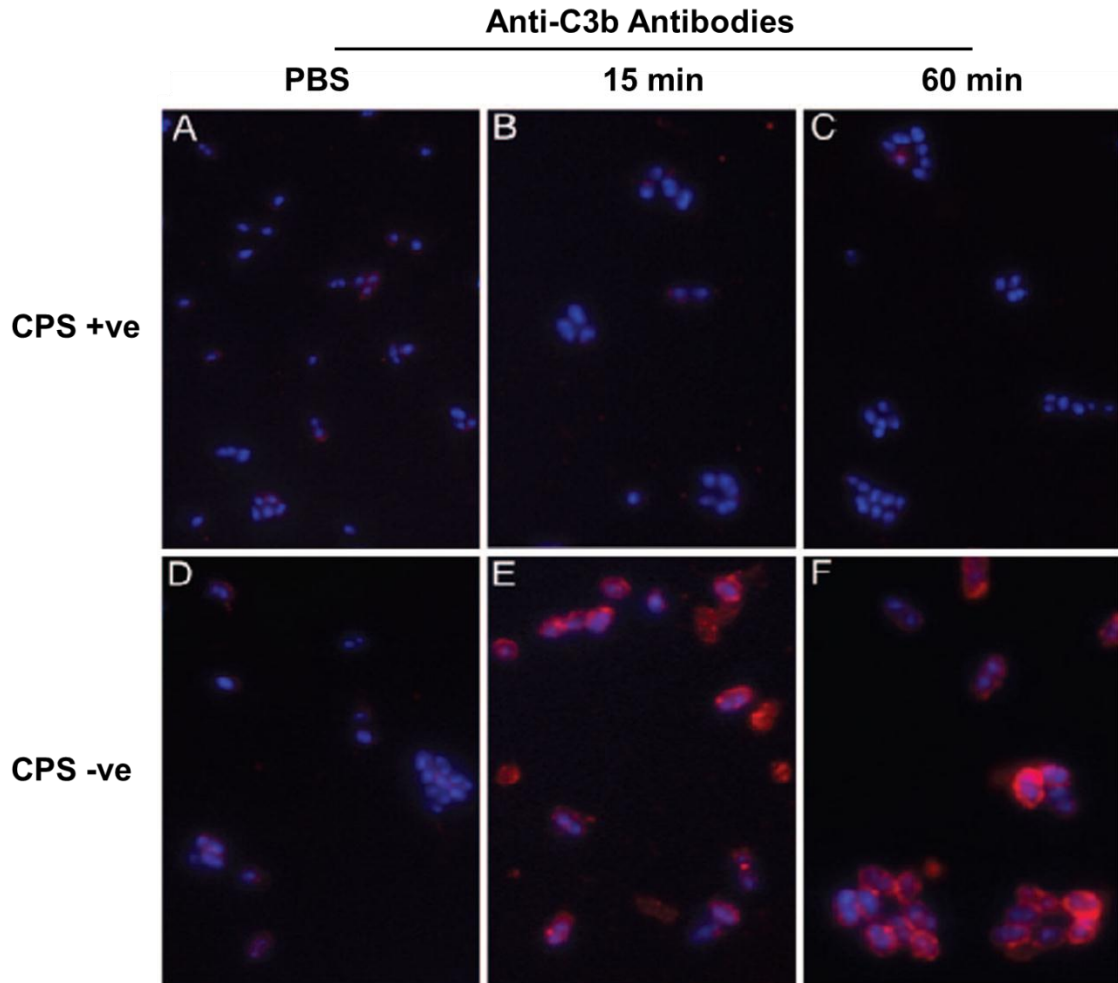


Figure 1.6: Immunofluorescence microscopy demonstrating decreased deposition of complement factor C3b in 10% human serum on the surface of CPS+/-ve strains of *B. pseudomallei*. *B. pseudomallei* cells were inoculated with 1) 10% human serum; 2) anti-C3b mouse monoclonal antibodies and 3) fluorophore labelled anti-mouse secondary antibody (red). Cells were also pre-stained with DAPI to identify the cell nucleus. Blue staining indicates DAPI stained bacteria and red staining indicates the deposition of C3b. Legend: A & D) cells incubated with PBS alone. B & E) cells incubated with 10% human serum for 15 minutes. C & F) cells incubated with 10% human serum for 60 minutes. Image reproduced with permissions from Reckseidler-Zenteno *et al.* Copyright American Society for Microbiology 2005⁴⁶.

1.1.3 Carbohydrate-based vaccines

Cell surface polysaccharides present an ideal candidate for use in vaccines as they are conserved and their presentation on the bacterial cell means they are highly accessible to the immune system. Carbohydrates are by themselves, poorly immunogenic and, furthermore, carbohydrate specific antibodies generally have low affinity when compared to protein-specific antibodies^{9, 47}. Traditionally, carbohydrate conjugate

vaccines were based on extracted polysaccharide material chemically conjugated to a carrier protein⁸. Conjugation of polysaccharides to a carrier protein was first established by Avery and Goebel,⁴⁸ who demonstrated that the coupling of *Pneumococcus* oligosaccharides to proteins rendered them immunogenic.

The poor immunogenicity of polysaccharides is as a result of the way in which polysaccharides generate an immune response. Polysaccharides are considered to be T-cell independent type 2 (TI-2) antigens based on their ability to stimulate B cells without the need for helper T-cells. The ability of polysaccharides to directly activate B cells arises from the cross-linking of IgM antigen receptors on the B-cell, facilitated by the polyvalent nature of polysaccharides⁴⁹. T-cell independent activation of B-cells generally results in the production of low affinity IgM antibodies and often does not generate memory B-cells. Coupling of polysaccharides to carrier proteins adds a T-cell dependant aspect to B-cell activation which facilitates the switching of B-cells into memory B-cells⁴⁹. In part it is this switching which enables glycoconjugate antigens to generate immunological memory for a specific antigen and thus act as vaccines⁸.

Carbohydrate based vaccines have been developed and are licensed, for a number three bacterial pathogens *Haemophilus influenzae* type b (Figure 1.7), *Neisseria meningitidis* (Figure 1.8) and *Streptococcus pneumoniae*⁵⁰.

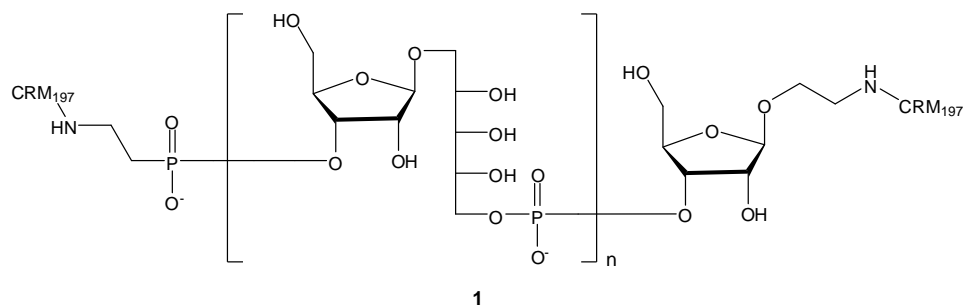
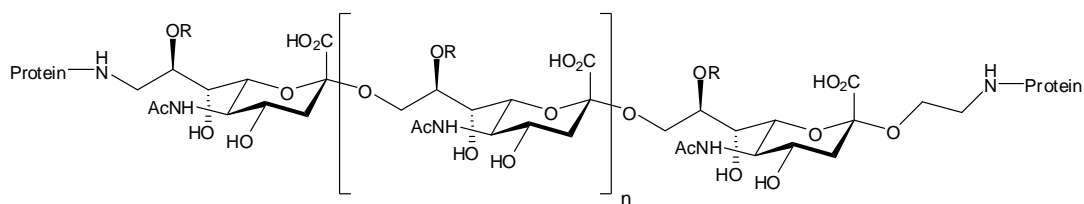


Figure 1.7: Structure of the Pfizer (Wyeth Lederle) *Haemophilus influenzae* Type b CPS vaccine, based on the linear β -linked poly-ribosyl ribitol phosphate capsular polysaccharide. The degree of polymerisation (n) is determined by the amount of periodate used in the oxidation of the native polysaccharide. The oxidised polysaccharide is reductively aminated to Diphtheria Toxin CRM₁₉₇ carrier protein to form the multivalent vaccine 1⁵⁰.



Wyeth Lederle vaccine: Protein = CRM₁₉₇; R = H or Ac (2)

Baxter Health vaccine: Protein = TetHc; R = H (3)

Figure 1.8: Structure of the Pfizer (Wyeth Lederle) (O-acetylated) and the Baxter Health (de-O-acetylated) *Neisseria meningitidis* Group C vaccine, based on the Group C α -(2,9) linked sialic acid capsular polysaccharide. Again the degree of polymerisation (n) is determined by the amount of periodate used in the oxidation of the native polysaccharide. The oxidised de-O-acetylated polysaccharide is reductively aminated to Diphtheria Toxin CRM₁₉₇ carrier protein (Pfizer) (Wyeth Lederle) (2) and the O-acetylated polysaccharide is reductively aminated to TetHc carrier protein (3)⁵⁰

There are three carbohydrate based *Streptococcus pneumoniae* vaccines currently available. Merck's Pneumovax 23 is comprised of purified capsular polysaccharide from the 23 most common serotypes. Owing to the lack of carrier protein this vaccine does not elicit immune memory and has low efficacy in young children⁵¹. The second vaccine is Pfizer (Wyeth's) PrevenarTM conjugate vaccine, which is comprised of capsular polysaccharides from a range of prevalent *S. pneumoniae* serotypes conjugated to a variety of carrier proteins⁵². Glaxo Smith Kline's Synflorix vaccine contains 10 CPS serotypes conjugated to carrier protein (DT and TT)⁵³. These vaccines are capable of eliciting immune memory and is effective in young infants⁵².

There is increasing research interest in the use of purified polysaccharide material to synthetic oligosaccharide fragments in glycoconjugate vaccines, alongside the continued use of natural polysaccharide material⁵⁴. In spite of the chemically demanding nature of carbohydrate synthesis, synthetic oligosaccharide fragments present an ideal antigen for carbohydrate vaccines⁹. The production, extraction and purification of bacterial polysaccharides can often be problematic⁵⁵, in particular when dealing with highly infectious bacteria such as *Yersinia pestis* or *Clostridium botulinum*, which require extensive containment facilities. It is also essential that all biological contaminants are removed from the polysaccharide extract in order to avoid adverse reactions, eg. septic shock syndrome⁵⁶. Extraction of polysaccharides affords a

polydisperse mixture of molecular masses, which upon conjugation with a protein will generate more diversity. The use of synthetic fragments allows for the preparation of well-defined glycoconjugate vaccines. The quality control and batch to batch consistency of oligosaccharide fragments is a distinct advantage, particularly in the eyes of regulatory bodies⁵⁷.

Furthermore, in conjunction with the shift to synthetic oligosaccharide fragments, there has also been a move to the use of fully synthetic carbohydrate vaccines⁵⁸⁻⁶¹. Along with the quality control benefits described above, one of the increasing concerns regarding the use of glycoconjugate vaccines is carrier induced epitopic suppression (CIES)⁶². CIES is the interference of pre-existing carrier protein antibodies on the development of immunity to conjugated antigens. Such strategies include the use of nanoparticles⁶³, liposomes⁶⁴ or peptides⁶⁵ to replace the traditional carrier proteins⁶⁶. The coupling of synthetic oligosaccharide epitopes to nanoparticles in combination with immunomodulating agents has been shown to be a promising step forward in the development of fully synthetic carbohydrate vaccines against *S. pneumoniae*^{63, 67}.

1.2 *Burkholderia pseudomallei*

B. pseudomallei is a Gram-negative bacteria which is the causative agent of melioidosis, a febrile illness with disease states such as pneumonia, septicaemia and chronic abscesses⁶⁸. The two main infection routes for *B. pseudomallei* are through breaks in the skin and inhalation of contaminated materials such as soil and water. Melioidosis is endemic to the sub-tropical regions of the globe (Figure 1.9) and as a result of the rise in transport of humans and animals is spreading at an ever increasing rate⁶⁹.

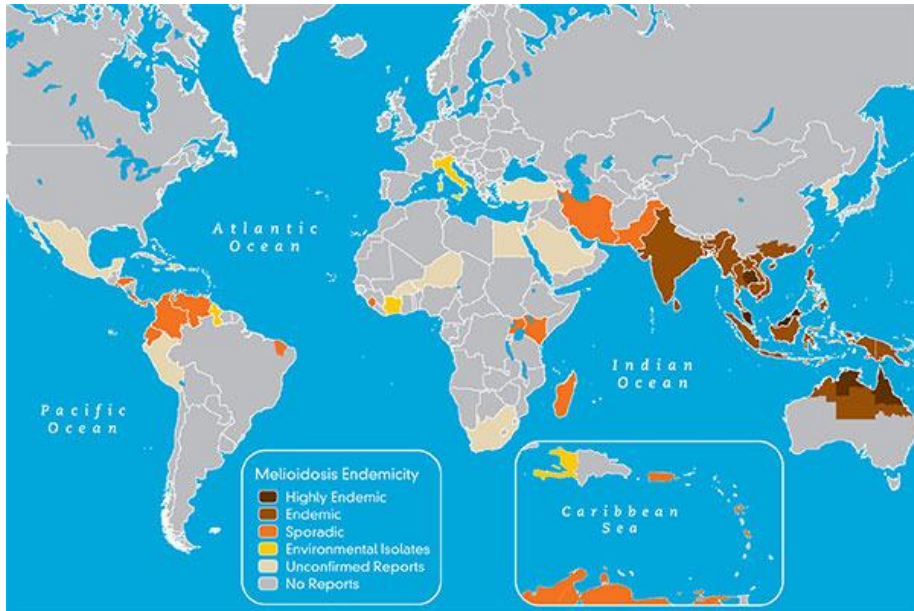


Figure 1.9: Global spread of melioidosis cases around the world in 2012. Image taken from the Centre for Disease Control website⁷⁰.

Melioidosis has two disease states; acute, where symptoms occur with 1-9 days post-infection, and chronic, where the infection can lay dormant for decades before symptoms are seen⁶⁹. There is currently no vaccine for melioidosis and treatment of the disease is often complicated. Like many other environmental bacteria, *B. pseudomallei* is highly resistant to a number of antibiotics⁷¹. As a result treatment involves lengthy intravenous regimens of antibiotics such as Meropenem and Ceftazidime⁷¹. Even with medical attention, the mortality rates associated with melioidosis are high, particularly in regions where access to advanced medical facilities is limited (Table 1.2)⁶⁸.

Mortality Rate for Melioidosis⁶⁸	
Antibiotics – Australia	10-20%
Antibiotics – Thailand	20-40%
No Antibiotics	>90%

Table 1.2: Mortality rates of melioidosis depending on treatment and access to advanced medical facilities⁶⁸.

On this basis and the relative ease at which this bacteria can be accessed the Centre for Disease Control (CDC) in the United States has classified *B. pseudomallei* as a category B Bio-terrorism agent⁷². The need for a vaccine for melioidosis is evident and there has been much research to this end.

1.2.1 Vaccination of *B. pseudomallei*

In 1993, Kanaphun *et al.* demonstrated that in endemic regions, such as North East Thailand, large proportions of the population tested seropositive for antibodies raised against *B. pseudomallei*. However, despite high exposure to the bacteria the incidence of melioidosis was relatively low⁷³. This demonstrated that those individuals who had been exposed to *B. pseudomallei* but not contracted melioidosis had developed protective immunity, indicating that vaccination against *B. pseudomallei* is possible. There have been a number of attempts to generate a vaccine for *B. pseudomallei* using different approaches.

Vaccination studies using live attenuated *B. pseudomallei* cell based vaccines have been widely investigated since the late 1950's⁷⁴. More recently, Stevens *et al.*⁷⁵ achieved partial immunity in mice with a *B. pseudomallei* mutant carrying a dysfunctional type-III secretion system. The use of live attenuated strains of bacteria is an effective means for vaccination against bacterial pathogens. This is based on the ability of the live bacteria to replicate in the host generating strong humoral and cell-mediated immune responses⁷⁶. Despite the efficacy of live attenuated vaccines, there as yet has not been a *B. pseudomallei* vaccine which has conferred full protective immunity in mice⁷⁷. There are also safety concerns regarding the use of live attenuated vaccines, particularly in immuno-compromised individuals, due to the potential for the bacteria to revert to a pathogenic state leading to infection⁷⁸. The use of dead whole cell vaccines has also been attempted for *B. pseudomallei* again with limited success⁷⁹⁻⁸¹. Despite providing short term protective immunity, when sacrificed, mice treated with dead *B. pseudomallei* cells were found to have very high bacterial concentration in major organs such as the spleen. This indicated that the use of dead whole cell vaccines was not providing sufficient protection against chronic infection, a pre-requisite for a *B. pseudomallei* vaccine candidate⁸¹.

In order to combat the safety and efficacy concerns associated with using whole cell (live-attenuated and whole-dead cell) vaccines, the majority of research into *B. pseudomallei* vaccines is focused on the development of sub-unit vaccines. Sub-unit vaccines use purified bacterial components to elicit an immune response in the host, meaning that as long as the material has been separated from any possibly reactogenic material (LPS etc.), the vaccine should be 100% safe⁷⁶. Sub-unit vaccines have been licensed in humans for tetanus and diphtheria (inactivated bacterial toxin vaccine) and pneumococcal and meningococcal disease (polysaccharide based vaccines Section **1.1.3**)^{78, 82}. The recent attempts for generation of a sub-unit vaccine for *B. pseudomallei* are summarised in Table **1.3**.

Antigen	Composition	Protection	References
LPS	Lipopolysaccharide	80% survival at day 14 after challenge with 4,300 x MLD	41
CPS	Polysaccharide	40% survival at day 14 after challenge with 4,300 x MLD	83
Flagellin	DNA	80-90% survival at day 14 after challenge with 100 x LD ₅₀	84-86
Flagellin	Protein	50% survival at day 7 after challenge with 100 x LD ₅₀	84, 86
Flagellin-CPS conjugate	Protein-Polysaccharide	Passive transfer of sera protected 40% of diabetic rats at day 8 after challenge with 400x LD ₅₀	86
BipB, BipC, BipD	Protein	No survival at day 5 after challenge with 30 x LD ₅₀	87
Omp85	Protein	70% survival at day 15 after challenge with 10 x LD ₅₀	88
EF-TU	Protein	Reduced colonisation after aerosol challenge with 1 x LD ₅₀ of <i>Burkholderia thailandensis</i>	89
BPSL2522 (Omp3)	Protein	50% survival at day 14 after challenge with 10 x LD ₅₀	90
BPSL2765	Protein	75% survival at day 14 after challenge with 10 x LD ₅₀	90
LoiC	Protein	80% survival at day 14 after challenge with 153 x MLD	91

Table 1.3: Details of sub-unit *B. pseudomallei* sub-unit vaccine candidates tested to date. Median lethal dose (MLD) is broadly equivalent to lethal dose 50% (LD₅₀), all experimental work was carried out in mice. Table adapted from Patel *et al*⁷⁷.

1.2.2 Virulence factors and pathogenicity of *B. pseudomallei*

A number of *B. pseudomallei* virulence factors have been identified and have been employed as potential vaccine candidates (Table 1.3). Polysaccharide virulence factors play a key role in the infection mechanism of *B. pseudomallei*, as previously described, the CPS-1 of *B. pseudomallei* is integral in the evasion of the hosts immune system by *B. pseudomallei* (Section 1.1.2.1)⁴⁶. There a couple of models which have been proposed for the role of LPS in the virulence mechanism of *B. pseudomallei*.⁹² The first focuses on the effect that LPS has on the formation of the MAC complex (Section 1.1.2.1). Activation of the complement system by LPS may occur far from the cell, preventing the formation of the MAC on the membrane surface of the cell. The second model proposes that the LPS is required for the correct presentation of the CPS-1 on the surface of the bacterial cell to facilitate its role as a virulence factor.⁹²

An important step in the infection mechanism of *B. pseudomallei* has been shown to be the injection of effector proteins into the host cells via the type three secretion system (TTSS-1) leading to the invagination of the bacteria⁹³. Mutations of the TTSS-1 gene cluster have been shown to lead to a substantial drop in virulence of the bacteria.⁷⁷ After internalisation, *B. pseudomallei* evades endocytic vacuoles through lysis of the endosome membrane⁹³. Pilatz *et al*⁹⁴ demonstrated *B. pseudomallei* can stimulate actin rearrangement/polymerisation at one pole of the cell, forming a protrusion. Through this protrusion *B. pseudomallei* can infect neighbouring cells, via endocytosis of this protrusion, without exposure to antibodies. A number of other putative virulence factors have also been identified for *B. pseudomallei* including; type IV pili for adhesion of the bacteria to host cells⁹³, a siderophore for iron acquisition⁹², various degradative enzymes including proteases and lipases⁹³, and quorum sensing molecules, which are yet to be identified⁹⁵.

1.2.3 Polysaccharides of *B. pseudomallei*

Of all the previous attempts for generation of a sub-unit vaccine for *B. pseudomallei* those involving the use of polysaccharide conjugates, with or without the addition of immunogenic peptides seemed to provide the most effective protection against lethal

1.2.3.1 *The capsular polysaccharide of B. pseudomallei*

The capsular polysaccharide was first identified as a primary virulence factor of *B. pseudomallei* by Reckseidler *et al.*¹⁰¹ Insertional inactivation of one of the glycosyltransferase genes for CPS-1 production resulted in a 10,000 fold reduction in virulence of the bacteria. It has been shown previously, Section 1.1.2.1 how CPS-1 acts as a virulence factor by interfering with the action of the complement system on *B. pseudomallei*, preventing opsonisation and subsequent phagocytosis. It has also been shown that biosynthesis of CPS-1 is up regulated during infection¹⁰². To date, all clinical isolated species of *B. pseudomallei* have been tested positive for the presence of CPS-1 giving a 100% correlation between virulence and capsule production, highlighting the vaccine potential of this polysaccharide¹⁰³. Sequencing of the genes responsible for the biosynthesis of the CPS-1 from *B. pseudomallei* revealed that it was most likely a group-III capsule, based on the presence of the *kps* locus. *Kps* loci are responsible for the translocation through and internalisation of capsular polysaccharides into the outer membrane of many bacteria, including *N. meningitidis* and *H. influenzae*¹⁰⁴. The presence of a diacylglycerophosphate group at the reducing terminus is a recurring phenomenon of group-III capsule bacteria¹⁰⁴. The presence of a diacylglycerol capping residue on the reducing terminus has implications on potential conjugation routes for the polysaccharide and will be discussed further in Section 3.2.2.

As discussed previously the options for the development of carbohydrate vaccines fall into two main categories: the extraction, purification and use of the intact polymer or the use of synthetic oligosaccharide fragments. The category III status of *B. pseudomallei* means that handling of the bacteria is restricted to labs with specialist containment facilities, such as those at DSTL-Porton Down. For these reasons, the use of the native polysaccharide as a vaccine candidate will not be discussed at this stage. The use of synthetic fragments of the CPS-1 (4) was the initial focus of this PhD project. The CPS-1 (4) of *B. pseudomallei* is a high molecular weight (ca. 200 kDa¹⁰⁵) homopolymer of 1,3-linked 2-O-acetyl-6-deoxy- β -D-manno-heptopyranoside residues (Figure 1.10).

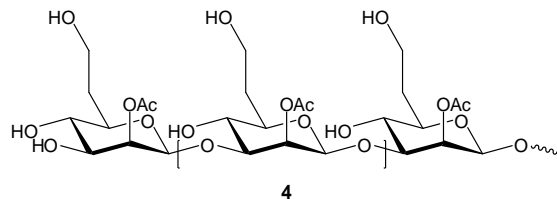


Figure 1.10: Structure of the capsular polysaccharide of *B. pseudomallei*.

The β -1,3 linkage of CPS-1 poses an interesting challenge for carbohydrate chemists. A discussion of the synthetic options for the synthesis of these polysaccharides can be found in the next section. However, the presence of the β -1,3 linkage also gives rise to questions regarding the global structure of the polysaccharide. The tendency of β -1,3-glucans to form helical structures (single and triple) has been well studied; lentinan (Sarko *et al.*¹⁰⁶), curdlan (Marchessault *et al.*¹⁰⁷) and schizophyllan (Fujita *et al.*¹⁰⁸). The propensity for β -1,3-glucans to form helical secondary structures gives some indication that β -1,3-mannans could adopt similar global structures. The development of secondary structures in polysaccharides is known to have an effect on the function of the polysaccharide. For example, heparin sulphate (HS) is a polysaccharide found on the surface of most cells in the form of a proteoglycan and is responsible for a variety of functions in the body. HS does not have a single defined structure; rather it is comprised of a disaccharide building block which, depending on the specific role of the molecule, has a variety of different pendant groups, as shown in Figure 1.11. A key role of HS in the body is the interaction of the polysaccharide with fibroblast growth factor (FGF) proteins, which are involved in the formation of blood clots. The presentation of the pendant sulphate groups on the helical structure of HS is essential for the interaction with FGF proteins¹⁰⁹. HS is an example of how the formation of a helix leads to the presentation of specific components of the native polysaccharide. The conformation of CPS-1 will have a direct impact on the presentation of epitope regions to the immune system. As such the global structure of CPS-1 must be considered as part of the vaccine development program.

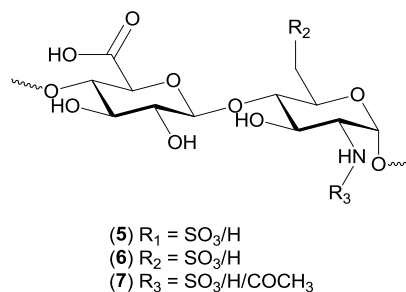


Figure 1.11: The general structure of heparin sulphate

Basic 3D modelling, using ChemDraw10 3D™, indicates that the CPS-1 (4) has the potential to adopt an extended helical structure (Figure 1.12).

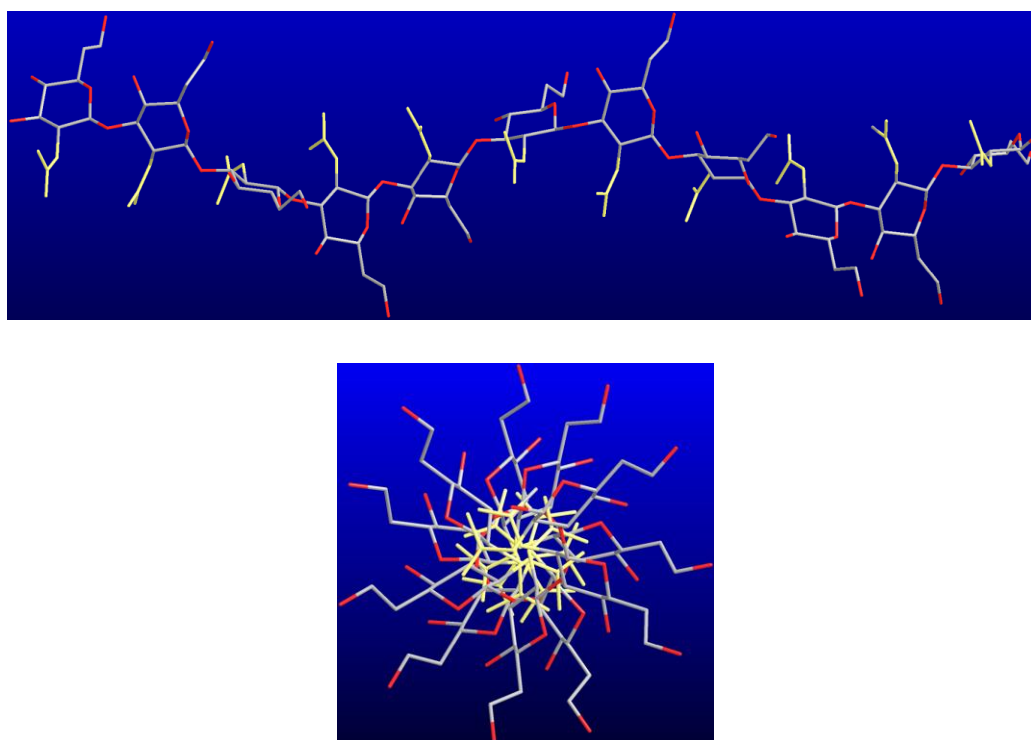


Figure 1.12: 3D representation of a CPS-1 fragment from *B. pseudomallei* demonstrating the formation of a helical structure. The 2-OAc groups have been highlighted in yellow for clarity. Images were produced using ChemDraw 3D and subjected to MM2 calculations.

If the capsular polysaccharide of *B. pseudomallei* does adopt a helical secondary structure, as predicted by the 3D models, then the conformational epitope of the polysaccharide must be considered. The formation of a helix by the CPS-1 (4), as

predicted above, leads to a number of important conformational changes. The first is the apparent burying of the 2-OAc (yellow) residue within the helix core. If this residue is buried within a helical structure, it implies that it may not be part of the CPS-1 (4) binding epitope and thus not required in synthetic mimics of the polysaccharide. The models also imply that, as a result of helix formation, the O-4 to O-7 region of the monosaccharide building blocks would be exposed and likely dominate any binding events with the host immune system (Figure 1.13). Although based on empirical evidence, and as such must be further investigated, these observations regarding the overall structure of the CPS-1 (4) provide useful insight into the requirements for synthetic antigens.

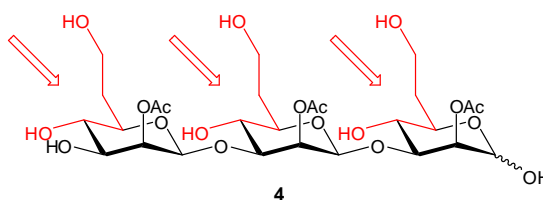


Figure 1.13: Structure of the capsular polysaccharide of *B. pseudomallei* with the predicted immuno-dominant region highlighted in red.

1.3 Synthetic strategy

There are three aspects to CPS-1 of *B. pseudomallei* (4) which make it an interesting and challenging synthetic target; i) the β -1,3-mannan configuration, ii) the unusual 6-deoxy-D-*manno*-heptose configuration and iii) the presence of the 2-*O*-acetyl group. As described above, it is our hypothesis that the acetyl group is buried within a helical core and as such is not a dominant factor in the immune system response to the native polysaccharide. The *Neisseria meningitidis* Group C vaccine produced by Baxter Health (3) is based on the de-*O*-acetylated CPS-1. This polysaccharide has proven to be as, if not more, immunogenic than the Wyeth Lederle (2) vaccine which is based on the natural *O*-acetylated polysaccharide⁵⁰. This suggests that the retention of *O*-acetyl groups present in natural polysaccharide is not always necessary for carbohydrate vaccine structures. On this basis, the synthetic strategies for the installation of the 2 *O*-acetyl group will not be discussed at this stage. The next section will give insight into

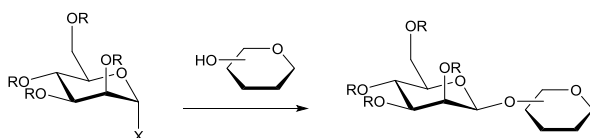
previous synthetic strategies for the synthesis of β -mannosides and the 6-deoxy-D-manno-heptose.

1.3.1 Synthesis of β -mannosides

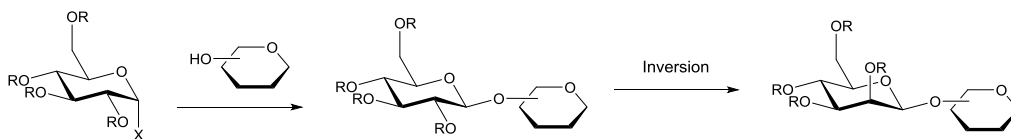
CPS-1 of *B. pseudomallei* is one of many examples of β -D-mannopyranosyl residues which are frequently found in nature. β -Linked mannopyranose is a common residue in many plant¹¹⁰ and microbial¹¹¹⁻¹¹⁴ polysaccharides providing biological rationale for their synthesis. However, the synthesis of oligosaccharides, such as fragments of the CPS-1 (**4**) from *B. pseudomallei* that contain repeating β -D-mannopyranose residues is a complex challenge for two reasons. **Thermodynamically** because the anomeric effect drives the formation of the α -linkage (1,2-*trans*) disfavouring the β -linkage (1,2-*cis*) and **kinetically**, as a result of the steric hindrance from the axial hydroxyl at the 2 position¹¹⁵. Over the years, as synthetic carbohydrate chemistry has developed a number of different synthetic strategies for β -linked mannopyranose oligosaccharide fragments have emerged. This next section focuses on some of the important works on the synthesis of β -mannosides.

The majority of synthetic strategies for the synthesis of β -mannosides can be put into two distinct categories, direct glycosylation and glycosylation-inversion strategies. (Scheme 1.1).

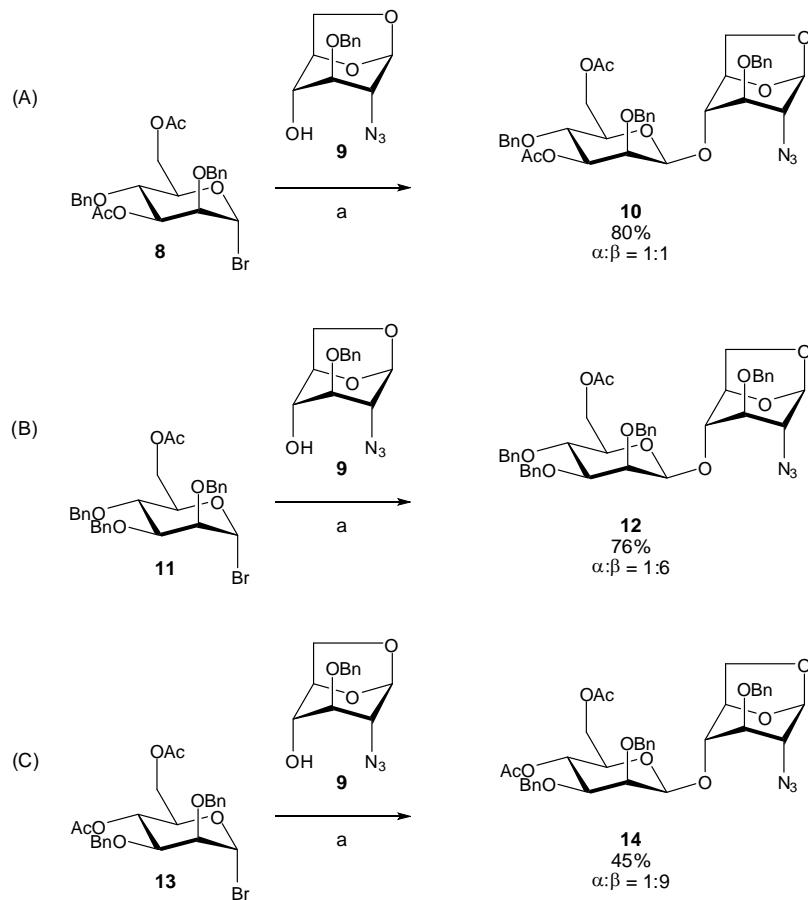
Direct Glycosylation Approach



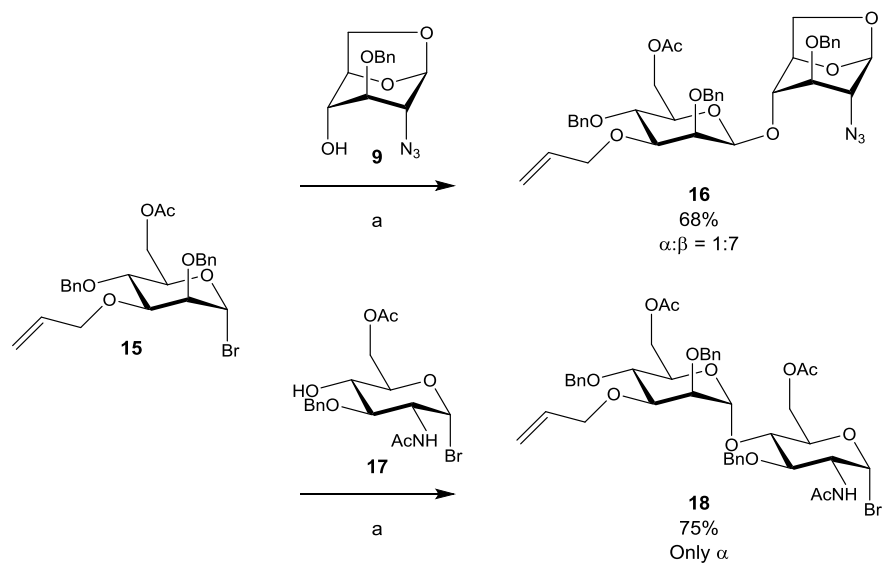
Glycosylation-inversion Approach



Scheme 1.1: Schematic representation of the two general approaches to β -mannoside synthesis, image adapted from Glycoscience, Fraser-Reid. B. O.¹¹⁶



Scheme 1.2: The effect of *O*-acetylation of mannosyl donors on the stereoselectivity of ‘insoluble’ silver salt promoted β -mannoside formation^{116 117}. Reagents and conditions: a) Ag silicate, DCM, rt, 2 h.



Scheme 1.3: Effect of acceptor reactivity on the stereoselective synthesis of β -mannosides from bromide (15) using silver silicate^{116 118}. Reagents and conditions: a) Ag silicate, DCM, rt, 2 h.

Initially β -mannosides were exclusively synthesised using α -mannosyl halides in the presence of a silver promoter such as silver oxide¹¹⁹. Later, the use silver Zeolite and silver silicate based promoters was pioneered by Paulsen¹²⁰ and Garegg¹²¹, respectively. The use of insoluble silver promoters leads to the formation of a 'surface-bound' intermediate and facilitates the S_N2 -like reaction between the glycosyl acceptor and activated donor¹¹⁶, giving high stereoselectivity. van Boeckel *et al.*¹²² demonstrated the use of the improved silver silica-alumina system which was shown to have higher reactivity than the silicate/Zeolite systems.

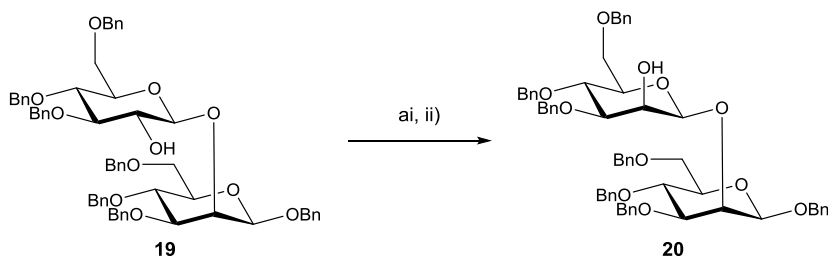
The role of protecting groups on the rate and the stereo-control of glycosylation reactions is widely not understood¹²³. The choice of protecting groups in both the donor and acceptor has a profound impact on the stereoselectivity of silver-promoted β -mannosidation reactions¹¹⁶. This is due to the fact that the successful synthesis of β -mannosides requires rapid displacement of the surface-bound donor. It is well established that the presence of ester-type protecting groups deactivates glycosyl donors.¹²⁴ The use of deactivated glycosyl donors¹²⁴, has been shown to result in the loss of stereoselectivity for the β -mannoside (Scheme **1.2 A**)¹¹⁶. However, van Boeckel *et al.*¹⁰⁹, demonstrated that the effect of *O*-acetyl groups on the stereoselectivity of the reaction is position dependant (Scheme **1.2 (B-C)**)^{116, 117}. The presence of an acetyl group in position-4 (**13**) was shown to be more stereoselective ($\alpha:\beta$, 1:9) when compared to the 2,3,4-tri-*O*-benzylated donor (**11**) ($\alpha:\beta$, 1:6) and the 3-*O*-acetylated donor (**8**)¹¹⁷. In the case of the acceptor, if the target hydroxyl group is sterically hindered and thus poorly reactive, the activated glycosyl donor is liberated from the surface into solution and the stereoselectivity of the reaction is lost as demonstrated by Paulsen *et al.*^{108,110} (Scheme **1.3**). Use of glycosyl acceptor (**15**) with bromide donor (**9**) showed high stereoselectivity ($\alpha:\beta$, 1:7), in comparison the use of acceptor (**17**) which has a higher relative steric hindrance, where only the α -anomer was formed^{116, 125}.

Since the initial work on β -mannoside synthesis using insoluble silver-salt promoters there have been a number of novel glycosyl donors developed for the synthesis of this difficult linkage. For example, the use of 1-*S*-benzoxazolyl (SBox) first demonstrated by

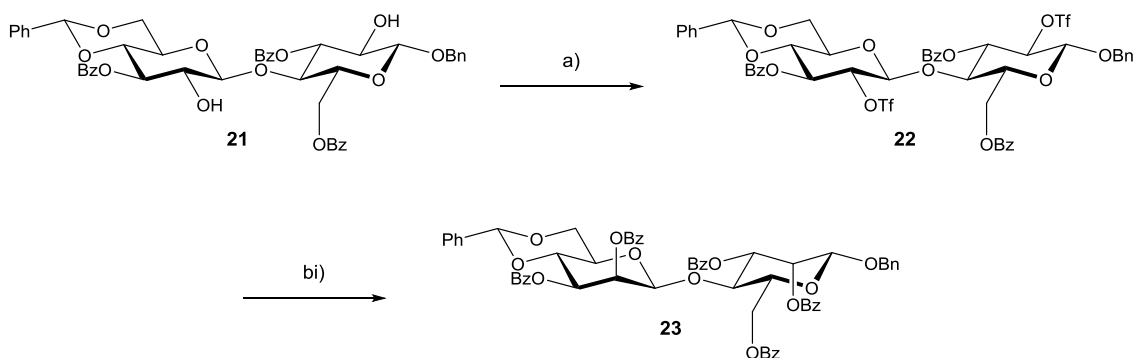
De Meo *et al*¹²⁶ or the use of naphthylthio glycosides as shown by Tatsuta and co-workers¹²⁷. The synthesis of β -linked *manno*-oligosaccharides (β -mannans) was originally attempted using the conventional method of glycosylation-inversion (Scheme 1.4).

There are two main routes¹¹⁶ for the inversion of C-2: (Scheme 1.4 (A)) two-step oxidation-reduction (Fraser-Reid *et al.*¹²⁸) and (B) two-step nucleophilic displacement (Twaddle *et al.*¹²⁹).

(A) Oxidation-reduction method



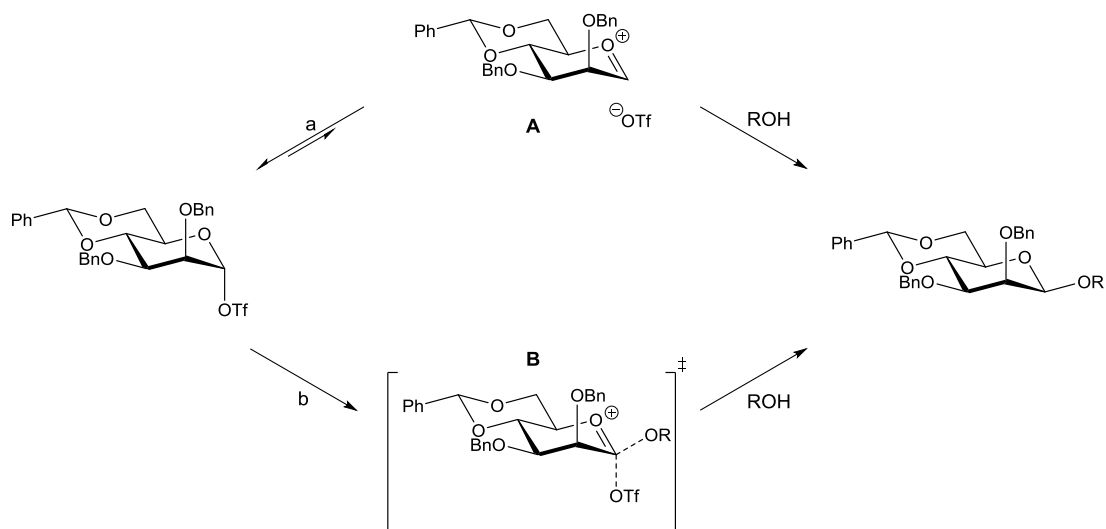
(B) Nucleophilic displacement method



Scheme 1.4: (A) Synthesis of β -1,2-linker mannobiose using the oxidation-reduction inversion methodology as described by Fraser-Reid *et al.* Reagents and conditions: ai) Swern oxidation; aii) L-Selectride;¹²⁸ (B) Synthesis of β -1,4-linked mannobiose using the nucleophilic displacement method as described by Twaddle *et al.*,^{129, 130} Reagents and conditions: a) Tf_2O , pyridine, DCM; b) Bu_4NOBz , toluene.

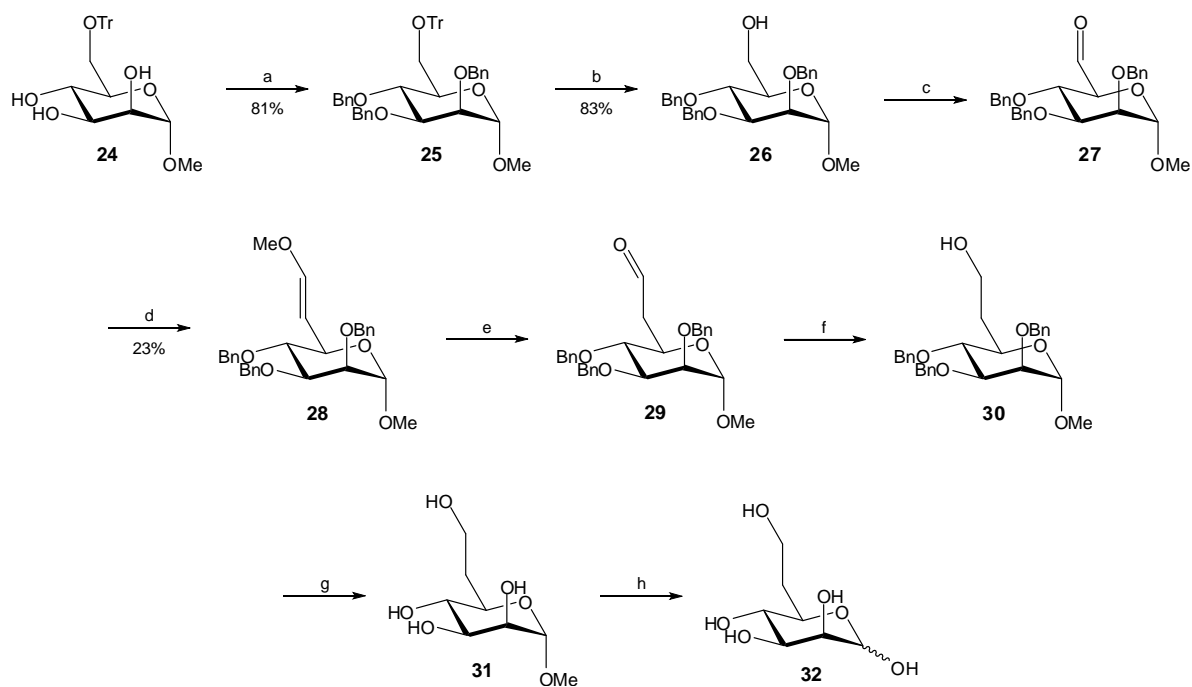
The direct synthesis of β -linked (-1,2-; -1,3- and -1,4-) mannans was demonstrated by Crich and co-workers^{131, 132} using 4,6-*O*-benzylidene and 4,6-*O*-*p*-methoxybenzylidene

acetal protected thioglycoside or sulfoxide donors in moderate yields and high β -stereoselectivity. Glycosyl sulfoxides, first employed by Kahne *et al.*¹³³ are highly reactive glycosyl donors. Crich demonstrated that pre-activation of 6,6-*O*-benzylidene acetal protected mannosyl sulfoxides with triflic anhydride ($\text{ Tf}_2\text{O}$) and 2,6-di-*tert*-butyl-4-methylpyridine (DTBMP) led to the synthesis of β -mannans¹³⁰. Two mechanisms have been suggested for the reaction (Scheme 1.5A) via contact ion-pair (**A**) (kinetic isotope analysis) and (**B**) through the α -triflate (α -triflate species (**B**) was observed by NMR analysis)^{134 116}.



Scheme 1.5: Proposed mechanism for the direct glycosylation of β -mannosides: a) via contact ion pair (A**) as predicted by kinetic isotope analysis and b) via α -triflate as predicted by detection of triflate (**B**) by NMR.**

Despite the complexity of the β -1,2-*cis* linkage, there have been great strides in the development of synthetic methodologies for the synthesis of these glycosides. However, the large-scale synthesis of β -*manno*-oligosaccharides is still a lengthy and challenging process. This section has given a brief insight into the some of the developments in this area over the last 30 years. There are many other routes which have not been discussed here, such as the intramolecular aglycon delivery (IAD) method described by Barresi and Hindsgaul¹³⁵ or the use of 1,2-*O*-stannylene acetals pioneered by Srivastava *et al.*¹³⁶. However, the synthesis of high-order β -*manno*-oligosaccharide still poses a challenging synthetic task for the most experienced of carbohydrate chemists.



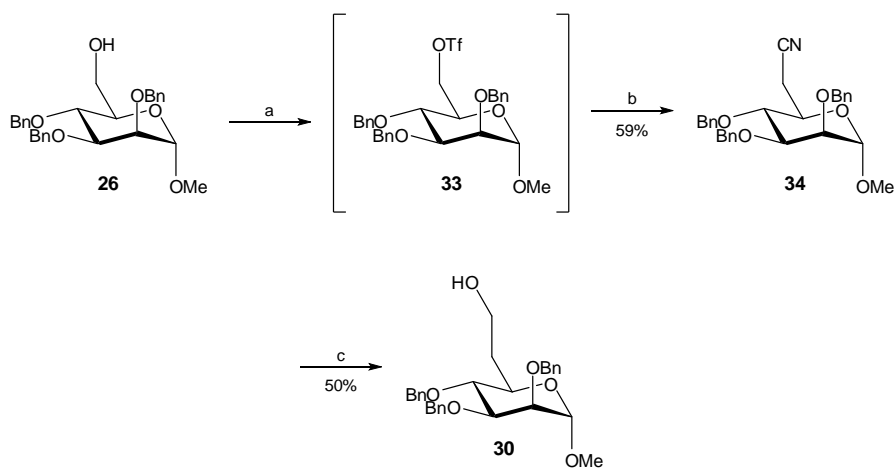
Scheme 1.6 Synthesis of 6-deoxy-D-manno-heptose (32) as reported by Boren *et al*¹³⁷. Reagents and conditions: a) NaH, BnCl, reflux, 6 h; b) 1 M HCl, acetone:H₂O (4:1), rt, 6 h; c) DCC, phosphoric acid, benzene:pyridine:DMSO (6:3:0.5), rt, 5 h; cii) oxalic acid, MeOH, rt, O/N, d) methoxymethyltriphenylphosphonium chloride, BuLi, Et₂O, -10°C – rt, 20 min – 18 h; e) 0.125 M H₂SO₄ aq, acetone, rt, 4 h; f) NaBH₄, H₂O:EtOH (19:1), rt, O/N; g) 5% Pd/C, EtOH, rt, O/N; h) 0.25 M H₂SO₄ aq, 100°C, O/N.

1.3.2 Synthesis of 6-deoxy-D-manno-heptose

Heptoses are important carbohydrates which occur in numerous structural variations in bacteria, such as lipo- or capsular polysaccharides¹³⁸. For example, L-*glycero*-D-*manno*-heptose, which is commonly found in the outer core regions of LPS¹³⁹ and is the building block of the *Yersinia pestis* capsular polysaccharide¹⁴⁰. 6-Deoxy heptoses have been shown to be a rare component of certain bacterial polysaccharides. The first 6-deoxy heptose isolated from bacteria was 6-deoxy-D-*manno*-heptose which was characterised as part of the LPS of *Yersinia pseudotuberculosis* group IIA¹⁴¹. Subsequently, this monosaccharide has been characterised in the polysaccharides of a number of different *Yersinia pseudotuberculosis*¹⁴² strains along with the *Burkholderia*^{96, 97, 143} strains described previously. Other 6-deoxy heptoses which have been characterised from bacterial polysaccharides include 6-deoxy-D-*altro*¹⁴⁴; -D-*talo*¹⁴⁵; -L-*galacto*¹⁴⁶ and L-*gulo*-heptose¹⁴⁷.

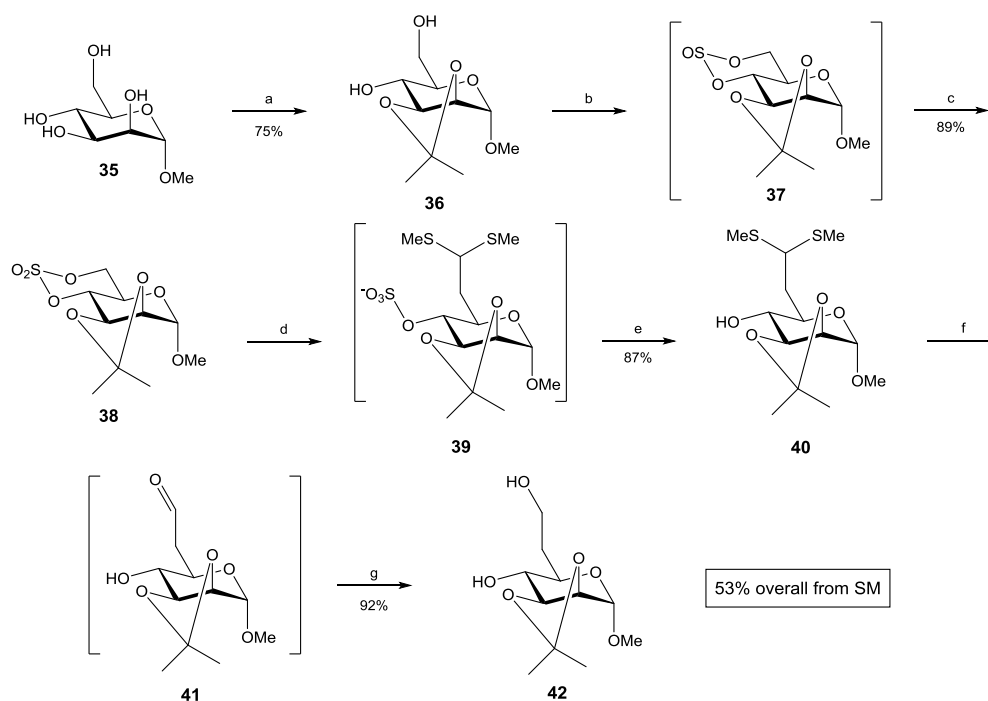
The synthesis of 6-deoxy-D-*manno*-heptose, the core building block of *B. pseudomallei* CPS-1 (**4**) was first reported by Boren *et al.*¹³⁷ from methyl 6-triphenylmethyl- α -D-mannoside (**24**) in 8 steps (Scheme 1.6). Installation of a trityl ether at the 6-position followed by global benzylation of the 2-, 3- and 4-positions and subsequent deprotection of the trityl group under acidic conditions afforded alcohol (**26**). Oxidation of the primary alcohol was carried out to generate aldehyde (**27**), which was converted to vinyl ether (**28**) though the use of methoxymethyltriphenylphosphonium chloride under Wittig conditions. Hydrolysis of vinyl ether (**28**) with mild acid conditions furnished aldehyde (**29**) which was reduced using NaBH₄ to afford methyl 2,3,4-tri-O-benzyl-6-deoxy- α -D-*manno*-heptose (**30**). The yield for the hydrolysis of the vinyl ether and the reduction of the corresponding aldehyde were not given in the original paper, but the low yield of the Wittig reaction (23%) demonstrates the need for development of this synthesis.

Aspinall *et al*¹⁴⁸ reported an improved synthesis for 6-deoxy-D-*manno*-heptose (**32**) again starting from methyl α -D-mannopyranose (Scheme 1.6). Primary alcohol (**26**) was synthesised under similar conditions as previous examples using a triphenylmethyl (trityl) and benzyl protecting groups. Triflate ester (**33**) was synthesised to facilitate the conversion to methyl 2,3,4-tri-O-benzyl- α -D-*manno*-heptopyranosiduronitrile (**34**) by cyanide displacement as described by Baer *et al*¹⁴⁹. A two-stage reduction using DIBAL-H and NaBH₄ was employed to converted nitrile (**34**) to the corresponding alcohol (**30**). The combined yield of 30% for the formation of nitrile (**34**) and subsequent reduction to afford protected 6-deoxy-heptose (**30**) was an improvement on the previous synthesis of 6-deoxy-*manno*-heptose¹³⁷.

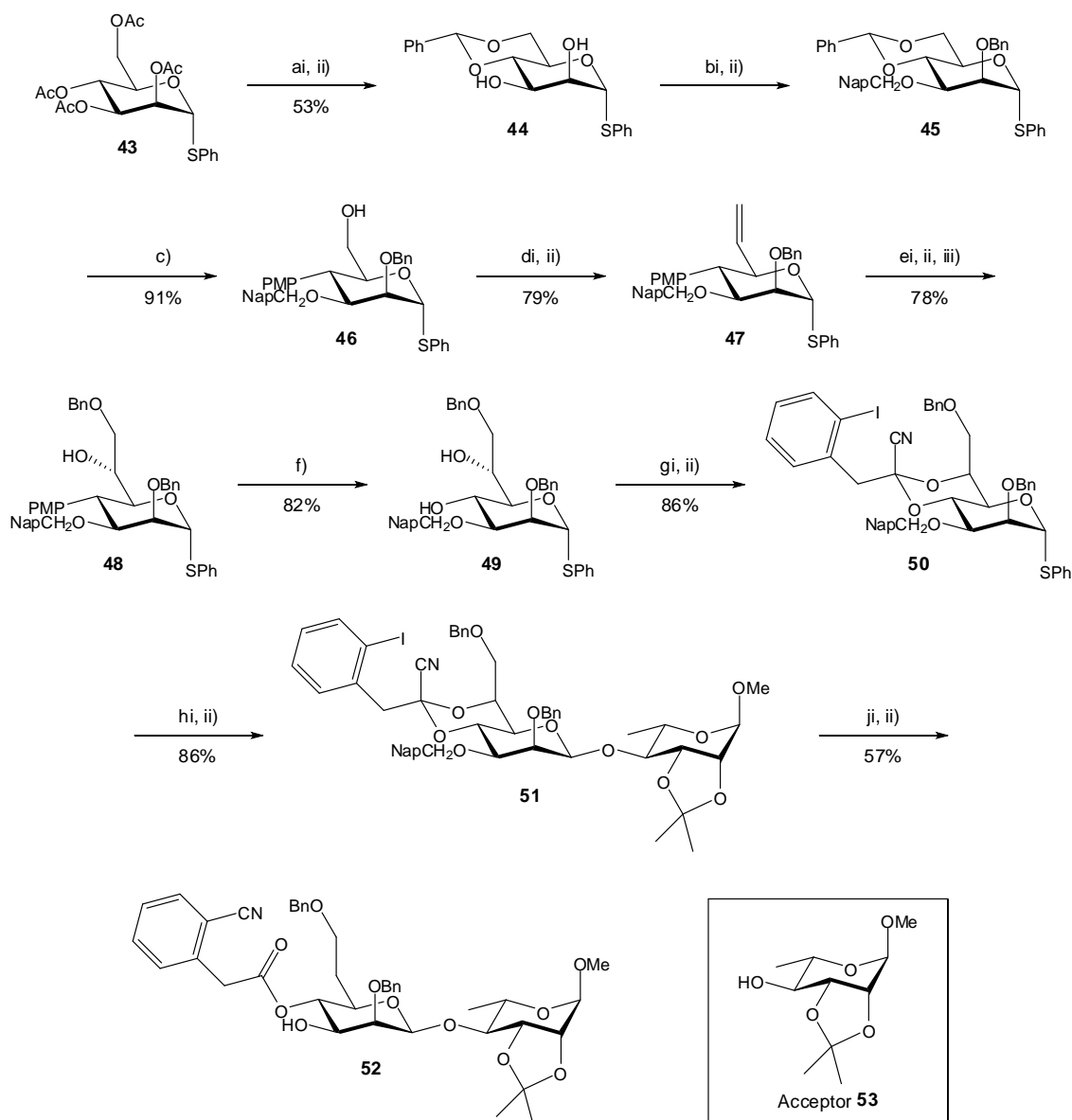


Scheme 1.7: Synthesis of methyl 2,3,4-tri-O-benzyl-6-deoxy- α -D-*manno*-heptose (**30**) as reported by Aspinall *et al*¹⁴⁸. Reagents and conditions: a) triflic anhydride, 2,6-*tert*-butylpyridine, DCM (abs), -10°C, 10 min; b) KCN, MeCN:H₂O (9:1), rt, 2 h; ci) 1 M DIBAL-H, toluene (abs), -20°C, 45 mins, cii) 2 M HCl, rt, 30 min, ciii) NaBH₄, MeOH, rt, 1 h.

van der Klein *et al*¹⁵⁰ demonstrated the use of cyclic sulphate intermediates for the synthesis of methyl α -D-*manno*-heptopyranose (**35**) (Scheme 1.8). Methyl 2,3-O-isopropylidene- α -D-*manno*-pyranose (**36**), was synthesised using graded, acid hydrolysis of 2,3:4,6-di-O-isopropylidene- α -D-*manno*-pyranose to generate the more thermodynamically stable monoacetal (**36**) in good yield¹⁵¹. Cyclic sulphate (**37**) was synthesised by reaction of monoacetal (**36**) with thionyl chloride in ethyl acetate-pyridine to form a cyclic sulphite intermediate, oxidation with sodium periodate in the presence of a ruthenium catalyst generated the corresponding 4,6-cyclic sulphate (**38**) in good yield 89%¹⁵⁰. Treatment of the cyclic 4,6-O-sulphate (**38**) with bis(methylthio)methyl-lithium, prepared by reaction of bis(methylthio)methane with butyl-lithium in THF/HMPA at -40°C , followed by mild acid hydrolysis afforded dithioacetal (**40**) in 87% yield. Protected 6-deoxy-heptose (**42**) was synthesised by reaction of dithioacetal (**40**) with *N*-bromosuccinimide to liberate aldehyde (**41**) which was subsequently reduced by NaBH_4 in overall yield of 53% (based on methyl α -D-mannopyranose **35**) to afford protected 6-deoxy-D-*manno*-heptopyranose (**30**)¹⁵⁰.



Scheme 1.8: Synthesis of 6-deoxy-D-*manno*-heptose (42**) via cyclic sulfate intermediates as described by van der Klein *et al*¹⁵⁰. Reagents and conditions: ai) DMP, *p*-toluenesulfonic acid, acetone, rt, 15 min, aii) 1 M NaHCO_3 aq, rt, 3 h; b) thionyl chloride, EtOAc:pyridine (16:1), rt, until completion TLC [3:97 acetone:DCM]; c) sodium periodate, $\text{RuCl}_3 \cdot \text{H}_2\text{O}$, rt, 1 h; d) bis(methylthio)methane, THF abs/HMPA, BuLi, -40°C , 1 h; e) H_2SO_4 (Conc.): H_2O (3:1), 50°C , 2 h; f) NBS, triethylammonium hydrogencarbonate, MeCN, 0°C , 5 min; g) NaBH_4 , EtOH, rt, 6 h.**



Scheme 1.9: Synthesis of β -1,3-linked disaccharide (57), containing a 6-deoxy-*manno*-heptose residue which has the 3 position selectively deprotected for subsequent glycosylation¹⁵². Reagents and conditions: ai) NH_3 , MeOH, rt, aii) $\text{PhCH}(\text{OMe})_2$, $\text{HBF}_4 \cdot \text{OEt}_2$, 0°C – rt; bi) dibutyltin oxide, 2-napthalene methyl bromide, benzene, reflux, bii) benzyl bromide, sodium hydride, THF, rt; c) DIBAL-H; di) DMSO, $(\text{COCl})_2$, Et_3N , dii) $\text{CH}_3\text{PPh}_3\text{Br}$, BuLi; ei) OsO_4 , NMNO, eii) Bu_2SnO , toluene, eiii) BnBr, CsF, DMF; f) 90% TFA, DCM; gi) 4,6-*O*-[1-cyano-2-(2-iodophenyl)ethylidene acetal]¹⁵², CSA, DCM, gii) TMSCN, $\text{BF}_3 \cdot \text{OEt}_2$, DCM; hi) DPSO, TTBP, Tf_2O , hii) acceptor (53)¹⁵², DCM; ji) Bu_3SnH , AIBN, Xylene, reflux, jj) DDQ

Work done by Crich and Banerjee¹⁵² on the synthesis of a tetrasaccharide subunit of the LPS of *Plesimonas shigelloides* provides a direct route to β -1,3-linked 6-deoxy-D-manno-heptosides. Scheme 1.9 combines both the C-6 extension step required for the synthesis of 6-deoxy-D-manno-heptose (**32**) and also the stereoselective β -1,3-mannose synthesis. The use of diol (**44**) enables the selective protection of the 3-OH with naphthalene ether by with dibutyltin oxide and 2-naphthylmethyl bromide¹⁵³. Selective deprotection of the 6-position with DIBAL-H afforded primary alcohol (**46**) which was converted to the corresponding olefin (**47**) by means of Swern oxidation. Heptose (**48**) was synthesised by treatment of olefin (**47**) OsO₄, before deprotection of the *p*-methoxyphenyl ether and installation of the 4,6-[1-cyano-2-(2-iodophenyl)ethylidene] acetal to afford (**50**). The use of 4,6-[1-cyano-2-(2-iodophenyl)ethylidene] acetal provides the required stereo-control for the synthesis of β -1,4-linked disaccharide (**50**), whilst also facilitating the formation of the 6-deoxy-heptose. The subsequent reductive radical fragmentation of protected heptose (**51**) with Bu₃SnH/AIBN in Xylene furnished the 6-deoxy heptose moiety (**52**)¹⁵⁴. Development of this route poses a viable option for the synthesis of oligosaccharide fragments of the CPS-1 of *B. pseudomallei*. However, optimisation of this route, along with inclusion of synthetic strategy for the installation of the acetyl group on the 2-position would be a lengthy and challenging process.

Prior to the start of this research project, Ancora Pharmaceuticals were contracted to undertake the synthesis of an octasaccharide fragment of the CPS-1 of *B. pseudomallei* (**4**) and, as a result, the synthesis of such compounds was not investigated as part of this thesis. Currently, we have been provided with a sample of the hexasaccharide (**54**) which will be discussed later in this project. The development of the synthetic procedure is still ongoing at Ancora, highlighting the complex synthetic challenge posed by this polysaccharide.

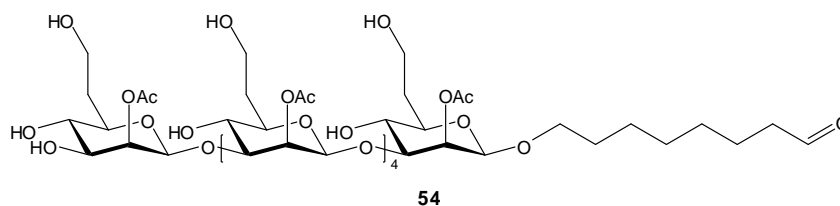


Figure 1.14: Structure of hexasaccharide fragment of CPS-1 produced by Ancora Pharmaceuticals.

1.4 General Aims of the Study

As highlighted earlier in this chapter, there is a need for the development of a successful vaccine for the pathogenic bacteria *B. pseudomallei*. The capsular polysaccharide of *B. pseudomallei* (4) has previously been shown to be a promising target for use in a carbohydrate vaccine (41). Traditionally carbohydrate vaccines have been based on extracted polysaccharide material, or oligosaccharide fragments, conjugated to carrier proteins. The synthesis of oligosaccharide fragments of CPS-1 (4) poses a complex synthetic challenge. As part of our research collaboration, Ancora Pharmaceutical were contracted to investigate the synthesis of an oligosaccharide CPS-1 fragment (54).

Despite the widespread use of oligosaccharide fragments in vaccine development, the application and immunological activity of monosaccharide antigens with respect to vaccine generation has not been systematically investigated. The primary aim of this study was to synthesise and assess the immunological activity of *B. pseudomallei* CPS-1 immunogens, both synthetic monosaccharides and natural polysaccharide isolates (Chapter 2). The use of a non-virulent *Burkholderia* strain for the production of CPS-1 was introduced to combat the health and safety concerns with working on a category three pathogen for the production of the natural polysaccharide (Chapter 3). Conjugation of the immunogens and immunisation trials in sheep were carried out for the production of polyclonal sera, which were subsequently analysed for immunological activity (Chapter 4). The second aim of the study was the development of a novel virus-like particle based carrier protein. The use of *in planta* expression of a chemically conjugatable Hepatitis B VLP was developed and underwent initial conjugation trials (Chapter 5).

1.5 References

1. A. Varki, R. Cummings, J. D. Esko, H. H. Freeze, P. Stabley, C. R. Bertizzi, G. W. Hart and M. E. Etzler, ed. C. Press, 2008, pp. 8-9.
2. Y. C. Lee and R. T. Lee, *Acc. Chem. Res.*, 1995, **28**, 321-327.
3. D. B. Werz, R. Ranzinger, S. Herget, A. Adibekian, C.-W. von der Lieth and P. H. Seeberger, *ACS Chemical Biology*, 2007, **2**, 685-691.
4. U. Aich and K. J. Yarema, in *Carbohydrate-based vaccines and immunotherapies*, John Wiley & Sons, Inc., 2008, DOI: 10.1002/9780470473283.ch1, pp. 1-53.
5. D. J. Miller and R. L. Ax, *Mol. Reprod. Dev*, 1990, **26**, 184-198.
6. E. E. Farmer, T. D. Moloshok, M. J. Saxton and C. A. Ryan, *J. Biol. Chem.*, 1991, **266**, 3140-3145.
7. N. Saha and K. K. Banerjee, *J. Biol. Chem.*, 1997, **272**, 162-167.
8. B. Kuberan and L. R. J., *Curr. Org. Chem.*, 2000, **4**, 653-677.
9. Z. Guo and B. G-J;, *Carbohydrate-based vaccines and immunotherapies*, Wiley, 2009.
10. J. B. Lowe, *Curr. Opin. Cell Biol.*, 2003, **15**, 531-538.
11. J. León, E. Rojo and J. J. Sánchez-Serrano, *J. Exp. Bot.*, 2001, **52**, 1-9.
12. N. Sharon and H. Lis, *Glycobiology*, 2004, **14**, 53R-62R.
13. P. Albersheim and A. J. Anderson-Prouty, *Annual Review of Plant Physiology*, 1975, **26**, 31-52.
14. N. Sharon and H. Lis, *Sci. Am.*, 1993, **268**, 82-89.
15. A. A. Fadl, J. Sha, G. R. Klimpel, J. P. Olano, D. W. Niesel and A. K. Chopra, *Infect. Immun.*, 2005, **73**, 1081-1096.
16. P. Messner and U. B. Sleytr, *Glycobiology*, 1991, **1**, 545-551.
17. K. Sandvig, B. Spilsberg, S. U. Lauvrak, M. L. Torgersen, T.-G. Iversen and B. O. van Deurs, *Int. J. Med. Microbiol.*, 2004, **293**, 483-490.
18. K. Bock, K.-A. Karlsson, N. Strömberg and S. Teneberg, in *The molecular immunology of complex carbohydrates*, eds. A. Wu and L. G. Adams, Springer US, 1988, vol. 228, ch. 7, pp. 153-186.
19. B. P. Cormack, N. Ghori and S. Falkow, *Science*, 1999, **285**, 578-582.
20. J. Ramana and D. Gupta, *PLoS ONE*, 2010, **5**, e9695.
21. W. Thomas, M. Forero, O. Yakovenko, L. Nilsson, P. Vicini, E. Sokurenko and V. Vogel, *Biophys. J.*, 2006, **90**, 753-764.

22. M. Rijavec, M. Müller-Premru, B. Zakotnik and D. Žgur-Bertok, *J. Med. Microbiol.*, 2008, **57**, 1329-1334.
23. R. Reis and F. Horn, *Gut Pathogens*, 2010, **2**, 8.
24. A. Kouki, R. J. Pieters, U. J. Nilsson, V. Loimaranta, J. Finne and S. Haataja, *Biology*, 2013, **2**, 918-935.
25. N. Juge, *Trends Microbiol.*, 2012, **20**, 30-39.
26. K. Julenius, A. Mølgaard, R. Gupta and S. Brunak, *Glycobiology*, 2005, **15**, 153-164.
27. B. A. Cobb and D. L. Kasper, *Eur. J. Immunol.*, 2005, **35**, 352-356.
28. A. Guichard, J. M. Park, B. Cruz-Moreno, M. Karin and E. Bier, *Proceedings of the National Academy of Sciences of the United States of America*, 2006, **103**, 3244-3249.
29. M. Lubran, *Annals of Clinical & Laboratory Science*, 1988, **18**, 58-71.
30. M. R. Wessels, C. E. Rubens, V.-J. Benedi and D. L. Kasper, *Proceedings of the National Academy of Sciences*, 1989, **86**, 8983-8987.
31. H. Levy, S. Weiss, Z. Altboum, J. Schlomovitz, I. Glinert, A. Sittner, A. Shafferman and D. Kobilier, *Infect. Immun.*, 2012, **80**, 2623-2631.
32. A. C. Hahn, C. R. Lyons and M. F. Lipscomb, *Hum. Immunol.*, 2008, **69**, 552-561.
33. L. G. Rahme, F. M. Ausubel, H. Cao, E. Drenkard, B. C. Goumnerov, G. W. Lau, S. Mahajan-Miklos, J. Plotnikova, M.-W. Tan, J. Tsongalis, C. L. Walendziewicz and R. G. Tompkins, *Proceedings of the National Academy of Sciences*, 2000, **97**, 8815-8821.
34. E. T. Rietschel, T. Kirikae, F. U. Schade, U. Mamat, G. Schmidt, H. Loppnow, A. J. Ulmer, U. Zähringer, U. Seydel and F. Di Padova, *The FASEB Journal*, 1994, **8**, 217-225.
35. N. Lapaque, I. Moriyon, E. Moreno and J.-P. Gorvel, *Curr. Opin. Microbiol.*, 2005, **8**, 60-66.
36. I. Lerouge and J. Vanderleyden, *FEMS Microbiol. Rev.*, 2002, **26**, 17-47.
37. A. H. M. Froon, M. A. Dentener, J. W. M. Greve, G. Ramsay and W. A. Buurman, *J. Infect. Dis.*, 1995, **171**, 1250-1257.
38. P. D. Marsh, *Caries Res.*, 2004, **38**, 204-211.
39. H. Koo, J. Xiao, M. I. Klein and J. G. Jeon, *J. Bacteriol.*, 2010, **192**, 3024-3032.
40. I. S. Roberts, *Annu. Rev. Microbiol.*, 1996, **50**, 285-315.
41. S. L. Reckseidler-Zeneto, *Capsular polysaccharides produced by the bacterial pathogen burkholderia pseudomallei*, InTech, 2012.

42. E. Benjamini and S. Leskowitz, *Immunology a short course*, Wiley-Liss, Second edn., 1991.
43. J. Thompson, Chapter 21: Complement system.
44. J. H. L. Playfair, *Immunology at a glance*, Blackwell Scientific Publications, Fourth edn., 1987.
45. B. Alberts, A. Johnson, J. Lewis, M. Raff, K. Roberts and P. Walter, *Molecular biology of the cell*, Garland Science, Fourth edn., 2002.
46. S. L. Reckseidler-Zenteno, R. DeVinney and D. E. Woods, *Infect. Immun.*, 2005, **73**, 1106-1115.
47. R. Adamo, A. Nilo, B. Castagner, O. Boutureira, F. Berti and G. J. L. Bernardes, *Chemical Science*, 2013, **4**, 2995-3008.
48. O. T. Avery and W. F. Goebel, *The Journal of Experimental Medicine*, 1929, **50**, 533-550.
49. K. E. Stein, *J. Infect. Dis.*, 1992, **165**, S49-S52.
50. W. Zou and H. J. Jennings, in *Carbohydrate-based vaccines and immunotherapies*, John Wiley & Sons, Inc., 2008, DOI: 10.1002/9780470473283.ch2, pp. 55-88.
51. A. E. Bridy-Pappas, M. B. Margolis, K. J. Center and D. J. Isaacman, *Pharmacotherapy: The Journal of Human Pharmacology and Drug Therapy*, 2005, **25**, 1193-1212.
52. A. de Roux, B. Schmöele-Thoma, G. R. Siber, J. G. Hackell, A. Kuhnke, N. Ahlers, S. A. Baker, A. Razmpour, E. A. Emini, P. D. Fernsten, W. C. Gruber, S. Lockhart, O. Burkhardt, T. Welte and H. M. Lode, *Clin. Infect. Dis.*, 2008, **46**, 1015-1023.
53. J. Croxtall and G. Keating, *Pediatric Drugs*, 2009, **11**, 349-357.
54. L. Morelli, L. Poletti and L. Lay, *Eur. J. Org. Chem.*, 2011, DOI: 10.1002/ejoc.201100296, 5723-5777.
55. M.-L. Hecht, P. Stallforth, D. V. Silva, A. Adibekian and P. H. Seeberger, *Curr. Opin. Chem. Biol.*, 2009, **13**, 354-359.
56. M. M. Dinges and P. M. Schlievert, *Infect. Immun.*, 2001, **69**, 1256-1264.
57. V. Johannes F.G, *FEBS Lett.*, 2006, **580**, 2945-2950.
58. S. F. Slovin, G. Ragupathi, S. Adluri, G. Ungers, K. Terry, S. Kim, M. Spassova, W. G. Bornmann, M. Fazzari, L. Dantis, K. Olkiewicz, K. O. Lloyd, P. O. Livingston, S. J. Danishefsky and H. I. Scher, *Proceedings of the National Academy of Sciences*, 1999, **96**, 5710-5715.
59. H. Xin, J. Cartmell, J. J. Bailey, S. Dziadek, D. R. Bundle and J. E. Cutler, *PLoS ONE*, 2012, **7**, e35106.

60. T. Buskas, P. Thompson and G.-J. Boons, in *Carbohydrate-based vaccines and immunotherapies*, John Wiley & Sons, Inc., 2008, DOI: 10.1002/9780470473283.ch9, pp. 263-311.
61. R. Lo-Man, S. Vichier-Guerre, R. Perraut, E. Dériaud, V. Huteau, L. BenMohamed, O. M. Diop, P. O. Livingston, S. Bay and C. Leclerc, *Cancer Res.*, 2004, **64**, 4987-4994.
62. M. P. Schutze, C. Leclerc, M. Jolivet, F. Audibert and L. Chedid, *The Journal of Immunology*, 1985, **135**, 2319-2322.
63. D. Safari, M. Marradi, F. Chiodo, H. A. Th Dekker, Y. Shan, R. Adamo, S. Oscarson, G. T. Rijkers, M. Lahmann, J. P. Kamerling, S. Penadés and H. Snippe, *Nanomedicine*, 2012, **7**, 651-662.
64. Y. Ikehara, M. Yamanaka and T. Yamaguchi, *J. Biomed. Biotechnol.*, 2010, **2010**.
65. S. Sarkar, S. A. Lombardo, D. N. Herner, R. S. Talan, K. A. Wall and S. J. Sucheck, *JACS*, 2010, **132**, 17236-17246.
66. R. Roy, *Drug Discovery Today: Technologies*, 2004, **1**, 327-336.
67. D. Safari, G. Rijkers and H. Snippe, *Chapter 24: The complex world of polysaccharides*, 2012, doi: 10.5772/48326
68. N. J. White, *The Lancet*, 2003, **361**, 1715-1722.
69. D. A. B. Dance, *Acta Trop.*, 2000, **74**, 115-119.
70. C. f. D. Control, Epidemicity of melioidosis infection.
71. T. J. J. Inglis, *Pharmaceuticals*, 2010, **3**, 1296-1303.
72. C. f. D. Control, Melioidosis.
73. P. Kanaphun, N. Thirawattanasuk, Y. Suputtamongkol, P. Naigowit, D. A. B. Dance, M. D. Smith and N. J. White, *J. Infect. Dis.*, 1993, **167**, 230-233.
74. A. M. Dannenberg and E. M. Scott, *The Journal of Experimental Medicine*, 1958, **107**, 153-166.
75. M. P. Stevens, A. Haque, T. Atkins, J. Hill, M. W. Wood, A. Easton, M. Nelson, C. Underwood-Fowler, R. W. Titball, G. J. Bancroft and E. E. Galyov, *Microbiology*, 2004, **150**, 2669-2676.
76. S. Liljeqvist and S. Ståhl, *J. Biotechnol.*, 1999, **73**, 1-33.
77. N. Patel, L. Conejero, M. d. Reynal, A. Easton, G. J. Bancroft and R. W. Titball, *Frontiers in Microbiology*, 2011, **2**, 198-Article 198.
78. L.-a. Pirofski and A. Casadevall, *Clin. Microbiol. Rev.*, 1998, **11**, 1-26.
79. J. L. Barnes and N. Ketheesan, *Immunol. Cell Biol.*, 2007, **85**, 551-557.

80. C. E. Razak, G. Ismail, N. Embin and O. Omar, *Malaysian Applied Biology Journal*, 1986, **15**, 105.
81. M. Sarkar-Tyson, S. J. Smither, S. V. Harding, T. P. Atkins and R. W. Titball, *Vaccine*, 2009, **27**, 4447-4451.
82. A. M. Fry, E. R. Zell, A. Schuchat, J. C. Butler and C. G. Whitney, *Vaccine*, 2002, **21**, 303-311.
83. M. Nelson, J. L. Prior, M. S. Lever, H. E. Jones, T. P. Atkins and R. W. Titball, *J. Med. Microbiol.*, 2004, **53**, 1177-1182.
84. H.-F. Chen, M.-H. Chang, B.-L. Chiang and S.-T. Jeng, *Vaccine*, 2006, **24**, 2944-2951.
85. C. Chen, D. Chen, J. Sharma, W. Cheng, Y. Zhong, K. Liu, J. Jensen, R. Shain, B. Arulanandam and G. Zhong, *Infect. Immun.*, 2006, **74**, 4826-4840.
86. P. J. Brett, D. C. Mah and D. E. Woods, *Infect. Immun.*, 1994, **62**, 1914-1919.
87. C. Druar, F. Yu, J. L. Barnes, R. T. Okinaka, N. Chantratita, S. Beg, C. W. Stratilo, A. J. Olive, G. Soltis, M. L. Russell, D. Limmathurotsakul, R. E. Norton, S. X. Ni, W. D. Picking, P. J. Jackson, D. I. H. Stewart, V. Tsvetnitsky, W. L. Picking, J. W. Cherwonogrodzky, N. Ketheesan, S. J. Peacock and E. J. Wiersma, *FEMS Immunology & Medical Microbiology*, 2008, **52**, 78-87.
88. Y.-C. Su, K.-L. Wan, R. Mohamed and S. Nathan, *Vaccine*, 2010, **28**, 5005-5011.
89. W. Nieves, J. Heang, S. Asakrah, K. Höner zu Bentrup, C. J. Roy and L. A. Morici, *PLoS ONE*, 2010, **5**, e14361.
90. Y. Hara, R. Mohamed and S. Nathan, *PLoS ONE*, 2009, **4**, e6496.
91. D. N. Harland, K. Chu, A. Haque, M. Nelson, N. J. Walker, M. Sarkar-Tyson, T. P. Atkins, B. Moore, K. A. Brown, G. Bancroft, R. W. Titball and H. S. Atkins, *Infect. Immun.*, 2007, **75**, 4173-4180.
92. D. DeShazer, P. J. Brett and D. E. Woods, *Mol. Microbiol.*, 1998, **30**, 1081-1100.
93. W. J. Wiersinga, T. van der Poll, N. J. White, N. P. Day and S. J. Peacock, *Nature Reviews Microbiology*, 2006, **4**, 272-282.
94. S. Pilatz, K. Breitbach, N. Hein, B. Fehlhaber, J. Schulze, B. Brenneke, L. Eberl and I. Steinmetz, *Infect. Immun.*, 2006, **74**, 3576-3586.
95. T. D'Cruze, L. Gong, P. Treerat, G. Ramm, J. D. Boyce, M. Prescott, B. Adler and R. J. Devenish, *Infect. Immun.*, 2011, **79**, 3659-3664.
96. M. B. Perry, L. L. MacLean, T. Schollaardt, L. E. Bryan and M. Ho, *Infect. Immun.*, 1995, **63**, 3348-3352.

97. C. Heiss, M. N. Burtnick, Z. Wang, P. Azadi and P. J. Brett, *Carbohydr. Res.*, 2012, **349**, 90-94.
98. M. Nimtz, V. Wray, T. Domke, B. Brenneke, S. Häussler and I. Steinmetz, *Eur. J. Biochem.*, 1997, **250**, 608-616.
99. K. Kawahara, S. Dejsirilert and T. Ezaki, *FEMS Microbiol. Lett.*, 1998, **169**, 283-287.
100. J. Cuccui, T. S. Milne, N. Harmer, A. J. George, S. V. Harding, R. E. Dean, A. E. Scott, M. Sarkar-Tyson, B. W. Wren, R. W. Titball and J. L. Prior, *Infect. Immun.*, 2012, DOI: 10.1128/iai.05805-11.
101. S. L. Reckseidler, D. DeShazer, P. A. Sokol and D. E. Woods, *Infect. Immun.*, 2001, **69**, 34-44.
102. H. Masoud, M. Ho, T. Schollaardt and M. B. Perry, *J. Bacteriol.*, 1997, **179**, 5663-5669.
103. D. E. Woods, *Molecular mechanisms of virulence of burkholderia pseudomallei and burkholderia mallei*, Horizon Bioscience, 2007.
104. C. Whitfield, *Annu. Rev. Biochem.*, 2006, **75**, 39-68.
105. A. E. Scott, S. M. Twine, K. M. Fulton, R. W. Titball, A. E. Essex-Lopresti, T. P. Atkins and J. L. Prior, *J. Bacteriol.*, 2011, **193**, 3577-3587.
106. T. L. Bluhm and A. Sarko, *Canadian Journal of Chemistry-Revue Canadienne De Chimie*, 1977, **55**, 293-299.
107. R. H. Marchessault, Y. Deslandes, K. Ogawa and P. R. Sundararajan, *Canadian Journal of Chemistry-Revue Canadienne De Chimie*, 1977, **55**, 300-303.
108. T. Yanaki, T. Norisuye and H. Fujita, *Macromolecules*, 1980, **13**, 1462-1466.
109. B. Mulloy, *An. Acad. Bras. Cienc.*, 2005, **77**, 651-664.
110. V. Pozsgay, B. Ernst, G. W. Hart and P. Sinaý, in *Carbohydrates in chemistry and biology*, Wiley-VCH Verlag GmbH, 2008, DOI: 10.1002/9783527618255.ch13, pp. 319-343.
111. L. Galbraith and S. G. Wilkinson, *Carbohydr. Res.*, 1997, **303**, 245-249.
112. P. L. Hackland, H. Parolis and L. A. S. Parolis, *Carbohydr. Res.*, 1988, **172**, 209-216.
113. Y.-M. Choy, G. G. S. Dutton and A. M. Zanlungo, *Can. J. Chem.*, 1973, **51**, 1819-1825.
114. J. Masuoka and K. C. Hazen, *Infect. Immun.*, 2004, **72**, 6230-6236.
115. H. Paulsen, *Angewandte Chemie International Edition in English*, 1982, **21**, 155-173.

116. A. Ishiwata and I. Yukishige, *Glycoscience: Stereoselective synthesis of beta-manno-glycosides*, Springer, 2008.
117. C. A. A. Van Boeckel, T. Beetz and S. F. Van Aelst, *Tetrahedron*, 1984, **40**, 4097-4107.
118. H. Paulsen and R. Lebuhn, *Liebigs Ann. Chem.*, 1983, **1983**, 1047-1072.
119. P. A. J. Gorin and A. S. Perlin, *Can. J. Chem.*, 1961, **39**, 2474-2485.
120. H. Paulsen and O. Lockhoff, *Chem. Ber.*, 1981, **114**, 3102-3114.
121. P. J. Garegg and P. Ossowski, *Acta Chem. Scand.*, 1983, **37**, 251.
122. C. A. A. van Boeckel, T. Beetz, A. C. Kock-van Dalen and H. van Bekkum, *Recl. Trav. Chim. Pays-Bas*, 1987, **106**, 596-598.
123. J. Guo and X.-S. Ye, *Molecules*, 2010, **15**, 7235-7265.
124. D. R. Mootoo, P. Konradsson, U. Udodong and B. Fraser-Reid, *JACS*, 1988, **110**, 5583-5584.
125. H. Paulsen, M. Heume, Z. Györgydeak and R. Lebuhn, *Carbohydr. Res.*, 1985, **144**, 57-70.
126. C. De Meo, M. N. Kamat and A. V. Demchenko, *Eur. J. Org. Chem.*, 2005, **2005**, 706-711.
127. K. Tatsuta and S. Yasuda, *Tetrahedron Lett.*, 1996, **37**, 2453-2456.
128. F. Mathew, M. Mach, K. C. Hazen and B. Fraser-Reid, *Synlett*, 2003, **2003**, 1319-1322.
129. G. W. J. Twaddle, D. V. Yashinsky and A. V. Nikolaev, *Organic & Biomolecular Chemistry*, 2003, **1**, 623-628.
130. D. Crich and S. Sun, *The Journal of Organic Chemistry*, 1997, **62**, 1198-1199.
131. D. Crich, A. Banerjee and Q. Yao, *JACS*, 2004, **126**, 14930-14934.
132. D. Crich, W. Li and H. Li, *JACS*, 2004, **126**, 15081-15086.
133. D. Kahne, S. Walker, Y. Cheng and D. Van Engen, *JACS*, 1989, **111**, 6881-6882.
134. D. Crich and N. S. Chandrasekera, *Angew. Chem. Int. Ed.*, 2004, **43**, 5386-5389.
135. F. Barresi and O. Hindsgaul, *JACS*, 1991, **113**, 9376-9377.
136. V. K. Srivastava and C. Schuerch, *Tetrahedron Lett.*, 1979, **20**, 3269-3272.
137. K. E. Hans. Boren, Per J. Garegg, Bengt Lindberg and Ake Pilotti, *Acta Chemica Scandinavia*, 1972, **26**, 4143-4146.

138. P. Kosma, *Curr. Org. Chem.*, 2008, **12**, 1021-1039.
139. S. G. Wilkinson, *Prog. Lipid Res.*, 1996, **35**, 283-343.
140. T. Ohara, A. Adibekian, D. Esposito, P. Stallforth and P. H. Seeberger, *Chem. Commun.*, 2010, **46**, 4106-4108.
141. K. Samuelsson, B. Lindberg and R. R. Brubaker, *J. Bacteriol.*, 1974, **117**, 1010-1016.
142. A. S. Shashkov*, Z. Pakulski*, B. Grzeszczyk and A. Zamojski, *Carbohydr. Res.*, 2001, **330**, 289-294.
143. D. P. AuCoin, D. E. Reed, N. L. Marlenee, R. A. Bowen, P. Thorkildson, B. M. Judy, A. G. Torres and T. R. Kozel, *PLoS ONE*, 2012, **7**, e35386.
144. J. Hoffman, B. Lindberg, J. Lönnngren and T. Hofstad, *Carbohydr. Res.*, 1976, **47**, 261-267.
145. G. O. Aspinall, A. G. McDonald, H. Pang, L. A. Kurjanczyk and J. L. Penner, *J. Biol. Chem.*, 1993, **268**, 18321-18329.
146. G. O. Aspinall, M. A. Monteiro, H. Pang, L. A. Kurjanczyk and J. L. Penner, *Carbohydr. Res.*, 1995, **279**, 227-244.
147. G. O. Aspinall, M. A. Monteiro and H. Pang, *Carbohydr. Res.*, 1995, **279**, 245-264.
148. G. O. Aspinall, A. G. McDonald and R. K. Sood, *Can. J. Chem.*, 1994, **72**, 247-251.
149. H. H. Baer, R. L. Breton and Y. Shen, *Carbohydr. Res.*, 1990, **200**, 377-389.
150. P. A. M. van der Klein and J. H. van Boom, *Carbohydr. Res.*, 1992, **224**, 193-200.
151. M. E. Evans and F. W. Parrish, *Carbohydr. Res.*, 1977, **54**, 105-114.
152. D. Crich and A. Banerjee, *JACS*, 2006, **128**, 8078-8086.
153. J. A. Wright, J. Yu and J. B. Spencer, *Tetrahedron Lett.*, 2001, **42**, 4033-4036.
154. D. Crich and A. A. Bowers, *The Journal of Organic Chemistry*, 2006, **71**, 3452-3463.

2 Chapter 2: Synthesis of monosaccharide antigens

2.1 Introduction

2.1.1 The monosaccharide antigens

The capsular polysaccharide (CPS-1) of *B. pseudomallei* (**4**) is a homopolymer of 1,3-linked 2-*O*-acetyl-6-deoxy- β -D-*manno*-heptopyranose residues, which as discussed in the previous chapter has been chosen as the target for this study¹. The chemical synthesis of this polymer provides an interesting synthetic challenge owing to the 1,2-*cis manno*-pyranose configuration, which is known to be one of the most taxing linkage in carbohydrate synthesis². The chemical synthesis is further complicated by the presence of the 2-*O*-acetyl group and the 6-deoxy-*manno*-heptopyranose structure of the monosaccharide unit, requiring the need for its multistep synthesis including the C-6 extension of D-mannose. A review of the synthetic strategies for the chemical synthesis of the β -1,3-mannans and 6-deoxy-*manno*-heptopyranose can be found in section **1.3**. Owing to the complex nature of the CPS-1 (**4**), the initial purposes of this study were to chemically synthesise a simplified monosaccharide component which can be derived from the CPS-1 of *B. pseudomallei* (**4**).

Much research has gone into the use of synthetic oligosaccharide fragments for the generation of immunological activity towards parent polysaccharides for the purpose of vaccine generation,^{3,4,5} however, the use of monosaccharides has not been systematically investigated. Sela *et al.*⁶ demonstrated that both normal and immune sera in animals contain carbohydrate active antibodies. Fractionation of the sera using a fetuin glycoprotein functionalised column, the authors partially purified Ig fractions which were shown to be specific for four monosaccharides present in fetuin, D-mannopyranose, sialic acid, D-galactopyranose and N-acetyl-D-glucosamine. Further to this, it has been shown that single monosaccharide modifications to polysaccharides can lead to selectivity towards the monosaccharide addition. For instance, Bromuro and co-workers showed that immunisation with synthetic β -glucan oligosaccharide (**55**) (Figure **2.1**) containing β -1,6 branches induced immunological activity to both β -1,3 glucan and the β -1,6 stub, where immunisation with synthetic β -glucan (**56**) only

resulted in activity towards β -1,3 glucans⁷. This suggests that the presentation of monosaccharides to the immune system may offer a route to the generation of a specific antibody response.

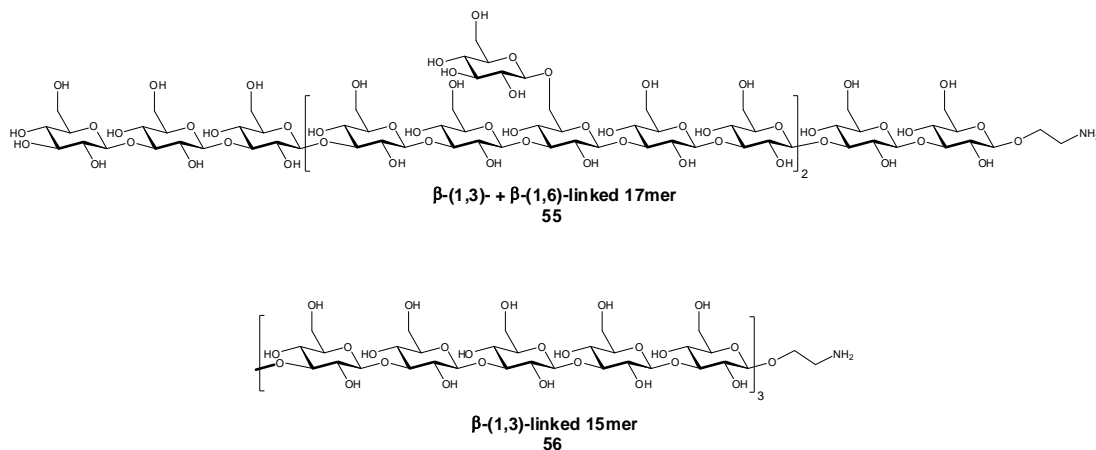


Figure 2.1: Structures of synthetic β -glucan oligosaccharides (53 and 54). Oligosaccharides were conjugated to diphtheria toxoid and immunological studies were carried out in mice⁷.

2.1.1.1 Carrier Proteins

The conjugation of carbohydrates to carrier proteins is essential for the development of a strong immune response and subsequent antibody generation (Section 1.3.3). There are a number of carrier proteins that have been used for the conjugation of carbohydrate antigens, such as KLH, which is routinely used for glycoconjugate research⁸. KLH is a large, heterogeneous glycoprotein with a molecular weight of 350-390 kDa and is highly immunogenic. It cannot be produced biochemically and is only obtained by purification from *Megathura crenulata*, the Keyhole Limpet⁹. Despite its inherent immunogenicity, and widespread use as the carrier protein of choice, KLH has a number of drawbacks. It forms large aggregates (4.5-13 MDa) and as a result is poorly soluble in water making it difficult to work with¹⁰. Aggregation of the sub-units poses another problem with the quantification of conjugation, as it cannot be analysed by MS or gel electrophoresis. The native glycosylation patterns of KLH also pose a significant problem for its use in this project. The presence of any additional carbohydrate moieties on the protein surface may interfere with the immunological recognition and activity of the monosaccharide haptens¹¹.

Alternatives to KLH, which have been used for conjugation of small molecule haptens are Bovine Serum Albumin (BSA)¹², Diphtheria Toxoid (DT)¹³ DT_{CRM197} (glutamic acid mutant)⁷ and Tetanus Toxin Heavy Chain Fragment (TetHc)¹⁴. Tetanus toxin is a potent neurotoxin which is produced by *Clostridium tetani* and consists of two polypeptides; the heavy chain (100,000 Da) and the light chain (50,000 Da). Mild enzymatic cleavage (papain) of tetanus toxin generates two major polypeptides, the larger of which is denoted as the TetHc fragment (50,000 Da). The TetHc fragment retains both the binding activity and internalization properties that are associated with the intact toxin resulting in high immunogenicity, but is non-toxic¹⁵. TetHc was an attractive option for this work as it can be readily expressed at high levels from *E. coli*¹⁴, has a high proportion of lysine residues for conjugation (33) and can be analysed by MALDI-ToF MS and SDS-PAGE¹⁶. These attributes make TetHc a very effective carrier protein and a good substitute for KLH.

A second set of glycoconjugates were made using BSA as the carrier protein. These conjugates were used in the immunological assessment of the monosaccharide antigen-derived antibodies. An alternative carrier protein is used for the immunological assessments to remove background activity of antibodies raised against the carrier protein (TetHc). BSA was selected for this role owing to its mainstream use as a carrier protein in immuno-assays and as a blocking agent¹⁷. Molecular models of both TetHc and BSA carrier proteins are shown in Figure 2.2, with the lysine residues, which were targeted for conjugation, highlighted in yellow.

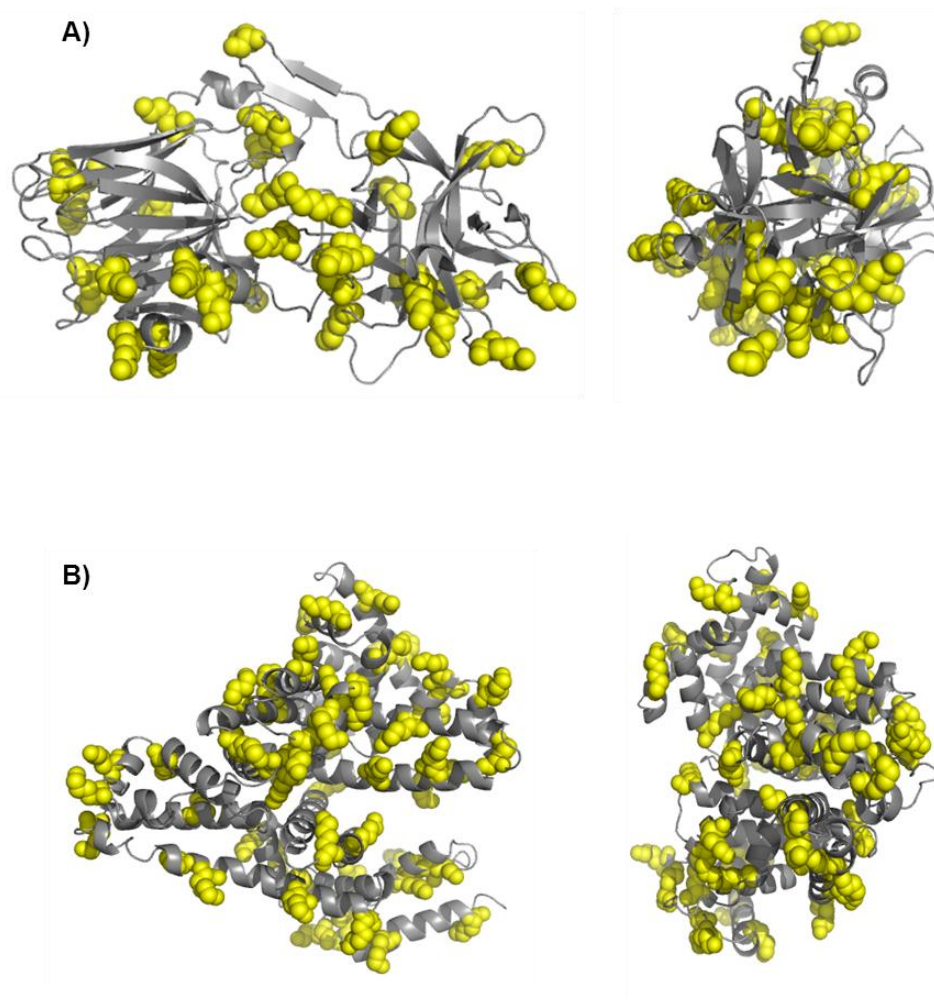


Figure 2.2: Models of A) TetHc fragment (right image rotated 90°) and B) BSA (right image rotated 90°). The lysine residues, which were targeted for conjugation are highlighted in yellow TetHc (33 residues) BSA (60 residues). Images were produced using PyMol with the help of E. O'Neill.

To investigate the potential of monosaccharide antigens, D-glucopyranose (**69**) and D-mannopyranose (**64**) haptens were synthesised and conjugated to protein. Immunisation in sheep, with the D-glucopyranose TetHc protein conjugate (**96**) was carried out to determine whether monosaccharide specific antibodies could be created. A D-manno-pyranose BSA conjugate (**93**) was also made in order to test the specificity of the D-glucopyranose derived antibodies. A CPS-1 monosaccharide, 6-deoxy-D-manno-heptose TetHc (**94**) protein conjugate was prepared to investigate the activity of monosaccharide derived antibodies against the intact capsular polysaccharide of *B. pseudomallei*. During this initial study into the potential of the monosaccharide antigen for CPS-1 (**4**), synthetic efforts for the 6-deoxy-D-manno-heptose hapten (**91**) were

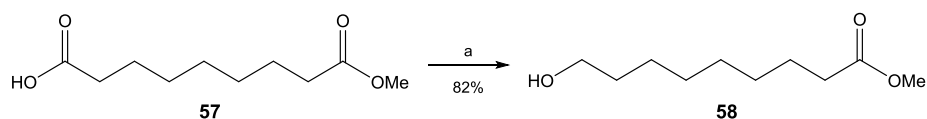
focused on the development of the α -configured compound. This was done to expedite the synthesis, avoiding the need for formation of the taxing β -1,2-*cis* linkage. As discussed in Section 1.2.2.1, based on molecular models, it was proposed that the C-4 to C-7 region of the monosaccharide building blocks would be the primary binding epitope for antibodies. By focusing on the most basic structural component of CPS-1 (4), the 6-deoxy-D-*manno*-heptopyranose monosaccharide (32), it was anticipated that switching from the β -configuration in the natural polysaccharide (4) to the α -configured monosaccharide hapten (91) would have minimal impact on antibody activity. Section 1.3.1 highlights some synthetic strategies which could be employed to synthesise the β -compound. The synthesis of 6-deoxy-D-*manno*-heptose (32) was made in accordance with literature precedence^{18, 19} (Section 1.3.2). Development of the synthetic protocol to facilitate multi-gram synthesis of the CPS-1 monosaccharide was also attempted.

2.2 Results and Discussion

2.2.1 Synthesis of 8-methoxycarbonyl octanol (58)

As described in Section 1.1.2, it is essential for carbohydrates to be conjugated to a carrier protein before they can be used as immunogens. There are a number of proteins which are used in carbohydrate based vaccines (Section 2.1.2). The conjugation chemistry of carrier proteins and carbohydrate antigens generally relies on the modification of carboxyl, hydroxyl, phenoxyl, hemiacetal, mercapto/disulphide and amino/imino functional groups²⁰. Different coupling strategies are employed depending on the nature of the antigen including direct activation and coupling of polysaccharides (reductive amination, cyanogen bromide activation) and the use of linker molecules for the conjugation of smaller antigens²¹⁻²⁴. In order to preserve the cyclic structure of monosaccharides, they were used in a form of glycosides attached to a linker with a reactive carboxyl group for conjugation to the carrier protein. Whilst there is a variety of different linkers which could be employed, we decided upon the use of an aliphatic chain linker. Building on the work done by Lemieux *et al.*²³ and Inman *et al.*²⁴ we used 8-methoxycarbonyl octanol (58) as the linker. This molecule was chosen as a result of its previous use in classical 1970's studies with di- and tri-saccharide haptens, the lack of any immuno-dominant functional groups, such as aromatics, the ease of synthesis and activation for conjugation^{23 25}.

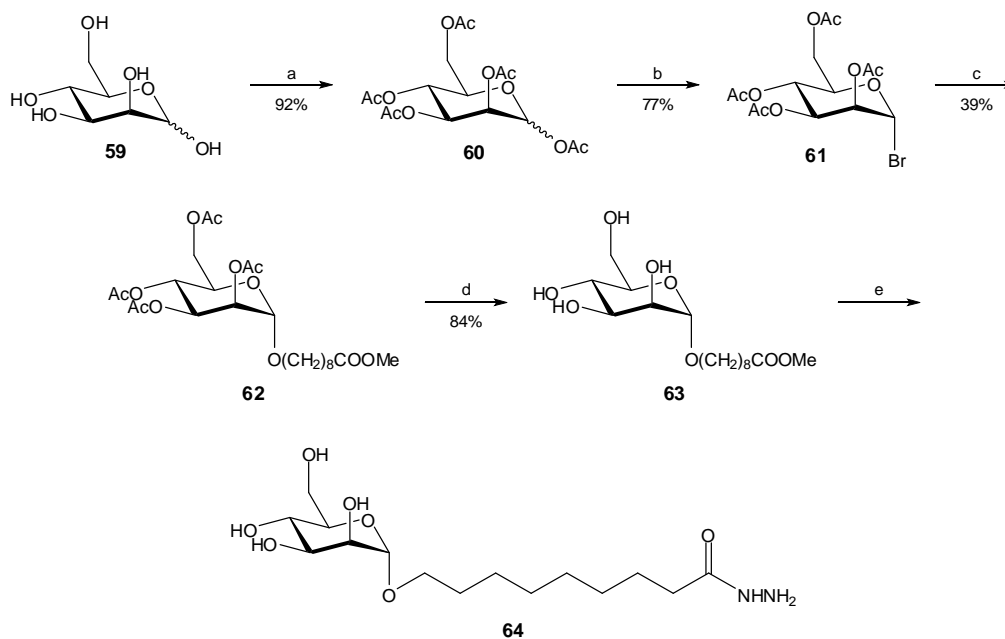
Prior to conjugation, the methyl ester (**58**) is readily converted to the corresponding acyl hydrazide using hydrazine monohydrate. Further activation of the hydrazide is required to facilitate the conjugation to lysine residues, which will be discussed later on in this chapter. Methyl ester (**58**) is available at scale through the borane-THF reduction of inexpensive mono-methyl azelate (**57**) in good yield, 82%, and was produced on a 16 gram scale (Scheme 2.1).



Scheme 2.1: Borane-THF reduction of mono-methyl azelate (57). Reagents and conditions: a) BH₃-THF, THF, -18°C – rt., 4.5 h

2.2.2 Synthesis of 8-(Hydrazinocarbonyl)octyl α -D-mannopyranoside (**64**)

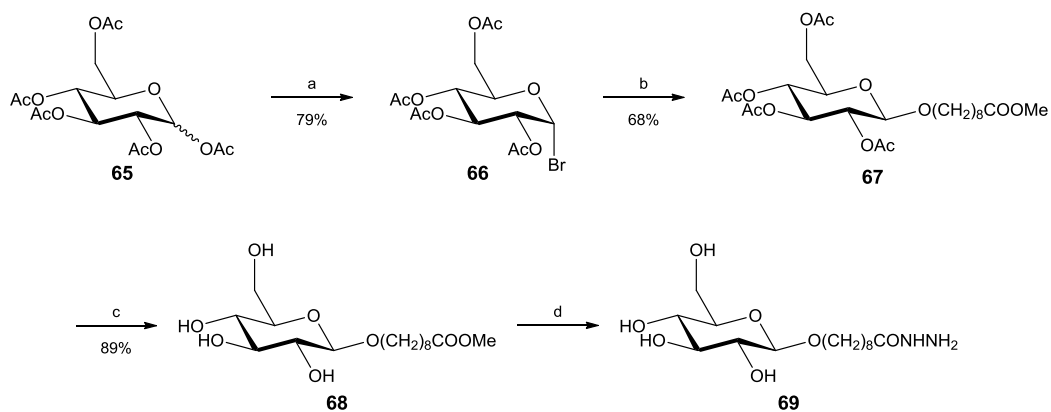
D-Mannose (**59**) was per-*O*-acetylated using the I₂/Ac₂O method as described by Kartha and Field²⁶. The anomeric acetate was converted to the bromide (**61**) by treatment with 33% HBr/AcOH, in preparation for glycosylation with the linker compound. Bromide (**61**) was glycosylated to linker (**58**) under Helferich conditions²⁷, the yield of the glycosylation was unusually poor (39%) with the major side-product being the acetylated linker molecule²³, indicating a high level of acetate migration during the reaction. However, owing to the fact that only small amounts of the D-mannose hapten (**64**) were required for the subsequent conjugation this was not investigated further. It should be noted that this is the reason why benzoyl protecting groups were used in the synthesis of the mannoheptose hapten (Scheme 2.6). Deacetylation was achieved using standard Zemplén conditions to afford the deprotected glycoside (**63**). This prospective hapten was subsequently activated for conjugation through the formation of the acyl hydrazide (**64**) using an excess of hydrazine monohydrate. This reaction was monitored through the loss of the OMe signal in the ¹H NMR spectrum and was shown to be quantitative after 4 h at 55 °C (Scheme 2.2).



Scheme 2.2: Synthesis of hydrazide (64). Reagents and conditions: a) I_2/Ac_2O , rt, 10 min; b) 33% w/v HBr/AcOH, DCE, $0^\circ C$ - rt, 3 h; c) $Hg(CN)_2$, $Hg(Br)_2$, 8-MCO, MS 4Å, DCE, rt, ON; d) NaOMe, MeOH, rt, 30 min; e) $NH_2NH_2 \cdot H_2O$, EtOH, $55^\circ C$, 4 h

2.2.3 Synthesis of 8-(hydrazinocarbonyl)octyl β -D-glucopyranoside (69)

The D-glucose hapten (69) was synthesised in the same fashion as the D-mannose hapten (64) above in good overall yield, (Scheme 2.3).



Scheme 2.3: Synthesis of hydrazide (69). Reagents and conditions: a) 33% w/v HBr/AcOH, DCM, $0^\circ C$ - rt, 3 h; b) $Hg(CN)_2$, $Hg(Br)_2$, 8-MCO, MS 4Å, DCE, rt, ON; c) NaOMe, MeOH, rt, 30 min; d) $NH_2NH_2 \cdot H_2O$, EtOH, $55^\circ C$, 4 h

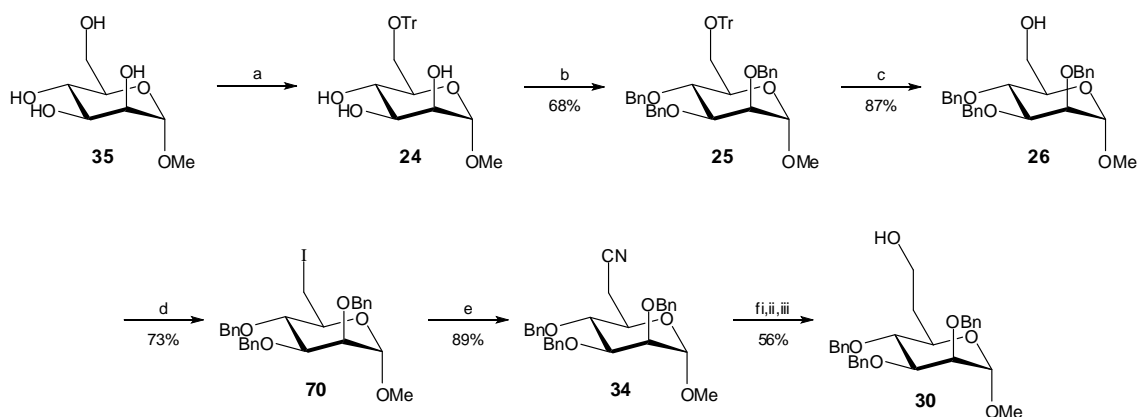
2.2.4 Synthesis of methyl 2,3,4-tri-*O*-benzyl 6-deoxy- α -D-*manno*-heptopyranoside (**30**)

Methyl 2,3,4-tri-*O*-benzyl- α -D-*manno*-pyranoside (**26**) was synthesised according to the procedure highlighted by Boren *et al.*¹⁸ (Scheme **2.4**). It was decided to adopt benzyl protecting groups for compatibility with the later DIBAL-H reduction step that is used for the C-6 extension. The 6-position of methyl mannoside was first selectively protected using triphenylmethylchloride in DMF with catalytic DMAP in good yield²⁸. Partial purification was performed in order to remove unreacted starting material. Thereafter, the 2-, 3- and 4-hydroxyl groups of trityl ether (**24**) were benzylated under Williamson conditions²⁹, with initial deprotonation with NaH in DMF, followed by the dropwise addition of BnBr to furnish (**25**). Attempts were made to carry out these two steps as a one-pot synthesis, but this was unsuccessful, due to complications with purification as a result of multiple impurities. The trityl protecting group was removed using standard acid hydrolysis with 90% TFA in DCM³⁰. It is worth noting that trityl alcohol can be triturated out of the reaction mixture using cold hexane before chromatography, in order to simplify the purification procedure.

Of the different routes for the C-6 extension step in the synthesis of 6-deoxy heptoses described previously, (Section **1.3.2**) the work done by Aspinall *et al.*¹⁹ was the most suitable for the expedient synthesis of 6-deoxy-*manno*-heptose (**32**). The reasonable yields and the use of relatively mild and cheap reagents made it an attractive option for potential development and scale-up. During their work (Scheme **1.7**), Aspinall and co-workers¹⁹ used a nucleophilic substitution of triflate (**33**) with cyanide for installation of the nitrile functionality. However, the associated yield of 50% for the two step reaction was lower than expected and it was felt that this could be improved upon through the use of iodine. The synthesis of methyl 6-deoxy-6-iodo- α -D-*manno*-pyranoside (**70**) was known³¹ to be simple and efficient and there are many literature precedents of the displacement of the iodide with cyanide which is easily achieved under Finkelstein conditions, following a simple S_N2 reaction mechanism³²⁻³⁴. The drawback of both iodide preparation and subsequent displacement procedure is that they required relatively long reaction times. Over the last decade, the use of microwave reactors for accelerated reactions has become more common-place. There has been a recent interest in the use of microwave conditions for carbohydrate synthesis, where it has

been shown to be an effective and expedient tool^{35, 36}. On this basis the use of microwave irradiation was trialled for the synthesis of the iodide (**70**) and nitrile (**34**).

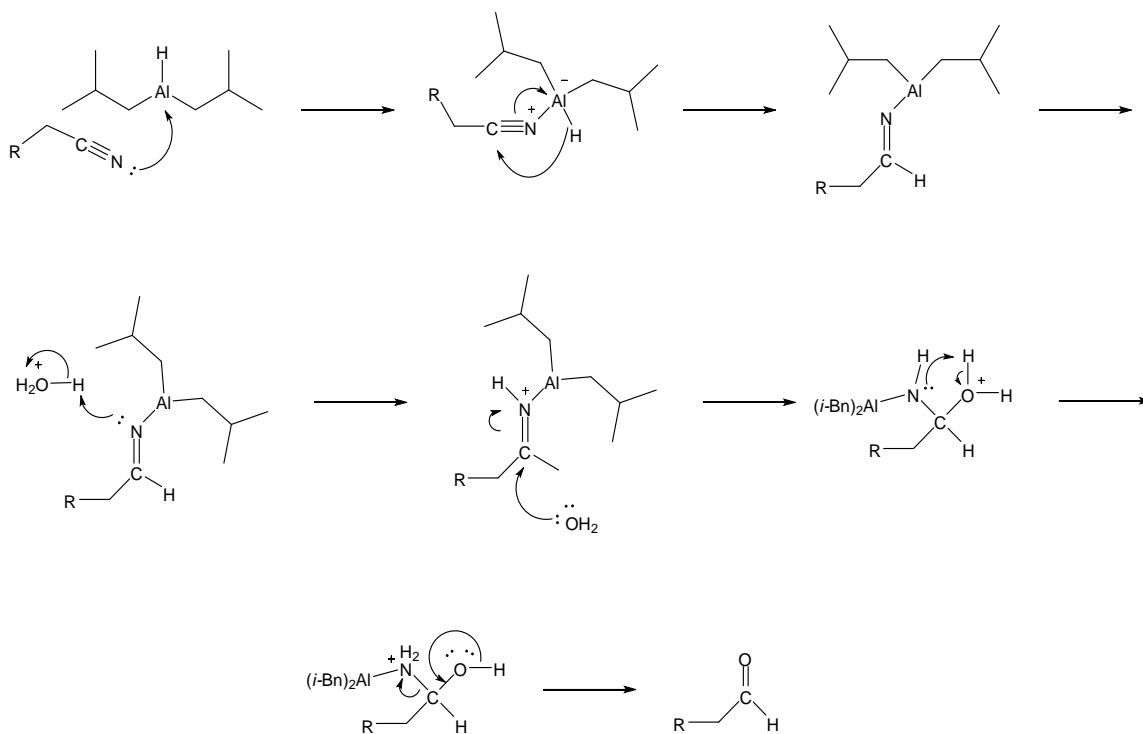
Iodide (**70**) was formed upon reflux of primary alcohol (**26**) with iodine, triphenylphosphine and imidazole in anhydrous toluene^{37, 38}. Initially this reaction was carried out under traditional reflux, but was also trialled under microwave conditions. The reaction time was cut down from 3 hours to 5 minutes, with an improvement in the yield, increasing from 73% to 81%. The nitrile functionality was introduced under Finkelstein conditions, by reaction of iodide (**70**) with excess sodium cyanide in DMF, in a microwave reactor. Due to accelerating effects of the microwave, the reaction was run without the use of a phase-transfer catalyst, which is usually required for this reaction³⁴. The reaction was initially optimised on a small scale to show completion in 3 h at 70°C.



Scheme 2.4: Synthesis of deoxy-D-manno-heptose (30). Reagents and conditions: a) Ph_3CCl , DMAP, DMF, 40°C, 16 h; b) BnBr , NaH, DMF, rt, 4 h; c) 90% TFA (aq.), DCM, rt, 30 min; d) I_2 , imidazole, PPh_3 , toluene, reflux, 4 h; e) NaCN, DMF, microwave, 70°C, 3 h; fi) DIBAL-H, toluene, -25°C, 45 min ii) 2M HCl, MeOH, rt, 45 min, iii) NaBH_4 , MeOH, rt, 30 min

Thin layer chromatography (TLC) analysis showed the reaction to be clean, and after purification of the product by passing the reaction mixture through a short bed of silica nitrile (**34**) was obtained in 89% yield (data not shown). The reaction was performed on a multi-gram scale with comparable results. The yield associated with the two steps (iodination and substitution with cyanide) was higher (67%) than that of the triflate ester

route¹⁹ (Scheme 1.7) (59%). For the reduction of the nitrile (**34**), we followed the procedure described by Aspinall *et al.*¹⁹ DIBAL-H was used to reduce the nitrile (**34**) to the imine in absolute toluene. Following the hydrolysis of the imine using aqueous HCl, the corresponding aldehyde was further reduced using NaBH₄ in MeOH to furnish protected 6-deoxy-D-*manno*-heptopyranose (**30**). The reaction mechanism of the DIBAL-H reduction and subsequent imine hydrolysis is described below (Scheme 2.5).



Scheme 2.5: Reaction mechanism for DIBAL-H reduction of the nitrile and subsequent imine hydrolysis down to the corresponding aldehyde

Attempts made to optimise the yield of the nitrile reduction led only to a modest improvement achieving 56% conversion over the three steps, compared to 50% stated in the literature¹⁹. Despite the modifications to the synthetic route, due to the use of bulky protecting groups and moderate yields associated with the steps, it still remains an impractical method for the large-scale synthesis of 6-deoxy-D-*manno*-heptopyranose (**32**). As a result attempts were made to employ a more efficient strategy, without the use of bulky protecting groups, which will be discussed in the next section.

2.2.5 Improvements to the synthetic route for 6-deoxy-D-*manno*-heptopyranose (32)

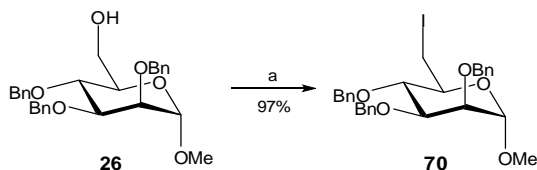
Efforts were subsequently made to develop a more robust and efficient synthetic route for 6-deoxy-D-*manno*-heptopyranose (32). The use of a synthetic oligosaccharide, for the generation of a carbohydrate based vaccine for *B. pseudomallei* would require multi-gram quantities for the starting monosaccharide for iterative synthesis. The current synthetic route to the protected 6-deoxy-D-*manno*-heptose monosaccharide (32), summarised in Scheme 2.4 is made up of 6 steps and has an overall yield of approximately 20%. Although this is a reasonable yield for a 6-step procedure, this chemistry was conducted only on small scale (1-3 grams of starting material). There are a number of technical issues which arise upon the scale-up of this route; this section deals with the attempted improvement of the synthesis of 6-deoxy-D-*manno*-heptopyranose (30).

2.2.5.1 The use of polymer bound triphenylphosphine

Although efficient on a small scale and an improvement on the previous syntheses by Boren *et al.*^{18, 39} and Aspinall *et al.*¹⁹, the current iodination procedure is not suited for scale-up^{18, 19}. The primary issue is associated with the purification of the product from the reaction mixture. During the reaction, triphenylphosphine oxide is generated, which is difficult to remove by column chromatography. When performed on small scale, two rounds of chromatography is sufficient to remove the PPh₃=O by product. However, on a large scale (10 – 20 grams), chromatography becomes impractical and precipitation of PPh₃O out of solution using non-polar solvents such as hexane or ether did not prove successful. Therefore attempts were made to use polymer-bound triphenylphosphine^{37, 40} (Sp-PPh₃) as a substitute for free triphenylphosphine, in order for the polymer bound PPh₃=O to be filtered off prior to chromatographic purification.

The reaction of I₂ with protected monosaccharide (26) was carried out in the presence of sp-PPh₃O in anhydrous toluene (Scheme 2.6) at 70°C for 4 hours. TLC and MALDI-ToF (data not shown) analysis confirmed complete conversion. The product was easily

separated from sp-PPh_3 and washed with NaHCO_3 and H_2O . TLC and MALDI-ToF analysis showed the reaction to be complete, chromatography purification was carried out and the product was isolated in a 97% yield.



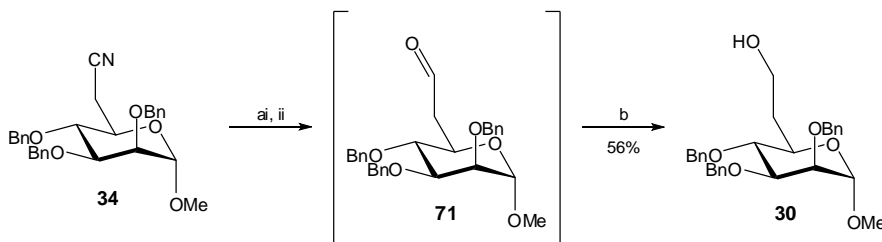
Scheme 2.6: Iodination of protected methyl mannoside (**26**) using Sp-PPh_3 . Reagents and conditions: a) Sp-PPh_3 , Imidazole, I_2 , toluene, reflux, 4 h

The yield of the reaction with free triphenylphosphine is 73%, with the majority of the losses being attributed to the chromatography steps needed for the purification of the product from triphenylphosphine oxide. The use of Sp-PPh_3 dramatically increases this yield, up to 97%, and presents an attractive replacement for triphenylphosphine. The cost of Sp-PPh_3 is approximately 15 times that of free PPh_3 and when used on large scale could become expensive. However, it is possible to reduce the $\text{Sp-PPh}_3=\text{O}$ generated during the reaction back to Sp-PPh_3 in quantitative yield using either alane (AlH_3) in THF ⁴¹ or trichlorosilane⁴². Owing to this, and the reduction in both energy and materials costs associated with the purification of the $\text{PPh}_3=\text{O}$, the use of polymer-bound triphenylphosphine for the large-scale synthesis of 6-deoxy-6-iodo derivatives is an effective and green alternative to the use of triphenylphosphine itself⁴³.

2.2.5.2 Nitrile reduction

One of the most inefficient steps of the described synthetic procedure on route to 6-D-deoxy-*manno*-heptose (**32**) is the three-step reduction of nitrile (**34**) down to primary alcohol (**30**). Over the course of the project this experiment was repeated several times, with the best yield being 56%, which was achieved when conducted on a 250 mg scale. When the scale of the reaction was increased, the yield dropped off dramatically. For example on a 1 gram scale the yield achieved was 37%, necessitating an alternative route. As discussed earlier in this chapter, there are a number of potential routes for the single carbon extension of a monosaccharide (summarised in Section 1.3.2). However, having adopted the iodide-nitrile route it was

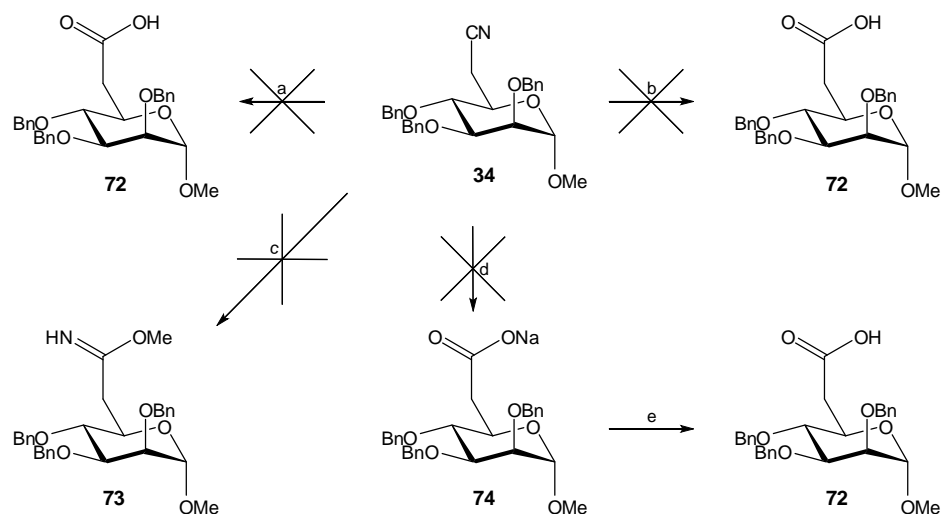
decided that efforts would be focused on improving the nitrile reduction, rather than developing a new route using previously studied methods. The current method of reduction uses DIBAL-H to reduce nitrile (**34**) down to the corresponding aldehyde (**71**), followed by further reduction of the aldehyde to the alcohol (**30**) (Scheme 2.7).



Scheme 2.7: Reduction of nitrile (34**) to alcohol (**30**) using DIBAL-H Reagents and conditions: a) DIBAL-H, toluene, -25°C, 45 min, ii) 2 M HCl, MeOH, rt, 45 min; b) NaBH₄, MeOH, rt, 30 min.**

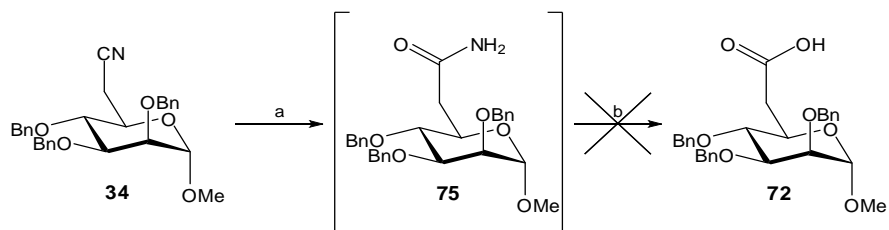
It could be possible to improve this procedure through the use of LiAlH₄ as the reducing agent for the aldehyde to alcohol step; however this is not desirable due to the health and safety issues associated with large-scale syntheses using LiAlH₄. Beyond the reduction of nitriles to aldehydes, the hydrolysis of nitriles presented an interesting option for this work. There are a number of routes which could be employed for the hydrolysis of a nitrile; acid-catalysed⁴⁴, base-catalysed⁴⁵ and enzymatic hydrolysis⁴⁶⁻⁴⁸. Although intriguing and desirable, the lack of commercial availability of these enzymes and the enzymatic hydrolysis of nitriles with nitrilases was not investigated as part of this study. Both acid- and base-catalysed reductions were trialled with no success, as described by Scheme 2.8.

The HCl promoted hydrolysis of nitrile (**34**) failed completely, with no consumption of the starting material being observed (TLC analysis or IR analysis) after 6 h at reflux temperature or in microwave reactor at 120°C. Both the reaction with H₂SO₄ and NaOH showed consumption of the starting material (TLC) analysis but both produced numerous degradation products. The use of sodium methoxide was also studied for the formation of the imidate (2-imido-2-methoxy-ethyl mannoside) (**74**) (Scheme 2.8), but again no reaction was observed after 24 hours at room temperature^{49, 50} or heating to 40 °C for 4



Scheme 2.8: Attempted hydrolysis of nitrile (**34**) using HCl, H₂SO₄ and NaOH Reagents and conditions: a) 4 M HCl, H₂O, reflux, 6 h; b) 4M H₂SO₄, H₂O, reflux, 2 h; c) 0.5 M NaOMe, MeOH, rt - 40°C, 24 h - 4 h d) 5 M NaOH, EtOH, reflux, ON; e) 4 M HCl, H₂O, rt, 30 min

Recently, Barragan-Montero *et al.*⁵¹, demonstrated the use of 30% H₂O₂ and NaOH for the hydrolysis of methyl 6-deoxy- α -D-*manno*-heptopyranosylurononitrile (**34**) in quantitative yield. The use of 30% aqueous hydrogen peroxide and sodium hydroxide was developed by Radziszewski *et al.*⁵² for the reduction of nitriles to amides, however further addition of NaOH/H₂O₂ upon formation of the amide, has shown to hydrolyse the amide down to the parent carboxylic acid⁴⁵. The use of NaOH/H₂O₂, in the presence of DMSO co-solvent, was trialed on protected nitrile (**34**). Unfortunately, even with the further addition of excess NaOH, it was not possible to proceed beyond the amide (**75**) with the protected material (Scheme 2.9)⁵³.

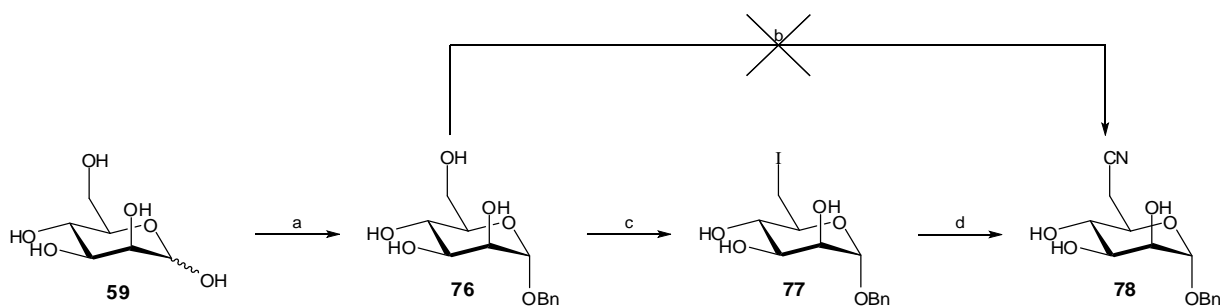


Scheme 2.9: Attempted hydrolysis of protected nitrile (**34**) with NaOH/H₂O₂. Reagents and conditions: a) NaOH, 30% H₂O₂, DMSO, rt, 36 h

At this stage, owing to the lack of success with the development of this route, and the requirement of bulky protecting groups work on this synthetic strategy was discontinued. Barragan-Montero *et al.*⁵¹ demonstrated that the NaOH/H₂O₂ hydrolysis of the free nitrile successfully generated the carboxylic acid. The development of efficient methodologies for the protecting group free synthesis of the free nitrile (**78**) were attempted next.

2.2.5.3 Protecting group-free synthesis of nitrile (**78**)

The synthesis of free nitrile (**78**) was attempted by two different methods, the first direct synthesis of the nitrile from benzyl- α -D-mannopyranoside (**76**) and secondly via the iodide (**77**) (Scheme 2.10).



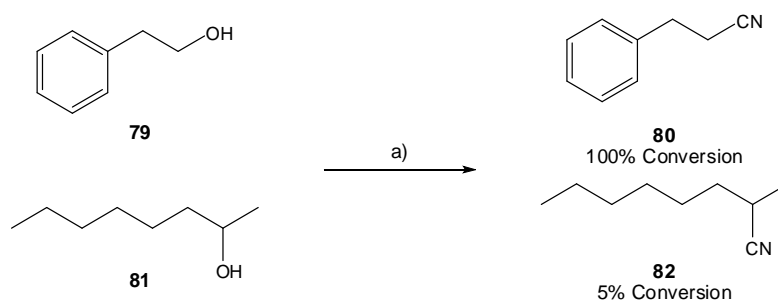
Scheme 2.10: Proposed route for the protecting group free synthesis of nitrile (**78**). Reagents and conditions: a) BnOH, AcCl, 50°C – rt, 1.5 h – 15 h, 96%; b) PPh₃, DDQ, *n*-Bu₄NCN, CH₃, rt, 2 h; c) PPh₃, Imidazole, I₂, THF, reflux, 2 h, 86%; d) NaCN, KCN/H₂O, rt, ON, quant.

Benzyl α -D-mannopyranoside (**78**) was synthesised according to the protocol described by Zunk *et al.*⁵⁴ in high yield (96%). The benzyl ether was used to protect the anomeric position and to simplify the synthetic manipulations as a result of improved solubility in organic solvents, and to aid with purification.

2.2.5.3.1 Direct synthesis of nitrile (**78**)

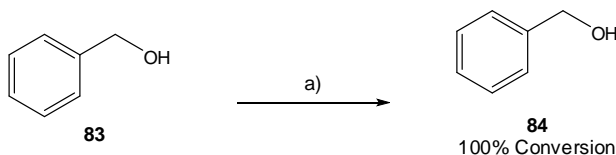
Iranpoor *et al.*^{55, 56} demonstrated the conversion of alkyl alcohols to alkyl halides using triphenylphosphine, 2,3-dichloro-5,6-dicyanobenzoquinone (DDQ) and quaternary ammonium halide salts. They further developed this work for the selective conversion

of primary alcohol (**79**) to the corresponding nitrile (**80**) with tetrabutylammonium cyanide in good yields in anhydrous acetonitrile⁵⁵.



Scheme 2.11: Direct synthesis of nitrile (**80**) from primary alcohol (**79**) as reported by Iranpoor *et al.*⁵⁵ The reaction was shown to be specific for primary alcohol (**79**) in the presence of secondary alcohol (**81**). Reagents and conditions: a) $\text{PPh}_3/\text{DDQ}/n\text{-Bu}_4\text{NCN}$, MeCN abs, rt, immediate.

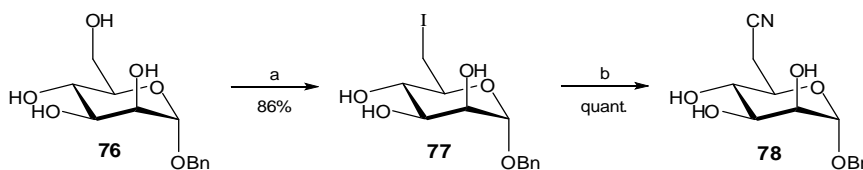
This reaction was repeated with benzyl α -D-mannopyranoside (**76**) in an attempt to furnish the desired nitrile (**78**) in one step (Scheme **2.10b**). Unfortunately, in our hands, this reaction was not successful, and no reaction was shown to have taken place after 2 hours (TLC and MALDI-ToF MS analysis, data not shown). It is worth noting that during the reaction there was no colour change from green to orange upon the addition of the substrate, which as described in the research paper indicates completion of the reaction⁵⁵. In order to assess whether the reaction conditions were correct, we repeated the reaction using benzyl alcohol (**83**) as the substrate, an example from the Iranpoor *et al.*⁵⁵ paper. This time, the indicative colour change occurred upon addition of the substrate and the reaction was shown to be successful by MALDI-ToF MS (Scheme **2.12**). The fact that the reaction was successful with the benzyl alcohol and not with monosaccharide (**76**) suggested that this system was not applicable for carbohydrates and was abandoned at this stage.



Scheme 2.12: Direct synthesis of benzyl nitrile (**85**) from benzyl alcohol (**84**), 100% conversion as shown by MALDI-ToF MS. Reagents and conditions: a) $\text{PPh}_3/\text{DDQ}/n\text{-Bu}_4\text{NCN}$, MeCN abs, rt, immediate

2.2.5.3.2 Indirect synthesis of nitrile (**78**) via the iodide (**77**)

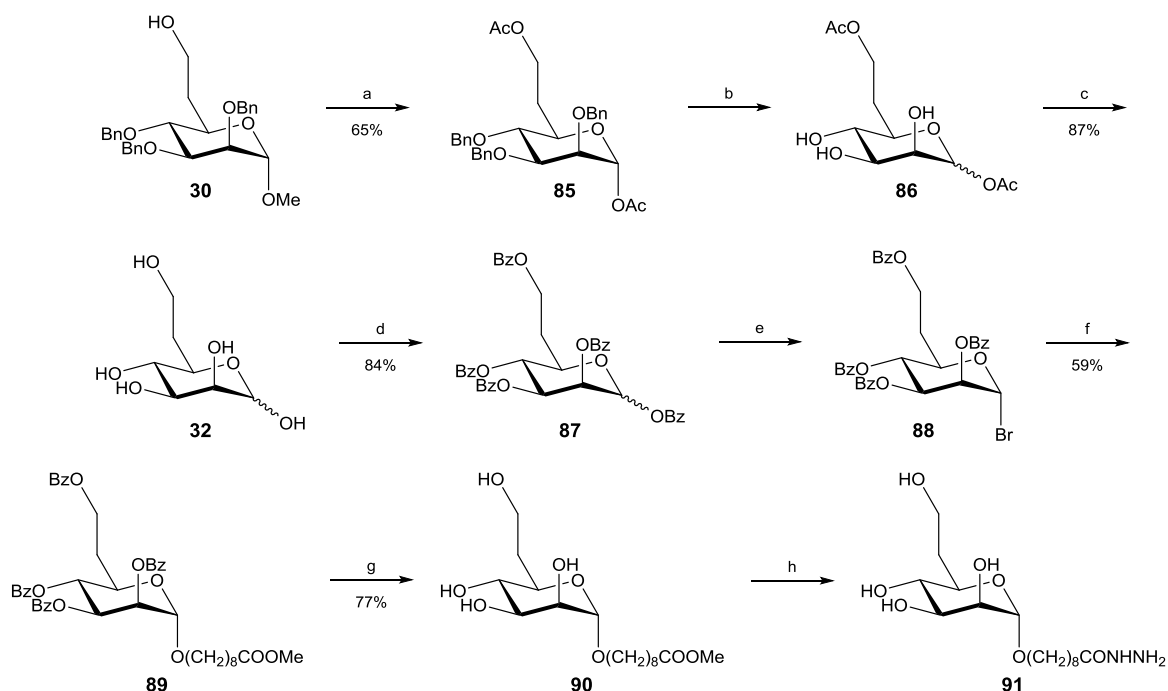
Iodide (**77**) was synthesised in good yield (86%) using the standard conditions of triphenylphosphine, imidazole and I₂ with anhydrous THF as the solvent. The removal of the PPh₃=O generated in the reactions is simplified due to the polar nature of the mobile phase used in the chromatography step [DCM:MeOH; 9:1]. Nitrile (**78**) was synthesised in quantitative yield using KCN in aqueous acetonitrile (Scheme 2.13). Therefore this route was the most efficient in transformation of mannosides into nitrile precursors of 6-deoxy-D-*manno*-heptopyranose (**32**) and has potential of further development into a scalable synthesis.



Scheme 2.13: Synthesis of nitrile (78**) without protecting groups. Reagents and conditions: a) PPh₃, Imidazole, I₂, THF, reflux, ON; b) KCN, MeCN:H₂O (1:1); rt, 15 h**

2.2.6 Synthesis of 8-(hydrazinocarbonyl)octyl 6-deoxy- α -D-*manno*-heptopyranoside (**91**)

To complete the synthesis of the 6-deoxy-D-*manno*-heptose hapten (**91**), the methyl glycoside had to be converted to the anomeric acetate *via* acetolysis with catalytic H₂SO₄ furnishing diacetate (**85**). The free 6-deoxy-D-*manno*-heptose was obtained through successive hydrogenation of the benzyl ethers and Zemplén deprotection. Per-O-benzoylation of 6-deoxy-D-*manno*-heptose (**32**) was carried out in order to avoid the acetate migration problem experienced in the mannose series (Section 2.2.2). Bromide (**88**) was synthesised by means of HBr/AcOH, purified by flash chromatography and directly glycosylated to linker (**58**) in overall yield of 59%. Deprotection of (**89**) via Zemplén deprotection afforded methyl ester (**9**) in 77% yield. The finished 6-deoxy-D-*manno*-heptose hapten (**91**) was furnished by conversion of the methyl ester (**90**) to the corresponding acyl hydrazide (**91**).



Scheme 2.14: Completion of heptose hapten synthesis (91). Reagents and conditions: a) H_2SO_4 (cat.), $\text{Ac}_2\text{O}/\text{AcOH}$, 0°C , 30 min; b) H_2 , Pd /C (cat.), EtOAc/EtOH , 40°C , 16 h; c) NaOMe , MeOH , rt, 30 min; d) BzCl , pyridine, rt, 16 h; e) 33% w/v HBr/AcOH , DCM , 0°C - rt, 3 h; f) $\text{Hg}(\text{CN})_2$, $\text{Hg}(\text{Br})_2$, 8-MCO, MS 4Å, DCE , rt, ON; g) NaOMe , MeOH , rt, 30 min; h) $\text{NH}_2\text{NH}_2 \cdot \text{H}_2\text{O}$, EtOH , 55°C , 4 h

2.3 Conjugation of monosaccharide haptens to carrier protein

2.3.1 Expression of His-tagged TetHc fragment in *E. coli*

An *E. coli* BL21 strain containing the pSK1-TetHc plasmid was provided by Dr A. Scott of DSTL-Porton Down. The cells were grown up in LB media (4 x 1 litre) to an optical density ($_{600\text{ nm}}$) of 0.8, at which point the expression of TetHc protein was induced by the addition of isopropyl β -D-1-thio-*galacto*-pyranoside (IPTG). After 16 hours incubation at 16°C the cells were harvested, lysed by means of a cell disrupter and the resulting cell debris was removed by centrifugation. The soluble protein was purified from the supernatant using an Äkta Xpress FPLC system (GE Healthcare) to afford pure protein at a yield of 55 mg/L of cell culture.

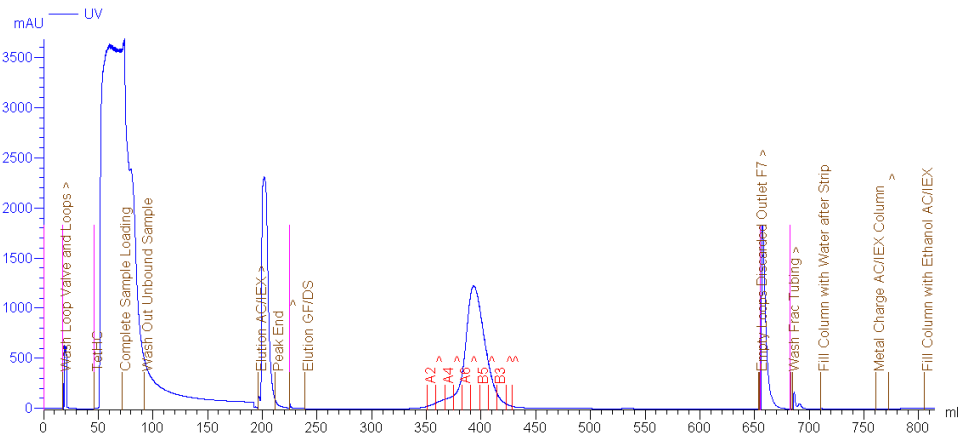


Figure 2.3: Chromatogram of TetHc fragment purification on Akta Xpress FPLC equipped with 1) Column HiTrap Ni-NTA column (5 ml, GE Healthcare); wash buffer [50 mM Tris-HCl, pH 8.0, 0.5 M NaCl, 30 mM imidazole]; eluent [50 mM Tris-HCl, pH 8.0, 0.5 M NaCl, 0.5 M imidazole]. 2) Superdex S75 XK26/60 column; eluent [50 mM HEPES, pH 7.5, 100 mM NaCl]; flow rate 3.2 ml/min.

SDS-PAGE analysis (Figure 2.4) showed successful expression and purification of TetHc fragment, with the fractions collected containing pure protein with the gel band corresponding to the standard supplied by DSTL.

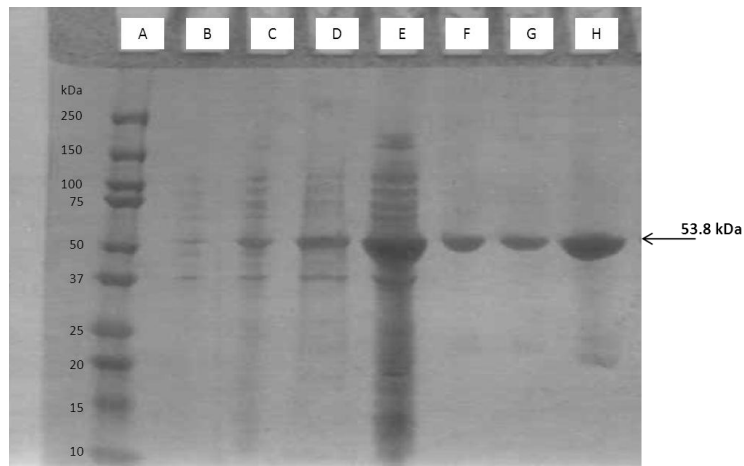


Figure 2.4: SDS-PAGE (Coomassie stained) analysis of fraction from Akta Xpress FPLC Sepharose S200 XK 26/60 column, flow rate 3.2 ml/min, eluent (20 mM HEPES, 150 mM NaCl, pH 7.5). Lanes: A) Kaleidoscope Ladder; B) Non-expressing cells (No IPTG); C) IPTG induced expressing cells; D) Total cell insoluble frac.; E) Total cell soluble frac.; F) Frac. A6; G) Frac. A8; H) Purified TetHc standard.

MALDI-ToF analysis was carried out on the intact protein as described in general methods section (7.1.3). The spectrum is shown below (Figure 2.5) with the main peak

at ca. 53 kDa corresponding the molecular weight of TetHc and the second peak corresponding to the $[M+2H]^{2+}$ ion.

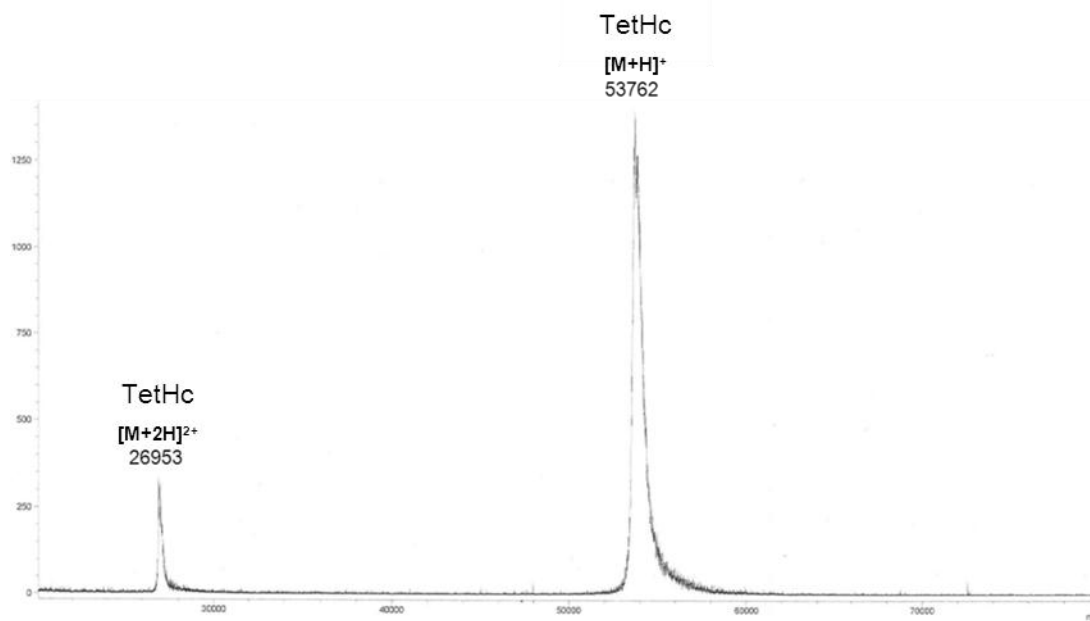
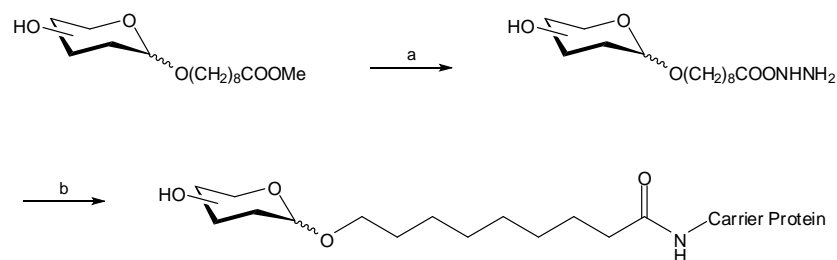


Figure 2.5: MALDI-ToF spectra of intact TetHc fragment

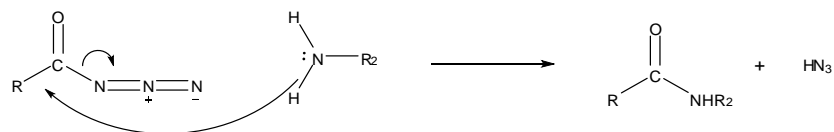
2.3.2 Conjugation of Haptens

In order to conjugate acyl hydrazide to the primary amines of lysine residues of the carrier protein, using an excess of acyl hydrazide which were initially converted to the corresponding acyl azides. This was achieved through oxidation using nitrous acid, which is formed *in situ* by reaction of *tert*-butyl nitrite with 4M HCl in DMF at -25°C (Section 6.1.1.2). The DMF solution containing the acyl azide was then added drop-wise to a cooled solution of protein in Borax/ KHCO_3 buffer (pH 9.0) (Scheme 2.15)²³.



Scheme 2.15: General reaction Scheme of glycoconjugate synthesis. Reagents and conditions: a) Hydrazine monohydrate, EtOH, 6 h, 55°C; bi) *tert*-butyl nitrite, 4M HCl, DMF, bii) TetHc, 0.08M Borax/0.35M KHCO₃, pH 9.0, O/N, 4°C.

The reaction between the acyl azide and lysine residues will only occur when the lysine side chain is in its free base form (Scheme 2.16)^{57 58}.



Scheme 2.16: Reaction mechanism for amide bond formation between acyl azide and lysine



Figure 2.6: SDS-Page analysis and FITC-ConA staining of Man-TetHc conjugate (92). Left Gel: Standard SDS-PAGE gel. Lanes: A) Kaleidoscope ladder; B) native TetHc fragment; C) Man-TetHc glycoconjugate (92); D) mix native TetHc and Man-TetHc conjugate (92). Right Gel: Western blot of SDS-PAGE gel. Lanes A) Kaleidoscope ladder; b) native TetHc fragment; C) Man-TetHc glycoconjugate (92) stained with FITC-ConA

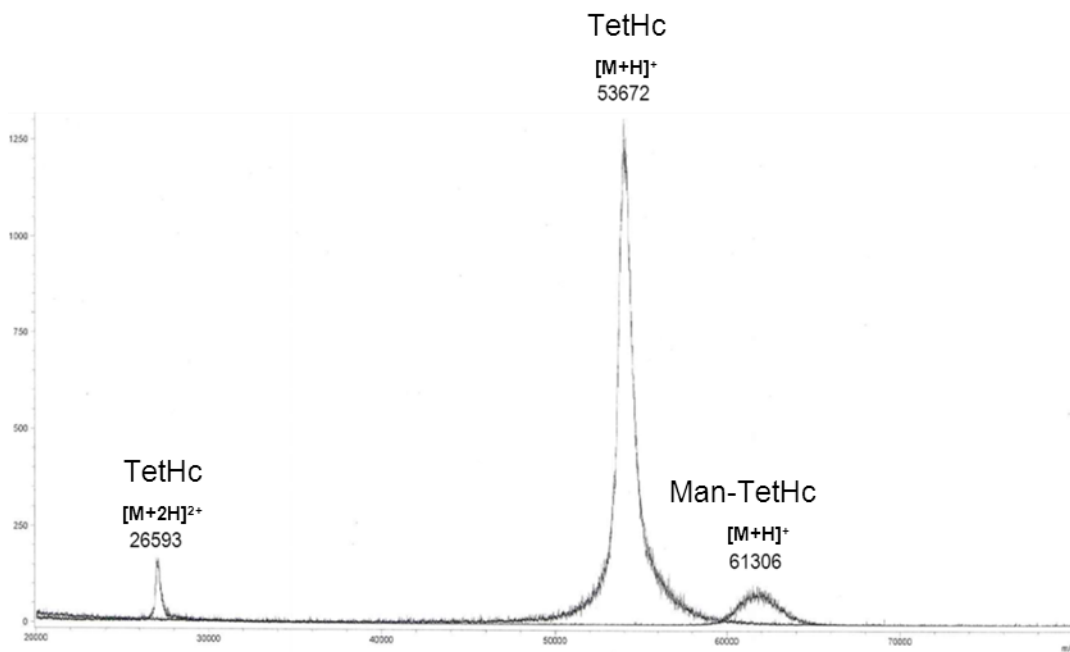


Figure 2.7: Overlay of MALDI-ToF spectra for native TetHc and Man-TetHc (92) glycoconjugates

2.3.2.1 Mannose-TetHc (Man-TetHc) Glycoconjugate (92)

The D-mannopyranose hapten (**64**) was successfully conjugated to TetHc carrier protein on a 6 mg scale. All protein conjugates were analysed using intact mass MALDI-ToF MS, SDS-PAGE and in the case of Man-TetHc, western blot analysis with (Fluorescein IsoThioCyanate) FITC-Concanavalin A (ConA). Con A is a carbohydrate lectin originally isolated from jack-bean and is known to specifically bind to α -D-mannose and α -D-glucose residues⁵⁹. MALDI-Tof MS is an ideal technique for the analysis of the glycoconjugates due to its soft ionisation with little fragmentation^{60, 61}. The glycoconjugates were analysed by MS following the procedure highlighted in general methods section (7.1.3). A number of matrices were trialled to generate spectra for these glycoconjugates. It was shown that a saturated solution of sinapinic acid [70% MeCN, 0.1% TFA] was the most suitable matrix for this work.

SDS-PAGE of the Man-TetHc conjugate (**92**) (Figure 2.6 (left)) demonstrated a band shift in the order of 5 – 10 kDa difference between native TetHc and the Man-TetHc conjugate (**92**). A western blot was taken of SDS-PAGE gel and stained using FITC-ConA, fluorescently labelled Concanavalin A and imaged using a fluorescence scanner at 495 nm (Figure 2.6 (right)). Only the Man-TetHc conjugate (**92**) was labelled by the FITC-ConA, indicating the successful conjugation and presentation of the mannose hapten on the surface of the TetHc carrier.

MALDI-ToF analysis confirmed conjugation at an average of 23 hapten units per TetHc molecule, giving a conjugation efficiency of 70% considering total number of available lysine residues (33) (Figure 2.7).

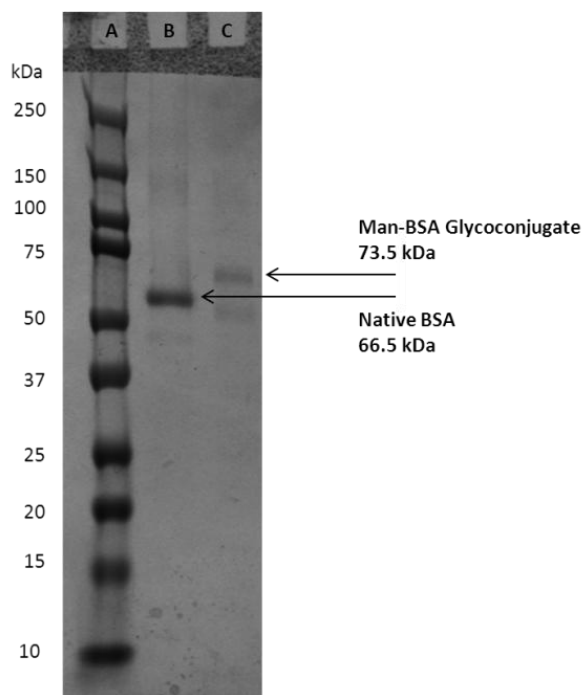


Figure 2.8: SDS-PAGE analysis of Man-BSA conjugate (91). Lanes: A) Kaleidoscope ladder; B) Native BSA; C) Man-BSA glycoconjugate (93).

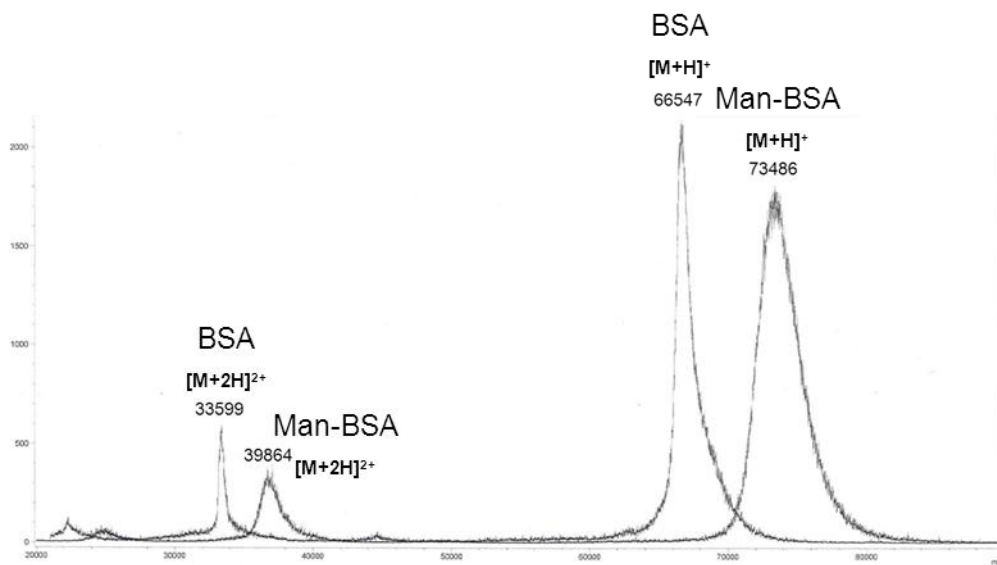


Figure 2.9: Overlay of MALDI-ToF spectra of native BSA and Man-BSA (93) conjugates

2.3.2.2 Mannose-BSA (Man-BSA) Glycoconjugate (93)

The D-mannose hapten (**64**) was successfully conjugated to the BSA carrier protein on an 11 mg scale. Figure **2.8** shows the SDS-PAGE analysis for the Man-BSA conjugate, with a corresponding band shift of approximately 7 kDa as calculated by MALDI-ToF MS (Figure **2.9**). MALDI-ToF analysis was carried out and gave an average of 20 mannose residues per BSA molecule, giving a conjugation efficiency of 33%. Comparing the MALDI-ToF data for the two generated glycoconjugates (Figure **2.8** and **2.9**) revealed a difference between the intensity of the molecular ions for Man-TetHc (**92**) and Man-BSA (**93**) glycoconjugates. The reason for the reduced intensity in the case of the Man-TetHc (**92**) conjugate is probably due to the poor solubility of the TetHc conjugate in the matrix solution. The shape and distribution of the MS peaks collected for both the Man-TetHc (**92**) and Man-BSA (**93**) samples indicates complete conjugation of all chemically addressable lysine residues. This is further backed up by the SDS-PAGE data, where the presence of distinct bands for the glycoconjugate represents complete reaction. Due to the large excess of hapten in the reaction, it is conceivable to assume that all the available lysine residues in both TetHc and BSA are successfully conjugated.

2.3.2.3 Glucose and Heptose Glyconjugates

The conjugation of the D-glucopyranose (**69**) and 6-deoxy-D-manno-heptopyranose (**91**) haptens to both TetHc and BSA carrier proteins was shown to be both efficient and reliable, with the conjugation efficiency (based on lysine coverage (conjugated lysine/total lysine content)x100) remaining consistent throughout the monosaccharide series. MALDI-ToF data for all glycoconjugates is detailed in Appendix **8.1**. The Glc-TetHc (**96**) and 6dHep-TetHc (**94**) monosaccharide antigens were used for antibody production by immunisation of sheep (Ig Innovations, South Wales). The BSA antigens were used in the immunological assessment of the TetHc conjugates, the results of which are discussed in Section **4**.

2.3.2.4 Summary of the monosaccharide hapten conjugation to TetHc and BSA

Glycoconjugate	Average Hapten per protein molecule	Conjugation Efficiency (conjugated lysine/total lysine)x100
6-Deoxy-mannoheptose-TetHc (6dManHep-TetHc) (94)	23	70%
6-Deoxy-mannoheptose-BSA (6dManHep-BSA) (95)	19	32%
Glucose-TetHc (Glc-TetHc) (96)	25	76%
Glucose-BSA (Glc-BSA) (97)	21	35%
Mannose-TetHc (Man-TetHc) (92)	23	70%
Mannose-BSA (Man-BSA) (93)	20	33%

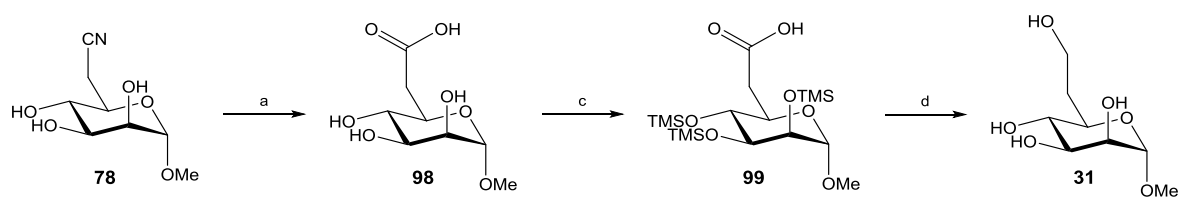
Table 2.1: Monosaccharide hapten-protein conjugates prepared in the current work

2.4 Conclusions

This chapter described the initial efforts for the synthesis of three monosaccharide haptens, 8-(methoxycarbonyl)octyl- α -D-mannopyranoside (**64**); 8-(methoxycarbonyl)octyl- β -D-glucopyranoside (**69**) and 8-(methoxycarbonyl)octyl-6-deoxy- α -D-mannoheptopyranoside (**91**). The syntheses of these compounds were based on methods of traditional carbohydrate chemistry and produced sufficient quantities of material for preparation of neoglycoconjugates required for immunological studies. The monosaccharide haptens were successfully conjugated to carrier proteins (TetHc and BSA) and used in immunisation trials. The description of these trials, along with the immunological assessment of the monosaccharide antigens is presented in Chapter 4.

However with the view of application of the 6-deoxy-D-manno-heptose (**32**) materials in vaccine development and oligosaccharide synthesis, large quantities (grams) of synthetic 6-deoxy-D-manno-heptose (**32**) will be required. Therefore, upon the successful synthesis of the monosaccharide haptens; efforts were made to streamline the synthesis of 6-deoxy-mannoheptose (**32**) for large scale production. Different strategies for the C-6 extension, along with protecting group-free synthetic routes were

investigated. Some success was achieved to this end; but optimisation of this approach is in on-going (Scheme 2.17).



Scheme 2.17: Improved synthesis of 6-deoxy-D-manno-heptose from free nitrile (79). Reagents and conditions: a) NaOH/30% H₂O₂, rt, 36 h; b) TMSCl, pyridine; 50°C – rt, 1 h – 18 h; s) BH₃-THF, THF, -20°C – rt, 1 h – 18 h

2.5 References

1. H. Masoud, M. Ho, T. Schollaardt and M. B. Perry, *J. Bacteriol.*, 1997, **179**, 5663-5669.
2. H. Paulsen, *Angewandte Chemie International Edition in English*, 1982, **21**, 155-173.
3. A. H. Lucas, M. A. Apicella and C. E. Taylor, *Clin. Infect. Dis.*, 2005, **41**, 705-712.
4. L. Morelli, L. Poletti and L. Lay, *Eur. J. Org. Chem.*, 2011, DOI: 10.1002/ejoc.201100296, 5723-5777.
5. P. Costantino, R. Rappuoli and F. Berti, *Expert Opinion on Drug Discovery*, 2011, **6**, 1045-1066.
6. B. A. Sela, J. L. Wang and G. M. Edelman, *Proceedings of the National Academy of Sciences*, 1975, **72**, 1127-1131.
7. C. Bromuro, M. Romano, P. Chiani, F. Berti, M. Tontini, D. Proietti, E. Mori, A. Torosantucci, P. Costantino, R. Rappuoli and A. Cassone, *Vaccine*, 2010, **28**, 2615-2623.
8. Z. Guo and B. G-J;, *Carbohydrate-based vaccines and immunotherapies*, Wiley, 2009.
9. T. Kurokawa, M. Wuhrer, G. Lochnit, H. Geyer, J. Markl and R. Geyer, *Eur. J. Biochem.*, 2002, **269**, 5459-5473.
10. R. Swerdlow, R. Ebert, P. Lee, C. Bonaventura and K. Miller, *Comp. Biochem. Physiol.*, 1996, **113B**, 537-548.
11. J. R. Harris and J. Markl*, *Micron*, 1999, **30**, 597-623.
12. J. Kubler-Kielb, T.-Y. Liu, C. Mocca, F. Majadly, J. B. Robbins and R. Schneerson, *Infect. Immun.*, 2006, **74**, 4744-4749.
13. E. Malito, B. Bursulaya, C. Chen, P. L. Surdo, M. Picchianti, E. Balducci, M. Biancucci, A. Brock, F. Berti, M. J. Bottomley, M. Nisum, P. Costantino, R. Rappuoli and G. Spraggon, *Proceedings of the National Academy of Sciences*, 2012, **109**, 5229-5234.
14. A. J. Makoff, S. P. Ballantine, A. E. Smallwood and N. F. Fairweather, *Nat. Biotechnol.*, 1989, **7**, 1043-1046.
15. M. Matsuda and M. Yoneda, *Biochem. Biophys. Res. Commun.*, 1977, **77**, 268-274.
16. K. Sinha, M. Box, G. Lalli, G. Schiavo, H. Schneider, M. Groves, G. Siligardi and N. Fairweather, *Mol. Microbiol.*, 2000, **37**, 1041-1051.

17. M. R. Arkin, M. A. Glicksman and H. Fu, *Inhibition of protein-protein interactions: Non-cellular assay formats*, Eli Lilly & Company and the National Center for Advancing Translational Sciences, 2012.
18. H. B. Boren, K. Eklind, P. J. Garegg, B. Lindberg and A. Pilotti, *Acta Chem. Scand.*, 1972, **26**, 4143-4146.
19. G. O. Aspinall, A. G. McDonald and R. K. Sood, *Can. J. Chem.*, 1994, **72**, 247-251.
20. B. Kuberan and L. R. J., *Curr. Org. Chem.*, 2000, **4**, 653-677.
21. D. S. Dalpathado, H. Jiang, M. A. Kater and H. Desaire, *Anal. Bioanal. Chem.*, 2005, **381**, 1130-1137.
22. J. Kohn and M. Wilchek, *FEBS Lett.*, 1983, **154**, 209-210.
23. R. U. Lemieux, D. R. Bundle and D. A. Baker, *JACS*, 1975, **97**, 4076-4083.
24. J. K. Inman, B. Merchant, L. Clafin and S. E. Tacey, *Immunochemistry*, 1973, **10**, 165-174.
25. K. Kai, J. Takeuchi, T. Kataoka, M. Yokoyama and N. Watanabe, *Tetrahedron*, 2008, **64**, 6760-6769.
26. K. P. R. Kartha and R. A. Field, *Tetrahedron*, 1997, **53**, 11753-11766.
27. K. Wada, T. Chiba, Y. Takei, H. Ishihara, H. Hayashi and K. Onozaki, *J. Carbohydr. Chem.*, 1994, **13**, 941-965.
28. C. Göllner, C. Philipp, B. Dobner, W. Sippl and M. Schmidt, *Carbohydrate Research*, 2009, **344**, 1628-1631.
29. L. J. Liotta and B. Ganem, *Tetrahedron Lett.*, 1989, **30**, 4759-4762.
30. K. K. Sadozai, J. K. Anand and S.-i. Hakomori, *Journal of Carbohydrate Chemistry*, 1994, **13**, 1037-1050.
31. S. K. Das, J.-M. Mallet and P. Sinaÿ, *Angewandte Chemie International Edition in English*, 1997, **36**, 493-496.
32. K.-S. Ko, C. J. Zea and N. L. Pohl, *JACS*, 2004, **126**, 13188-13189.
33. S. J. Marsh, K. P. R. Kartha and R. A. Field, *Synlett*, 2003, 1376-1378.
34. M. T. C. Pedrosa, R. B. Alves, M. A. F. Prado, J. D. de Souza Filho, R. J. Alves and N. B. D'Accorso, *J. Carbohydr. Chem.*, 2003, **22**, 433-442.
35. F. Langa, P. de la Cruz, A. de la Hoz, A. Diaz-Ortiz and E. Diez-Barra, *Contemporary Organic Synthesis*, 1997, **4**, 373-386.
36. P. Lidström, J. Tierney, B. Wathey and J. Westman, *Tetrahedron*, 2001, **57**, 9225-9283.

37. B. Classon, Z. C. Liu and B. Samuelsson, *J. Org. Chem.*, 1988, **53**, 6126-6130.
38. R. Caputo, H. Kunz, D. Mastroianni, G. Palumbo, S. Pedatella and F. Solla, *Eur. J. Org. Chem.*, 1999, 3147-3150.
39. K. E. Hans. Boren, Per J. Garegg, Bengt Lindberg and Ake Pilotti, *Acta Chemica Scandinavia*, 1972, **26**, 4143-4146.
40. G. Anilkumar, H. Nambu and Y. Kita, *Organic Process Research & Development*, 2002, **6**, 190-191.
41. F. Sieber, P. Wentworth, J. D. Toker, A. D. Wentworth and W. A. Metz, *J. Org. Chem.*, 1999, **64**, 5188-5192.
42. D. Castro, L. Boiani, D. Benitez, P. Hernández, A. Merlino, C. Gil, C. Olea-Azar, M. González, H. Cerecetto and W. Porcal, *European Journal of Medicinal Chemistry*, 2009, **44**, 5055-5065.
43. G. Gelbard, in *Handbook of green chemistry and technology*, Blackwell Science Ltd, 2007, DOI: 10.1002/9780470988305.ch8, pp. 150-187.
44. F. Effenberger, B. Hörsch, S. Förster and T. Ziegler, *Tetrahedron Lett.*, 1990, **31**, 1249-1252.
45. C. V. Magatti, J. J. Kaminski and I. Rothberg, *The Journal of Organic Chemistry*, 1991, **56**, 3102-3108.
46. A. Deraadt, H. Griengl, N. Klempier and A. E. Stutz, *J. Org. Chem.*, 1993, **58**, 3179-3184.
47. M. A. Cohen, J. Sawden and N. J. Turner, *Tetrahedron Lett.*, 1990, **31**, 7223-7226.
48. H. Kakeya, N. Sakai, T. Sugai and H. Ohta, *Tetrahedron Lett.*, 1991, **32**, 1343-1346.
49. A. V. Malkov, A. Liddon, P. Ramirez-Lopez, L. Bendova, D. Haigh and P. Kocovsky, *Angewandte Chemie-International Edition*, 2006, **45**, 1432-1435.
50. S. I. van Kasteren, S. J. Campbell, S. Serres, D. C. Anthony, N. R. Sibson and B. G. Davis, *Proceedings of the National Academy of Sciences*, 2009, **106**, 18-23.
51. V. Barragan-Montero, A. Awwad, S. Combemale, P. d. S. Barbara, B. Jover, J.-P. Moles and J.-L. Montero, *Chem med chem*, 2011, **6**, 1771-1774.
52. G. B. Payne, P. H. Deming and P. H. Williams, *J Org Chem*, 1961, **26**, 659-663.
53. S. D. Cho, Y. D. Park, J. J. Kim, J. R. Falck and Y. J. Yoon, *Bull. Korean Chem. Soc.*, 2004, **25**, 407-409.
54. M. Zunk and M. J. Kiefel, *Tetrahedron Lett.*, 2011, **52**, 1296-1299.

55. N. Iranpoor, H. Firouzabadi, B. Akhlaghinia and N. Nowrouzi, *J. Org. Chem.*, 2004, **69**, 2562-2564.
56. N. Iranpoor, H. Firouzabadi, G. Aghapour and A. R. Vaezzadeh, *Tetrahedron*, 2002, **58**, 8689-8693.
57. I. André, S. Linse and F. A. A. Mulder, *JACS*, 2007, **129**, 15805-15813.
58. J. Cuadros, L. Aldega, J. Vetterlein, K. Drickamer and W. Dubbin, *J. Colloid Interface Sci.*, 2009, **333**, 78-84.
59. R. Loris, D. Maes, F. Poortmans, L. Wyns and J. Bouckaert, *J. Biol. Chem.*, 1996, **271**, 30614-30618.
60. D. J. Harvey, *Mass Spectrom. Rev.*, 1999, **18**, 349-450.
61. S. L. Cohen and B. T. Chait, *Anal. Chem.*, 1996, **68**, 31-37.

3 Production and characterisation of capsular polysaccharide from *Burkholderia thailandensis*

3.1 *Burkholderia thailandensis*

Access to the CPS-1 of *B. pseudomallei* (4) is essential for this project, both for the analysis of generated antibodies and for the use of the intact polysaccharide and fragments thereof, in vaccination trials. Previous attempts by collaborators to extract and purify the CPS-1 from native *B. pseudomallei* (4) have failed (Section 3.2.1) and due to the stringent health and safety requirements for working with a category III pathogen, it was not possible to work with this bacterium at JIC. However, the availability of a non-pathogenic strain of *Burkholderia* which produces CPS-1 (4) would be a great step forward for this work.

Burkholderia thailandensis is a closely related species to *B. pseudomallei*, but is essentially non-virulent¹. The lethal dose in mice for *B. thailandensis* (E264 strain) is 1000 fold greater than that of *B. pseudomallei*,² with infection only occurring in severely immuno-compromised individuals^{3,4}. Originally being classified as *pseudomallei*-like, it was not until 1998 when Brett and co-workers proposed that, due to the several differences from *B. pseudomallei*, it be classified as a distinct species, *B. thailandensis*⁵. *B. thailandensis* is usually distinguished from *B. pseudomallei* through its ability to assimilate arabinose⁴. Due to its avirulent nature, unlike *B. pseudomallei*, *B. thailandensis* does not require category III laboratory facilities and is not designated as a biosecurity threat. This makes it much easier to study and work with, and as a result it represents a vital tool for studying the pathogenesis of *B. pseudomallei*⁶. The lack of virulence of *B. thailandensis* compared to *B. pseudomallei* is attributed to several genetic differences between the two species^{7, 8}. Research has shown that *B. thailandensis* (E264) produces a structurally similar LPS (100) to *B. pseudomallei*, but does not CPS-1(4)⁹.

As discussed in Section 1.1.1.1, the encapsulation of *B. pseudomallei* with CPS-1 (4) is essential for virulence of the bacterium. The absence of CPS-1 (4) in *B. thailandensis* E264, as a result of the lack of the CPS-1 biosynthesis gene cluster, is considered to be a predominant factor in its attenuated virulence. In an attempt to

understand more about the avirulent nature of *B. thailandensis*, Sim and co-workers¹⁰ conducted a pan-genome array study to isolate new strains of *B. thailandensis*. Within their study they found numerous strains of *B. thailandensis* that differed from the reference E264 strain. However, two strains were of particular note; *B. thailandensis* E555 – isolated from soil in Indonesia and *B. thailandensis* CDC3015869 – isolated from human sera in USA. Both of these strains appeared to have lost the exopolysaccharide (EPS) gene cluster present in E264 and replaced it with a novel genomic region (300 kb), similar to the *B. pseudomallei* CPS-1 gene cluster. Comparison between a wild type *B. pseudomallei* strain (BpK96243) CPS-1 cluster and the novel genomic region found in *B. thailandensis* highlighted a protein similarity of 96% (nucleotide similarity 93.4%)¹⁰.

The presence of a *B. pseudomallei*-like gene cluster was further confirmed using immunofluorescence microscopy (Figure 3.1). *B. thailandensis* E264 and E555 were stained with 4,6-diamidino-2-phenylindole (DAPI), a blue fluorescent stain which binds to DNA identifying the nucleus of the cell. Fluorescently labelled monoclonal antibodies specific for CPS-1 (4) were used to highlight the presence of CPS-1 (4) in the E555 strain, demonstrated by the red staining in Figure 3.1 B.

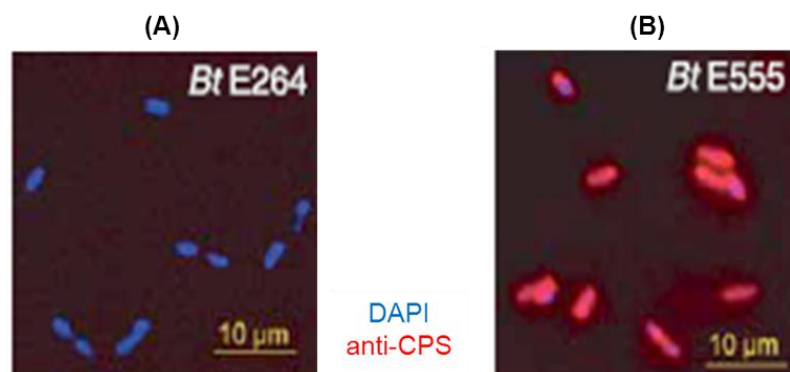


Figure 3.1: Confirmation of CPS-1 (4) expression by *B. thailandensis* E555 by immunofluorescence analysis. Cell nucleus stained blue (DAPI) and presence of CPS-1 (4) was visualised with a fluorescently labelled anti-CPS-1 antibody (red). Image adapted from Sim and co-workers¹⁰

Having identified an essentially avirulent strain of *Burkholderia* which produces the 1,3-linked 2-O-acetyl-6-deoxy- β -D-manno-heptopyranoside CPS-1 (4), recent data from Scott and co-workers¹¹ summarised the potential use of live *B. thailandensis* E555 bacteria as a vaccine candidate against *B. pseudomallei* infection. As

discussed in the Section 1.2.1, there have been a number of studies looking at the use of attenuated *B. pseudomallei* cells in vaccinations, which have shown to confer a degree of immunity in mice¹². However, there are growing safety concerns regarding the use of using live-attenuated bacteria in vaccinations¹³. The data published by Scott and co-workers¹¹ demonstrated that immunisation with live *B. thailandensis* E555 led to the development of protective immunity in mice. Although a significant step forward in this area, the use of bacteria, regardless of its avirulent nature, is still not desirable in the eyes of the regulatory bodies. *B. thailandensis* E555 does however pose a viable option for large scale production of the CPS-1 (4), which is thought to be the key for the development of a successful vaccine for *B. pseudomallei*¹⁴ (Section 1.2.1). To date all evidence for the production of a similar polysaccharide by E555 is based on genomic analysis and immunoblotting with monoclonal antibodies raised against *B. pseudomallei* (K96243) whole cells. This chapter details the production, extraction and first full characterisation of the capsular polysaccharide from *B. thailandensis* E555.

3.2 Results and discussion

3.2.1 NMR characterisation of CPS-1 (4) from *B. pseudomallei*

Prior to investigation into the use of *B. thailandensis* E555 for the production of CPS-1 (4), the extraction and purification of CPS-1 (4) from *B. pseudomallei* was attempted by our collaborators at DSTL-Porton Down. Two samples of polysaccharide extract from *B. pseudomallei* (K96243) were provided by Dr A. Scott for characterisation. One sample had been extracted from *B. pseudomallei* grown in LB-Lennox media and one was extracted from bacteria grown on solid agar as part of an investigation into the effects of growth conditions on CPS-1 (4) production. Initial immunological studies indicated the presence of CPS-1 (4) through the use of a monoclonal antibody (mAb 41VH12) raised against intact *B. pseudomallei* cells.

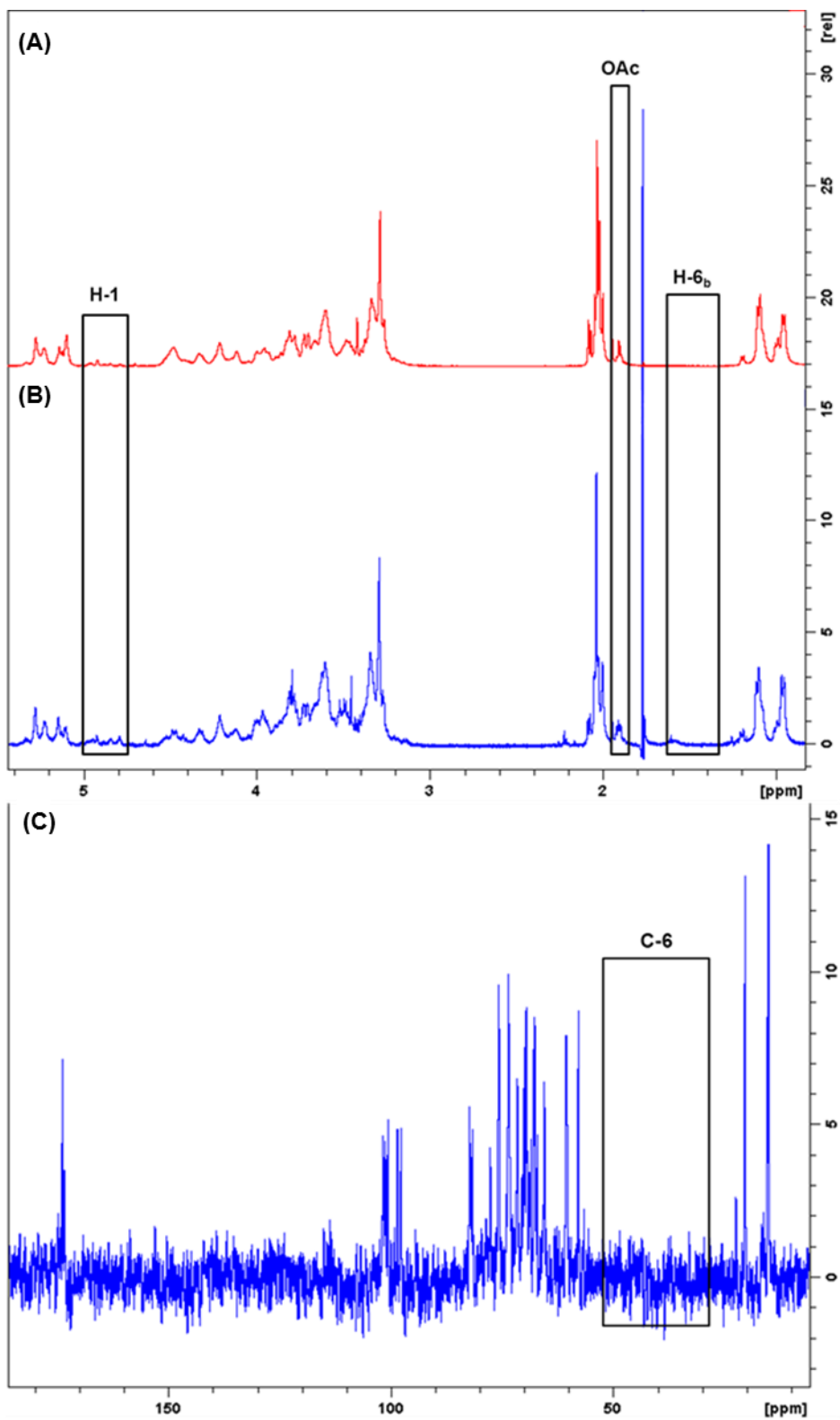


Figure 3.2: ^1H NMR (400 MHz; D_2O): (A) extract from *B. pseudomallei* grown on solid media; (B) extract from *B. pseudomallei* grown in LB-Lennox media; (C) ^{13}C NMR (100 MHz, D_2O) for *B. pseudomallei* grown on solid media.

Figure 3.3 demonstrates that the mAb 4IVH12 antibody recognises material in both aqueous extractions of heat-inactivated *B. pseudomallei* (K96243) (cell washings) and on the whole bacterial cell.

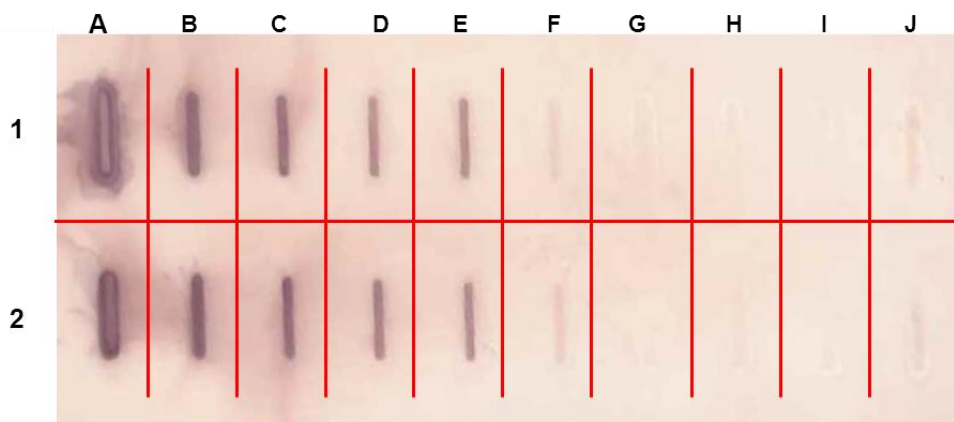


Figure 3.3: Slot-blot data for 1 *B. pseudomallei* K96243 cells indicating the presence of CPS-1 material. Lanes: A) cell wash; B) cell wash 1/10; C) cell wash 1/100; D) cell wash 1/1000; E) 1 $\mu\text{g/ml}$ cells; F) 0.1 $\mu\text{g/ml}$ cells; G) 0.01 $\mu\text{g/ml}$ cells; H) blank; I) *E. coli* cell wash; J) 1 $\mu\text{g/ml}$ *E. coli* cells. Rows: 1 & 2 (duplicates)) samples made using 1 mg of *B. pseudomallei* K96243 cells, grown under standard conditions.

However, proton and carbon NMR (Figure 3.2) of both polysaccharide samples indicated no presence of 2-*O*-acetyl-6-deoxy-*D*-manno-heptopyranoside, when compared to the literature NMR data^{15, 16}. This was highlighted by the absence of peaks at *ca.* 4.9 ppm (H-1), 2 ppm (OAc) and 1.8 ppm (H-6_b) as shown in the ¹H NMR spectrum (Figure 3.2 (A & B)). ¹³C NMR data (Figure 3.2 C) were collected for the polysaccharide extract isolated from cells grown on solid media and further confirmed the absence of 2-*O*-acetyl-6-deoxy-*D*-manno-heptopyranoside. The absence of a peak at *ca.* 35 ppm, corresponding to the deoxy C-6 carbon in 6-deoxy-*D*-manno-heptose (32), confirms that the polysaccharide extracted from *B. pseudomallei* is not CPS-1 (4), as predicted by the antibody experiment (Figure 3.3).

B. pseudomallei produce 5 other polysaccharides (Section, 1.2.2, Table 1.4) alongside CPS-1 (4), many of which have been characterised by NMR. However, due to the complexity of the collected NMR data, the elucidation of the structure of the polysaccharide(s) present in this sample would be non-trivial. However, acid hydrolysis and subsequent monosaccharide analysis of the samples was carried out

in attempt to identify the monosaccharide components of the *B. pseudomallei* extract.

3.2.1 Monosaccharide component analysis of *B. pseudomallei* polysaccharide extracts

The *B. pseudomallei* (K96243) polysaccharide extract (solid media) was subjected to exhaustive acid hydrolysis down to monosaccharide components as described in experimental Section 7.1.6. Monosaccharide component analysis was conducted using a Dionex ICS-5000 high-performance ion chromatography system with a CarboPac PA20 column. Isocratic elution with 8 mM NaOH was shown to provide the best separation of 6 monosaccharide standards (Section 7.1.7.1). Monosaccharide analysis of the polysaccharide extract from *B. pseudomallei* (K96243) indicated the presence of at least 5 monosaccharides. Spiking experiments (Figure 3.5) were carried out using both 6-deoxy-D-mannoheptopyranose (CPS-1) and 6-deoxy-L-talopyranose (LPS) (Figure 3.4) in an attempt to detect the presence of either CPS-1 (4) or LPS (100) in this sample.

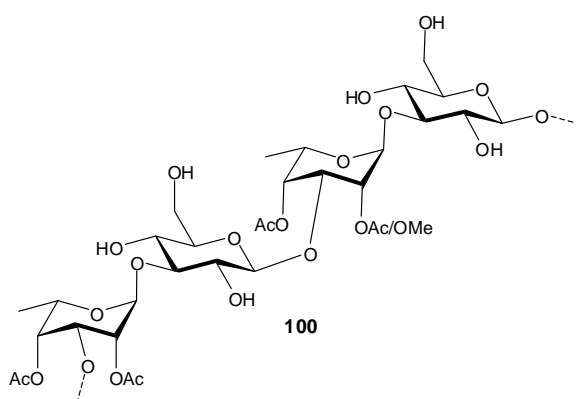


Figure 3.4: Structure of LPS of *B. pseudomallei* (100).

Based on these experiments (Figure 3.5), along with the NMR data, it was possible to conclude that neither CPS-1 (4) nor LPS (100) were present. The capsular polysaccharide of *B. pseudomallei* is the current focus of this study; as a result of the lack of this polysaccharide further work into the elucidation of the composition of this polysaccharide sample was not carried out. However, based on the collected data it is possible to postulate the presence of multiple polysaccharides, which could be further investigated at a later stage if appropriate.

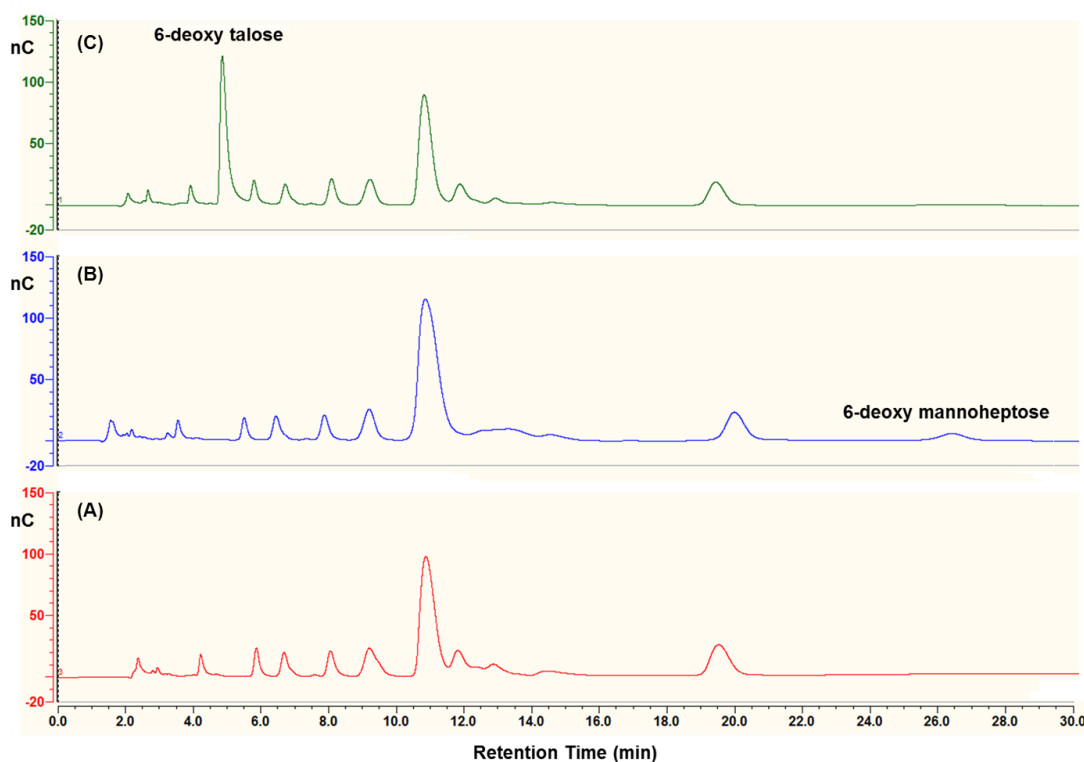


Figure 3.5: Monosaccharide component analysis of polysaccharide hydrolysate of *B. pseudomallei* cells grown on solid media. Dionex CarboPac PA 20 column (3 x 150 mm); Dionex CarboPac PA-100G Guard column (2 x 50 mm); flow rate 0.25 ml/min; 8 mM NaOH isocratic elution; 25°C; 10 μ l (2 μ g) injection; pulsed amperometric detection (Au electrode). Trace: (A) 10 μ l (2 μ g) of *B. pseudomallei* polysaccharide extract; (B) 10 μ l (2 μ g) of *B. pseudomallei* polysaccharide extract spiked with 10 μ M 6-deoxy-D-manno-heptose (32); (C) 10 μ l (2 μ g) of *B. pseudomallei* polysaccharide extract spiked with 100 μ M 6-deoxy-L-talose.

Owing to the lack of success with the extraction of the capsular polysaccharide by collaborators, we were provided with an authentic sample of *B. pseudomallei* CPS-1 (4) extracted by the Brett group in South Alabama, for use as a reference sample. The collected ^1H and HSQC data are shown in Table 3.1 and are consistent with the published data¹⁷.

	<i>H-1</i>	<i>H-2</i>	<i>H-3</i>	<i>H-4</i>	<i>H-5</i>	<i>H-6</i>	<i>H-7</i>
→3)-2-O-Ac-β-D-6dHepP-(1→	4.86	5.24	3.92	3.44	3.44	1.67/ 2.11	3.71
	<i>C-1</i>	<i>C-2</i>	<i>C-3</i>	<i>C-4</i>	<i>C-5</i>	<i>C-6</i>	<i>C-7</i>
	95.9	69.5	78.8	68.9	72.7	33.3	57.9
	<i>H-1</i>	<i>H-2</i>	<i>H-3</i>	<i>H-4</i>	<i>H-5</i>	<i>H-6</i>	<i>H-7</i>

Table 3.1: ¹H NMR (400 MHz, D₂O) and ¹³C NMR (100 MHz, D₂O) data for CPS-1 (4) sample isolated from *B. pseudomallei*^{11,13}.

3.2.2 Extraction of CPS-1 from *B. thailandensis*

Heiss and co-workers⁹ showed that the LPS (**100**) from *B. thailandensis* E264 is structurally identical to that of *B. pseudomallei* (Figure 3.4). The multiple genome alignment conducted by Sim and co-workers¹⁰ demonstrated strain E555 also has the potential to produce a similar LPS (**100**) structure. As the extraction method for the LPS (**100**) is identical to that of CPS-1 (4), an LPS-deficient mutant of *B. thailandensis* E555 was made in an attempt to simplify the extraction and purification procedure for CPS-1. The mutant strain of E555 was provided to us by our collaborator Dr A. Scott (DSTL-Porton Down) and was prepared using a pKNOCK plasmid¹⁸ inserted into the *wbil* gene to knock out LPS biosynthesis. The *wbil* gene is conserved in many LPS biosynthesis gene clusters and encodes for an oligosaccharide dehydratase/epimerase. Deletion of this gene has been shown to abrogate LPS biosynthesis in similar *B. pseudomallei* strains^{19,20}.

The *B. thailandensis* E555 $\Delta wbil$ Km^R strain was grown overnight at 37 °C in LB-Lennox media in the presence of kanamycin. The cells were collected by centrifugation and re-suspended in water, the mixture was added to hot aqueous phenol and the polysaccharide was extracted according to the method described by Burtnick and co-workers¹⁵. The crude carbohydrate material was sequentially treated with DNase, RNase and Proteinase K to digest DNA, RNA and proteins respectively before ultracentrifugation was carried out to isolate the polysaccharide.

After the crude polysaccharide sample had been collected by ultra-centrifugation a ¹H NMR spectrum was acquired (Appendix 8.2) in order to confirm the presence of

the polysaccharide. Despite the crude nature of the polysaccharide sample it was possible to see the presence of the 2-OAc peak at *ca.* 2.0 ppm. The crude preparation was lyophilised to afford 635 mg of extract. The next stage of the procedure was the acid cleavage of the lipid from the polysaccharide. As described in Section 1.2.2.1 the *B. pseudomallei* CPS-1 is a group III capsule²¹ determined by the presence of the *kps* loci in the CPS-1 biosynthetic cluster²². Currently the exact nature of the lipid anchor of CPS-1 (**4**) in *B. pseudomallei* is unknown. The *WcbA* and *wcbO* genes in the CPS-1 cluster are known homologs of the LipA and LipB proteins in *Neisseria meningitidis*²³. The *LipA* and *LipB* genes were originally thought to be responsible for the addition of a phospholipid-anchor onto the CPS-1 of *N. meningitidis*. However, Tzeng *et al*²⁴ demonstrated that these genes (homologs of *KpsC* and *KpsS* in *E. coli* (K5 - 12) were required for the translocation and expression of the polysaccharide on the cell surface, but not the addition of an anchoring group²⁴. It is believed (personal communication B. Wren (LSHTM) and N. Harmer (Exeter)) that *B. pseudomallei* CPS-1 (**4**) is assembled on a glycosylated phosphatidylglycerol (**101**) (Scheme 3.1), similar to that of the group III capsule of *S. pneumoniae*²⁵. Further genetic and biochemical analysis is required in order to validate this theory. However, if this is the case, mild acid hydrolysis of the lipid moiety will furnish the glycerol capped polysaccharide (**102**) and not a reducing terminus. The potential capping of the reducing termini has implications on the formation of CPS-1-glycoconjugates and will be discussed further in Chapter 4.

The crude carbohydrate preparation (320 mg) was treated with 2% AcOH for 4 hours at 100°C to remove the lipid carrier²⁶ (Scheme 3.1) by cleavage of the phosphate diester bond. After 4 hours, the solution was clarified by centrifugation (40 mins, 8,000 *rcf*) and lyophilised to afford the cleaved polysaccharide as a white powder (130 mg).

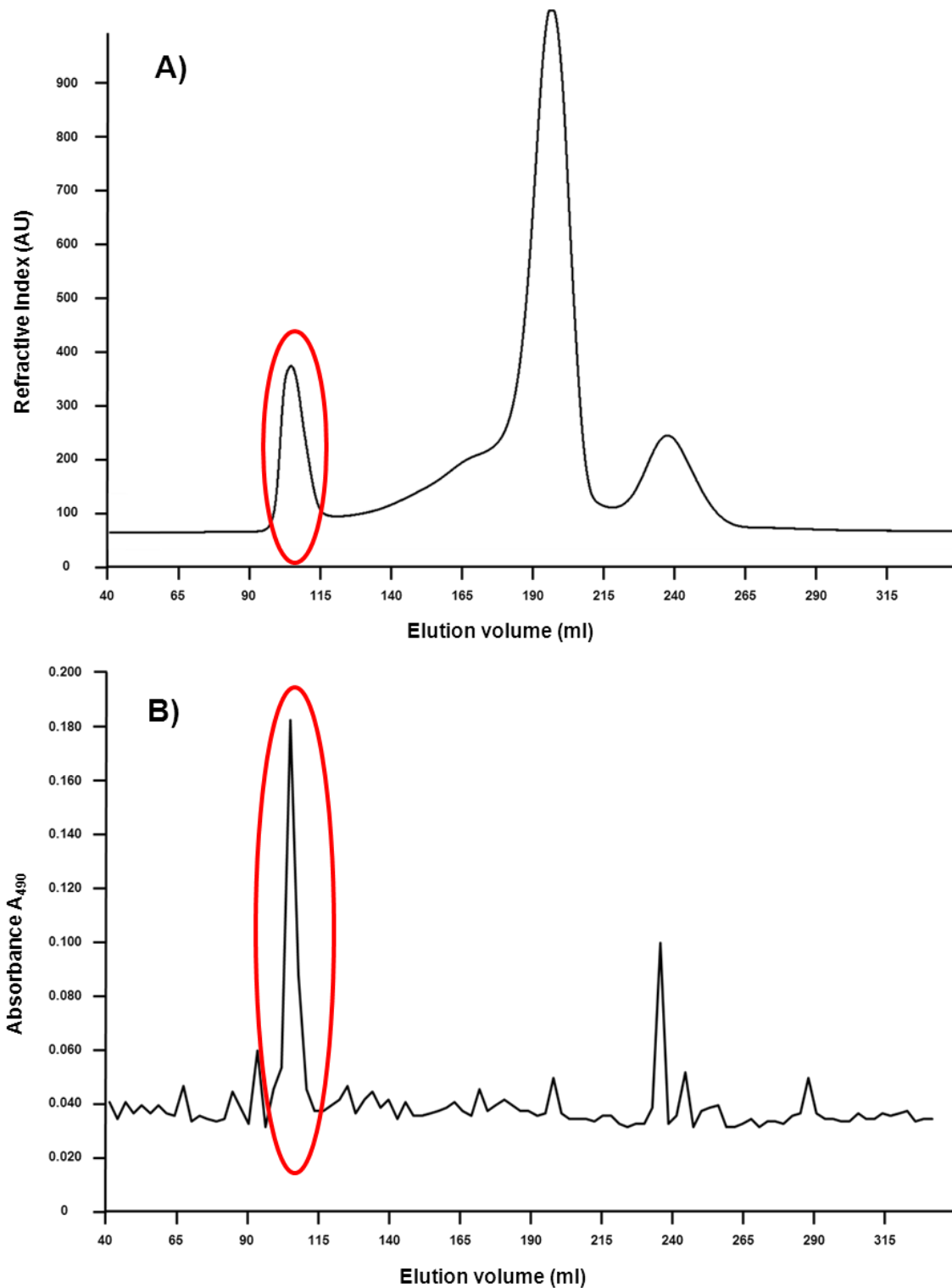
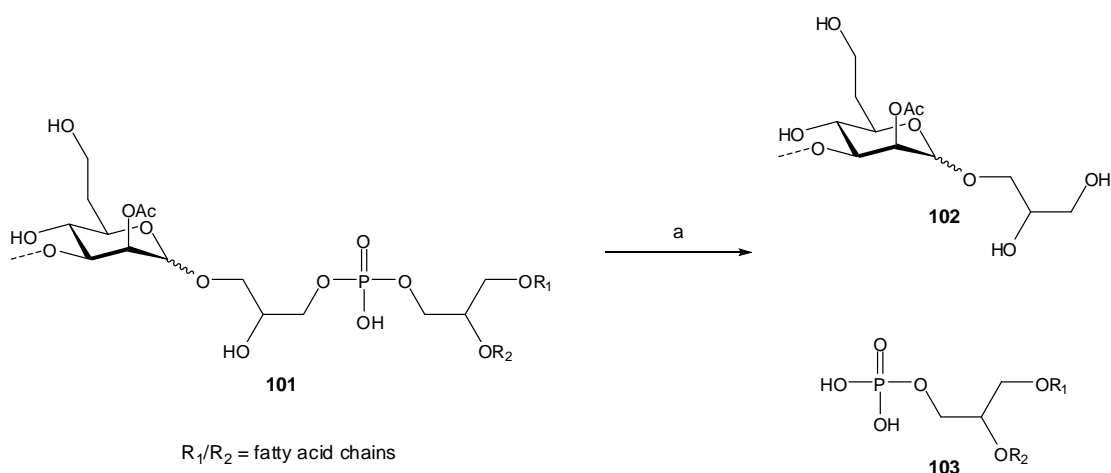


Figure 3.6: (A) Refractive index trace of GPC purification of *B. thailandensis* CPS-1. Sephadex G50 XK 26/40 column, flow rate 0.5 ml/min; eluent MQ-H₂O, sample loaded 1.5 ml at 20 mg/ml, fractions (collected 40 – 290 ml) collected for 6 min (3 ml). (B) results from phenol:sulphuric acid assay.



Scheme 3.1: Mild acid cleavage of lipid from glycerol-CPS-1 (101). Reagents and conditions: a) 2% AcOH, 100 °C, 4 h.

Purification of the CPS-1 extract from *B. thailandensis* E555 $\Delta wbiI$ (Bth-CPS-1 **104**) was subsequently achieved using gel permeation chromatography (GPC) to separate the cleaved capsular polysaccharide from the lower molecular weight impurities (Figure **3.6**). The collected fractions were assayed using the high throughput phenol-sulphuric acid assay as described by Masuko *et al*²⁷ (Section **7.1.5**). Figure **3.6** shows the refractive index trace from the GPC purification (**A**) and the corresponding phenol-sulphuric acid assay results (**B**).

The GPC trace (Figure **3.6 (A)**) shows three major peaks, with due to its size (predicted from western blot *ca.* 200 kDa)¹⁵, the Bth-CPS-1 (**104**) was expected to reside in the initial peak. The phenol:sulphuric acid assay (Figure **3.6 (B)**) confirmed that the first peak contained carbohydrate with the second peak containing no carbohydrate. The third peak contained traces of carbohydrate, but due to the nature of the purification, this was believed to be low molecular weight impurity from the bacteria and media, and were consequently discarded. The carbohydrate containing fractions were combined and lyophilised to afford Bth-CPS-1 (**104**) (5 mg from 30 mg) which was characterised using NMR (**3.2.4**), monosaccharide analysis (**3.2.5**) and capillary electrophoresis (**3.2.6**).

Table 3.2 details the starting and resulting weight from each step of the extraction and purification procedure.

Method	Starting Weight (mg)	Weight (mg)
Ultra-centrifugation	4 L of bacterial culture	635
Acid Hydrolysis	320	135
GPC purification	30	5

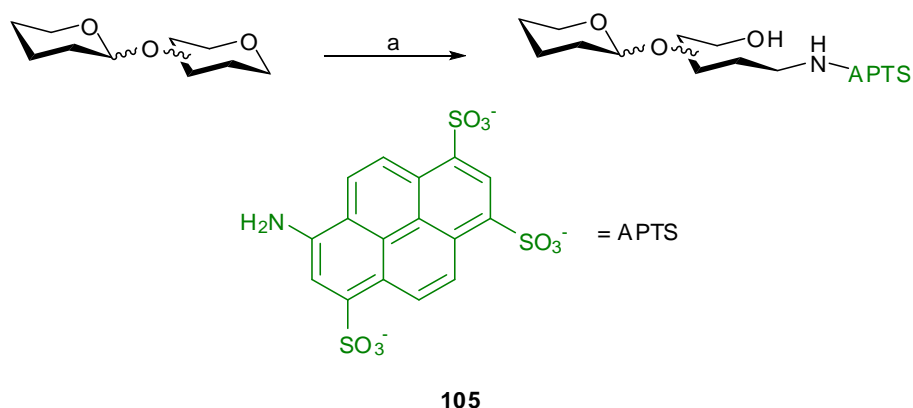
Table 3.2: Starting and resulting weight from each step of the Bth-CPS-1 (104) extraction and purification.

Based on extrapolation of the final weight of polysaccharide it is estimated that approximately 100 mg of Bth-CPS-1 (104) could be purified from the 4 litres of starting culture. This number is aligned with an ELISA estimate for Bth-CPS-1 (104) concentration on live *B. thailandensis* E555 $\Delta wbil$ cells (24 $\mu\text{g/ml}$) which was performed by collaborators at DSTL-Porton Down, subsequent to our extraction and NMR analysis (Table 3.3).

Sample	Average CPS-1 concentration ($\mu\text{g/ml}$)
<i>B. thailandensis</i> E555 (live)	22
<i>B. thailandensis</i> (Heat-killed)	8
<i>B. thailandensis</i> E555 $\Delta wbil$ (live)	24
<i>B. thailandensis</i> E555 $\Delta wbil$ (Heat-killed)	5

Table 3.3: Concentration of Bth-CPS-1 (104) present in *B. thailandensis* E555 cells before and after heat-kill treatment as determined by ELISA. (Personal communication, Marc Bayliss - DSTL).

In order to determine whether the lipid cleavage step had afforded a reducing terminus, or as expected the Bth-CPS-1 (104) molecule is capped with glycerol the purified polysaccharide was reductively aminated with 8-aminopyrene-1,3,6-trisulfonic acid (105) (APTS) (Scheme 3.2). The reaction was purified by means of a 30% mono:bis (38:2) acrylamide gel.



Scheme 3.2 Reductive amination of carbohydrate and APTS (**105**). Reagents and conditions: a) APTS, NaCNBH₃, 0.2M AcOH, THF, 37°C 18 h.

Fluorescence imaging of the gel suggested that traces of CPS-1 material had been successfully labelled with APTS (**105**) (Figure 3.7). Unfortunately, owing to the size of the Bth-CPS-1 (**104**), further analysis of this reaction was not trivial. This result demonstrates that a small population of Bth-CPS-1 (**104**) material may not be capped with glycerol and may be available for conjugation by reductive amination. However, it may be that the band corresponds to a small proportion of uncapped Bth-CPS-1 (**104**), or an unrelated polysaccharide (Section 3.2.3), and does not disprove the current hypothesis that Bth-CPS-1 (**104**) is capped with glycerol.

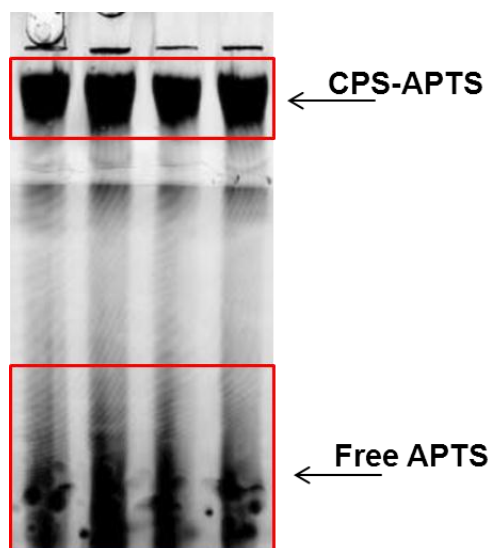


Figure 3.7: Fluorescence image of APTS-labelled CPS-1 confirm the presence of a reducing terminus. 30% mono:bis (38:2) acrylamide Tris-borate gel [100 mM; pH 8.2].

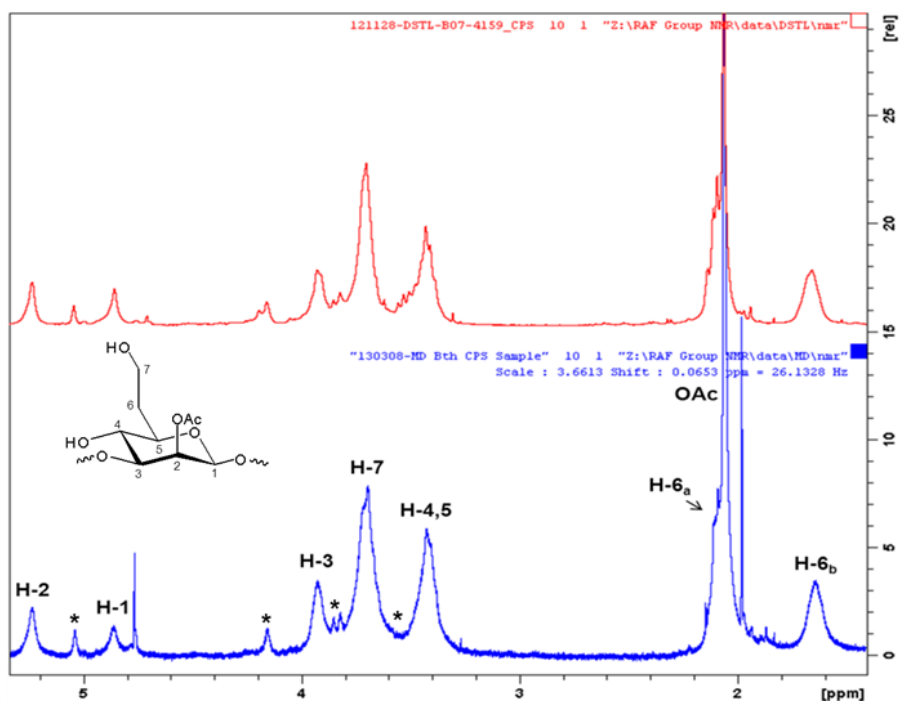


Figure 3.8: Comparison of ^1H (400 MHz, D_2O) (Red) spectrum from the authentic CPS-1 from *B. pseudomallei* (4) and (blue) the ^1H spectrum of the polysaccharide sample extracted from *B. thailandensis* E555 Δwbil (104).

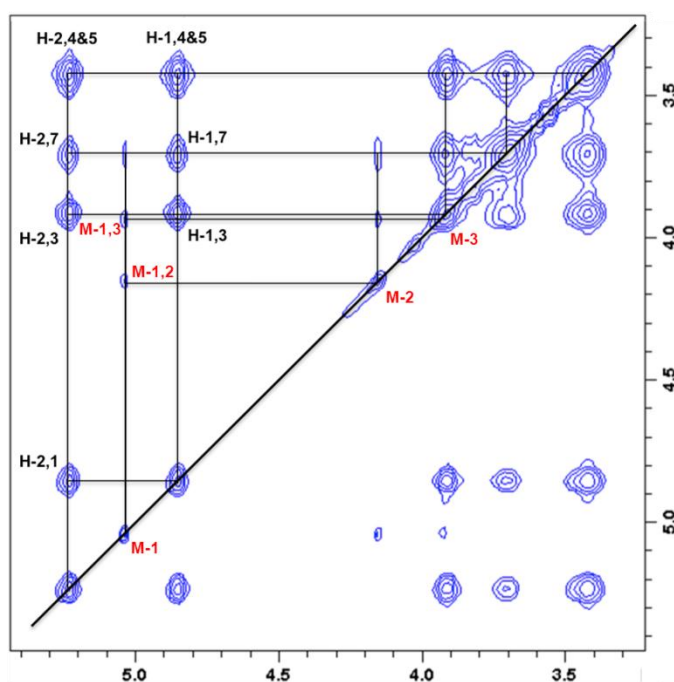


Figure 3.9: NOESY spectra *B. thailandensis* Bth-CPS-1 (104) sample. 2-O-acetyl-6-deoxy-D-manno-heptopyranose signals (black) and D-mannopyranose signals (red) with NOE coupling pattern illustrated.

3.2.3 NMR characterisation of CPS-1 extract from *B. thailandensis* E555 $\Delta wbil$

Comparison of the ^1H NMR spectra (Figure 3.8) for the authentic *B. pseudomallei* CPS-1 (**4**) sample (obtained from the Brett group¹⁵) and Bth-CPS-1 (**104**) indicated that E555 produced the same $\rightarrow 3$ -2-O-Ac- β -D-6dHepp-(1 \rightarrow) polymer (**4**) as the native *B. pseudomallei*. The two proton spectra are identical with all of the diagnostic peaks aligned, indicating the same structure in both compounds. The other major spin system (highlighted *) present in the NMR data was attributed to an α -1,3-mannan polymer (**106**), which is known to be produced by both *B. pseudomallei* and *B. mallei* strains¹⁷. A NOESY experiment (Figure 3.9) was performed to confirm the identity of the mannan polymer.

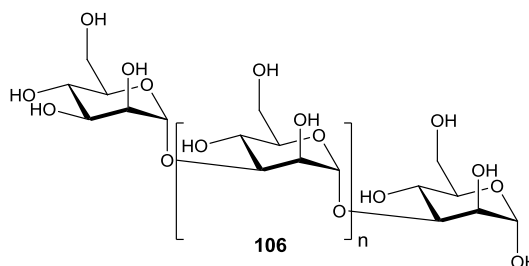


Figure 3.10: Structure of α -1,3-mannan polymer (**106**) that was co-purified with Bth-CPS-1 from *B. thailandensis* E555 $\Delta wbil$.

The NOE coupling (Figure 3.9) demonstrates (M-1,2; M-1,3 and M-2,3 pattern as shown) that the main impurity belongs to a distinct polysaccharide which corresponds to the published data for the α -1,3-D-mannan (**106**)¹⁷. The pattern also shows that there is no discernible coupling between the *B. thailandensis* E555 $\Delta wbil$ 2-O-acetyl-6-deoxy-D-manno-heptose polymer (**104**) and the α -1,3-D-mannan polymer (**106**). The current hypothesis in the field is that these are two separate polysaccharides produced by the bacteria¹⁷ (based on NOE patterns), however, to date, there has been no conclusive evidence of this point. Further work (Section 3.3) is needed to prove whether these are in fact two separate homopolymers or a blockwise-assembled heteropolymer. HSQC data (Figure 3.11) were also collected and the overlay of the reference *B. pseudomallei* CPS-1 (**4**) sample and the *B. thailandensis* E555 $\Delta wbil$ Bth-CPS-1 (**104**) mutant (Figure 3.11) further confirms the structure of the CPS-1. Corresponding ^{13}C data were also collected and are shown in the appendix (Appendix 8.3).

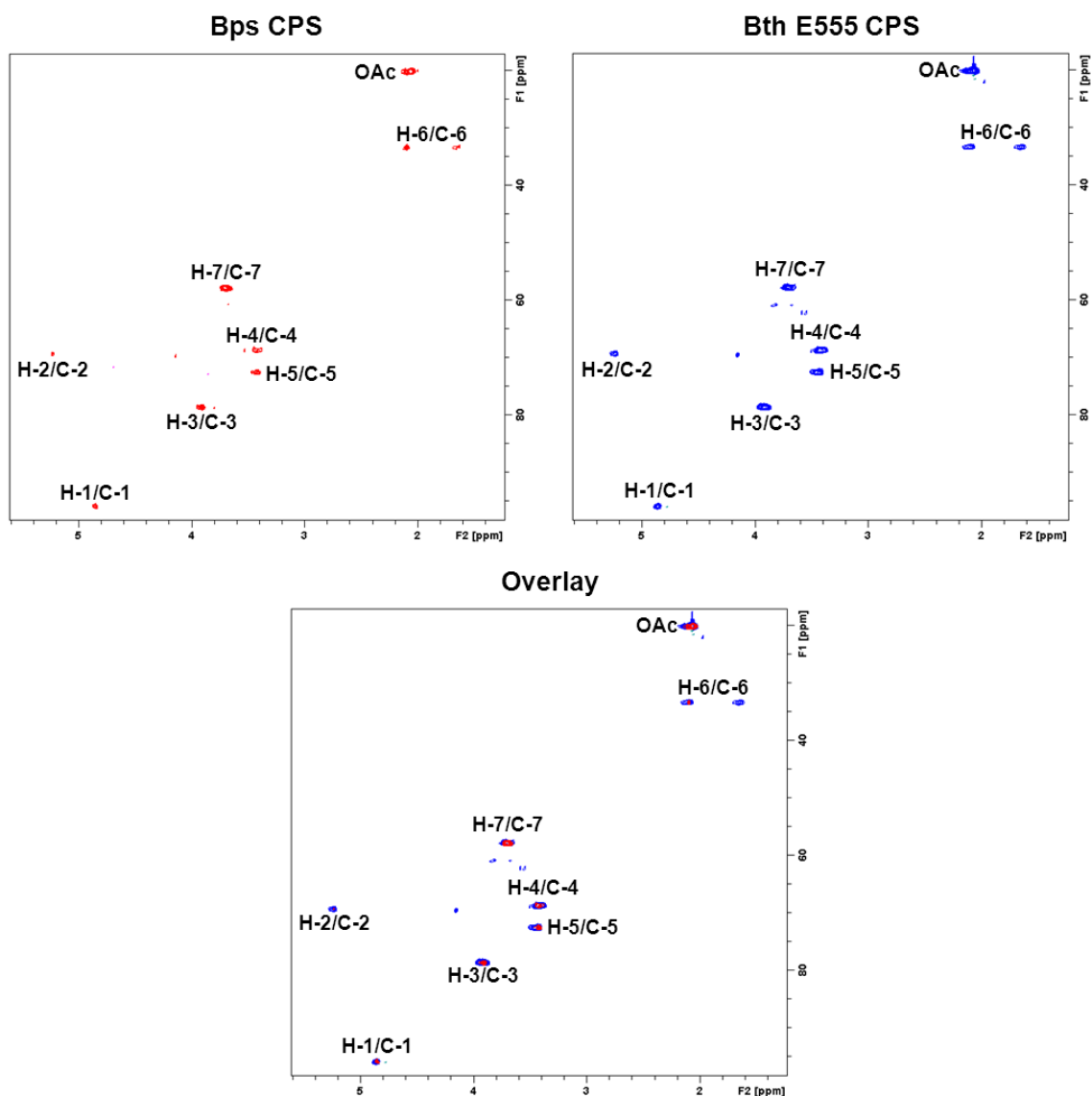


Figure 3.10: HSQC (D₂O) spectra for CPS-1 samples from (left): *B. pseudomallei* CPS-1 (4) and (right) *B. thailandensis* E555 Δ *wbil* CPS-1 (104) and overlay (Bottom): Red CPS-1 (4); Blue Bth E555 Δ *wbil* E555 CPS-1 (104).

The presence of the α -1,3-D-mannan (**106**) polymer is unique to *Burkholderia* species, that produce 2-O-acetyl-6-deoxy-D-manno-heptopyranse CPS-1 (**4**) (*B. pseudomallei*) and (**104**) (*B. thailandensis* E555 Δ *wbil*). Studies on the LPS and OPS produced by *B. thailandensis* E264 by Heiss and co-workers⁹ clearly showed the lack of the α -1,3-D-mannan polymer (**106**) in the polysaccharide extract of this bacterium. The only noticeable genomic difference between the E264 and E555 strains (disregarding the taurine metabolism genome cluster and lipocalins present in E555) is the presence of the Bps-like CPS-1 cluster¹⁰. This suggests that

enzymes for the production of both the mannan polymer (**106**) and CPS-1 (**4** and **104**) are encoded on the same Bps-CPS like gene cluster.

B. thailandensis (E555) represents the third species of *Burkholderia* which produces the 2-O-acetyl-6-deoxy-D-manno-heptose capsule (**4**) along with *B. pseudomallei* and *B. mallei*. All three of these species produce both the CPS-1 (**4**) and α -1,3-mannan (**106**) polysaccharides, but in different ratios, as shown in Table 3.4.

Bacterial Species	CPS-1	(α -1,3)-D-mannan
<i>B. pseudomallei</i>	93% ^a (82%) ^b (72%) ^c	7% ^a (18%) ^b (28%) ^c
<i>B. thailandensis</i> E555 ($\Delta wbil$)	73% ^b	27% ^b
<i>B. mallei</i>	52% ^a	48% ^a

Table 3.4: Polysaccharide content of the three different *Burkholderia* species. A) Data taken from Heiss and co-workers¹⁷ b) NMR integration value from authentic CPS-1 sample 1 Paul Brett; c) NMR integration value for authentic CPS-1 sample 2 (Paul Brett).

The data displayed for *B. pseudomallei* were taken from Heiss and co-workers¹⁷ compiled from both NMR data and monosaccharide composition analysis (gas chromatography) to determine the polysaccharide ratio of 93:7 (CPS-1:mannan). However, the NMR data that was collected (JIC) on two separate polysaccharide samples that were provided the Brett lab (in brackets) were distinctly different to the data shown in reference¹⁷ (Figure 3.12). Based on integration of the H-1 signals in the NMR spectra the mannan (**106**) accounts for 18% of polysaccharide sample 1 and 28% of polysaccharide sample 2 (proton NMR in Appendix 8.4). This indicates that there may be batch to batch variability in the composition of the CPS-1 polysaccharide(s). The ratio of mannan:CPS-1 may depend on the production environment of the bacteria; media, light, temperature and oxygen levels have all been shown to affect the composition of different bacterial polysaccharides^{28 29}.

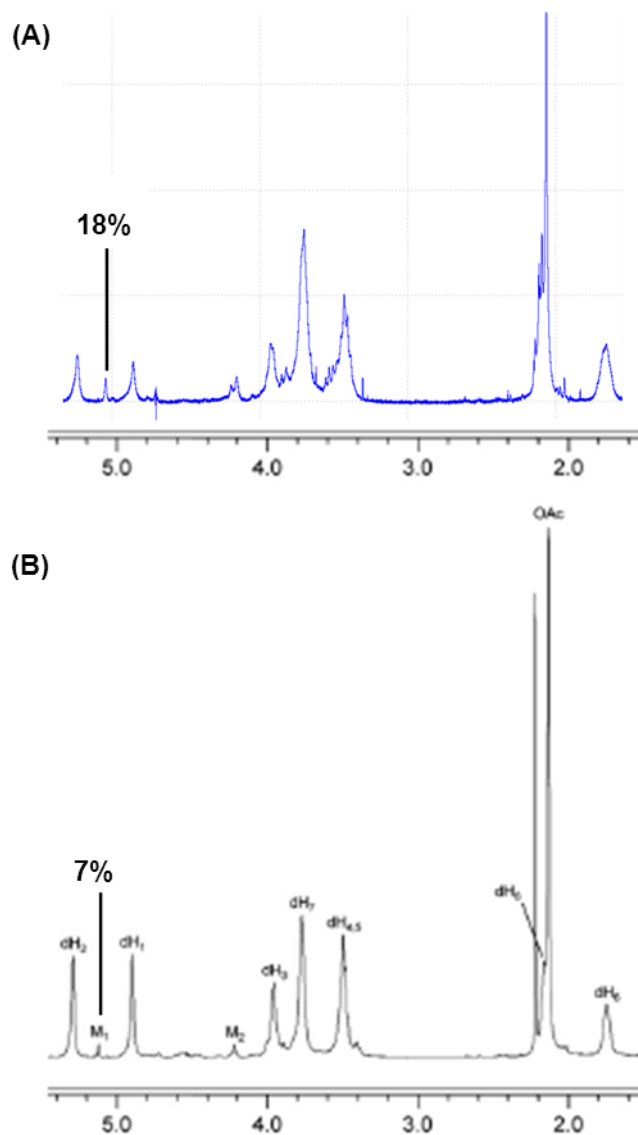


Figure 3.12: ¹H NMR (400 MHz, D₂O) of *B. pseudomallei* polysaccharide extract. (A) Polysaccharide extract from *B. pseudomallei* extracted by Brett lab and sent to JIC; (B) Reproduced with permissions, Copyright Elsevier from Heiss and co-workers¹⁷.

There is also a disparity between the monosaccharide analysis and the NMR integration ratios in the *B. thailandensis* E555 Δwbl mutant data. NMR integration estimates the mannan content to be as high as 27%, whereas monosaccharide analysis estimates the mannan content to only be ca. 10% (Figure 3.16). It is not only the ratio of CPS-1:mannan that differs between the species, the CPS-1 (**4**) in *B. pseudomallei* is estimated to be ca. 200 kDa in length, whereas that of *B. mallei* is estimated to be 145 kDa based on SDS-PAGE and alignment with protein standards. Analysis of the *B. thailandensis* E555 Δwbl capsule (**104**) by Scott and

co-workers (Figure 3.13) showed that it was of a similar size (200 kDa) to that of *B. pseudomallei* (4) (K96243)¹¹.

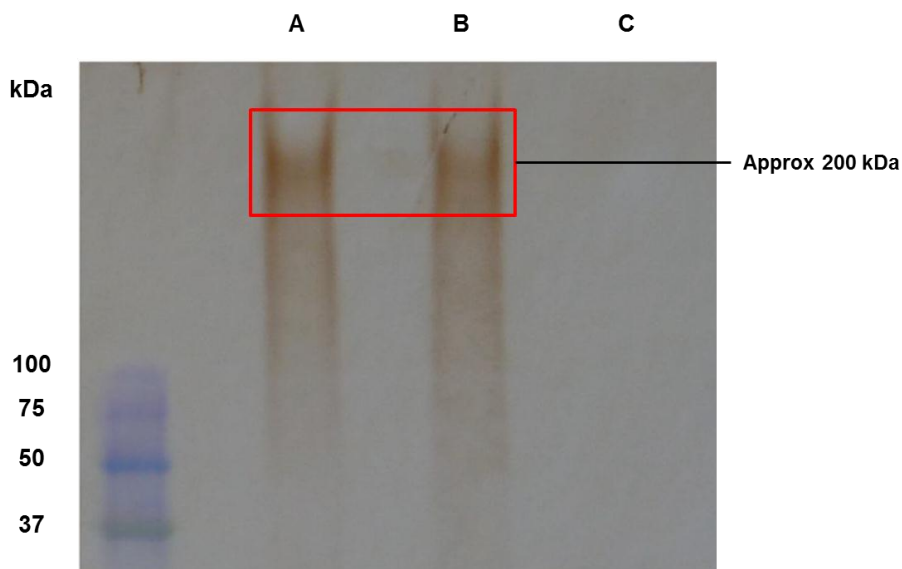


Figure 3.13: Immunoblot of CPS-1 produced by (A) *B. pseudomallei* (4) (K96243); (B) *B. thailandensis* E555 $\Delta wbil$ (98) and (C) *B. thailandensis* E263. Reproduced with permission from Scott and co-workers¹¹.

3.2.4 Monosaccharide analysis of CPS-1 extracted from *B. thailandensis* E555 ($\Delta wbil$ pKNOCK-KmR mutant)

Bth-CPS-1 (104) was subjected to full acid hydrolysis according to general protocol 7.1.6. The acid hydrolysed Bth-CPS-1 (104) extract was injected onto the Dionex system as before (Figure 3.14). Of the three peaks present in the Bth-CPS-1 (104) sample, two have been identified as 6-deoxy-D-manno-heptopyranose (A) and D-mannopyranose (B), both of which were elucidated using spiking experiments (Figures 3.15 & 3.16).

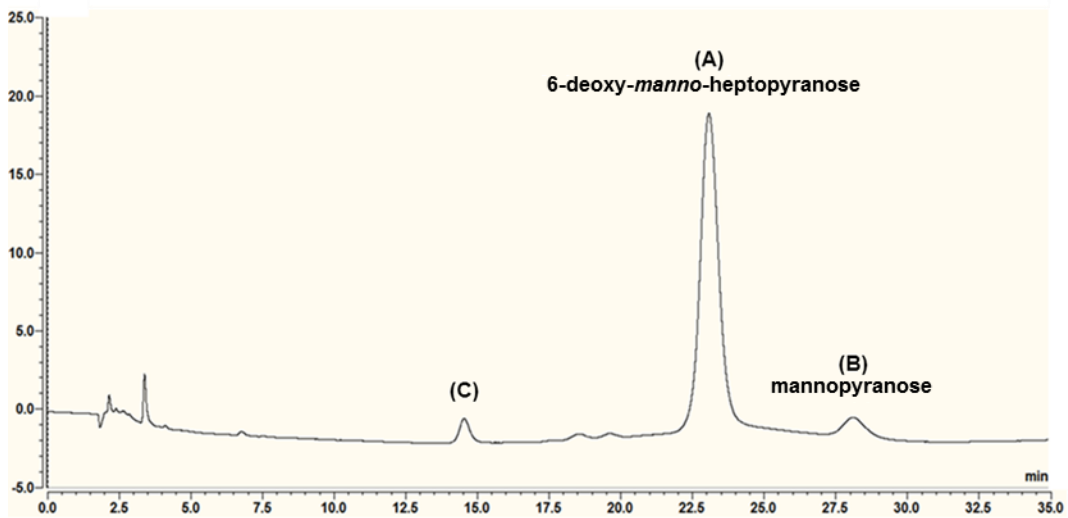


Figure 3.14: Chromatogram of CPS-1 extract monosaccharide analysis. Dionex CarboPac PA 20 column (3 x 150 mm); Dionex CarboPac PA-100G Guard column (2 x 50 mm); flow rate 0.25 ml/min; 8 mM NaOH isocratic elution; 25°C; 10 μ l (2 μ g) injection; pulsed amperometric detection (Au electrode).

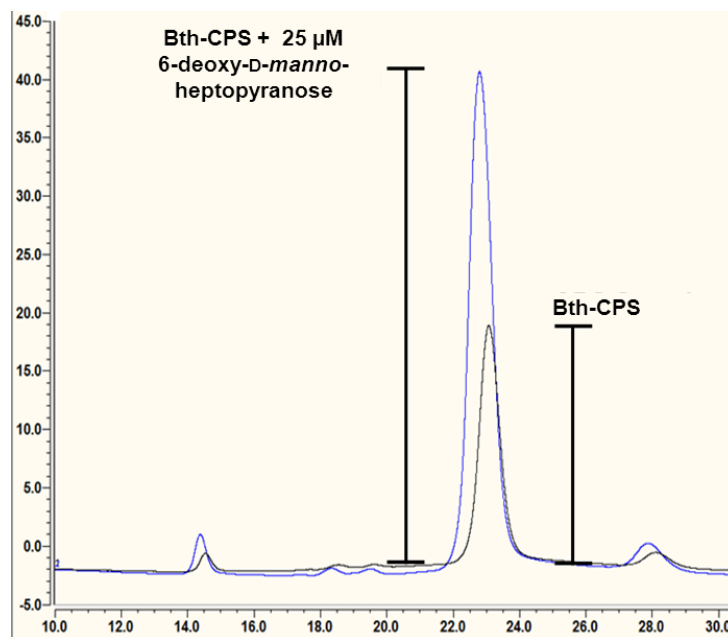


Figure 3.15: Zoomed in region of the Bth-CPS-1 (98) monosaccharide analysis. (Blue) Bth-CPS-1 sample; (Black) Bth-CPS-1 sample spike with 25 μ M 6-deoxy-D-manno-heptopyranose standard. Dionex CarboPac PA 20 column (3 x 150 mm); Dionex CarboPac PA-100G Guard column (2 x 50 mm); flow rate 0.25 ml/min; 8 mM NaOH isocratic elution; 25°C; 10 μ l (2 μ g) injection; pulsed amperometric detection (Au electrode).

The increase in relative peak height when the Bth-CPS-1 (**104**) sample was spiked with the heptose monosaccharide (25 μM) confirms the main structural component of this polysaccharide is 6-deoxy-D-manno-heptopyranose (**32**) (Figure 3.15). The D-mannopyranose experiment below (Figure 3.16) shows an increase in the integration of the smaller peak when D-mannose is co-injected with the sample, thus confirming the identity of the peak as D-mannose.

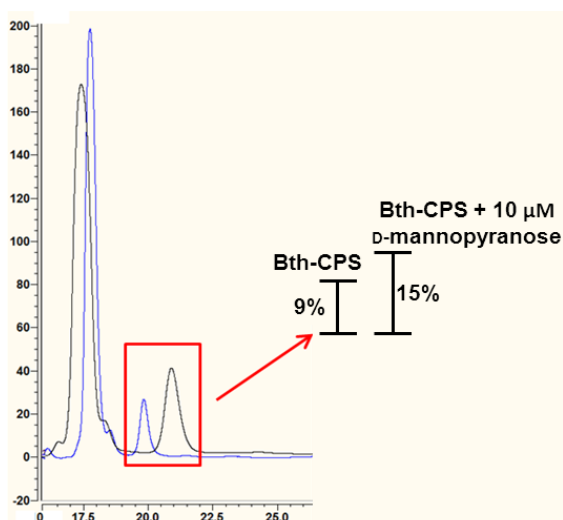


Figure 3.16: Monosaccharide analysis of CPS-1. (Blue) CPS-1 sample; (Black) CPS-1 sample spiked with 10 μM mannose standard. Dionex CarboPac PA 20 column (3 x 150 mm); Dionex CarboPac PA-100G Guard column (2 x 50 mm); flow rate 0.25 ml/min; 8 mM NaOH isocratic elution; 25°C; 10 μl (2 μg) injection; pulsed amperometric detection (Au electrode).

The identity of the first peak (Figure 3.14, peak **C**) is still unknown, experiments (data not shown) were run to determine whether the peak corresponded to 6-deoxy-L-talose, one of the constituents of *B. thailandensis* LPS (**100**) or L-rhamnose, part of the CP-2 polysaccharide (Section 1.2.2). Both of these experiments proved that neither 6-deoxy-talopyranose or rhamnopyranose were present in the Bth-CPS-1 (**104**) sample, indicating the lack of LPS (**100**) or CP-2 in the polysaccharide extract. The peak accounts for 3-4% of the trace and cannot be seen in NMR studies. Owing to this it was left unidentified for the purposes of the current study.

3.2.5 Partial acid hydrolysis and capillary electrophoresis experiments

As part of the vaccine development project the use of both intact CPS-1 (**4**) and fragments of the CPS-1 are to be investigated. After successful extraction and purification of Bth-CPS-1 (**104**) from the non-pathogenic strain *B. thailandensis* E555 $\Delta wbiI$ the partial acid hydrolysis of Bth-CPS-1 (**104**) backbone was attempted. A search of the literature found several methods for the incomplete hydrolysis of polysaccharides^{30 31}. Di and co-workers³² carried an extensive study into the effects of temperature, strength and volume of acid used on partial hydrolysis of polysaccharides from fruiting spores of Lingzhi mushrooms. It was concluded that 1 mL of 0.75 M H₂SO₄ in a sealed vial at 85°C were the optimal conditions for partial hydrolysis of polysaccharides. BaCO₃ was used for the neutralisation of the acid due to the poor solubility of BaSO₄, which is formed during the neutralisation and can be easily removed by centrifugation.

The next stage was to label the crude oligosaccharide preparation with a fluorescent tag for analysis with capillary electrophoresis (CE). Previously, the Field lab has demonstrated the high sensitivity and resolution of CE can be implemented for the analysis of carbohydrates³³. CE analysis separates ions based on their electrophoretic mobility with the use of a strong voltage and laser-induced fluorescence detection (LIF)³⁴. In order for the neutral oligosaccharides to be compatible with CE analysis they must first be labelled with a charged fluorescent tag. The reductive amination of carbohydrates with APTS (**105**) (Scheme **3.2**) for the labelling of carbohydrates for CE has been shown to be highly efficient and reproducible (88% yield for maltose)³⁵.

The oligosaccharide fragments were successfully labelled with APTS (**105**) as described in experimental Section **7.3.4**. After purification by gel electrophoresis the APTS labelled oligosaccharides were extracted and injected onto the CE.

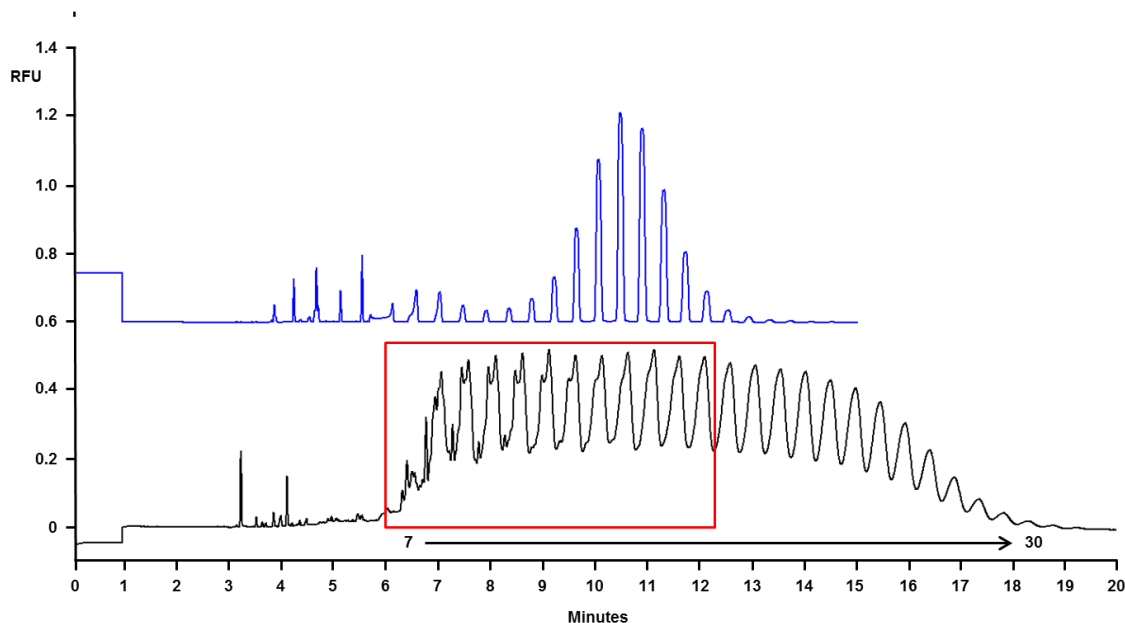


Figure 3.17: CE trace of APTS labelled CPS-1 oligosaccharides. (Top) Glucose ladder (Bottom) CPS-1 oligosaccharides labelled with APTS.

The CE trace above (Figure 3.17) demonstrates the successful partial hydrolysis of the native Bth-CPS-1 (**104**) using 0.75 M H₂SO₄, to afford CPS-1 oligosaccharides ranging from DP 7 to ca. 30. In the dp 7-15 region (highlighted in red box) the resolution is sufficient to pick up two distinct oligosaccharides for each peak. Due to the mild conditions needed for the partial hydrolysis full deacetylation of the polysaccharide would not occur resulting in a mixture of *O*-acetylated and de-*O*-acetylated species, giving rise to the double peaks. In order to verify this, the sample was de-*O*-acetylated with hydrazine monohydrate at elevated temperature and run on the CE again. The contraction of the two peaks into a single peak confirmed the presence of both *O*-acetylated and de-*O*-acetylated residues in the oligosaccharide polymers (Figure 3.18).

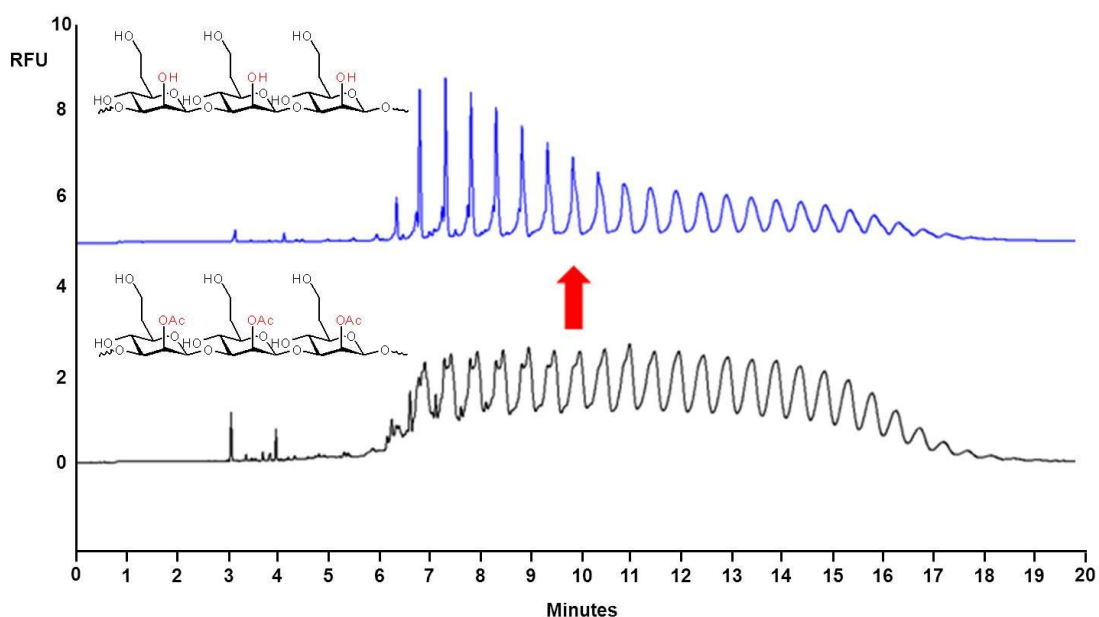


Figure 3.18: CE trace for the deacylation of Bth-CPS-1 oligosaccharides. (Top) fully deacylated CPS-1 oligosaccharides. (Bottom) Mixed CPS-1 oligosaccharides.

The CE trace of the lower bands (Sample 2, Section 7.3.4) indicated the presence of lower weight (dp 1-6) oligosaccharides from the mild acid hydrolysis. There is currently work on-going to develop the acid hydrolysis procedure to enable tailoring of the hydrolysis to produce products of more defined length.

3.3 Conclusions

The lack of CPS-1 (**4**) in either *B. pseudomallei* extracts, both of which reacted positively with the mAb 4IVH12 raised against heat-killed *B. pseudomallei* cells, highlights issues regarding the use of antibody identification of CPS-1 (**4**). During their work on the characterization of the *B. pseudomallei* (K96243) CPS-1 coding region, Cuccui and coworkers²¹ demonstrated that the 4V1H12 mAb was a reliable tool for the detection of CPS-1 (**4**) in a range of *B. pseudomallei* mutants. We have also shown that the antibody is reactive to purified CPS-1 extracted from both *B. pseudomallei* (**4**) and *B. thailandensis* E555 $\Delta wbiI$ (**104**). However, owing to the results described in Section 3.2.1, the use of the mAb 4IVH12 is not sufficient for the confirmation of extractable quantities of material. This is probably down to the inherent sensitivity of the antibody detection versus NMR and monosaccharide analyses. It is assumed that there are small traces of the CPS-1 (**4**) material

present in this sample, which can be detected by the blot technique but cannot be purified and characterised by NMR.

The fact that no CPS-1 (4) can be purified from these samples can possibly be attributed to the heat-kill treatment which was carried out during the culturing of the bacteria. Owing to the stringent health and safety requirements of working with *B. pseudomallei* at DSTL-Porton Down, the bacteria must be heated to 80°C for 4 hours before being sterility checked. Subsequently to our NMR analysis collaborators on the growth optimisation of *B. thailandensis* E555 $\Delta wbil$ has shown there is a dramatic reduction in the quantity of CPS-1 (4 & 104) on the bacteria post heat-kill treatment (Table 3.3).

Sample	Average CPS-1 concentration ($\mu\text{g/ml}$)
<i>B. thailandensis</i> E555 (live)	22
<i>B. thailandensis</i> (Heat-killed)	8
<i>B. thailandensis</i> E555 $\Delta wbil$ (live)	24
<i>B. thailandensis</i> E555 $\Delta wbil$ (Heat-killed)	5

Table 3.3: Concentration of Bth-CPS-1 (104) present in *B. thailandensis* E555 cells before and after heat-kill treatment as determined by ELISA. (Personal communication, Marc Bayliss - DSTL).

During the heat-kill procedure it is believed that CPS-1 (4) is shed into the media, as the cells are harvested by centrifugation, it is expected that the majority of the CPS-1 (4) is lost at this stage in the supernatant, which was discarded. In order for the successful purification of CPS-1 (4) from *B. pseudomallei* bacteria, the supernatant from the heat-kill procedure must be retained and analysed for polysaccharide content.

This chapter has discussed the first structural characterisation of the $\rightarrow 3$)-2-O-Ac- β -D-6dHepp-(1 \rightarrow) capsular polysaccharide (4) of *B. pseudomallei* produced by a similar non-pathogenic strain, *B. thailandensis* E555 $\Delta wbil$ (Bth-CPS-1 (104)). Owing to the size (ca. 200 kDa) of the capsular polysaccharide isolated from the *Burkholderia* strains, in depth characterisation and analysis of the structure of the

intact polysaccharide is non-trivial. NMR data has provided some insight into the structural similarities between the Bth-CPS-1 (**104**) isolated from *B. thailandensis* E555 $\Delta wbi1$ and the CPS-1 (**4**) previously isolated from both *B. pseudomallei* and *B. mallei*. Based on these findings it can be concluded that the main structural component of this polymer is based on the 6-deoxy-mannoheptopyranose (**32**). However, during the course of the NMR characterisation a number of inconsistencies have been observed. The presence of an α -1,3-mannan polymer (**106**) has shown to be present in all CPS-1 samples to a varying degree. It has been shown that this variation is not solely based on strain, but also as a result of batch to batch variability from the same strain. Full extraction, purification and characterisation of the mannan polymer has, as yet not been achieved. If, as currently believed in the field, these are two separate polymers, the role of the α -1,3-mannan (**106**) polymer on the virulence of *B. pseudomallei* needs to be investigated. Currently the CPS-1 'specific' monoclonal antibodies used in *Burkholderia* research have been raised against whole *Burkholderia* cells. These antibodies have been shown on numerous occasions to be reactive towards purified CPS-1 samples that contain a degree of mannan polymer (**106**), making it unclear which epitope the antibodies are in fact binding to. If the mannan component is dominant in immune recognition, the use of synthetic oligosaccharide fragments of CPS-1 derived antibodies may not be sufficient to provide protective immunity against *B. pseudomallei*.

With regard to the use of CPS-1 (**4**) conjugate vaccines, the presence of the mannan polymer (**106**) is less complex. In fact having both the CPS-1 (**4**) and mannan (**106**) polysaccharides conjugated to a carrier protein may be advantageous for antibody generation and subsequent protection. From a regulatory point of view, however, it may be essential for full characterisation of all constituent parts of the glycoconjugate before clinical trials are established. To this end, work needs to be under-taken to gain more insight into the nature and role of the mannan (**106**) component. As previously stated, the only discernible difference between *B. thailandensis* E264 and E555 is the presence of the *B. pseudomallei* CPS-1-like genome cluster. This cluster is assumed to be responsible for the synthesis of both CPS-1 and mannan polysaccharide. Mutation of the three putative glycosyltransferases (*WcbB*, *WcbE* and *WcbH*)²¹ in the CPS-1 cluster coupled with extraction and structural analysis of polysaccharide products could

help to elucidate the nature of the mannan polymer (**106**). A further characterisation of the mAb 4IVH12 monoclonal antibody is discussed in Section **4.4.3** & **4.4.4**.

However, the successful production of CPS-1 in an avirulent strain of bacteria is a great step forward in the vaccine development program for *B. pseudomallei*. Through the use of *B. thailandensis* E555 $\Delta wbiI$ the large scale fermentation of Bth-CPS-1 (**104**) is now a possibility, enabling its use in immunisation trials. It has been shown that the capsule can be partially hydrolysed to produce oligosaccharide fragments; both O-acetylated and de-O-acetylated which are suitable for conjugation. Currently there is on-going work into the optimisation of the partial acid hydrolysis of the polysaccharide and the conjugation of Bth-CPS-1 (**104**) and corresponding oligosaccharide fragments for immunisation trials. The Bth-CPS-1 (**104**) was then taken forward for use in the immunological assessment of the mAb 4IVH12 monoclonal antibody and the 6dHep-TetHc (**95**) derived polyclonal antibodies.

3.4 References

1. V. Wuthiekanun, M. D. Smith, D. A. B. Dance, A. L. Walsh, T. L. Pitt and N. J. White, *J. Med. Microbiol.*, 1996, **45**, 408-412.
2. W. J. Wiersinga, A. F. De Vos, R. De Beer, C. W. Wieland, J. J. T. H. Roelofs, D. E. Woods and T. Van Der Poll, *Cell. Microbiol.*, 2008, **10**, 81-87.
3. M. B. Glass, J. E. Gee, A. G. Steigerwalt, D. Cavuoti, T. Barton, R. D. Hardy, D. Godoy, B. G. Spratt, T. A. Clark and P. P. Wilkins, *J. Clin. Microbiol.*, 2006, **44**, 4601-4604.
4. N. Lertpatanasuwan, K. Sermsri, A. Petkaseam, S. Trakulsomboon, V. Thamlikitkul and Y. Suputtamongkol, *Clin. Infect. Dis.*, 1999, **28**, 927-928.
5. P. J. Brett, D. DeShazer and D. E. Woods, *Int. J. Syst. Bacteriol.*, 1998, **48**, 317-320.
6. A. Haraga, T. E. West, M. J. Brittnacher, S. J. Skerrett and S. I. Miller, *Infect. Immun.*, 2008, **76**, 5402-5411.
7. M. T. G. Holden, R. W. Titball, S. J. Peacock, A. M. Cerdeno-Tarraga, T. Atkins, L. C. Crossman, T. Pitt, C. Churcher, K. Mungall, S. D. Bentley, M. Sebahia, N. R. Thomson, N. Bason, I. R. Beacham, K. Brooks, K. A. Brown, N. F. Brown, G. L. Challis, I. Cherevach, T. Chillingworth, A. Cronin, B. Crosssett, P. Davis, D. DeShazer, T. Feltwell, A. Fraser, Z. Hance, H. Hauser, S. Holroyd, K. Jagels, K. E. Keith, M. Maddison, S. Moule, C. Price, M. A. Quail, E. Rabinowitsch, K. Rutherford, M. Sanders, M. Simmonds, S. Songsivilai, K. Stevens, S. Tumapa, M. Vesaratchavest, S. Whitehead, C. Yeats, B. G. Barrell, P. C. F. Oyston and J. Parkhill, *Proc. Nat. Acad. Sci. U.S.A.*, 2004, **101**, 14240-14245.
8. Yu. Y, H. S. Kim, H. H. Chua, C. H. Lin, S. H. Sim, D. Lin, A. Derr, R. Englels, D. DeShazer, B. Birren, W. C. Nierman and P. Tan, *BMC Microbiol.*, 2006, **6**, 1 - 17.
9. C. Heiss, M. N. Burtnick, I. Black, P. Azadi and P. J. Brett, *Carbohydr. Res.*, 2012, **363**, 23-28.
10. B. M. Q. Sim, N. Chantratita, W. F. Ooi, T. Nandi, R. Tewhey, V. Wuthiekanun, J. Thaipadungpanit, S. Tumapa, P. Ariyaratne, W.-K. Sung, X. H. Sem, H. H. Chua, K. Ramnarayanan, C. H. Lin, Y. Liu, E. Feil, M. Glass, G. Tan, S. Peacock and P. Tan, *Genome Biology*, 2010, **11**, R89.
11. A. E. Scott, T. R. Laws, R. V. D'Elia, M. G. M. Stokes, T. Nandi, E. D. Williamson, P. Tan, J. L. Prior and T. P. Atkins, *Clinical and Vaccine Immunology*, 2013, **20**, 1041-1047.
12. R. P. Beasley, G. Chin-Yun Lee, C.-H. Roan, L.-Y. Hwang, C.-C. Lan, F.-Y. Huang and C.-L. Chen, *The Lancet*, 1983, **322**, 1099-1102.
13. V. Johannes F.G, *FEBS Lett.*, 2006, **580**, 2945-2950.
14. M. N. Burtnick, C. Heiss, R. A. Roberts, H. P. Schweizer, P. Azadi and P. J. Brett, *Frontiers in cellular and infection microbiology*, 2012, **2**, 108.

15. M. N. Burtnick, C. Heiss, R. A. Roberts, H. P. Schweizer, P. Azadi and P. J. Brett, *Frontiers in cellular and infection microbiology*, 2012, **2**.
16. Y. A. Knirel, N. A. Paramonov, A. S. Shashkov, N. K. Kochetkov, R. G. Yarullin, S. M. Farber and V. I. Efremenko, *Carbohydr. Res.*, 1992, **233**, 185-193.
17. C. Heiss, M. N. Burtnick, Z. Wang, P. Azadi and P. J. Brett, *Carbohydr. Res.*, 2012, **349**, 90-94.
18. M. F. Alexeyev, *BioTechniques*, 1999, **26**, 824-828.
19. A. Tuanyok, J. K. Stone, M. Mayo, M. Kaestli, J. Gruendike, S. Georgia, S. Warrington, T. Mullins, C. J. Allender, D. M. Wagner, N. Chantratita, S. J. Peacock, B. J. Currie and P. Keim, *PLoS Negl Trop Dis*, 2012, **6**, e1453.
20. D. DeShazer, P. J. Brett and D. E. Woods, *Mol. Microbiol.*, 1998, **30**, 1081-1100.
21. J. Cuccui, T. S. Milne, N. Harmer, A. J. George, S. V. Harding, R. E. Dean, A. E. Scott, M. Sarkar-Tyson, B. W. Wren, R. W. Titball and J. L. Prior, *Infect. Immun.*, 2012.
22. C. Whitfield, *Annu. Rev. Biochem*, 2006, **75**, 39-68.
23. S. L. Reckseidler, D. DeShazer, P. A. Sokol and D. E. Woods, *Infect. Immun.*, 2001, **69**, 34-44.
24. Y.-L. Tzeng, A. K. Datta, C. A. Strole, M. A. Lobritz, R. W. Carlson and D. S. Stephens, *Infect. Immun.*, 2005, **73**, 1491-1505.
25. R. T. Cartee, W. T. Forsee and J. Yother, *J. Bacteriol.*, 2005, **187**, 4470-4479.
26. M. Caroff, A. Tacken and L. Szabó, *Carbohydr. Res.*, 1988, **175**, 273-282.
27. T. Masuko, A. Minami, N. Iwasaki, T. Majima, S.-I. Nishimura and Y. C. Lee, *Anal. Biochem.*, 2005, **339**, 69-72.
28. G. A. Somerville and R. A. Proctor, *Microbiology and Molecular Biology Reviews*, 2009, **73**, 233-248.
29. S. Burdman, E. Jurkevitch, M. a. E. Soria-Díaz, A. M. G. Serrano and Y. Okon, *FEMS Microbiology Letters*, 2000, **189**, 259-264.
30. W. H. Jiang, J. T. Wotach, R. L. Keil and V. P. Bhavanandan, *Biochemistry Journal*, 1998, **331**, 193-199.
31. Z. El-Rassi, *Carbohydrate Analysis by Modern Chromatography and Electrophoresis*, Elsevier, 2002.
32. X. Di, K. K. C. Chan, H. W. Leung and C. W. Huie, *J. Chromatogr. A*, 2003, **1018**, 85-95.
33. E. Prifti, S. Goetz, S. A. Nepogodiev and R. A. Field, *Carbohydr. Res.*, 2011, **346**, 1617-1621.

34. R. A. Evangelista, M.-S. Liu and F.-T. A. Chen, *Anal. Chem.*, 1995, **67**, 2239-2245.
35. M. G. O'Shea, M. S. Samuel, C. M. Konik and M. K. Morell, *Carbohydr. Res.*, 1998, **307**, 1-12.

4 Chapter 4: Immunological assessment of anti-monosaccharide antibodies

This chapter describes the preliminary immunological assessment of the anti-monosaccharide polyclonal sheep sera. Enzyme-linked immunosorbent assays (ELISAs) and slot-blot techniques were used to determine the activity and specificity of the polyclonal sera to the cognate monosaccharide. Based on the results obtained, four more monosaccharide haptens were developed in an attempt to further investigate the antigenic potential of monosaccharide haptens. Analysis of anti-CPS-1 monoclonal antibody (mAb 4IVH12) and the 6dHep-TetHc polyclonal serum with the Bth-CPS-1 extract (**106**) was also carried out.

4.1 Generation of polyclonal antibodies

In collaboration with Ig Innovations, polyclonal antibodies to the 6dHep-TetHc (**94**) and Glc-TetHc (**96**) antigens were raised in sheep (2 sheep per antigen). Sheep were chosen as the animal model due to previous experience of industrial collaborators, Mologic, who have experienced a number of antigens which have successfully generated antibodies in ovine systems when other systems have failed (eg. mice and rabbits). Mologic have demonstrated the successful generation of ovine antibodies against a broad range of antigens, including carbohydrates and it was felt that this model offered the highest chance for success for the monosaccharide antigens (personal communication Mark Davis, Mologic).

Two sheep per antigen were immunised as described in experimental section **7.4.1**; the schedule for the immunisations is described below (Figure **4.1**). Serum samples from 0, 6, 10, 14 & 18 weeks were collected and analysed for immunological activity.

Action	Description	Week(s)
Pre-immune serum collection	Pre-immune sample blood collected, serum isolated from clot via centrifugation	0
Primary immunisation	0.5 mg of antigen for 2 sheep; emulsion made up with saline and Freund's Complete Adjuvant (CFA) 6 x injection sites per sheep	0
Re-immunisation	0.25 mg of antigen for 2 sheep, emulsion made up with saline and Freund's Incomplete Adjuvant (IFA) 6 x injection sites per sheep	4, 8, 12,16
Bleeds	Sample blood collected, serum isolated from clot via centrifugation	6, 10, 14, 18

Figure 4.1: Immunisation schedule for antibody generation at Ig-innovations.

The primary immunisation included Freund's Complete Antigen (CFA) which comprises a water/oil emulsion in the presence of inactivated Mycobacterial cells. CFA is used as an immunopotentiator and is known to enhance the reaction of a given antigen¹. The use of adjuvants, particularly those containing bacterial cells (CFA), is strictly regulated in antibody generation due to the negative effects on the host^{2 3}. For this reason, re-immunisations were performed with the addition of Freund's Incomplete Adjuvant (IFA), which is based simply on a water/oil emulsion. Emulsion based adjuvants such as CFA/IFA act as 'depot' adjuvants, which protect the antigen from degradation and expulsion from the host system along with dilution effects. In doing this the adjuvant achieves slow-release of intact antigen extending the period of exposure to the host's immune system. This results in the continual activation of the antibody generating cells leading to improved levels of antibody production¹.

4.1.1 Kinetics of the immune response

Re-immunisation with an antigen is required for the development of cellular memory by the immune system and the generation of highly specific antibodies. Upon initial immunisation (priming), the generation of antibodies is slow, with a latent period of up to 2 weeks, depending on the species, after which time the production of antibodies begins. IgM (macroglobulin) is typically the first class of antibody

produced during an immune response, followed by IgG. Even with the use of adjuvants, initial antibody production generally ceases entirely after 3-4 weeks⁴. However, re-immunisation with the same antigen leads to constant stimulation of the immune system and the development of a stronger immune response. After the priming event, the latent period is much shorter with the secondary immunisation and the amount, type and quality of antibodies is increased. There is also an increase in class switching from IgM to IgG, with IgG antibodies appearing in much higher concentrations (Figure 4.2)⁵.

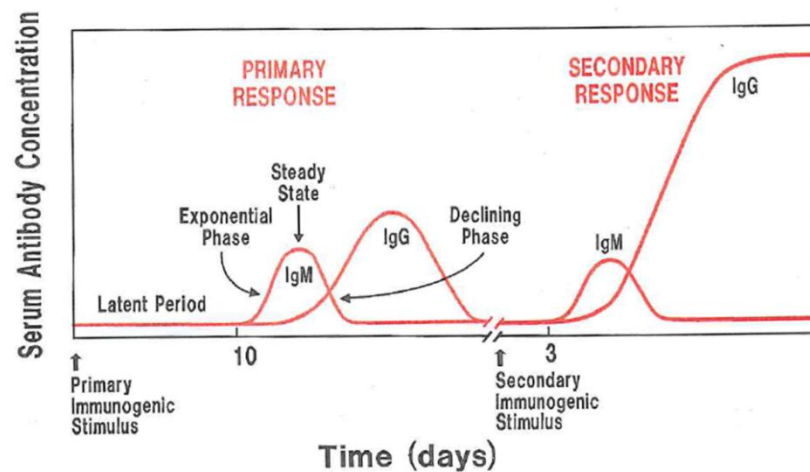


Figure 4.2: Kinetics of an immune response. The latent period is the time taken for B-cells to come into contact with antigen and start producing antibodies. The length of the latent period is dependent on the species, antigen and adjuvant used. Figure reproduced with permissions from Immunology: a Short Course Copyright John Wiley and Sons 2009⁵.

Affinity maturation of the antibodies⁶ occurs as a result of a B-cell selection process. The differentiation of B-cells into antibody producing plasma cells is triggered by the binding of B-cells to the antigen. As the concentration of antibody increases in the blood there is greater competition between the B-cells and antibody for the free antigen. As a result only the B-cells with high-affinity receptors located on their surface will be able to bind to the antigen and thus differentiate into plasma cells. This preferential selection of B-cells leads to the development of antibodies with high antigen affinity^{5,7}.

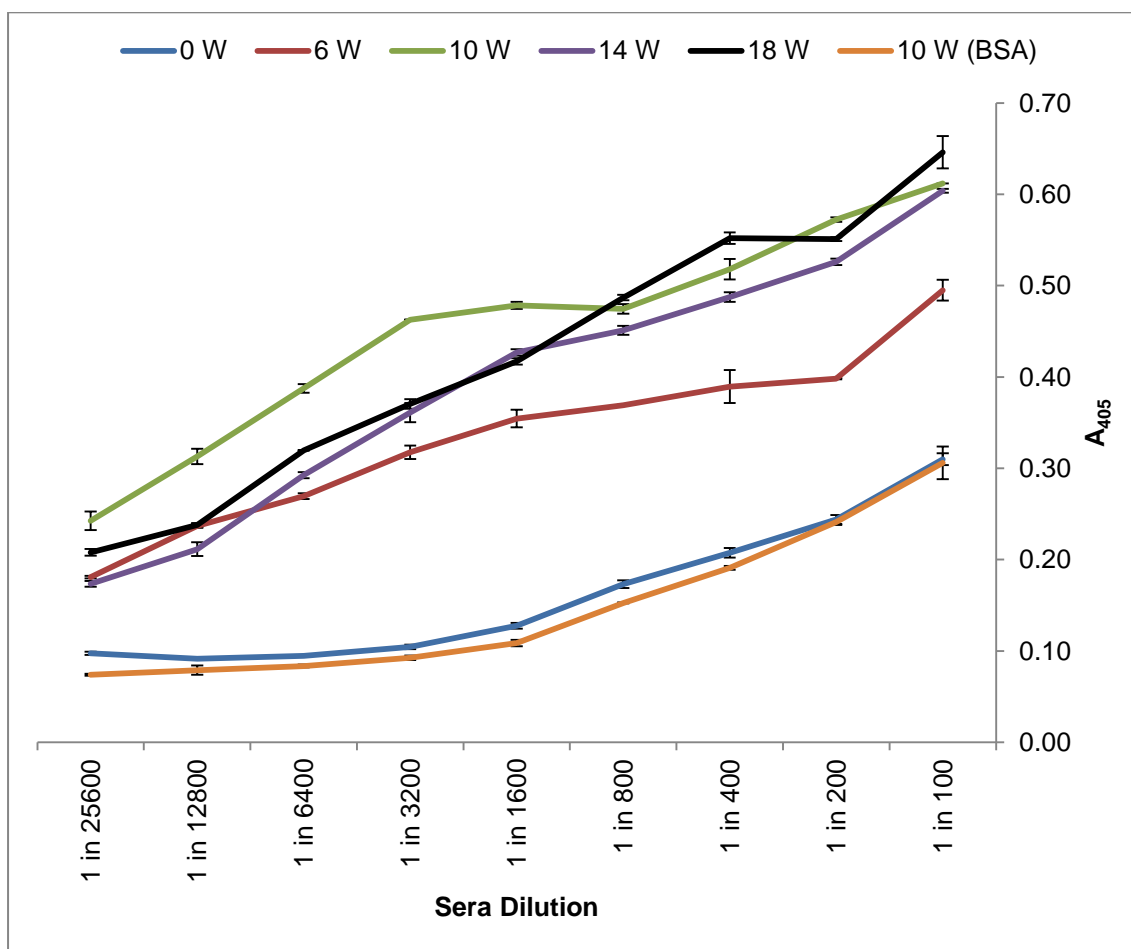


Figure 4.3: ELISA of Glc-TetHc sera (0, 6, 10, 14 & 18 W) activity against Glc-BSA (50 µg/ml) unless specified, on the plate. Legend: (blue) 0 week Glc-TetHc sera; (red) 6 week Glc-TetHc sera; (green) 10 week Glc-TetHc sera; (purple) 14 week Glc-TetHc sera; (black) 18 week Glc-TetHc sera and (orange) 10 week Glc-TetHc sera against BSA (50 µg/ml) on plate. Data were recorded in triplicate using standard ELISA protocol 7.4.2.1.

4.2 Results and discussion

4.2.1 ELISA analysis of glucose derived antibodies

ELISA analysis was carried out on the glucose antigen (**96**) derived sera (Figure 4.4) in order to determine the activity and specificity of the generated antibodies.

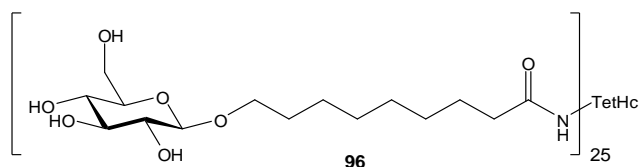


Figure 4.4: Structure of Glc-TetHc antigen

Figure 4.3 demonstrates that the Glc-TetHc derived sera have activity towards the Glc-BSA glycoconjugate immobilised on the surface of the ELISA plate. Both negative controls [pre-immune (blue) and 10 W – BSA (orange)] showed some activity towards the Glc-BSA antigen. The activity of the pre-immune samples (blue) demonstrates the native background binding of the sheep sera to the Glc-BSA conjugate, prior to immunisation with target antigen. The 10 week-BSA activity (orange) demonstrates the background binding of the sheep sera to the carrier protein (BSA) used during the ELISA analysis. The activity of the 10 W serum against the BSA control was comparable to that of the pre-immune serum towards the Glc-BSA conjugate. This demonstrates that polyclonal sheep sera do not have pre-existing activity towards the BSA carrier or the Glc-BSA conjugate. As a result, any observed activity of the immune sera (6, 10, 14, 18 weeks) above this baseline activity (blue and orange) represents specific activity of the polyclonal sera towards the target hapten (**69**). All of the immune sera (6, 10, 14, 18 weeks) were shown to have activity which was significantly higher than the baseline activities (blue and orange), demonstrating the specific binding to the D-glucose hapten (**69**). At high sera concentrations (dilution factor 1 in 100 – 1 in 800) there is a distinct difference in response between the 6 (red) week sample and the later bleeds (10 (green), 14 (purple) & 18 (black) weeks). This increase in response is a result of a longer time period between immunisation and bleed and is consistent with antibody affinity maturation. After 10 W the antibody response appears to indicate that antibody maturation is complete. Figure 4.3 shows data for the response of combined

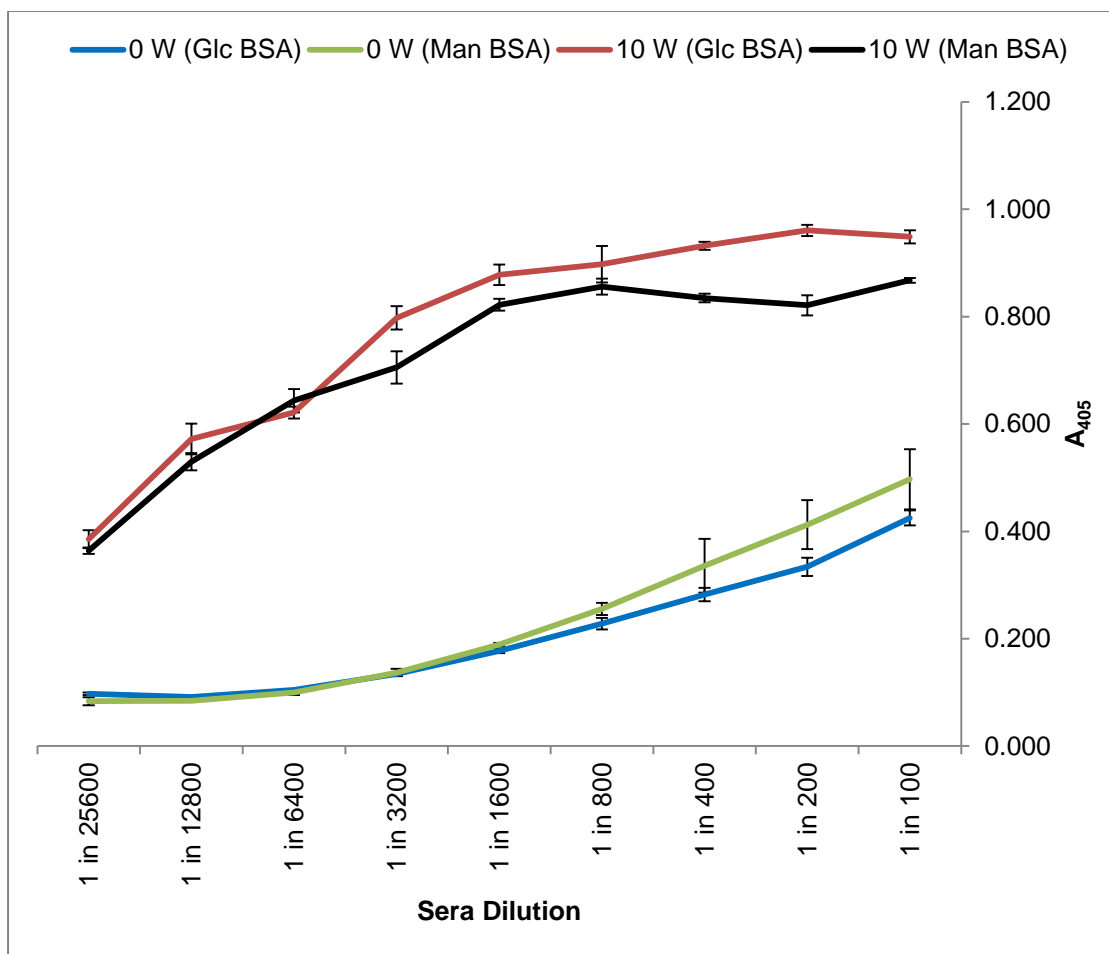


Figure 4.5: ELISA of Glc-TetHc sera (0 & 10 weeks) activity against Glc-BSA (50 $\mu\text{g/ml}$) or Man-BSA (50 $\mu\text{g/ml}$) on the plate. Legend: (blue) 0 weeks Glc-TetHc sera against Glc-BSA on plate; (green) 0 weeks Glc-TetHc sera against Man BSA on plate; (red) 10 weeks Glc-TetHc sera against Glc-BSA on plate; (black) 10 weeks Glc-TetHc sera against Man-BSA on plate. Data was recorded in triplicate using standard ELISA protocol 7.4.2.1.

Glc-TetHc sera from two sheep (CF1497 and CF1498); ELISA experiments were also carried out on the individual serum samples and the results were shown to be analogous to the combined data (Appendix 8.5) and as a result all subsequent ELISA were carried out using combined sera from both animals.

In order to determine whether there was any antibody specificity for the monosaccharide motif, the combined 10 week Glc-TetHc serum was analysed against both the Glc-BSA and Man-BSA conjugates (Figure 4.5). The pre-immune serum was again shown to have low background activity towards the Glc-BSA (blue) and Man-BSA (green) conjugates, indicating that any observed activity of the sample sera (10 weeks) was as a result of the polyclonal sera binding to the target hapten. The 10 week sera were selected at this stage as it gave the strongest response against the Glc-BSA in previous ELISA experiments (Figure 4.3). The 10 week serum was shown to have a slightly reduced activity towards the Man-BSA conjugate (black) when compared to the Glc-BSA activity (red), at high sera concentration (1 in 100 – 1 in 3200 dilution factor). This indicated that the Glc-TetHc polyclonal antibodies have limited selectivity towards the D-glucose hapten (69) over D-mannose hapten (64).

Competition ELISA experiments were designed in order to further investigate the activity and specificity of the polyclonal sera.

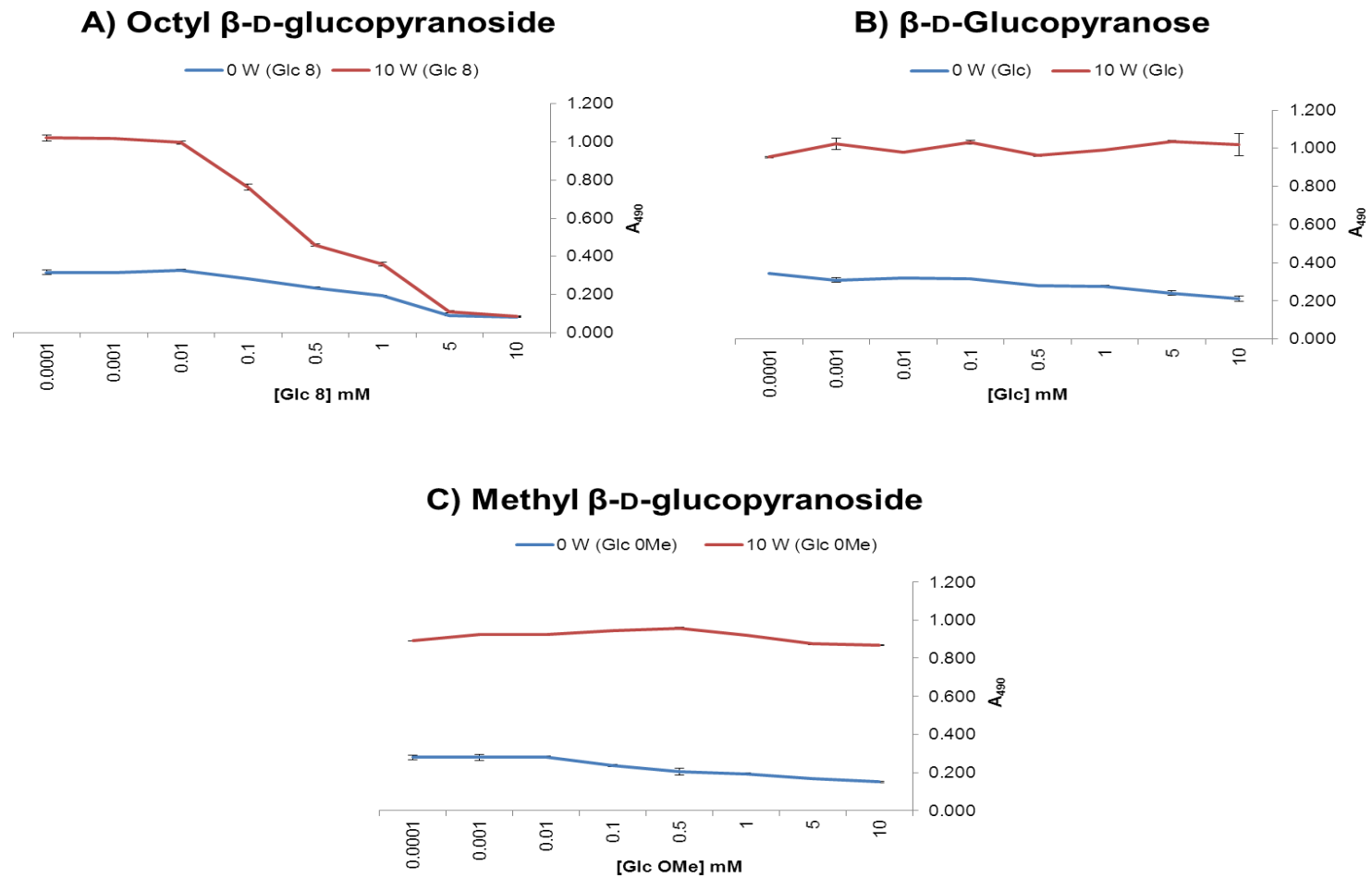


Figure 4.6: Competition ELISA results from Glc-TetHc (0/10 Week; 1 in 1600 dilution) sera against Glc-BSA (50 μ g/ml) on plate pre-incubated with serial dilutions of: A) octyl β -D-glucopyranoside; B) D-glucopyranose and C) methyl β -D-glucopyranoside. Legend: (Red) 10 Weeks sample 1 in 1600 dilution; (Blue) 0 Weeks sample 1 in 1600 dilution. Experiment was run according to standard competition ELISA protocol 7.4.2.1.

4.2.1.1 Competition ELISAs with Glc-TetHc polyclonal sera

Glc-TetHc sera (0 (blue) & 10 (red) weeks, 1 in 1,600 dilution) were pre-incubated with serial dilutions of a) octyl β -D-glucopyranoside; b) D-glucopyranose and c) methyl β -D-glucopyranoside (Figure 4.6 (A-C)). The competition ELISA experiments with D-glucopyranose and methyl β -D-glucopyranoside suggest that the antibodies are unable to bind to the free monosaccharides in solution (Figure 4.6 (B-C)). Octyl β -D-glucopyranoside (4.6 A) shows good competition for binding with the 10 week (red) Glc-TetHc serum. There is also inhibition of the pre-immune serum (blue) in the presence of octyl β -D-glucopyranoside at high concentration. This may indicate that the octyl β -D-glucoside has a general inhibition effect on antibody binding as a result of its surfactant properties. However, octyl β -D-glucoside is routinely used as a detergent in immunofluorescence assays at concentrations of 0.5% - 0.1% (17- 3 mM) to remove background antibody binding⁸. As such, it is not expected that the presence of octyl β -D-glucoside as a surfactant is sufficient to impact on specific antibody binding, indicating that the combined monosaccharide-linker motif is required for binding of the polyclonal antibodies to the target D-glucose hapten (69). The fact that the generated antibodies are shown to bind to octyl β -D-glucopyranoside could explain the activity of the Glc-TetHc sera towards the Man-BSA glycoconjugate (93) (Figure 4.5). Polyclonal serum contains multiple antibodies with different specificities and binding epitopes, and as such, antibodies raised against the linker may be present. This would lead to positive binding of the serum to the Man-BSA glycoconjugate, thus masking any monosaccharide specific antibodies.

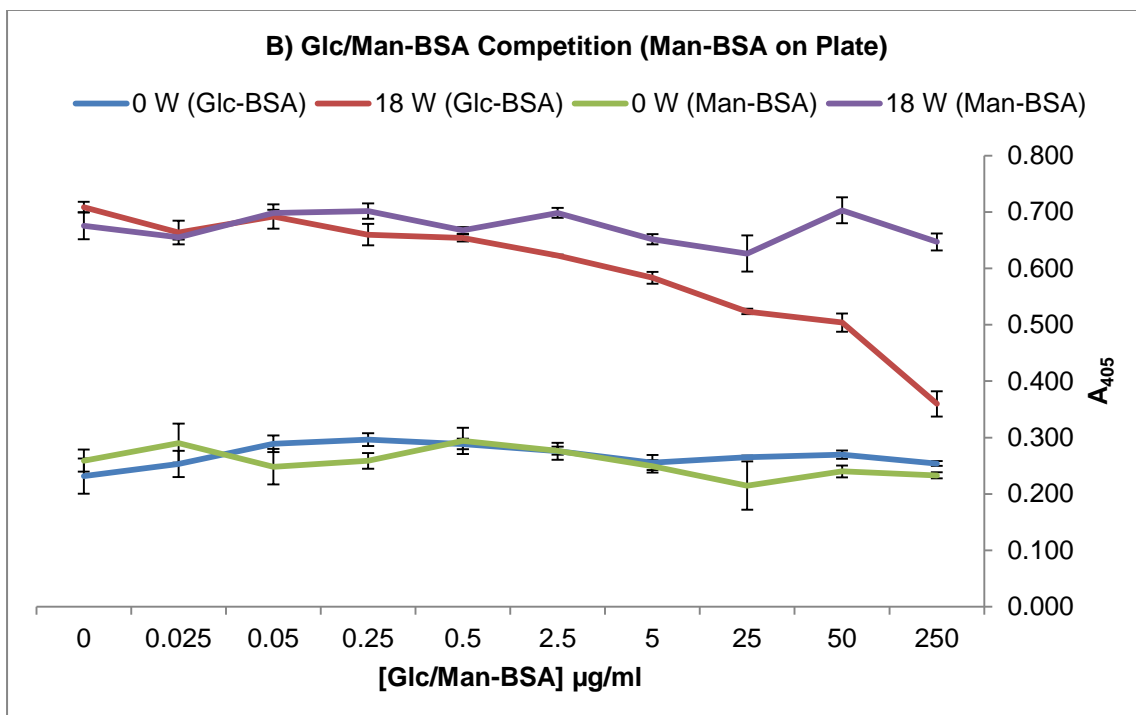
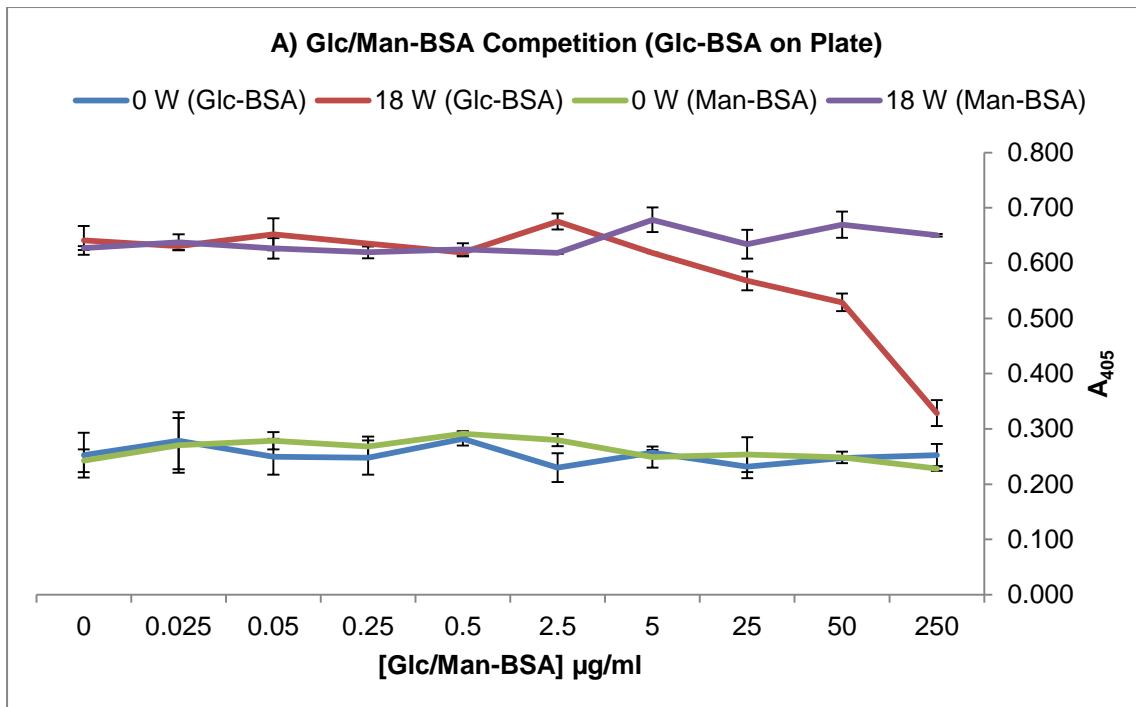


Figure 4.7: Man-BSA and Glc-BSA competition ELISA results from Glc-TetHc (0/18 week; 1 in 1600 dilution) sera against A) Glc-BSA (50 µg/ml) and B) Man-BSA (50 µg/ml) on plate pre-incubated with serial dilutions of Man-BSA (0 W – green and 18 W – purple) and Glc-BSA (0W – blue and 18 W – red). Legend: (blue) 0 weeks 1 in 1600 dilution Glc-TetHc sera pre incubated with Glc-BSA; (red) 18 weeks 1 in 1600 dilution Glc-TetHc sera pre incubated with Glc-BSA; (green) 0 weeks 1 in 1600 dilution Glc-TetHc sera pre incubated with Man-BSA; (purple) 18 weeks 1 in 1600 dilution Glc-TetHc sera pre incubated with Man-BSA. Experiment was run according to standard competition ELISA protocol 7.4.2.1 and results were recorded in triplicate.

Competition experiments with Glc-BSA (**97**) and Man-BSA (**93**) (Figure **4.7A** and **B**) demonstrate that the Glc-TetHc derived sera possess some degree of specificity towards the D-glucose hapten (**69**). Both the competition experiments with the 18 week Glc-TetHc serum and Glc-BSA glycoconjugate (red) show positive binding to the Glc-BSA in solution. However, the competition experiments with the Man-BSA (purple) indicate that the polyclonal antibodies do not bind to the Man-BSA in solution. The observation that the Glc-TetHc serum reacts positively with the Man-BSA glycoconjugate when it is bound on the surface of the ELISA plate, but not when in solution indicates that the binding event to Man-BSA may be concentration dependent. When bound to the plate the Man-BSA will be at a much higher localised concentration than in solution. This effect may facilitate the binding of the antibodies to the non-cognate antigen when it is surface bound, however further investigation is required to verify this observation. It is known from previous competition experiments (Figure **4.7 A**) that the monosaccharide-linker motif is required for antigen binding. The fact that the linker molecule is the same in both the Man-BSA and Glc-BSA conjugates further implies that the background binding may be as a result of the alkyl linker. Attempts were made to further deconvolute the activity of the polyclonal antibodies and are described in Section **4.3**.

The evidence presented so far suggests that there is some degree of monosaccharide specificity present in the Glc-TetHc derived antibodies. This monosaccharide specificity is further demonstrated in the slot-blot analysis, which is described in Section **4.2.3**.

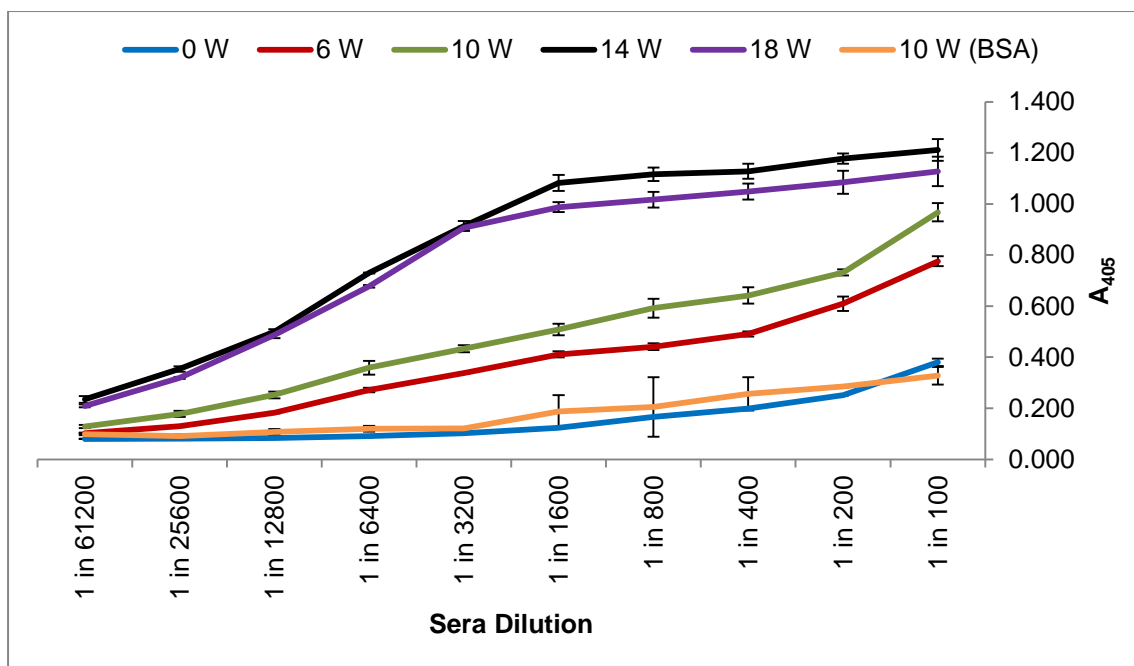


Figure 4.8: ELISA of 6dHep-TetHc sera (0, 6, 10, 14 & 18 W) activity against Hep-BSA (50 µg/ml) unless specified, on the plate. Legend: (blue) 0 week 6dHep-TetHc sera; (red) 6 week 6dHep-TetHc sera; (green) 10 week 6dHep-TetHc sera; (purple) 14 week 6dHep-TetHc sera; (black) 18 week 6dHep-TetHc sera and (orange) 10 week 6dHep-TetHc sera against BSA (50 µg/ml) on plate. Data was recorded in triplicate using standard ELISA protocol 7.4.2.1.

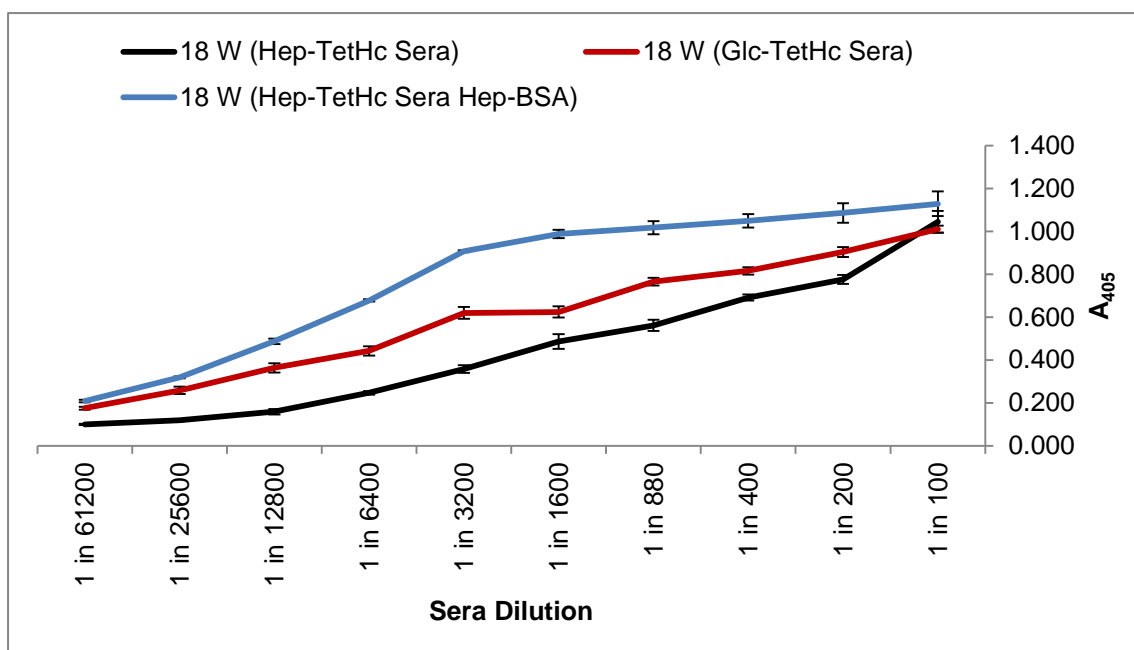


Figure 4.9: ELISA of 6dHep-TetHc sera (10 W – black) and Glc-TetHc sera (10 W – red) activity against Glc-BSA (50 µg/ml) and Hep-BSA (50 µg/ml) on the plate. Legend: 0 W Glc-BSA (black) 18 weeks 6dHep-TetHc sera against Glc-BSA on plate; (red) 10 weeks Glc-TetHc sera against Glc-BSA on plate; (blue) 18 weeks 6dHep-TetHc sera against Hep-BSA on plate. Data was recorded in triplicate using standard ELISA protocol 7.4.2.1.

4.2.2 ELISA analysis of heptose derived antibodies

The 6-deoxy-D-mannoheptose TetHc antigen (**94**) derived sera were analysed by ELISA in order to determine the activity of the antibodies towards the target 6-deoxy-D-*manno*-heptose hapten (**91**).

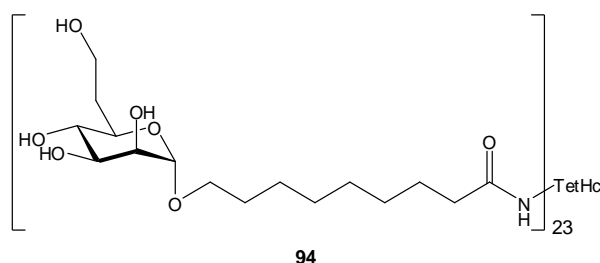


Figure 4.10: Structure of the 6-deoxy-D-mannoheptose TetHc antigen (**94**).

Figure **4.8** again shows the time-dependent maturation of antibody affinity towards the target hapten (**91**). The maturation of antibody activity towards the antigen is slower than that of the glucose antigen (Figure **4.3**) with the response developing until week 14. There are a number of potential reasons behind this phenomenon including differences in the immunisation formulations or a delayed/poor immune response to the 6-deoxy-D-*manno*-heptopyranose antigen by the sheep as a result of the increased complexity of the antigen. However this result clearly shows the development of an antibody response to the 6dHep-TetHc antigen (**94**).

The 6dHep-TetHc serum (18 weeks) was analysed against the Glc-BSA glycoconjugate, in parallel with the Glc-TetHc serum (18 weeks) (Figure **4.9**). The result shows a reduced response of the 6dHep-TetHc sera (black) against Glc-BSA when compared to the Glc-TetHc sera (red). The result is even more obvious when the response of the 6dHep-TetHc sera against Glc-BSA (black) is compared to that of the 6dHep-TetHc sera against 6dHep-BSA (blue) when performed under the same conditions. The much higher activity of the 6dHep-TetHc sera against the 6dHep-BSA, compared to that against Glc-BSA, again demonstrates the potential monosaccharide specificity of the generated antibodies. This result is further confirmed by the slot-blot analysis of the polyclonal antibodies Section **4.2.3**.

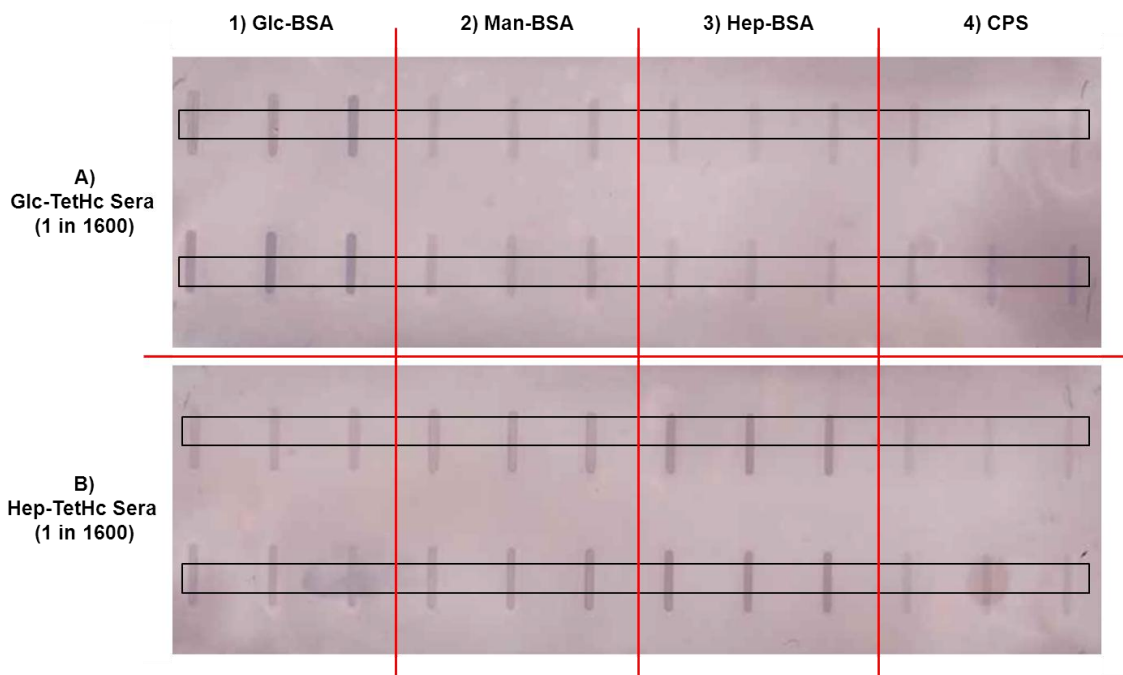


Figure 4.11: Slot blot analysis of A) Glc-TetHc serum (18 W; 1 in 1600 dilution) and B) 6dHep-TetHc serum (18 W; 1 in 1600 dilution) against 1) Glc-BSA (50 µg/ml); 2) Man-BSA (50 µg/ml); 3) Hep-BSA (50 µg/ml) and CPS-1 (50 µg/ml). Data was recorded in sextuplicate using slot-blot protocol 7.4.3.

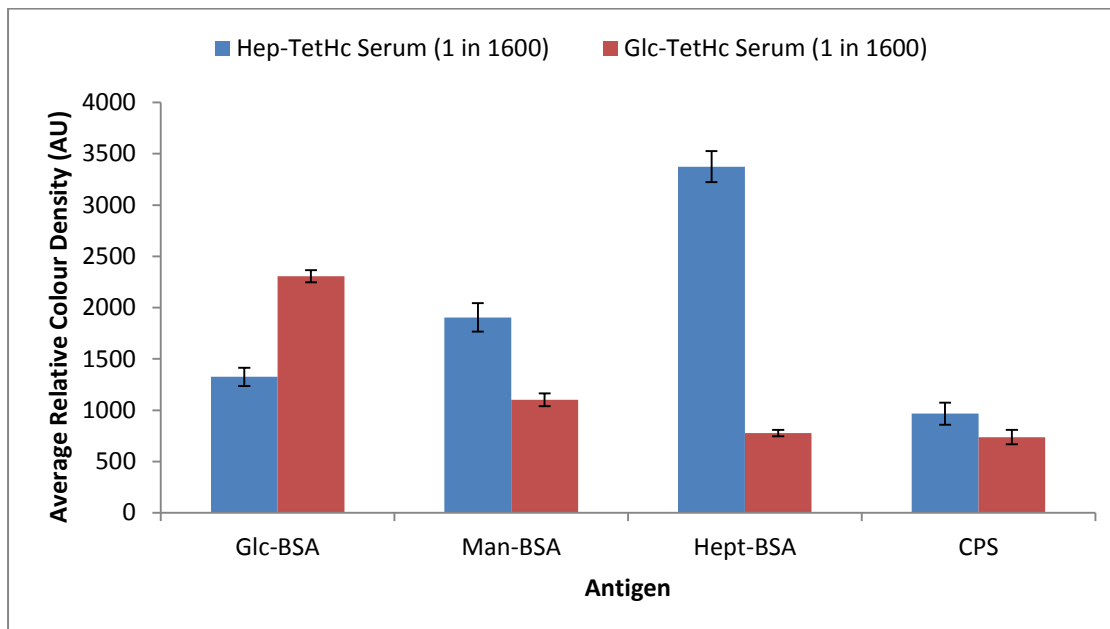


Figure 4.12: Colourimetric density analysis of the blot images using Image-J. Legend: (blue) 6dHep-TetHc serum (18 W; 1 in 1600 dilution); (red) Glc-TetHc serum (18 W; 1 in 1600 dilution).

4.2.3 Slot-blot analysis of monosaccharide derived antibodies

Slot-blot analysis of both sets of polyclonal sera (Glc-/Hep-TetHc; 18 W; 1 in 1600 dilution) further demonstrated the monosaccharide specificity of both sets of antibodies. Figure 4.11 shows the blot membranes from both experiments; it is evident that there is some degree of background binding of the antibodies to all of the antigens, as shown in the ELISA experiments (Figures 4.5 and 4.9). However, the positive signal is markedly stronger with the Glc-TetHc serum and Glc-BSA and the 6dHep-TetHc serum and Hep-BSA. Colourimetric analysis of the blots was carried out using Image-J gel analysis software. The black rectangles (Figure 4.11) represent the sample areas selected for the analysis. Image-J⁹ is used to compare the colourimetric density (intensity) of bands on gels/western blots and can be used to quantify the antibody response to the chosen antigen. The relative density of bands, with the background colour (BSA control) subtracted, was calculated and the average for each antigen was plotted on a column graph (Figure 4.12).

Figure 4.12 shows that both sets of antigens are specific towards the cognate antigen, confirming the conclusions of the ELISA analysis. Again, background binding of the antibodies to the non-cognate antigens was observed. In both cases, the antibodies are more reactive towards the Man-BSA glycoconjugate when compared to the other non-cognate antigen. This result is not surprising as *D-manno*-pyranose is structurally more similar to both antigens than 6-deoxy-*D-manno*-heptose and *D-gluco*-pyranose (Figure 4.13).

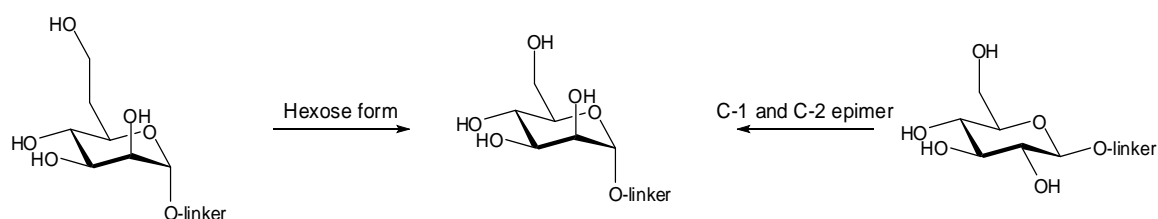


Figure 4.13: Structural differences between the three monosaccharide motifs

This result demonstrates that the background binding is not solely dependent on the presence of the linker molecule, as there is differentiation between the three

antigens by both the Glc-TetHc sera and the 6dHep-TetHc sera. This highlights the different specificities of the polyclonal sera and the need for affinity purification of the antibodies followed by further analysis. The lack of binding of the 6dHep-TetHc sera to the CPS-1 on the blot indicates that monosaccharide derived antibodies are not sufficient for the recognition of CPS-1 of *B. pseudomallei*; see section 4.4.3 for further analysis.

4.3 Enhancement of the antigenicity of the monosaccharide antigens

The ELISA and slot-blot analyses suggest that the immune system is capable of distinguishing between monosaccharide structures such as D-*manno*-pyranose, D-*gluco*-pyranose and 6-deoxy-D-*manno*-heptose. However, it is apparent that the linker molecule is playing an important role in the binding of the antibodies to the antigens as demonstrated by the background binding seen throughout the analyses. In an attempt to increase the antigenicity of the monosaccharide antigens and to remove the binding effect of the linker motif, a two sided strategy was employed.

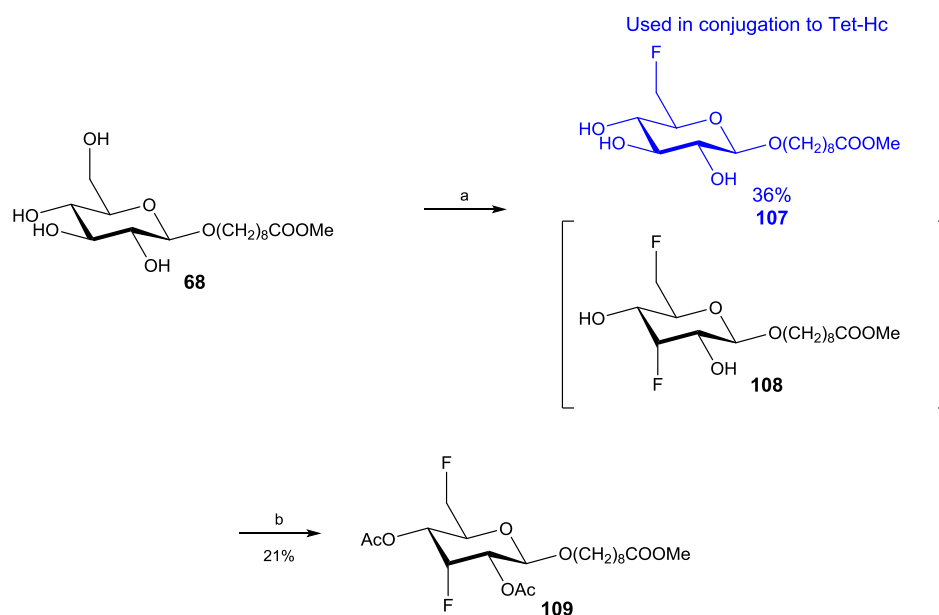
The first strategy involved the use of fluorine to boost the immunogenicity of the glucose antigen. Fluorine has been widely applied in medicinal chemistry (Flurithromycin¹⁰ and Efavirenz¹¹) for decades. Currently 20-25% of the drugs currently in the production pipeline contain at least one fluorine atom in their structure¹². Recently there has been an interest in using fluorine to increase the activity of carbohydrate based antigens, with particular focus on anti-cancer vaccines. A key process in the evolution and malignancy of many cancers is the development of abnormal glycosylation patterns known as, tumour associated carbohydrate antigens (TACA), on tumour cells surfaces¹³. It has been shown that TACAs can be used to not only distinguish between cancer types but also help to understand the developmental stage of the cancer¹⁴. As a result, there has been a concerted effort into the development of TACA derived cancer treatments and preventative vaccines. However, despite initial promise, vaccines based on natural TACA structures are not sufficient for the development of IgG antibodies and subsequent T-cell dependent immunity¹⁵. This is based on the fact that a number of TACAs are also presented by 'normal' cells at reduced levels, and as such are regarded as 'self' by the immune system¹⁶. There is also an issue with metabolic

stability of the natural carbohydrate antigens as a result of degradation by carbohydrate active enzymes, which can severely impact on efficacy¹⁵. The inclusion of fluorine molecules into the structures of TACAs is one method in which these problems can be avoided. It has been shown that the fluorination of carbohydrate based antigens (STn antigen¹⁷ MUC1 glycopeptide¹⁸) can lead to increased immunogenicity and specificity of antibodies to the natural antigen, along with increased metabolic stability. On this basis, a 6-deoxy-6-fluoro-D-glucopyranose hapten (**111**) was synthesised and again sheep were immunised, in collaboration with Ig Innovations, for antibody generation in an attempt to generate a more specific immune response to the cognate glucose hapten.

The second strategy involved the synthesis of a second set of monosaccharide antigens (section **4.3.2**) based on the same conjugation chemistry but with a thiol-linked three-carbon linker (3-methyl mercaptopropionate). The second generation of antigens will be conjugated to BSA carrier protein and used for the further evaluation of the specificity of the monosaccharide antibodies. It was anticipated that by using BSA conjugates of the monosaccharide antigens with shortened linker in ELISA and blot analysis any activity and resulting specificity would be focused upon the monosaccharide motifs and not the carrier protein or linker molecule.

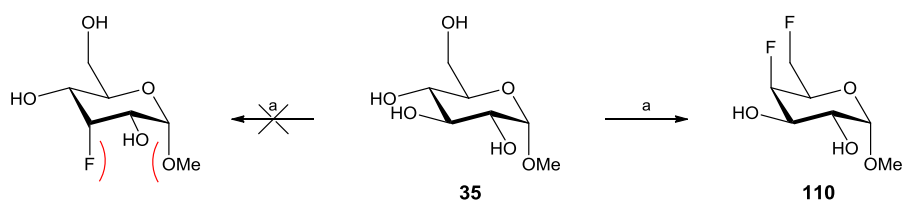
4.3.1 Synthesis of 6-deoxy-6-fluoro-D-glucose TetHc antigen (112)

8-(Methoxycarbonyl)octyl 6-deoxy-6-fluoro-D-glucopyranoside (**107**) was synthesised in one step from 8-(methoxycarbonyl)octyl- β -D-glucopyranoside (**68**) using diethylaminosulfur trifluoride in moderate yield of 36% (Scheme **4.1**)^{19 20}. Purification of the reaction by flash chromatography afforded a second, less polar compound, which was isolated, per-O-acetylated in-order to facilitate NMR characterisation and identified by NMR (¹H, ¹³C and ¹⁹F). The acetylated byproduct was shown to be 8-(methylcarbonyl)octyl 2,4-di-O-acetyl-3,6-di-deoxy-3,6-di-fluoro- β -D-*allo*-pyranoside (**109**), identified by the characteristic coupling constants in the ¹H NMR data; [H-4 $J_{3,4} = 3.5$ Hz and $J_{4,5} = 10.0$ Hz]²¹. The splitting patterns in both the ¹H and ¹³C NMR spectra place the second fluorine atom in an axial configuration at the C-3 position. ¹³C NMR spectra for (**107**) and (**109**) are displayed in Appendix **8.6**.



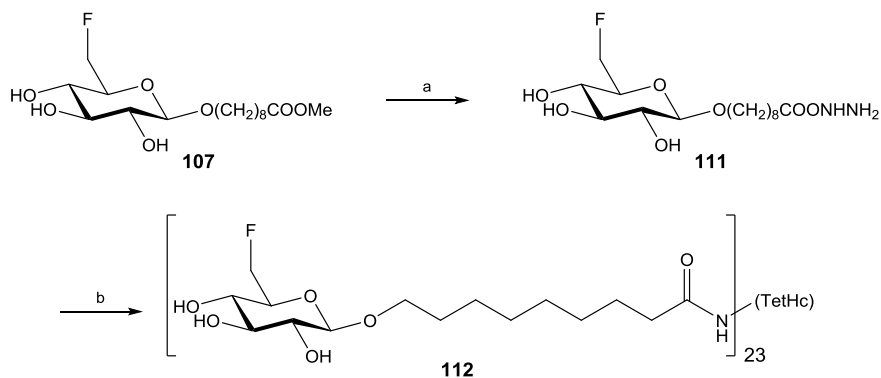
Scheme 4.1: Synthesis of 8-(methoxycarbonyl) 6-deoxy-6-fluoro-β-D-glucopyranoside (108) and 8-(methoxycarbonyl)-2,4-di-O-acetyl-3,6-dideoxy-3,6-difluoro-β-D-allo-pyranose (109). Reagents and conditions: a) DAST, DCM (abs), -40°C – rt, 1 h; b) Ac₂O, pyridine, rt, O/N.

Owing to the D-allose configuration of this compound, further investigation into this compound was not carried out; however, it does pose an interesting observation from a mechanistic point of view. It has been shown previously by Somawardhana²² and Card¹⁹ that treatment of methyl α-D-glucopyranoside with DAST under the same conditions described here leads to the formation of methyl 4,6-dideoxy-4,6-difluoro-α-D-galactopyranoside (Scheme 4.2). It is known that anomeric configuration has an effect on the reactivity of the *endo*-cyclic hydroxyls of monosaccharides, as first described by a series of tosylation experiments of α/β-D-*gluco*-pyranoside conducted by Compton²³. However, the S_N2 mechanism of fluorination results in an inversion of stereochemistry. Owing to this, formation of the 3-deoxy-3-fluoro-α-glucopyranose will be sterically hindered due to predominant 1,3-diaxial interactions leading to the formation of the 4-deoxy-4-fluoro product (Scheme 4.2).



Scheme 4.2: Synthesis of methyl 4,6-dideoxy-4,6-difluoro- α -D-galacto-pyranoside (**110**) from methyl α -D-gluco-pyranoside with DAST. Reagents and conditions: a) DAST, DCM (abs), -40°C – rt, 1 h

The 6-deoxy-6-fluoro- β -D-glucopyranoside derivative (**107**) was converted to the acyl hydrazide (**111**) by reaction with hydrazine monohydrate at 50°C . The TetHc 6-deoxy-6-fluoro conjugate (6D6FGlc-TetHc) (**112**) was synthesised by the standard conjugation protocol as described in Section 2.3.2 (Scheme 4.3). The MALDI-ToF and SDS-Page analysis of the 6D6FGlc-TetHc glycoconjugate indicated an average of 23 haptens per protein, giving a conjugation efficiency of 70% (MALDI-ToF data shown in Appendix 8.7). The 6D6FGlc-TetHc conjugate was submitted to Ig Innovations for antibody generation.



Scheme 4.3: Conjugation of 8-(methoxycarbonyl)octyl-6-deoxy-6-fluoro- β -D-glucopyranoside (**107**) to TetHc carrier protein. Reagents and conditions: a) NH_2NH_2 , EtOH, 4 h, 55°C ; bi) *tert*-butyl nitrite, 4 M HCl, DMF, bii) TetHc, 0.08M Borax/0.35M KHCO_3 , pH 9.0, O/N, 4°C .

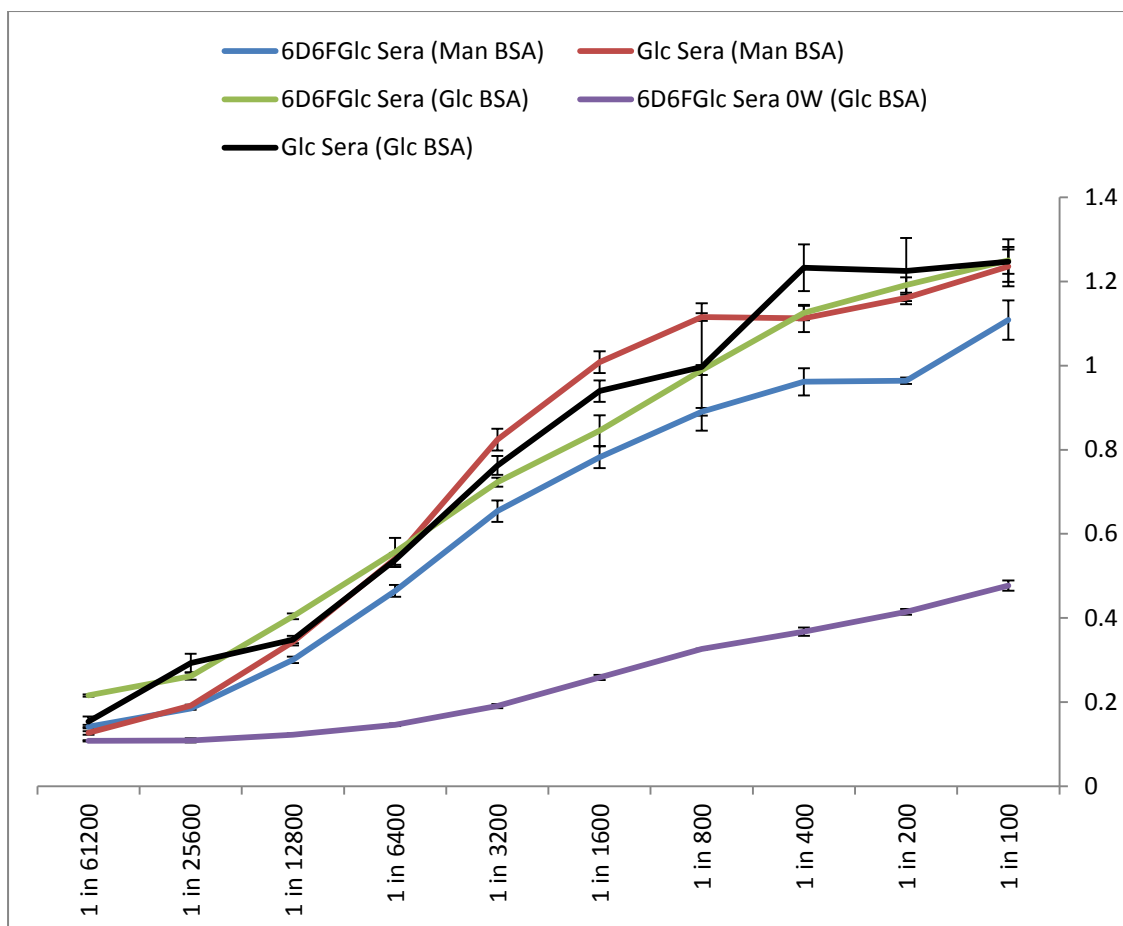


Figure 4.14: ELISA assessment of 6D6FGlc-Sera against Glc-BSA (50 µg/ml) and Man-BSA (50 µg/ml) on plate. Legend: (purple) 0 W 6D6FGlc-TetHc sera against Glc-BSA (50 µg/ml); (blue) 18 W 6D6FGlc-TetHc sera against Man-BSA (50 µg/ml); (green) 18 W 6D6FGlc-TetHc sera against Glc-BSA (50 µg/ml); (black) 18 W Glc-TetHc sera against Glc-BSA (50 µg/ml); (red) 18 W Glc-TetHc sera against Man-BSA (50 µg/ml).

4.3.1.1 Immunological assessment of the 6D6FGlc-TetHc sera

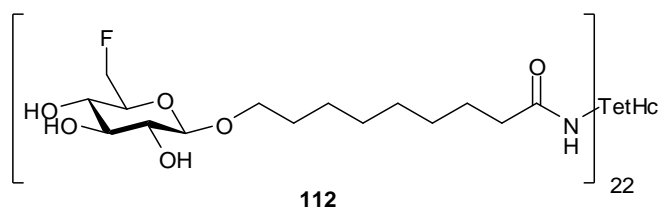
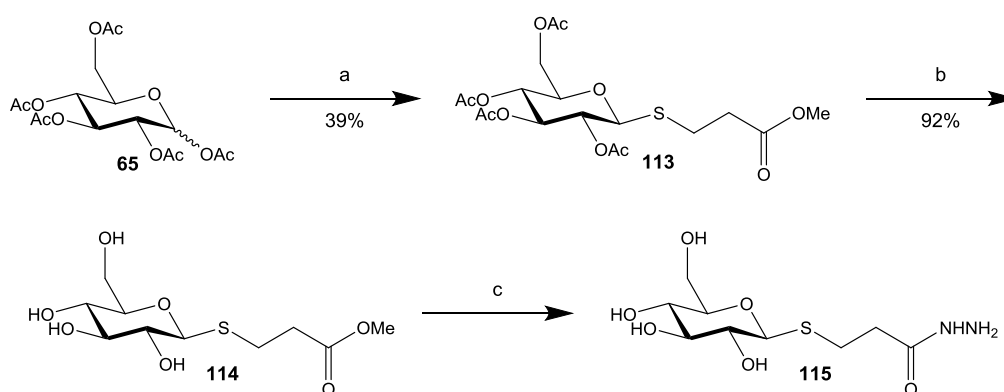


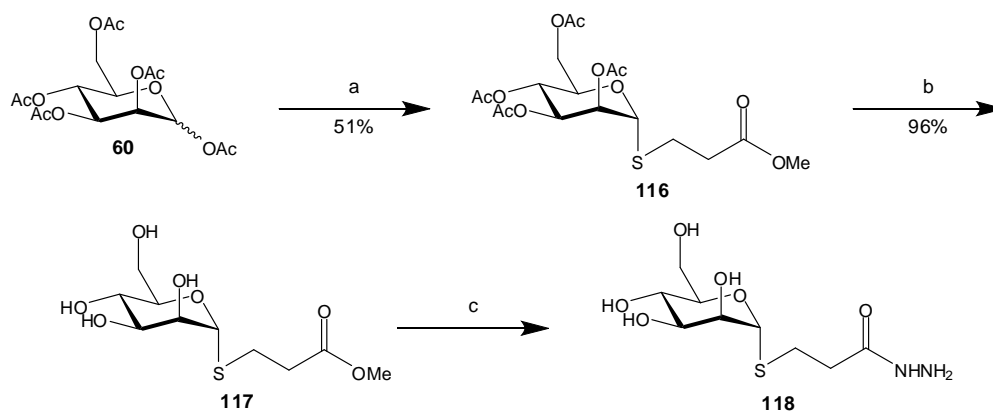
Figure 4.15: Structure of the 6d6FGlc-TetHc antigen (112)

The activity profile of the 6d6FGlc-TetHc (**112**) derived antibodies (Figure 4.14) (pre-immune (purple) and 18 weeks against Glc-BSA (green) and Man-BSA (blue) conjugates is similar to the Glc-TetHc sera (Figure 4.14 (Glc-BSA (red) and Man-BSA (black))). The activity of the 6d6FGlc-TetHc sera indicated that antibodies raised against the 6-fluorinated D-glucose antigen recognise the native unfluorinated D-glucose hapten (**69**). Due to the variable nature of polyclonal sera, and the effect of the alkyl linker on specificity (Section 4.2) at this stage, it was not possible to make direct comparisons regarding the relative activities of the Glc-TetHc and 6d6FGlc-TetHc derived sera. In order to determine the impact of fluorination on activity and specificity of the derived antibodies, a much more detailed analysis of the antibodies is required. Ideally, generation of monoclonal antibodies specific for the fluorinated (**111**) and native D-glucose hapten (**69**) would be produced. This would allow for the binding kinetics of both antibodies to be determined and provide insight into the immunological impact of fluorination. This work was not conducted as part of this study, but the preliminary activity result is encouraging and indicates that further development and investigation of the fluorinated haptens would be warranted.

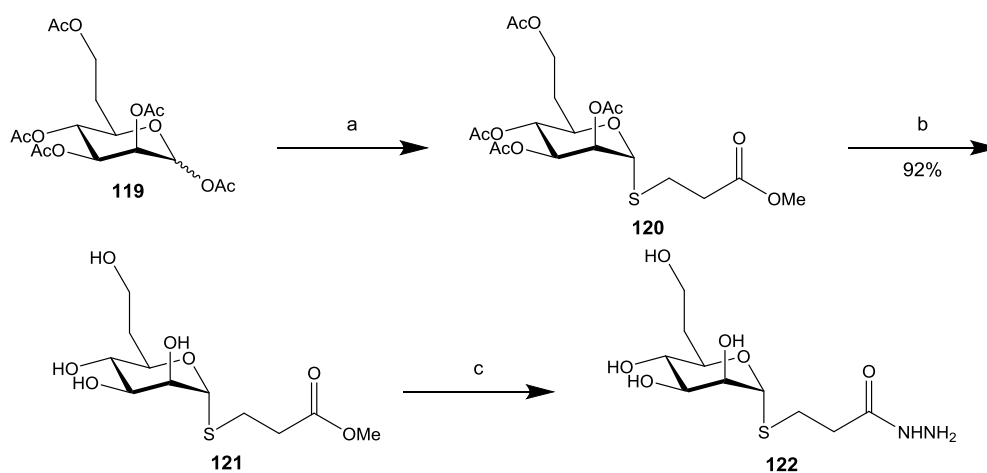
D-Gluco-compound



D-Manno-compound



D-Manno-hepto-compound



Scheme 4.4: Synthesis of the short linker haptens. Reagents and conditions: a) $\text{BF}_3 \cdot \text{OEt}_2$, DCM, $0^\circ\text{C} - \text{r.t.}$, O/N; b) NaOMe, MeOH, rt, 30 min; c) $\text{NH}_2\text{NH}_2 \cdot \text{H}_2\text{O}$; EtOH, 55°C , 4 h.

4.3.2 Synthesis of short linker haptens

A second generation of monosaccharide haptens was developed through the use of 3-methylmercaptopropionate in an attempt to further investigate the specificity of the anti-monosaccharide antibodies. In order to simplify the synthesis of the short linker haptens, methyl 3-mercaptopropionate was selected as the new linker. The use of thiol based linker in these conjugates will further differentiate the linker moiety from the original 8-methoxycarbonyl octanol linker. It also allows for the direct synthesis of the conjugates from the per-*O*-acetylated monosaccharides²⁴. These haptens will help to establish whether the apparent specificity of the sheep sera raised against the monosaccharide antigens is conferred by the carbohydrate motifs or as part of a combined monosaccharide-linker epitope.

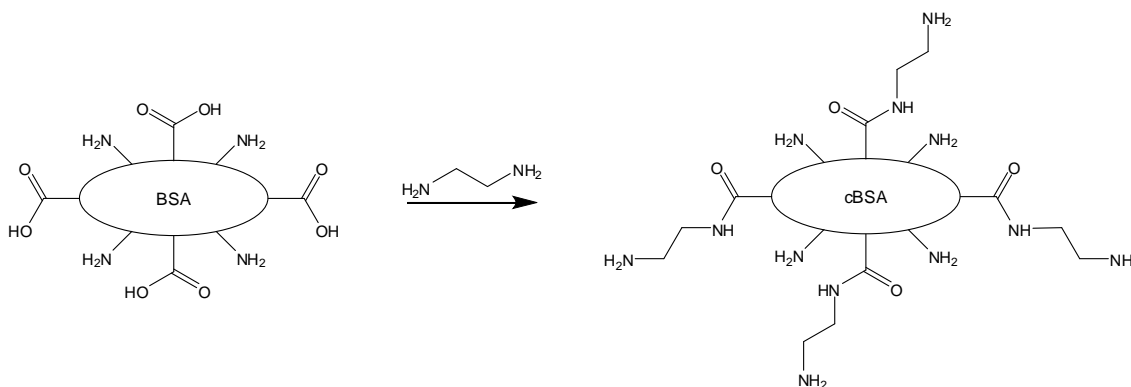
The short linker haptens were all synthesised in three steps from the per-*O*-acetylated monosaccharides (Scheme 4.4). Boron trifluoride diethyl etherate-promoted glycosylation was achieved in moderate yield for all three conjugates, followed by global deacetylation under Zemplén conditions. The per-*O*-acetylated 6-deoxy-*D*-manno-heptopyranoside (**120**) was provided by Giulia Pergolizzi (Field Lab). Acyl hydrazides were formed upon reaction of the methyl ester with hydrazine monohydrate at elevated temperature as described earlier for (**64**, **69** and **91**, Section 2.2). Conjugation to carrier protein and use of the second-generation antigens is ongoing in the Field group.

4.4 Immunological assessment of anti-CPS-1 monoclonal antibody

4.4.1 Conjugation of CPS-1 to cBSA carrier protein

The use of the native capsular polysaccharide for the immunological assessment of the potential vaccine candidates is an important part of the larger vaccine development project. The direct loading of polysaccharides on to polystyrene ELISA plates has been shown to be inconsistent, even at high loading concentrations²⁵. There are a number of methods which can be employed to improve binding of polysaccharides to ELISA plates, such as covalent attachment²⁵, conjugation to a carrier protein,²⁶ or antibody capture ELISA²⁷. As previously described the mAb 4IVH12 antibody, raised against intact K96243 *B. pseudomallei* cells was available to us²⁸. However, use of this monoclonal antibody in capture ELISA assays was unexpectedly not possible due to cross-reactivity between the secondary antibody (anti-sheep) used for the detection of sheep sera and the mouse monoclonal. To overcome this problem the conjugation of CPS-1 to cationised BSA was attempted. The conjugation of *B. pseudomallei* CPS-1 (4) to cBSA has previously been described by Burtnick *et al*²⁹.

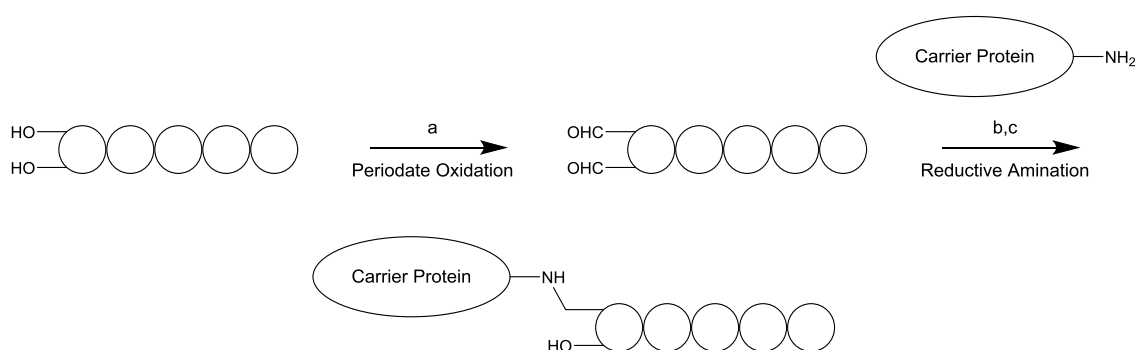
cBSA was chosen as the carrier protein in this instance in order to follow the protocol established by Burtnick *et al*²⁹. cBSA is native BSA which has been treated with an excess of ethylenediamine, essentially capping all negatively charged residues with primary amines (Scheme 4.5). This increases the number of conjugation sites, whilst also making the carrier more immunogenic than the native protein³⁰.



Scheme 4.5: Schematic representation of the synthesis of cBSA from native BSA with ethylenediamine.

Burtnick *et al*²⁹ used periodate oxidation of CPS-1 to afford non-reducing terminal aldehydes. Two vicinal diols (axial-equatorial or equatorial-equatorial) are required for formation of the intermediate oxidation complex³¹. As a result of the β -1,3-linkage of the Bth-CPS-1 (**104**) periodate oxidation can only occur at the non-reducing terminus where the 3-OH and 4-OH are correctly orientated for periodate oxidation. This method provides a simple route to the selective installation of aldehydes at the non-reducing terminus of the Bth-CPS-1 (**104**) which can be exploited for the chemical modification of the polysaccharide.

In section 3.3.2 the successful reductive amination of CPS-1 to aminopyrene trisulfonic acid (APTS) (**105**) is described. However, as the efficiency of this reaction was not fully investigated it was decided to proceed with the periodate oxidation to ensure successful coupling of the cBSA to the carrier protein. The native Bth-CPS-1 (**104**) (5 mg) was successfully conjugated to the carrier protein on a 1:1 ratio with the carrier protein as described by Burtnick and co-workers (Scheme 4.6). After the periodate oxidation step the sample was purified using a PD-10 column before reductive amination with cBSA. The reaction was terminated with the addition of NaBH₄ and extensively dialysed against MQ-H₂O and lyophilized to afford CPS-1-cBSA glycoconjugates (6 mg).



Scheme 4.6: Schematic representation of CPS-1 conjugation to carrier protein. Reagents and conditions: a) NaIO₄, PBS, rt, 40 mins; b) 1M NaBH₃CN in 10 mM NaOH, PBS, rt, 4d; c) 1M NaBH₄ in 10 mM NaOH.

An initial SDS-PAGE gel was run on the glycoconjugates sample (Figure 4.16) using cBSA as the standard. Coomassie staining of the initial gel revealed bands at

70, 150 and 250 kDa corresponding to cross-linked cBSA as a result of cationization. The presence of a protein band at +250 kDa (red box) indicated the successful conjugation of the oxidised CPS-1 to cBSA. In contrast to the data published by Burtnick *et al.*³² a large proportion of the cBSA remained unmodified. This may be as a result of difference between the Bth-CPS-1 (**104**) and the *B. pseudomallei* CPS-1 (**4**) polysaccharides that was used in the two experiments. Currently studies are under way in the Field lab regarding the use of both polysaccharides for conjugation in order to determine the cause of this observation.

Size exclusion chromatography (S200 column) was performed to remove unreacted cBSA and isolate the high molecular weight material (red box) (Figure 4.17).

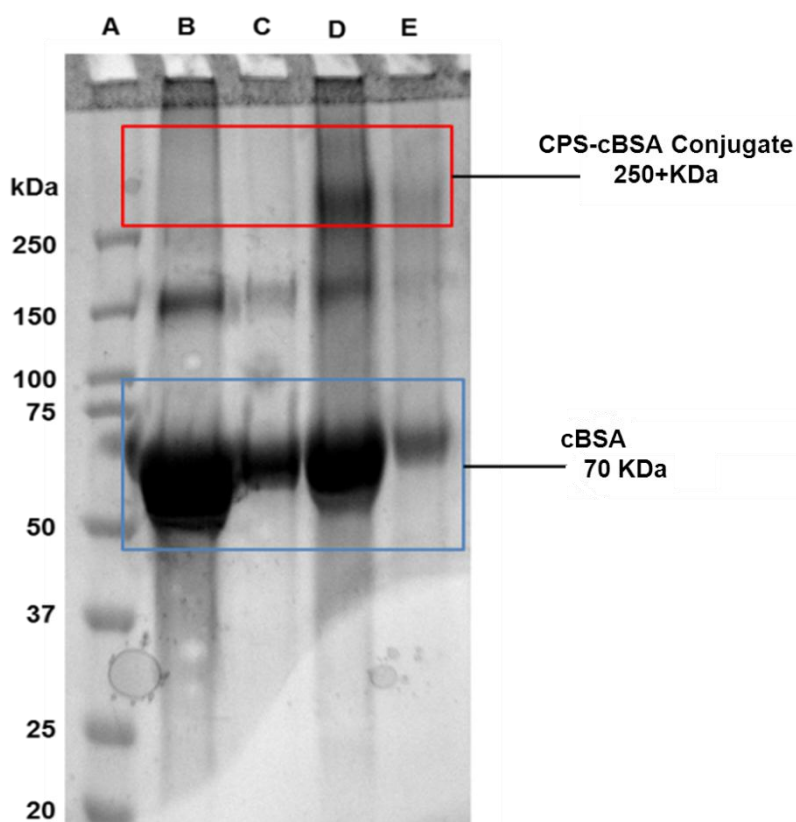


Figure 4.16: SDS-PAGE gel of cBSA conjugation reaction. Lanes: A) Kaleidoscope ladder; B) cBSA (2 mg/ml); C) cBSA (0.5 mg/ml); D) Glycoconjugate (2 mg/ml); E) Glycoconjugate (0.5 mg/ml)

Isocratic elution (50 mM HEPES; pH 7.5, 150 mM NaCl) of the glycoconjugates sample was done on an S200 HR (Superdex) column XK26/60 and fractions (1 ml)

were collected and analysed using the high-throughput phenol-sulphuric acid assay to determine the carbohydrate content (Figure 4.17).

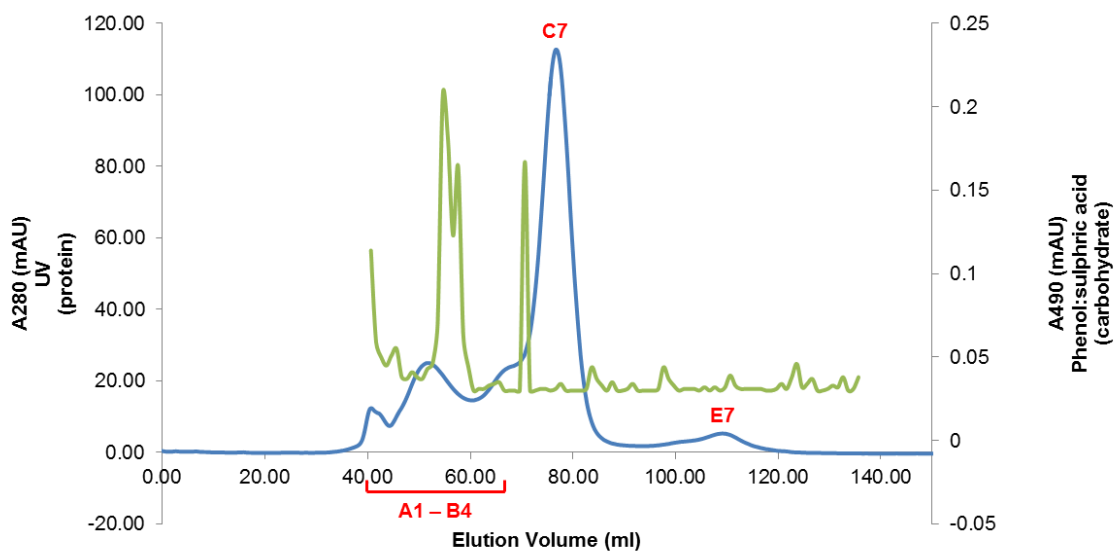


Figure 4.17: Size exclusion chromatography of CPS-1-cBSA glycoconjugate. XK26/60 S200 HR column (Superdex); flow rate 1 ml/min; eluent 50 mM HEPES, pH 7.5, 150 mM NaCl; sample loaded 500 μ l and 12 mg/ml; fractions (40 – 150 ml) 1 ml. Series (Blue) UV trace (A_{280}) protein content; (Green) Phenol:sulphuric acid assay (A_{490}) carbohydrate content. Fractions taken for SDS highlighted in red.

A selection of fractions were taken from the peaks of interest (UV and carbohydrate active) and run on SDS-PAGE gel and western blot using the ant-CPS-1 monoclonal antibody (mAb 4IVH12) (Figure 4.18).

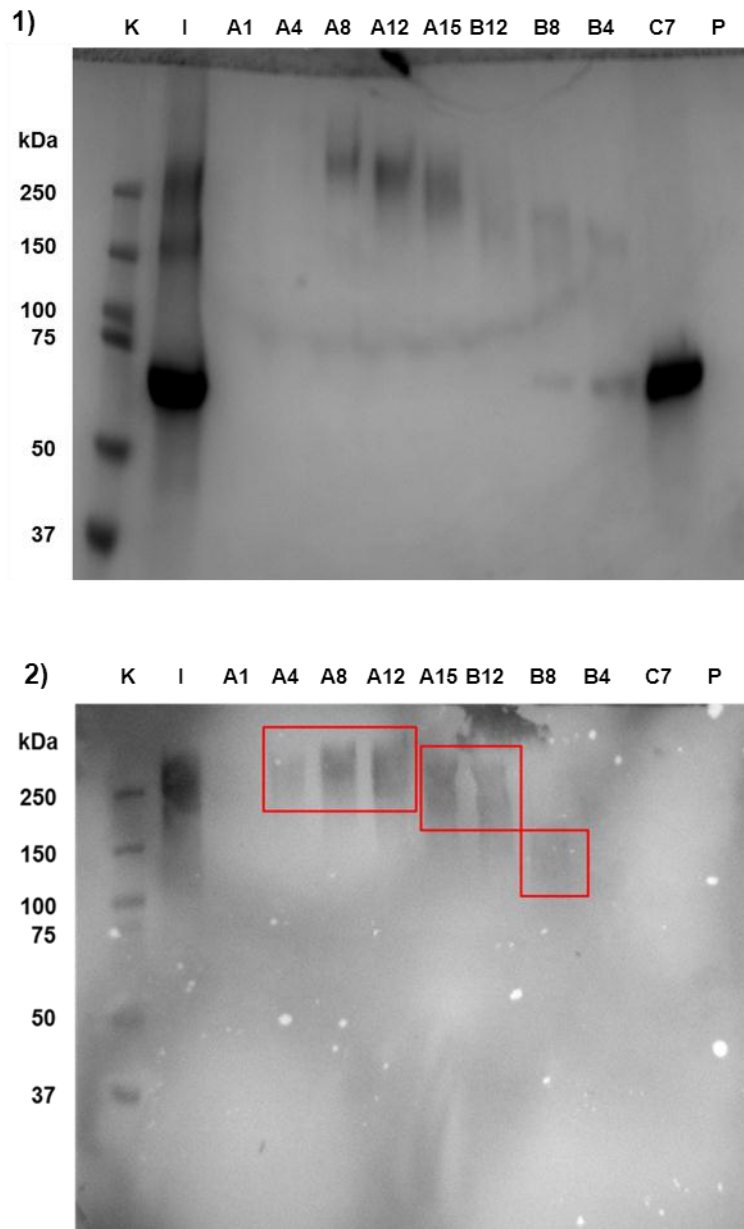


Figure 4.18: 1) Coomassie stained SDS-PAGE gel of fractions taken from SEC of CPS-1-cBSA glycoconjugate; 2) Western blot of SDS-PAGE gel. Lanes: K) Kaleidoscope ladder; I) Initial sample; A1) Fraction A1; A2) Fraction A4; A8) Fraction A8; A12) Fraction A12); A15) Fraction A15; B12) Fraction B12; B8) Fraction B8; B4) Fraction B4); C7) cBSA; P) CPS-1 sample (0.5 mg/ml)

The western blot analysis indicates the conjugation of Bth-CPS-1 (**104**) to the carrier protein and subsequent purification from excess cBSA. The SEC elution pattern, SDS-PAGE and western blot analyses suggests a series of glycoconjugates with varying molecular weights were produced (highlighted in red box Figure 4.18). Using a set of protein standards it is possible to estimate the molecular weight of the different conjugates from the SEC elution pattern.

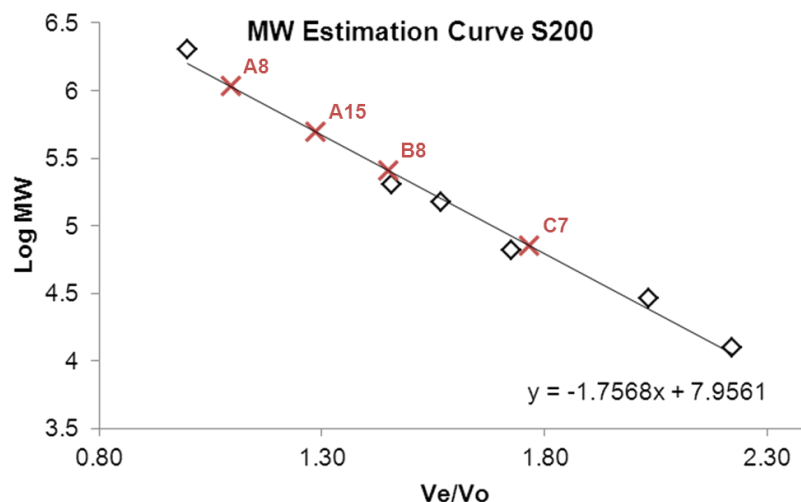


Figure 4.19: Calibration curve for molecular weight prediction using the S200 SEC column. Standards (black diamonds left to right): blue dextran – 2000 kDa; β -amylase – 200 kDa; ADH – 150 kDa; BSA – 66 kDa; carbonic anhydrase - 29 kDa; cytochrome C – 12.4 kDa. Fractions (red crosses): A8 – 1000 kDa; A15 – 500 kDa; B8 – 250 kDa; C7 – 70 kDa. V_e – elution volume of sample; V_o – void volume of column (43.22 ml).

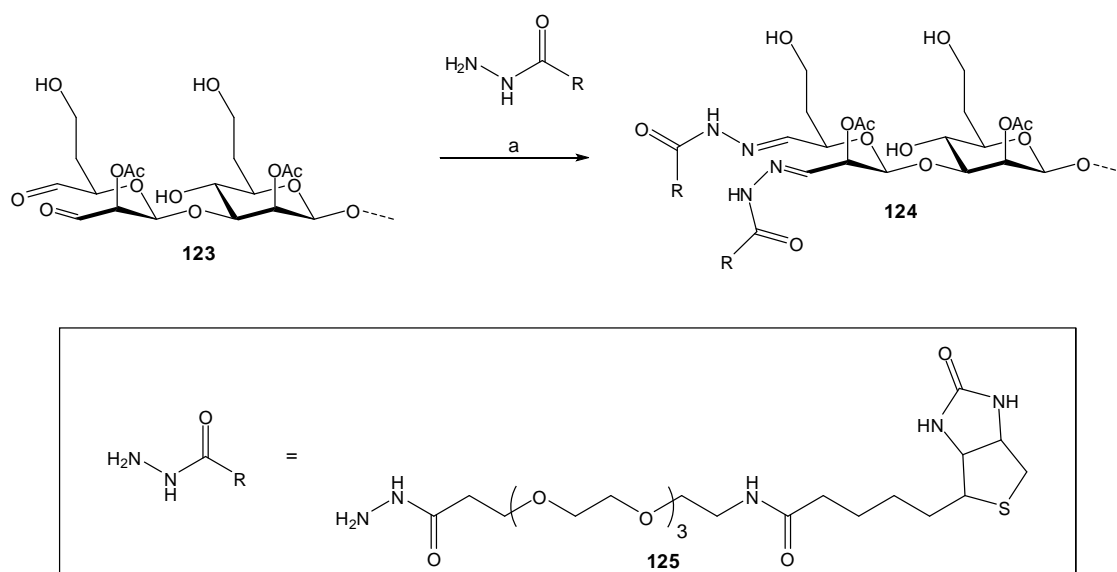
The molecular weight estimation (Figure 4.19) confirms the data from the SDS-PAGE gel and western blot indicating the successful purification of the Bth-CPS-1-cBSA conjugates from the native cBSA (fraction C7 – predicted MW of 70 kDa). Molecular weight estimations of the three sets of bands in the western blot predict conjugates of 1000 kDa (fraction A8); 500 kDa (fraction A15) and 250 kDa (fraction B8). It is important to note that owing to the fact that CPS-1 will behave differently to the globular protein standards the molecular weight estimations can only act as rough guides.

However, it does indicate the generation of glycoconjugates with different Bth-CPS-1 loadings, which can be isolated using chromatography. The isolation and extraction of Bth-CPS-1 (**104**) will afford a polydisperse population of different

polysaccharide chain lengths. Our collaborators (DSTL-Porton Down) have demonstrated using SDS-PAGE, that the Bth-CPS-1 (**104**) is approximately 200 kDa in size (Figure **3.12**). However, an accurate determination of the molecular weight of the Bth-CPS-1 (**104**) population is not possible. The distribution of the Bth-CPS-1-cBSA glycoconjugates could arise from the conjugation of different polymer lengths to the cBSA. This highlights one of the issues of using isolated polysaccharide material for the purposes of vaccine generation. One other explanation for series of conjugates is the possibility of the cross-linking of cBSA molecules with CPS-1. The use of the periodate oxidation step for the generation of aldehyde moieties means that there is potential for reductive amination to occur at both ends of the polysaccharide. As described previously (Section **3.2.2**), it is believed that CPS-1 is capped with a glycerol glycoside, if this is the case periodate oxidation of the glycerol moiety will occur, forming aldehydes available for reductive amination with the carrier protein. Owing to the complex and heterogeneous nature of the conjugation products another route for the loading of CPS-1 on 96-well plates for ELISA analysis was required. However, the conjugation of intact CPS-1 is part of the larger vaccine development program and development of this conjugation protocol is currently on going in the Field group.

4.4.2 Biotinylation of CPS-1

The use of biotinylated CPS-1 in conjunction with streptavidin labelled plates offered a simple and efficient method of attaching CPS-1 to an ELISA plate. As shown in the previous section, the periodate oxidation of CPS-1 is an effective route for the generation of aldehyde groups which can be used to functionalise the CPS-1 polymer. The oxidised Bth-CPS-1 (2 mg) was reacted with EZ-link Hydrazide-PEG₄-biotin³³ (**125**) (Pierce Biotechnology, Thermo Fischer) and purified using a PD-10 desalting column to afford biotinylated CPS-1 (**125**) (2 mg) for use in ELISA analysis (Scheme **4.7**).



Scheme 4.7: reaction of oxidised CPS-1 (123) with EZ-link Hydrazide-PEG₄-Biotin PEG 4. Reagents and conditions: a) 0.1 M NaPO₄, 0.15 M NaCl, pH 7.2, rt, 2 h.

In order to confirm the successful biotinylation of the Bth-CPS-1 (104) an immunofluorescence experiment was employed using streptavidin coated microscope slides. A pattern was drawn on the microscope slide using the biotinylated CPS-1. After incubation with mAb 41VH12 (K69243) antibody and a fluorescent secondary antibody (Alexa 566-anti-mouse, Invitrogen) fluorescence imaging was done. Figure 4.20 shows the detection of biotinylated CPS-1 on the surface of the microscope slide, confirming the successful attachment of biotinylated CPS-1 to a streptavidin surface.

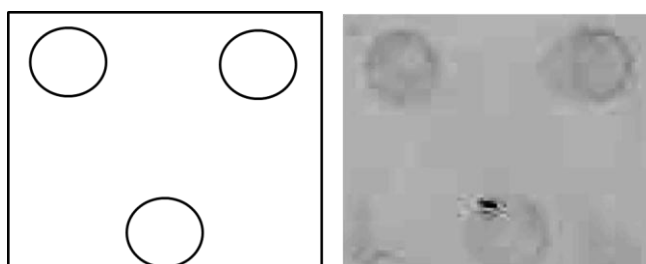


Figure 4.20: Left) Schematic representation of pattern drawn on streptavidin coated microscope slide with biotinylated CPS-1. Right) Fluorescence image of microscope slide demonstrating the successful biotinylation of CPS-1 and subsequent attachment to a streptavidin coated surface.

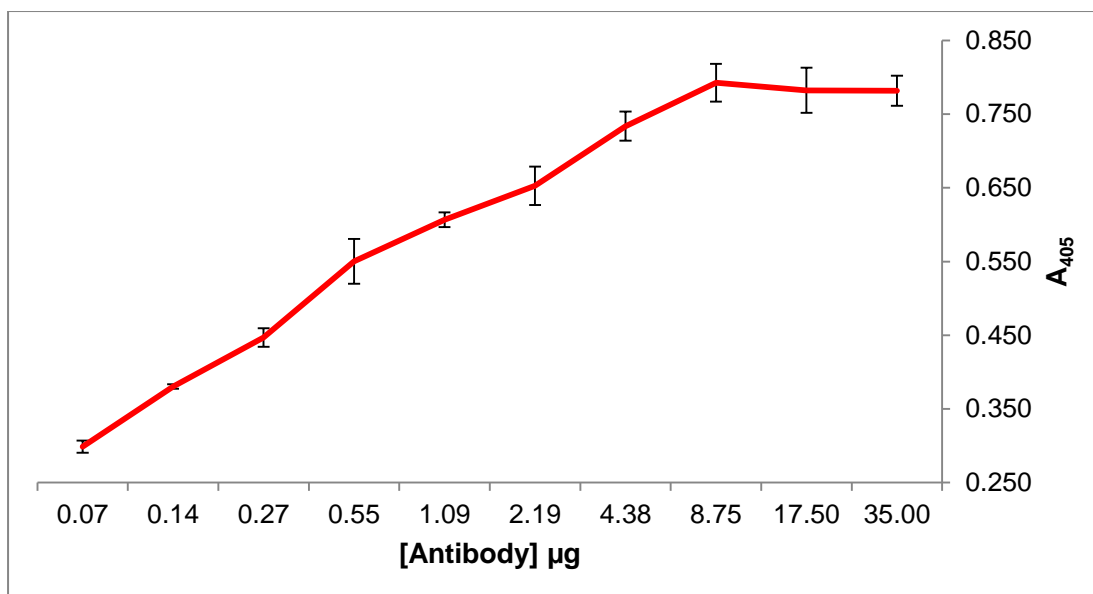


Figure 4.21: ELISA of anti-*B. pseudomallei* (K69243) mAb 4IVH12 activity against biotin-CPS-1 (2 µg/ml) on streptavidin coated plate. Data was collected in duplicate following CPS-1 ELISA protocol 7.4.2.3

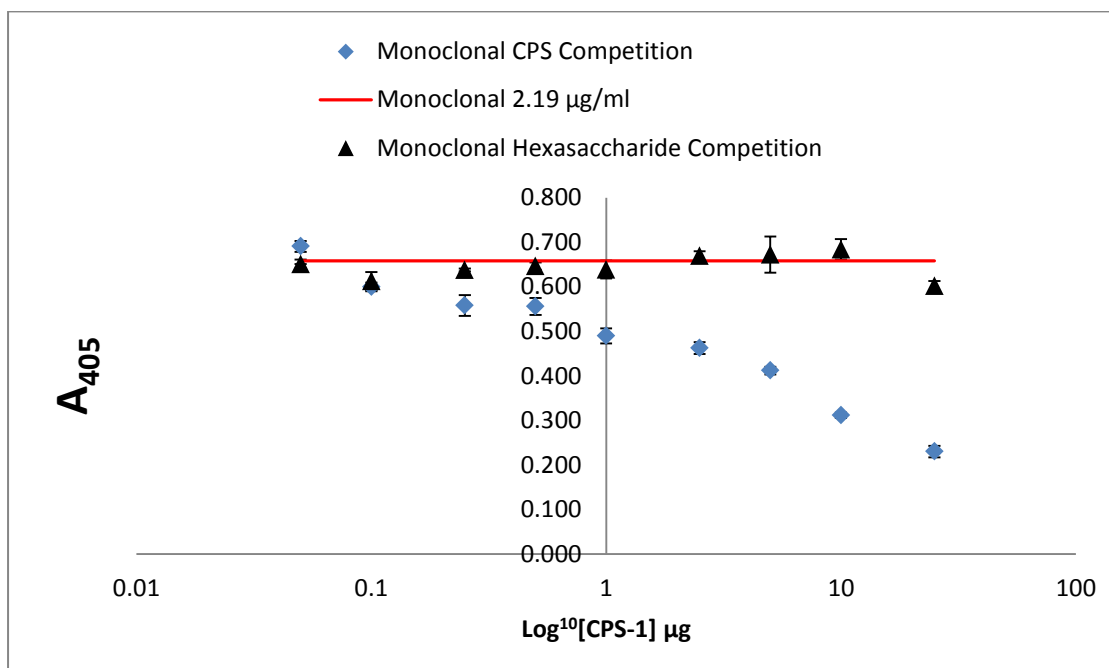


Figure 4.22: Competition ELISA of anti-*B. pseudomallei* (K69243) mAb 4IVH12 (2.19 µg/ml) with purified CPS-1 and Ancora hexasaccharide at varying concentrations (25 – 0.5 µg/ml) against biotin-CPS-1 on the plate (2 µg/ml). Legend: Red) Response of anti-*B. pseudomallei* (K69243) 4IVH12 mAb antibody (2.19 µg/ml) against biotin-CPS-1 under normal conditions; blue diamond) response of anti-*B. pseudomallei* (K69243) monoclonal antibody (2.19 µg/ml) against biotin-CPS-1 with CPS-1 (25 – 0.5 µg/ml) in competition; black triangle) response of anti-*B. pseudomallei* (K69243) mAb 4IVH12 (2.19 µg/ml) against biotin-CPS-1 with Ancora hexasaccharide (25 – 0.5 µg/ml) in competition. Data was collected in triplicate following ELISA protocol 7.4.2.3

4.4.3 ELISA assessment of monoclonal antibody against CPS-1

In order to determine that the biotinylated CPS-1 (**124**) was suitable for ELISA based assays, the binding of the monoclonal antibody was assessed using a streptavidin-coated ELISA plate. The concentration dependent response of the anti-*B. pseudomallei* (K69243) monoclonal antibody demonstrates that the use of biotin-CPS-1 (**124**) and streptavidin coated plates was suitable for the ELISA analysis of the monoclonal antibody (Figure **4.21**). In an attempt to investigate the validity of a synthetic oligosaccharide fragment of CPS-1 for use in a potential *B. pseudomallei* vaccine a competition ELISA with the synthetic Ancora hexasaccharide (**54**) and CPS-1 was carried out (Figure **4.22**).

Anti-*B. pseudomallei* (K69243) mAb 4IVH12 (4.38 µg/ml in PBS_T) was incubated with equal volumes of CPS-1 and equal volumes of hexasaccharide (50 µg/ml – 0.1 µg/ml in PBS_T) for 30 minutes at 37°C. Antibody concentration of 4.38 µg/ml was chosen, as upon incubation with equal volumes of antigen would give a final volume of 2.19 µg/ml. At 2.19 µg/ml, mAb 4IVH12 demonstrates 60% of maximum activity under the conditions of the ELISA assay. Using this concentration ensures that saturated binding of the antibody solution is not achieved and that any competition is clearly visible during the experiment.

The result from the competition ELISA experiment with the Ancora hexasaccharide and the MAb 4IVH12 antibody indicates that there is no recognition of the synthetic hexasaccharide by the monoclonal antibody. This result raises questions about the validity of either the use of synthetic oligosaccharide fragments of CPS-1 as vaccine candidates, or the use of the anti-*B. pseudomallei* (K69243) monoclonal. The 4IVH12 monoclonal (anti-CPS-1) antibody used in this research was raised against heat-inactivated *B. pseudomallei* cells²⁸. As a result of the nature of the mAb, it is not possible for conclusions to be made at this stage. Immunisation trials with the synthetic hexasaccharide are planned for the future and should provide further insight into the potential of synthetic antigens. It has also been shown that heat inactivation of *B. pseudomallei* dramatically decreases the CPS-1 content around the cells, which may have a negative impact of anti-CPS-1 antibody generation (M. Bayliss, personal communication, Table **3.3**). The MAb 4IVH12 antibody was characterised by the authors using western blot and immunofluorescence

techniques. It was shown that the antibody was reactive and specific to; a high-molecular weight polysaccharide component, which was not LPS and was located on the surface of the bacterial cell. Based on these observations, it was concluded that the 4IVH12 mAb was specific for the capsular polysaccharide of *B. pseudomallei*²⁸. Subsequently, AuCoin and co-workers raised another monoclonal antibody (mAb 3C5) specific for *B. pseudomallei* CPS-1 in a similar fashion³⁴. Both monoclonal antibodies have been shown to be highly reactive to all CPS-1-producing strains of *B. pseudomallei* and *B. mallei*^{28, 34}. The monoclonal antibody was also shown not to react towards CPS-1 deficient strains of *Burkholderia* (*B. thailandensis* E264)^{15, 18}. In the case of the mAb 4IVH12 we have shown (section 3.2.1) that the antibody is reactive towards CPS-1 positive *B. thailandensis* E555 ($\Delta wbiI$) strain. However, extraction and characterisation of CPS-1 material from *B. pseudomallei*³⁵, *B. mallei*^{28, 35} and *B. thailandensis* (E555) $\Delta wbiI$ (this thesis) has shown high levels of an α -1,3-mannan polysaccharide (**106**) contaminant (Section 3.2.3). We have shown that the level of mannan content is variable not only between *Burkholderia* species, but also between different polysaccharide extractions (Table 3.4). The presence of the mannan polymer is thought to be linked to the CPS-1-genome cluster and thus it can be expected that all CPS-1 positive strains of *Burkholderia* will also produce the mannan polysaccharide. These observations, along with the lack of specificity of the mAb 4IVH12 antibody towards the Ancora hexasaccharide indicate that the epitope of the monoclonal may not be the -3)-2-O-acetyl-6-deoxy- β -D-manno-heptose-(1- polysaccharide as previously assumed, but could possibly be associated with an alternative *Burkholderia* polysaccharide, such as the α -1,3-mannan²⁸.

The lack of activity of the 4IVH12 antibody against the hexasaccharide (**54**) could also be associated with the global presentation of the polysaccharide. As discussed in Section 1.2.2.1 basic 3D modelling of the CPS-1 suggest that it may form a helical structure. The conformation of the polymer may be radically different from an oligosaccharide fragment and as such the hexasaccharide may not be sufficient for recognition by the antibody at these concentrations (25 - 0.05 μ g/ml).

At this stage the detailed immunological assessment of the 6dHep-TetHc derived antibodies against the purified Bth-CPS-1 (**104**) material was not possible due to time constraints. ELISA analysis using the biotinylated CPS-1 (**124**) was attempted

but all experiments failed as a result of activity of sheep derived sera against the streptavidin plates. An experiment was run with just the commercial streptavidin plates and the sheep sera (0 & 18 W) and both were shown to be equally reactive to the plate. However, the slot-blot analysis of the 6dHep-TetHc sera (section 4.2.3) indicates that the sera are not active towards the native polysaccharide. Investigations into the monoclonal antibody activity towards the Ancora hexasaccharide (54) have highlighted the possibility that the global structure of the CPS-1 may play an important role in the recognition of this polysaccharide and as a result antibodies raised using mono-/oligo-saccharide fragments of the CPS-1 may not be sufficient. Further analysis of the 6dHep-TetHc sera was performed using an Octet 96Red biosensor system (ForteBio) and is described in Section 4.5.

4.5 Octet analysis

The Octet 96Red biosensor system (FortéBio) was used to further investigate the binding of the mAb 4IVH12 and the 6dHep-TetHc derived sera to CPS-1 extracted from *B. thailandensis* E555 Δwbl . The Octet system uses biolayer interferometry to detect binding onto the surface of a functionalised disposable biosensor. The dip and read format of the Octet systems negates the need for microfluidics giving it a distinct advantage over other techniques, such as SPR (Biacore)³⁶.

Initial attempts were made to use anti-mouse IgG (Fc Capture (AMC)) functionalised biosensors to immobilise mAb 4IVH12 anti-CPS-1 antibody on the surface of the biosensor. Detection of binding of the immobilised antibody and the CPS-1 in solution was difficult with only a low response being observed. In order to assess both the binding of mAb 4IVH12 and the Hept-TetHc sera to CPS-1, streptavidin biosensors were used to immobilise biotinylated CPS-1 (124).

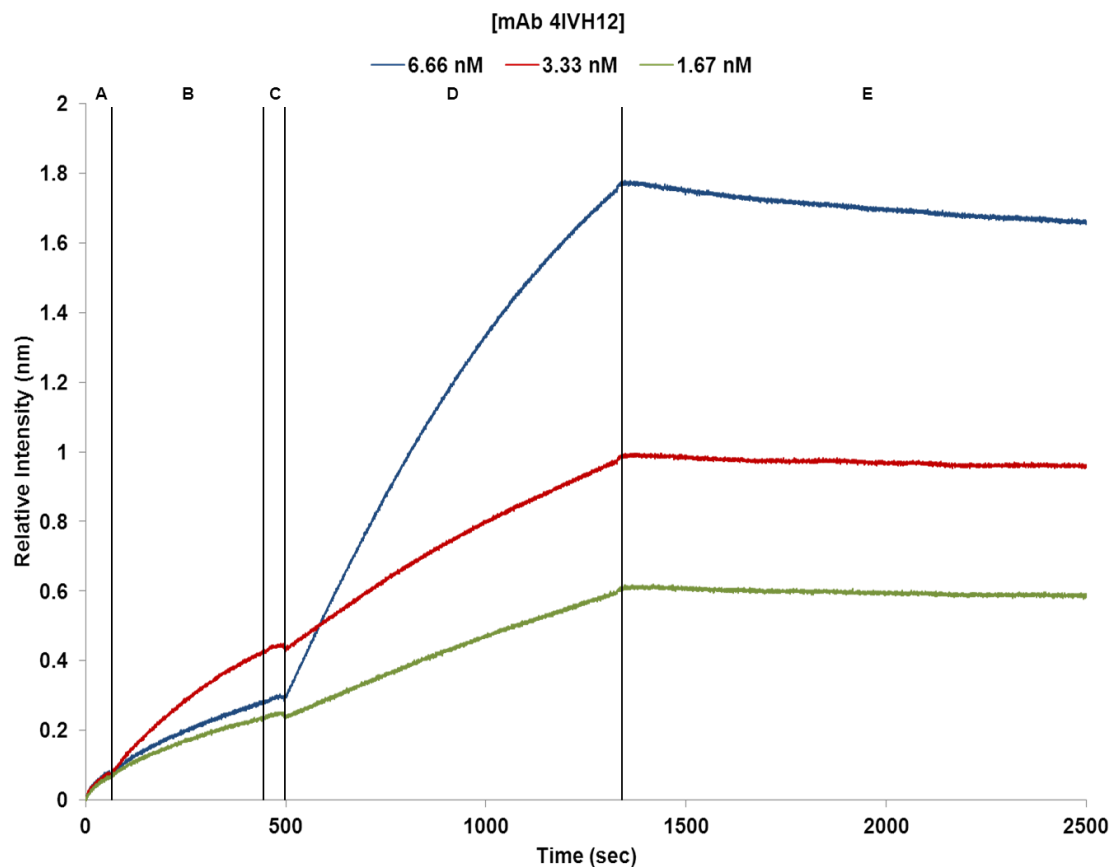


Figure 4.23: Octet analysis of mAb 4IVH12 binding to biotin-CPS-1 immobilised (10 $\mu\text{g/ml}$) on the surface of streptavidin biosensors. Legend: (blue) 6.66 nM mAb 4IVH12; (red) 3.33 nM mAb 4IVH12; (green) 1.67 nM mAb 4IVH12. Work flow: A) Initial baseline for biosensor stabilisation (60 seconds); B) loading of biotinylated CPS-1 (400 Seconds); C) baseline stabilisation (60 seconds); D) binding of antibodies to immobilised CPS-1 (900 Seconds); E) dissociation of antibodies (1200 seconds).

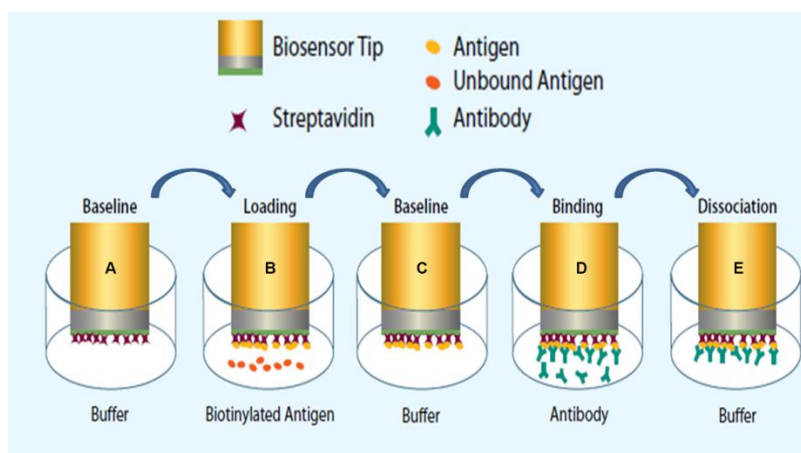


Figure 4.24; Schematic representation of the octet experiment for mAb 4IVH12. Workflow: A) Initial baseline for biosensor stabilisation (60 seconds); B) loading of biotinylated CPS-1 (400 Seconds); C) baseline stabilisation (60 seconds); D) binding of antibodies to immobilised CPS-1 (900 Seconds); E) dissociation of antibodies (1200 seconds). Image adapted from ForteBio Octet Brochure³⁷

Figure **4.23** shows the binding curves of three different concentrations (6.66 nM, 3.33 nM and 1.67 nM) of mAb 4IVH12 with biotinylated CPS-1 immobilised on streptavidin biosensors. The binding curves for mAb 4IVH12 indicates strong binding of the antibody to the biotinylated CPS-1 (**124**), with a slow dissociation rate [k_d 2.27×10^{-5} 1/s. The equilibrium dissociation constant (k_{on}/k_{off}) of mAb 4IVH12 to the biotinylated CPS-1 was calculated, (using ForteBio Octet analysis software) to be 2.66×10^{-11} M ($R^2 = 0.99$) demonstrating the low nanomolar affinity of the monoclonal antibody for the biotinylated Bth-CPS-1 preparation (**124**).

Next the binding of the combined heptose sera to the immobilised biotinylated CPS-1 (10 $\mu\text{g}/\text{ml}$) was assessed using the Octet instrument. Previously, assessment of the binding was attempted using ELISA and slot blot analysis, however due to high background binding this was not possible. It was believed that due to the sensitivity of the Octet system it would be possible to deconvolute specific binding from background binding. Serial dilutions of the pre-immune sera were analysed as reference samples and the data were subtracted from the corresponding 18 week sera data. This normalised the data removing the non-specific binding element of the pre-immune sera leaving only binding of the immune sera. The data were corrected to the baseline and the 25-point moving average response was plotted against time (Figure **4.25**).

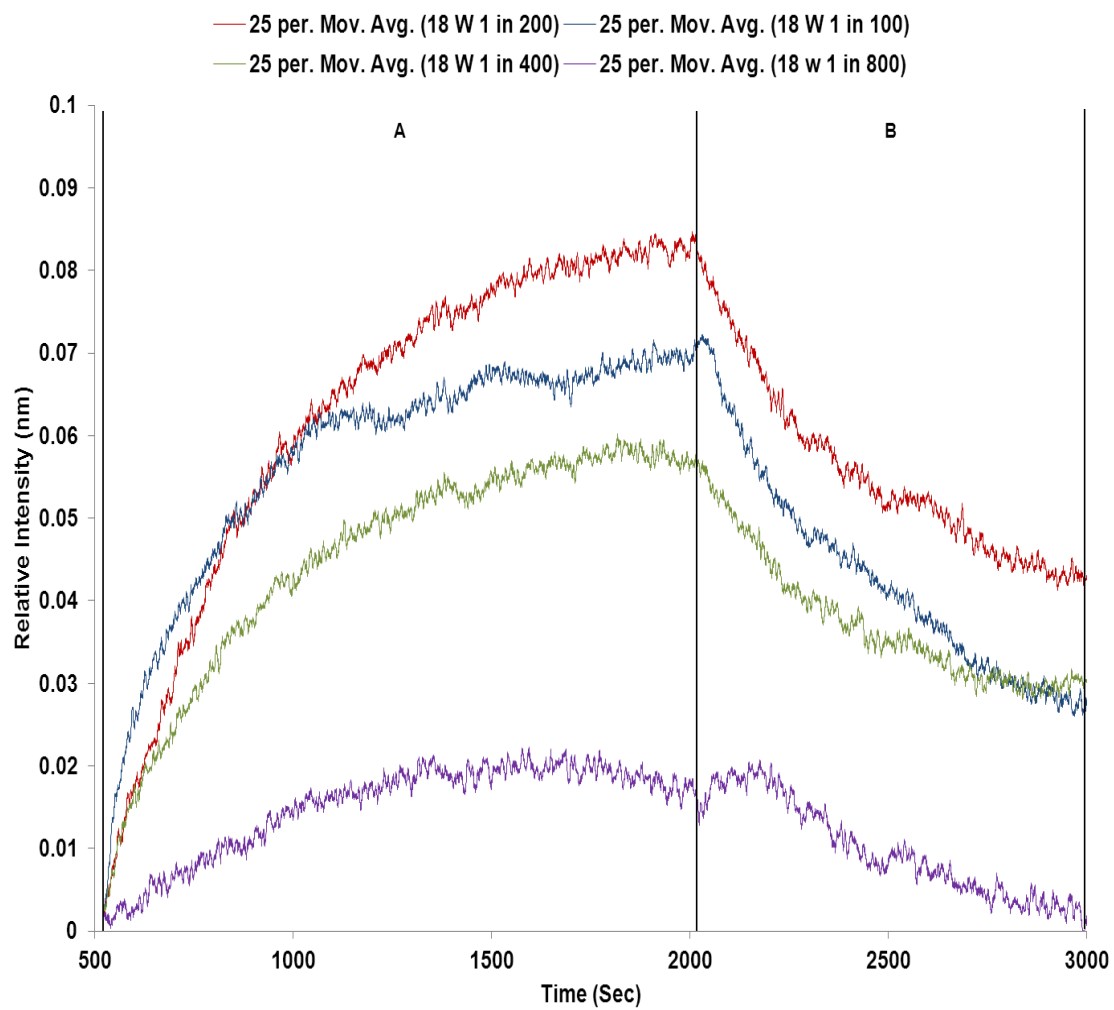


Figure 4.25: The normalised binding curves for the 18 W heptose sera. Legend: (blue) 18 W 1 in 100 dilution; (red) 18 W 1 in 200 dilution; (green) 18 W 1 in 400 dilution and (purple) 18 W 1 in 800 dilution. (A) association step (1500 sec); (B) dissociation step (1000 sec). Data was normalised by subtraction of pre-immune binding from 18 week binding and corrected to the baseline. 25-point moving average of the data was plotted.

Figure 4.24 demonstrates that when the background binding of the pre-immune sera is removed, there is some binding of the 6dHep-TetHc polyclonal sera to the immobilised capsular polysaccharide. The binding only occurs at very high sera concentration, with no binding observed below the 1 in 400 dilution factor. However, the binding profile observed in the high sera concentrations (1 in 100 (blue); 1 in 200 (red); and 1 in 400 (green)) resemble a typical antibody-antigen binding curve. This result indicates that there is potential binding of the monosaccharide derived antibodies to the cognate polysaccharide CPS-1

4.6 Conclusions and future directions

This chapter has detailed the preliminary immunological assessment of anti-monosaccharide raised antibodies. Monosaccharide specificity was observed in both the D-glucose and 6-deoxy-D-manno-heptose derived antibodies. However there were high levels of background binding to the non-cognate haptens throughout. The initial immunological assessment of the D-glucose derived polyclonal sera (Glc-TetHc) has demonstrated that antibodies with specificity for different monosaccharides can be produced. ELISA and slot-blot analysis has shown that the Glc-TetHc sera have higher binding towards the Glc-BSA glycoconjugate when compared to the Man-BSA and 6dHep-BSA (Section 4.2.1). Further analysis of the polyclonal antibodies, including the use of the second generation antigens (short-linker), is required to further understand the binding specificity of the polyclonal antibodies. By using a shortened/different linker it may be possible to determine the role of the linker molecule on antibody binding affinity to the target monosaccharide. Immunisation with monosaccharide conjugates employing a series of linker molecules could help elucidate the ideal linker for the presentation of monosaccharides to the immune system

Polyclonal antibodies raised against the 6-deoxy-6-fluoro-D-glucose hapten (117) (Section 4.3.2) were shown to bind to the native D-glucose BSA conjugate (97). Affinity purification of the polyclonal sera using immobilised D-glucose hapten (69) would remove some background binding which would facilitate the further characterisation of the antibodies. The Octet Red96 biosensor system provides a high-throughput platform for the kinetic analysis of antibody binding. After purification of the Glc-TetHc and 6d6FGlc-TetHc sera, binding kinetics analysis

using the Octet system should help to elucidate the specificities of the antibodies and determine the effects of fluorination of the monosaccharide antigen.

Analysis of the 6dHep-TetHc derived sera activity towards the biotinylated Bth-CPS-1 (**124**) using ELISA was not possible due to the high background activity of the polyclonal sera against the streptavidin coated plates. However, octet analysis of the 6-deoxy-D-heptose monosaccharide-derived antibodies suggested that some binding to the cognate CPS-1 occurred. In order to confirm this, the Octet analysis (Section **4.5**) needs to be repeated using all of the available immune sera samples (6, 10, 14 & 18 weeks). If the observed binding is a result of specificity towards the cognate polysaccharide, maturation of the binding profile would be observed. If successful, purification of the antibodies and characterisation of the binding of the antibodies to native CPS-1 on the surface of the *B. thailandensis* E555 $\Delta wbiI$ mutant will be required. Immunofluorescence and ELISA analysis will provide some information regarding the potential application of the monosaccharide antigen in vaccination studies.

Further investigation of the mAb 4IVH12 anti-CPS-1 monoclonal antibody using biotinylated CPS-1 showed it to have low nanomolar affinity. However, detection of binding to the synthetic Ancora hexasaccharide (**54**) was not observed. It was concluded that either CPS-1 forms a global structure, thus presenting a conformational epitope which is required for recognition by the monoclonal antibody. As such, the synthetic hexasaccharide will not present the same conformational epitope and mAb 4IVH12 will not bind. Alternatively, the monoclonal antibody, which was raised against heat-inactivated *B. pseudomallei* cells, is specific for another epitope such as the α -1,3-mannan polymer also produced by *B. pseudomallei* and *B. thailandensis* E555 $\Delta wbiI$ (Section **3.2.1** & **3.2.2**). Understanding the role of the α -1,3-mannan in the virulence of *B. pseudomallei* and its potential as a vaccine candidate is important to this project. Currently CPS-1 extracts from three strains of *Burkholderia* (*B. pseudomallei*, *B. mallei* and *B. thailandensis* E555) have been shown to contain the mannan polysaccharide to varying degrees (Section **3.2.2**). Access to the purified polysaccharides will enable further investigation and understanding of the role of these two polysaccharides and inform decisions regarding their use as vaccine candidates.

4.7 References

1. H. F. Stils, *ILAR Journal*, 2005, **46**, 280-293.
2. C. F. M. Hendriksen, *ILAR Journal*, 2005, **46**, 227-229.
3. P. Chiarella, E. Massi, M. De robertis, E. Signori and V. M. Fazio, *Exp. Opin. Bio. Ther.*, 2007, **7**, 1551-1562.
4. B. Guy, in *Carbohydrate-Based Vaccines and Immunotherapies*, John Wiley & Sons, Inc., Editon edn., 2008, pp. 89-115.
5. E. Benjamini and S. Leskowitz, *Immunology A Short Course*, Second edn., Wiley-Liss, 1991.
6. H. N. Eisen and G. W. Siskind, *Biochemistry*, 1964, **3**, 996-1008.
7. J. H. L. Playfair, *Immunology at a Glance*, Fourth edn., Blackwell Scientific Publications, 1987.
8. D. Bhattacharyya, A. T. Hammond and B. S. Glick, Editon edn., 2009, vol. 619, pp. 403-410.
9. C. A. Schneider, W. S. Rasband and K. W. Eliceiri, *Nat. Methods*, 2012, **9**, 671-675.
10. D. Saverino, E. A. Debbia, A. Pesce, A. M. Lepore and G. C. Schito, *J. Antimicrob. Chemother.*, 1992, **30**, 261-272.
11. D. W. Haas, H. J. Ribaud, R. B. Kim, C. Tierney, G. R. Wilkinson, R. M. Gulick, D. B. Clifford, T. Hulgand, C. Marzolini and E. P. Acosta, *AIDS*, 2004, **18**, 2391-2400.
12. S. Purser, P. R. Moore, S. Swallow and V. Gouverneur, *Chem. Soc. Rev.*, 2008, **37**, 320-330.
13. J. Zhu, J. D. Warren and S. J. Danishefsky, *Exp. Rev. Vac.*, 2009, **8**, 1399-1413.
14. S.-i. Hakomori, *Cancer Res.*, 1996, **56**, 5309-5318.
15. J. Yan, X. Chen, F. Wang and H. Cao, *Organic & Biomolecular Chemistry*, 2013, **11**, 842-848.
16. S. Hakomori, *Ann. Rev. Immunol.* 1984, **2**, 103-126
17. F. Yang, X.-J. Zheng, C.-X. Huo, Y. Wang, Y. Zhang and X.-S. Ye, *ACS Chemical Biology*, 2010, **6**, 252-259.
18. T. Oberbillig, C. Mersch, S. Wagner and A. Hoffmann-Roder, *Chem. Commun.*, 2012, **48**, 1487-1489.
19. P. J. Card, *J. Org. Chem.*, 1983, **48**, 393-395.
20. V. Dinoiu, *Rev. Roum. Chim.*, 2007, **52**, 219-234.

21. E. Lee, P. Browne, P. McArdle and D. Cunningham, *Carbohydr. Res.*, 1992, **224**, 285-289.
22. C. W. Somawardhana and E. G. Brunngaber, *Carbohydr. Res.*, 1981, **94**, C14-C15.
23. J. Compton, *JACS*, 1938, **60**, 395-399.
24. K. Czifrak and L. Somsak, *Carbohydr. Res.*, 2009, **344**, 269-277.
25. S. Zielen, M. Bröker, N. Strnad, L. Schwenen, P. Schön, G. Gottwald and D. Hofmann, *J. Immunol. Methods*, 1996, **193**, 1-7.
26. B. M. Gray, *J. Immunol. Methods*, 1979, **28**, 187-192.
27. J. E. Sippel and N. I. Girgis, *The American Journal of Tropical Medicine and Hygiene*, 1991, **45**, 676-682.
28. J. F. Ellis, Thesis: Antibody detection of *Burkholderia pseudomallei* and *Burkholderia mallei* University of Aston in Birmingham, 2000.
29. M. N. Burtnick, C. Heiss, R. A. Roberts, H. P. Schweizer, P. Azadi and P. J. Brett, *Frontiers in cellular and infection microbiology*, 2012, **2**, 108.
30. A. Muckerheide, R. J. Apple, A. J. Pesce and J. G. Michael, *J. Immunol.*, 1987, **138**, 833-837.
31. K. A. Kristiansen, A. Potthast and B. E. Christensen, *Carbohydr. Res.*, 2010, **345**, 1264-1271.
32. M. N. Burtnick, C. Heiss, R. A. Roberts, H. P. Schweizer, P. Azadi and P. J. Brett, *Frontiers in cellular and infection microbiology*, 2012, **2**.
33. Q. Wang and L. E. Limbird, *J. Biol. Chem.*, 2002, **277**, 50589-50596.
34. D. P. AuCoin, D. E. Reed, N. L. Marlenee, R. A. Bowen, P. Thorkildson, B. M. Judy, A. G. Torres and T. R. Kozel, *PLoS ONE*, 2012, **7**, e35386.
35. C. Heiss, M. N. Burtnick, Z. Wang, P. Azadi and P. J. Brett, *Carbohydr. Res.*, 2012, **349**, 90-94.
36. Y. Abdiche, D. Malashock, A. Pinkerton and J. Pons, *Anal. Biochem.*, 2008, **377**, 209-217.
37. Octect Red96 Biosensors, ForteBio, ed. ForteBio, Editon edn., 2008. <http://www.fortebio.com/octet-RED96.html>

5 Hepatitis B core Antigen Virus-like Particle carrier protein

5.1 Introduction

The role of carrier proteins has been pivotal in the development of polysaccharide conjugate vaccines for diseases caused by *Haemophilus influenza*, *Neisseria meningitidis* and *Streptococcus pneumonia*. However, it has become apparent that as the use of these vaccines becomes more widespread, the potential for immunological interference caused by the carrier protein increases. This interference is described as carrier-induced-epitopic suppression (CIES). CIES describes how pre-existing antibodies to the carrier protein can reduce the immunological efficacy of the conjugated hapten. Figure 5.1 highlights the three possible mechanisms by which CIES can affect the immunogenicity of haptens conjugated to carrier proteins¹.

Figure 5.1 **A** shows the normal interaction of a conjugate vaccine with the immune system, the carrier protein enables the T-cell dependant recognition of the conjugate antigen. This is the basis of the cooperative effect which is the driving force behind the use of carrier proteins such as Diphtheria Toxoid (DT_{CRM197}). Figure 5.1 **B** highlights how the presence of anti-carrier protein antibodies can lead to steric hindrance, effectively blocking the hapten molecule from the immune system (B-cells) leading to a poor response and thus fewer antibodies. Figure 5.1 **C** shows how the recognition of the carrier protein can dominate the T-helper cell response through competitive mechanisms and lead to low yield of anti-hapten antibodies. In Figure 5.1 **D** the presence of T-regulatory cells specific for the carrier proteins can negatively affect anti-hapten responses.

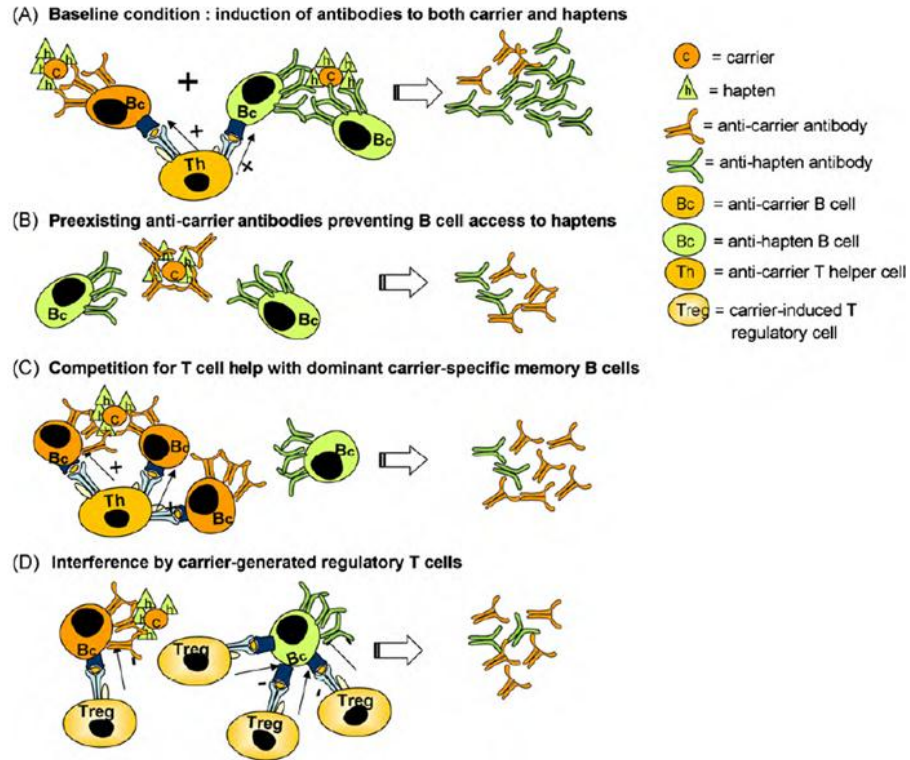


Figure 5.1: Schematic representation of mechanisms for CIES, reproduced with permissions from Dagan¹ *et al.*; Copyright Elsevier 2010.

Research has also shown that when compared to other carrier proteins such as diphtheria toxin, the use of Tet-Hc in conjugate vaccines results in increased CIES effects, necessitating higher vaccine doses¹. As a result there has been movement towards the use of novel carrier protein in glycoconjugate vaccines to combat this problem, with the use of virus-like particles (VLPs) as vaccine carriers becoming an attractive option².

Since the idea of using VLPs in vaccinations was first introduced in the 1980's by Maupas³ *et al.* and Krugman^{4 5} *et al.* during their work on Hepatitis B vaccines, there has been significant interest in the area⁶. VLPs are multiprotein structures which mimic the structure of the native virus, but do not have the viral genomic information and as a result are non-replicative². Owing to this, VLPs avoid the need for attenuation or inactivation highlighting their potential as safe vaccine carriers². The repetitive, organised structure of VLPs leads to cross-linking of B-cell receptors making VLPs capable of inducing strong B-cell responses without the need for

adjuvants or high vaccine doses^{2, 7, 8}. As a result of these factors VLPs are a safe, potent and cost effective means of vaccine generation.

There are currently a small number of commercially available VLP-based vaccines in use around the globe (Table 4.1), with a great many more undergoing clinical trials^{2, 9}.

Vaccine	Vaccination Target	Manufacturer
Engerix [®]	Hepatitis B (HBV)	GSK
Ceravix [®]	Human papillomavirus (HPV)	GSK
Recombivac HB [®]	Hepatitis B (HBV)	Merck
Gardasil [®]	Human papillomavirus (HPV)	Merck

Table 5.1: Table listing commercially available VLP based vaccines in use as of 2013².

Currently the available VLP-based vaccines are used for vaccinating against the virus from which the VLP is derived (i.e. Ceravix is a HPV based VLP vaccine for HPV infection). These vaccines use the structural mimicry of the VLPs towards the native virus to elicit an immune response and generate protective immunity². However, due to their highly repetitive and immunogenic structure there has been recent interest in using VLPs as antigen carriers for other bacterial (tuberculosis)¹⁰, viral (dengue)¹¹ and protozoan (malaria)¹² infections. Much of this research has focused on the use of hepatitis B derived VLP carrier proteins¹³.

5.1.1 Hepatitis B virus

Hepatitis B Virus (HBV) is a DNA virus which infects the liver causing both acute and chronic liver infections. It is widespread throughout the globe, with sub-Saharan Africa and East Asia being most affected, where up to 10% of the adult population are infected. Annually hepatitis B infects 2 billion people and accounts for 600,000 deaths (WHO Hepatitis B Fact Sheet N^o204, 2013). The HBV particle (Figure 5.2) consists of an exterior lipid envelope, the surface antigen (HBs-Ag) and an interior nucleocapsid, the core antigen (HBcAg)^{13, 14}. HBeAg is an extracellular form of HBcAg and plays an important role in the identification of chronic Hepatitis B patients¹⁵. The nucleocapsid encapsulates the HBV genome and the polymerase required for viral replication¹⁶. The surface antigen consists of a lipid envelope

embedded with three different glycoproteins (large, middle and small surface antigens), which are required for the adhesion and infection of host cells¹³. The particles were first identified by Dane *et al.* in 1970, using electron microscopy, and are now referred to as Dane particles¹⁷.

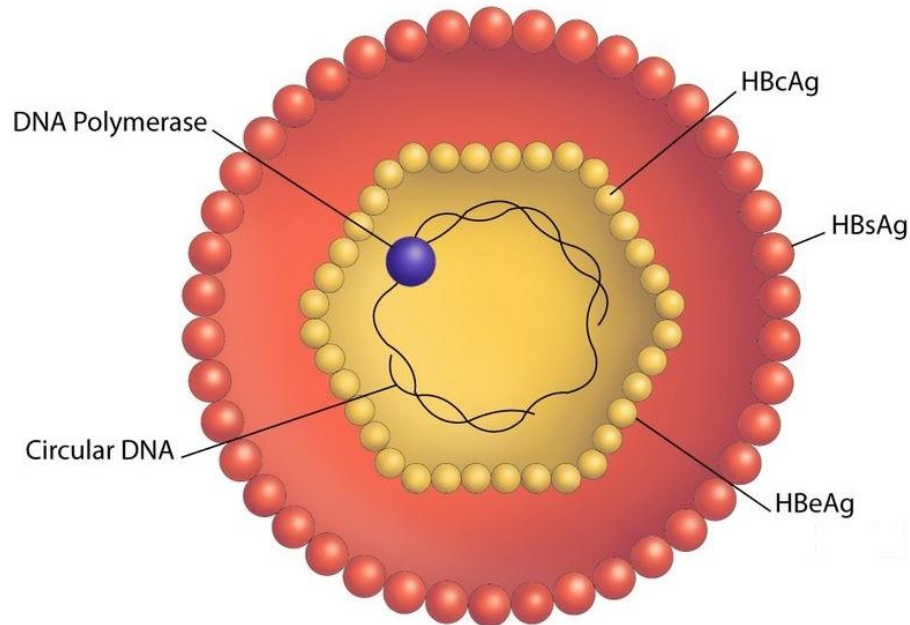


Figure 5.2: Structure of the hepatitis B virus (picture taken from Johns Hopkins Bloomberg School of Public Health Website)¹⁸.

The current hepatitis B vaccine program is VLP-based (Engerix and Recombivac HB) and uses the HBsAg of the hepatitis B viron¹⁹. However, owing to the highly immunogenic nature of the core antigen (HBcAg) there has been increased research in using this VLP as a novel protein carrier for vaccines. HBcAg has been previously shown to be an excellent antigen carrier platform²⁰ with strong immunogenicity and adjuvanting properties. The strong self-adjuvanting properties of HBcAg are as a result of the fact that HBcAg can act as both a T-cell dependent and T-cell independent antigen^{21, 22}. HBcAg is a 21.5 kDa protein (Figure 5.3), with two HBcAg monomers forming a dimer through disulphide bridges (Figure 5.3 yellow), which acts as the building block for the capsid shell. The capsid shell has an icosahedral shape (Figure 5.4) and either consists of 180 (30 nm; T=3 particle) or 240 (34 nm T=4 particle) copies of the HBcAg protein¹⁴.

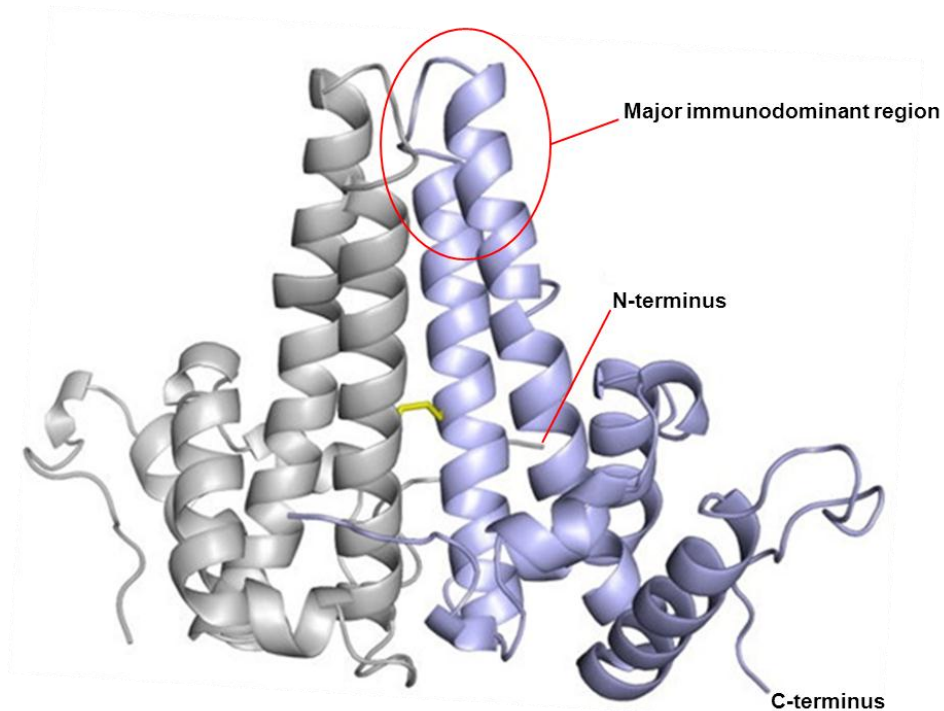


Figure 5.3: Structure of HBcAg dimer (monomer in purple). Image reproduced from Wynne *et al.* Copyright Elsevier 1999²³.

The HBcAg dimer has three primary sites for insertion of an antigenic epitope (hapten) for presentation, the C-terminus, N-terminus and the major immunodominant region (MIR) (Figure 5.3). The N-terminal domain is necessary for the assembly of the HBc monomers into the global VLP structure^{2,14}. Owing to its requirement for particle assembly, hapten attachment/insertion at this site is problematic. The C-terminus is arginine-rich and is responsible for nucleic acid-binding and not necessary for particle assembly²⁴. The MIR region (amino acids 74-89) at the top of the 'spike' (E1 loop) that is formed by the arrangement of two α -helices, is highly immunogenic. The MIR has been shown to be the main region of shared antigenicity between the two forms of this protein (HBcAg and HBeAg), indicating that it is the primary immunogenic site in both assembled VLPs and free core protein monomers²⁵. Modification and insertion of epitopes into this region has been the most successful for the generation of highly reactive recombinant VLPs^{2,26}. There have been a number of efforts focused on the insertion of peptide sequences into the MIR of HBcAg, which are detailed in the following references^{2,13,27,28}.

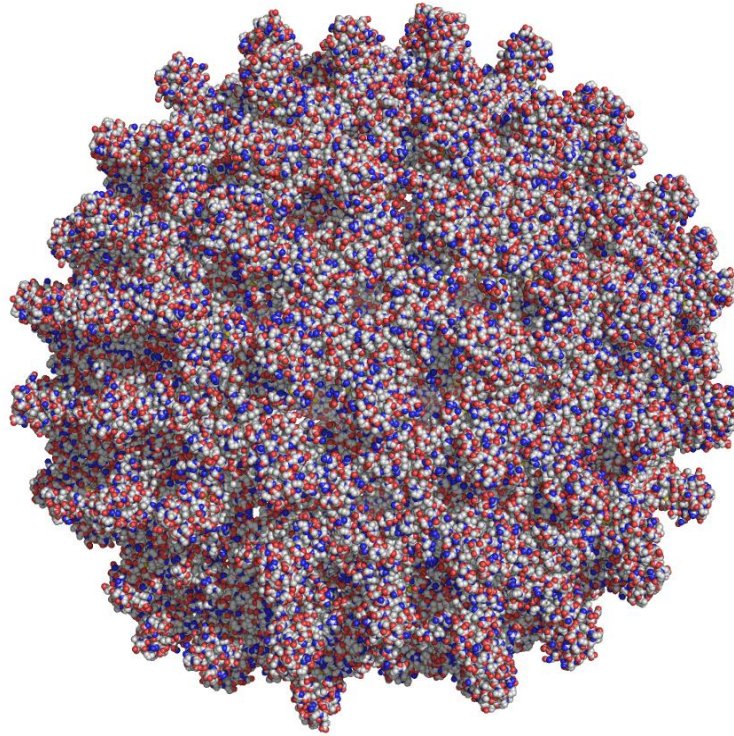


Figure 5.4: Image of the HBcAg VLP (T=3 particle) PDB code: IQGT, model produced using PyMol.

Figure 5.4 shows the global structure of the HBcAg VLP, with the E1 loops protruding from the particle surface offering the ideal site for antigen attachment¹³.

5.1.2 HBcAg tandem core

The development of HBcAg based vaccines is dependent on the successful insertion of the antigen of choice into the MIR region of the E1 loop²⁹. The location of the MIR and the proximity of the two loops in the dimer (Figure 5.3) mean that the presence of large peptides or highly charged inserts, can lead to stereo/electronic effects which can adversely affect particle assembly. In order for the successful insertion of large peptides into the MIR, the N- and C- terminus of the peptide insert must naturally be in close proximity to avoid steric constraint on the insert or be attached by long flexible linkers³⁰. The inclusion of large proteins in the MIR of the HBcAg monomer can also lead to steric interference on the assembly of the dimer building block. In an attempt to combat this, groups in Leeds (Rowlands) and Oxford (Stuart) developed tandem core technology, which is currently licensed by our collaborators, iQur²¹. Utilising computational analysis, gene constructs were

produced in order to fuse two HBcAg core monomers together through a flexible peptide linker (Figure 5.5)²¹.

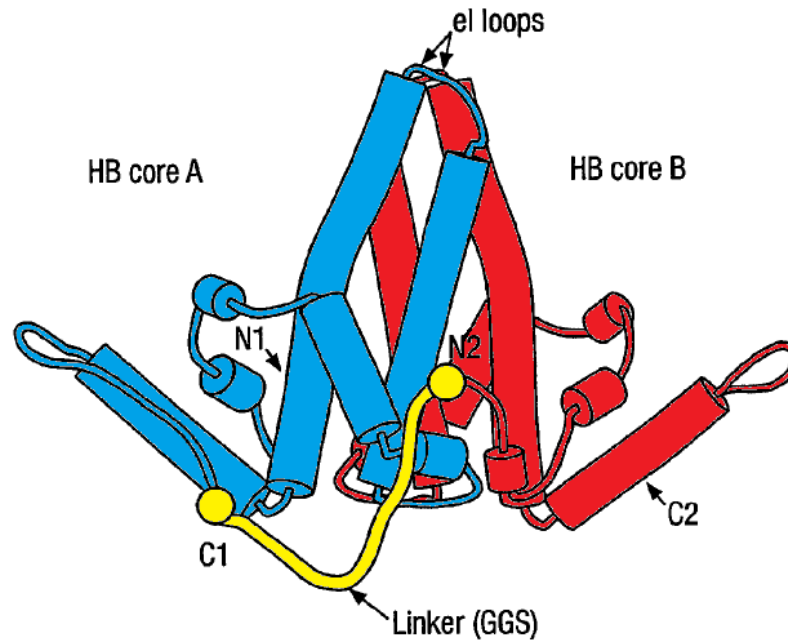


Figure 5.5: Schematic of the tandem HBcAg core with two HBcAg monomers fused together with a flexible peptide linker highlighted in yellow (adapted from Gehin *et al*²¹).

The fusion of two HBcAg monomers to form a single peptide increases the versatility of the HBcAg as a vaccine carrier in two ways. Through the inclusion of distinct restriction sites in the two E1 loops each loop can be addressed independently to either produce a bivalent platform (Figure 5.6a) or a system where the antigen is only inserted a single E1 loop (Figure 5.6b) removing the potential for steric hindrance associated with double insertion (Figure 5.6c).

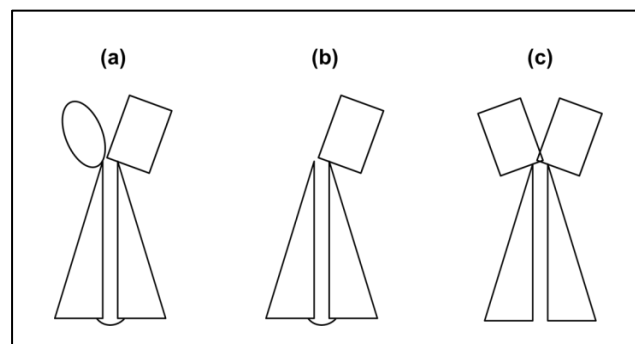


Figure 5.6: Schematic representation illustrating (a) the development of a bivalent platform using tandem technology, (b) the insertion of antigen into a single E1 loop with tandem technology and (c) the steric hindrance that is associated with the use of wild-type HBcAg core.

In comparison to the current studies using the tandem-core technology, our research efforts were focused on the development of a chemically addressable HBc-Ag carrier protein. Instead of engineering genetic constructs for the insertion of a single protein epitope into the MIR of the HBc-Ag protein, we designed a short peptide insert which would allow chemical conjugation of synthetic antigens to the E1-loop.

5.1.2.1 The peptide insert

As described earlier in this thesis, the development of a carbohydrate vaccine for *B. pseudomallei* has involved the chemical conjugation of haptens (**69** and **91**) to surface lysine residues present in TetHc. In order to make use of the existing haptens we decided to focus on the insertion of lysine residues into the MIR of the HBcAg protein (in both the *wild type* monomer and the tandem core), in an attempt to furnish a chemically addressable HBcAg VLP. In 2002³¹, Jegerlehner *et al.* demonstrated the insertion of a single lysine into the MIR sequence and used a hetero-bifunctional linker to conjugate a series of antigens to the VLP. During this work the authors attempted coupling of antigens to both the wt-HBcAg and their lysine-modified variant. The coupling efficiency of the unmodified wild-type VLP was shown to be less than 5%³¹. There are only two native lysines in each HBcAg monomer, both of which are buried in the VLP shell upon assembly, masking them from chemical modification. This highlights the need for the insertion of chemically addressable groups, such as lysine, for the development of a platform carrier protein.

We wanted to build on the positive results of the multivalent display of the heptose antigen (**91**), discussed in Chapters **2** and **4**, through the use of an oligo-lysine insert. It was hoped that through the use of an oligo-lysine insert at the tip of the MIR region, the organised and repetitive structure of the VLP could be exploited. The repetitive presentation by the VLP would result in B-cell cross-linking, mimicking a natural polysaccharide immune response, whilst still having T-cell dependant activation as a result of the protein carrier.

However, it was thought that the insertion of an oligo-lysine insert would lead to a large charge imbalance in the particle, making the tips of the E1-loop positively charged. This could not only affect the assembly of the dimers into viable VLPs, but also the immunogenic properties of the assembled VLP. In order to combat this it was decided to flank the poly-lysine insert with aspartate residues and thus balance the positive charge. Glycine spacers were also used at each end of the insert to separate the sequence from the native peptide. Inserted in the DNA sequence that codes for the E1 loop are two restriction sites (AseI and Sall) which are used in the development of new VLP constructs. The section between the two restriction sites codes for a 10 amino acid sequence. It has been shown previously that it is possible to insert entire proteins into the MIR of the HBcAg protein³². However, these studies involved extensive optimisation of the expression and purification techniques to afford valid recombinant VLPs³⁰. In order to reduce the likelihood of preventing particle assembly, a small peptide insert of similar size (14 amino acids) to the original sequence was designed. The peptide insert was comprised of Glycine-(Aspartate)₃-(Lysine)₆-(Aspartate)₃-Glycine (D₃K₆D₃), in an attempt to maximise the number of lysine residues, without dramatically increasing the size of the insert. It was anticipated that the inclusion of four extra amino acids would not have a negative effect on particle assembly; however this could only be determined experimentally. A model of the new HBcAg monomer was produced using PyMol (Figure 5.7) with the inserted peptide sequence highlighted in yellow (lysine) and blue (aspartate).

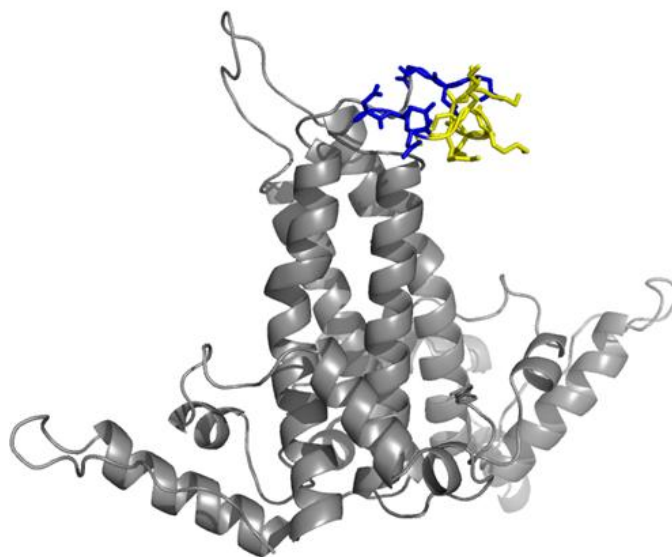


Figure 5.7: Structure of *wt*-HBcAg dimer with new protein insert (Lys - yellow, Asp - blue). Structure modelled using PyMol and PDB structure 1QGT.

5.1.3 VLP production

VLPs have been produced for approximately 40 different viruses using at least 5 different expression systems² [*Baculovirus* and insect cells^{27, 33}; mammalian cells³⁴; bacteria (*E. coli*)³⁴; yeast (*S. cerevisiae*)³⁵ and plants²⁸ (tobacco³⁶, potato², tomato² and soybean²). Previously, our collaborators (iQur) attempted the production of a similar tandem core HBcAg in yeast (*S. cerevisiae*) with limited success. There is anecdotal evidence to suggest that plants offer a more suitable platform for the folding of the complex VLP structures than other expression systems, such as yeast (personal communication, M. Whelan, iQur Ltd; G. Lomonossoff, JIC). Both the quality and yield of VLPs produced in plants have been shown to be higher when compared to expression in yeast³².

In 1998, Tsuda *et al.*³⁷ achieved the first expression of HBcAg in transgenic tobacco plants. Using full length viral vectors from Cowpea Mosaic Virus (CPMV) and Potato Virus X, the Lomonossoff group first achieved transient expression of HBcAg in 2006, with comparable yields (10 mg/kg fresh weight tissue) to that achieved using stable transgenic lines³⁸. In 2008, through the use of the patented pEAQ-*HT* expression system developed by the Lomonossoff group, the transient expression of HBcAg was achieved with much improved yields (1 g/kg FWT). Owing to this and due to the expertise and previous success of HBcAg production *in planta* by the Lomonossoff group (JIC), efforts were focused on expression of the D3K6D3 VLP in *Nicotiana benthamiana* using the pEAQ-*HT* expression system developed by the Lomonossoff group.

5.1.3.1 The pEAQ-*HT* expression system

The pEAQ-*HT* (easy and quick) expression system is a transient expression system specifically designed to give high-level expression of proteins in plants³⁹⁻⁴¹. pEAQ-*HT* is based on the cloning of the desired gene between a modified 5'-untranslated region (5'-UTR) and 3'-UTR of Cowpea mosaic virus (CPMV) RNA-2^{39, 40}. The map for the tandem-core HBcAg plasmid is detailed in Appendix 8.8.

Through the use of the pEAQ-*HT* expression system, it is possible to generate proteins in extremely high yield, without the need for viral replication in the host,

removing the need for plant pathogen regulations. It has been shown that the yields associated with the pEAQ-*HT* systems are equivalent to the highest reported yields for systems which rely on viral replication³⁹. Expression of VLP proteins by means of the pEAQ-*HT* system has shown to be an effective and efficient method for producing fully assembled particles *in planta*^{28,40}. Agroinfiltration of plants utilises the delivery of *Agrobacterium* into viable plant leaf tissue by vacuum infiltration⁴² (large scale) or by direct pressure infiltration into the abaxial air space of leaves⁴³ (small scale). Once located into the plant cells, the *Agrobacterium* uses horizontal gene transfer to transfer the desired genetic information from the bacteria to the plant.

5.2 Results and Discussion

5.2.1 Production of the D3K6D3 pEAQ-*HT* wt/t-HBcAg plasmids

In order to produce both the wild type and tandem core (D3K6D3 VLPs *in planta*, new pEAQ-*HT* plasmids first had to be generated, with the assistance of H. Peyret (Lomonossoff group). Wild type and tandem pEAQ-*HT*-t-HBcAg-EL (tandem) and pEAQ-*HT*-wt-HBcAg-EL (wild type) expression plasmids were kindly donated by the Lomonossoff group (JIC).

Restriction digests (AseI & Sall) of both plasmids was carried out using standard conditions and the samples were run on a 0.8% agarose gel. The corresponding bands were excised from the gel and the plasmids were extracted using Qiaquick gel extraction kit (Qiagen). The forward and reverse primers were annealed and the ligation reactions were carried out using a 3:1 ratio of insert to plasmid backbone. After overnight incubation at 16 °C, Top10 chemically competent *E. coli* cells (Invitrogen) were transformed with the plasmids. Colony PCR and sequencing was used to confirm the successful cloning of the wt/t-HBcAg D3K6D3 plasmids. Once the plasmids (*wt*-D3K6D3HBcAg and *tandem*-D3K6D3HBcAg) had been successfully cloned, *Agrobacterium tumefaciens* LBA4404 cells were transformed by electroporation. After recovery on ice, the cells were plated out on to agar supplemented with kanamycin and rifamycin. After incubation for 3 days at 27°C, colony PCR was performed and the reactions were analysed by ethidium bromide-stained agarose gel electrophoresis (Figure 5.11).

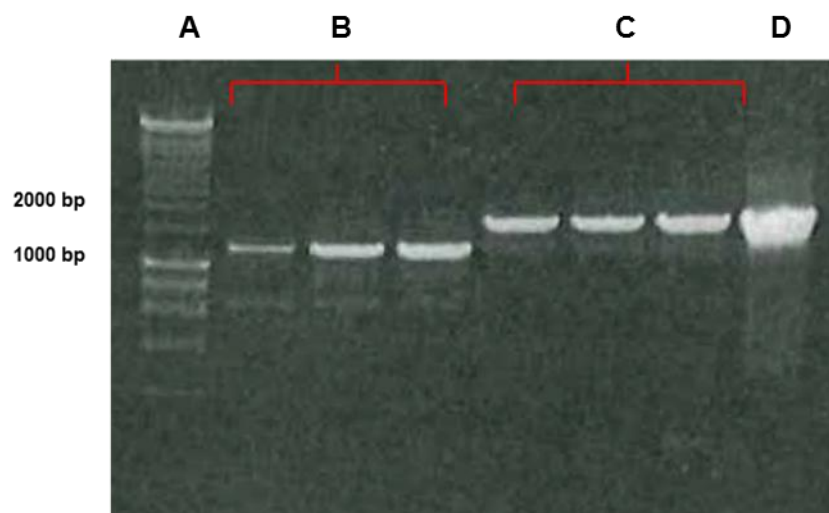


Figure 5.8: Agarose gel of colony PCR of *A. tumifaciens* transformation. Lanes: A) Ladder (Hyperladder 1; Bioline); B) pEAQ-HT-wt-HBcAg D3K6D3; C) pEAQ-HT-t-HBcAg D3K6D3; D) PCR positive control. D3K6D3 insert size is 1.59 kDa, recombinant D3K6D3 wt-HBcAg vector is 1288 bp (B); recombinant D3K6D3 t-HBcAg (C) vector is 1835 bp.

Figure 5.8 highlights the successful cloning, expression and amplification of the D3K6D3 HBcAg plasmids in agrobacterium. The bands at approximately 1800 and 1200 bp correspond to the monomeric and tandem recombinant plasmids respectively.

5.2.2 *In planta* expression of the VLPs

A trial *in planta* expression was conducted using three *A. tumifaciens* clones carrying the D3K6D3 wt/t-HBcAg plasmids, as judged by colony PCR. Infiltration solutions of the cells containing pEAQ-HT-wt/t-HBcAg D3K6D3 plasmids were made up in MMA [10 mM MES, 10 mM MgCl₂, 100 μM acetosyringone, pH 5.7] buffer supplemented with acetosyringone and used to infiltrate the youngest leaves of two plants. Acetosyringone is a phenolic plant compound which is secreted during infection and has been shown to up-regulate *Agrobacterium* infiltration^{44,45}. Pre-incubation of *Agrobacterium* with acetosyringone in MMA buffer, which is designed to mimic the environment of the cell leaf activates the cells and leads to improved expression levels⁴⁴. Six days post infiltration (dpi) the leaves were harvested and a single disc (10 mm diameter) was cut from each infiltrated leaf. The six discs from each plant were collected and extracted in both HBV extraction buffer (HBex) and phosphate buffer in order to determine the best extraction buffer. After extraction, the plant material was removed via centrifugation and the crude VLP extracts were loaded onto a LDS-PAGE gel for western blot analysis.

A western blot of the LDS-PAGE gel was taken and detected using mouse anti-hepatitis B virus core antigen antibody [10E11] (AbCam), which recognises the first 10 amino acids of the N-terminus. Enhanced chemiluminescence techniques were used for visualization and the blot was scanned using an Imagequant LAS 500 scanner (Figure 5.9).

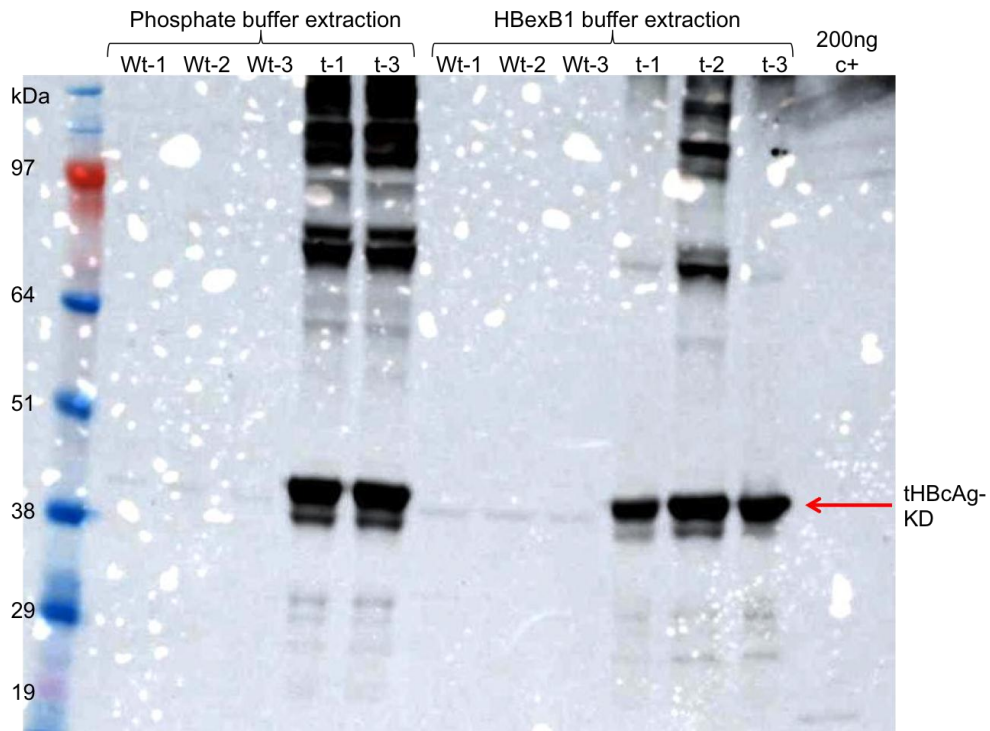


Figure 5.9: Western blot of trial expression for D3K6D3 wt-HBcAg and D3K6D3 t-HBcAg VLPs extracted in PBS and HBex buffer systems. Lanes: D3K6D3 wild type monomer (Wt 1-3); D3K6D3 tandem core (t 1-3); positive control C⁺ wt-HBcAg (200 ng). Primary antibody: mouse anti-Hepatitis B core antigen (10E11 AbCam) (1 in 1000); secondary antibody: goat anti-mouse IgG HRP labelled (1 in 3000); detection method enhanced chemiluminescence.

Figure 5.9 demonstrates the successful *in planta* expression of the t-HBcAg D3K6D3 VLP. There was no expression of the wt-HBcAg D3K6D3 with any of the plasmid preparations. This result ratifies the use of the tandem core particle over the monomeric core as discussed in the introduction section of this chapter. It is assumed that the inclusion of the highly charged D3K6D3 insert in the E1 loop of the monomer prevents the assembly of the dimer building blocks, halting VLP assembly. Based on the results of these blots, the modified D3K6D3 tandem core VLP presents a viable option for the generation of a chemically addressable VLP carrier. A larger scale preparation of the D3K6D3 tandem core VLPs was carried out using 13 plants, the leaves of which were again harvested 6 dpi.



Figure 5.10: (Left) *Nicotiana benthamiana* leaf being infiltrated with *agrobacterium* solution. (Right) Infiltrated plants.

Once harvested the protein was extracted from the plant material, again using phosphate and HBex buffer. The crude material was isolated on a sucrose gradient (20 – 60%) via ultracentrifugation and the fractions were analysed by LDS-PAGE (Figure 5.11).

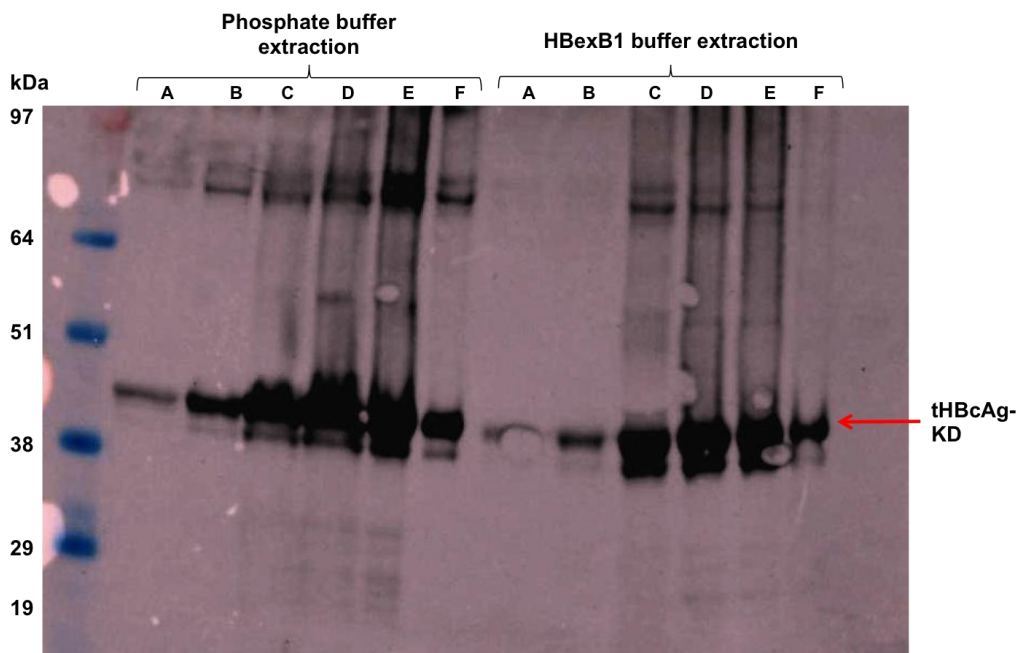


Figure 5.11: Coomassie stained LDS-PAGE gel of VLP purification sucrose gradients. Lanes: A) Supernatant; B) 20% sucrose; C) 30% sucrose; D) 40% sucrose; E) 50% sucrose; F) 60% sucrose

The 30-50% sucrose fractions were collected and extensively dialysed against 200 mM AmBic buffer. An estimation of the expression levels, based on standards, was made and shown to be in the region of 0.4 mg of protein per gram of plant tissue.

Once dialysed the samples were concentrated by speed vac and submitted for TEM analysis (Figure 5.12).

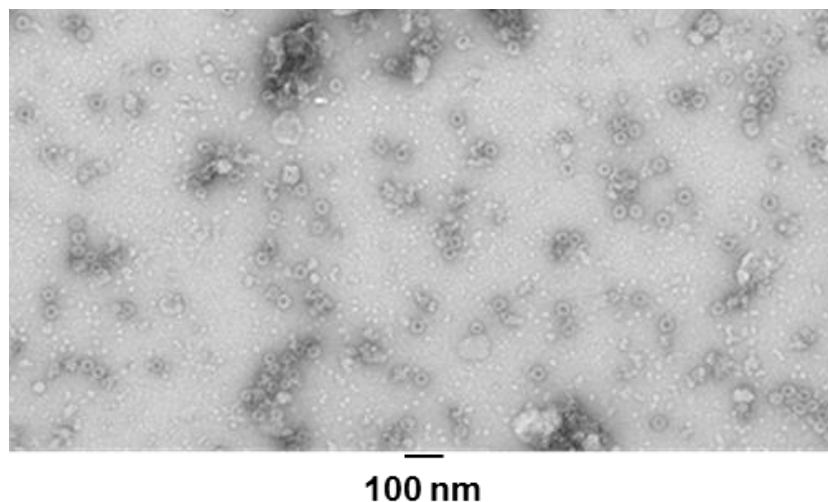


Figure 5.12: Negatively stained TEM image of D3K6D3 tandem core VLP (14,500x).

Figures 5.12 and 5.13 confirm the successful production of fully assembled D3K6D3 tandem core VLPs. The image shows that the virus like particles have a tendency for self-aggregation, which has been seen before with modified tandem core particles. However, the problem may be accentuated by electrostatic interactions generated by the highly charged insert. The aggregation may impact on the availability of the lysine residues for conjugation, but this could only be assessed through experimental analysis. The assembled VLPs are approximately 30 nm in diameter as shown below.

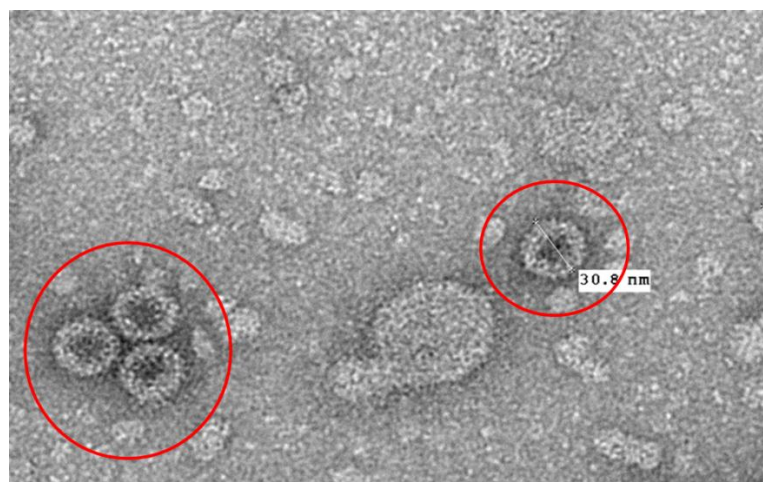


Figure 5.13: Zoomed in TEM image of D3K6D3 tandem core VLP (50,000x).

5.2.3 Conjugation with FITC

In order to assess the availability of the inserted lysine residues for conjugation, the fluorophore, fluorescein isothiocyanate (FITC) was used. MALDI-ToF MS has been instrumental in the analysis of the TetHc glycoconjugates (Chapter 2) but was not successful for the VLP monomer. MALDI-ToF MS was conducted on the pure VLP sample but no peak was detected at 42.6 KDa, the mass of the tandem core monomer. On this basis, FITC was selected to aid with the identification and characterisation of the VLP conjugates. The reaction between the isothiocyanate group and the lysine residue is similar to that of the acyl azide reaction used previously in this study. Approximately 500 µg of crude VLP was reacted with a large excess of FITC in conjugation buffer [0.08M Na₂B₄O_{7.10}H₂O; 0.35m KHCO₃; pH 9.0] overnight. After extensive dialysis the crude conjugation was concentrated and run on SDS-PAGE and agarose gels.

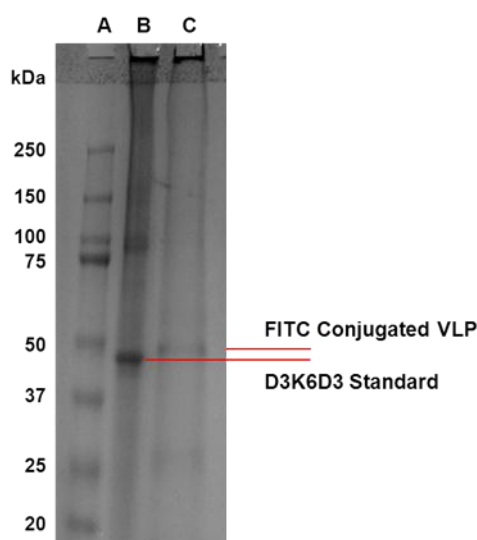


Figure 5.14: Coomassie stained SDS-PAGE gel of FITC conjugated VLP. Lanes: A) kaleidoscope ladder; B) D3K6D3 VLP standard; C) FITC Conjugated D3K6D3 VLP.

Figure 5.14 above shows a small band shift from the unmodified VLP sample to the FITC conjugation reaction, indicating that the conjugation of FITC to the D3K6D3 VLP had been successful. A second SDS-PAGE gel was visualised using a fluorescence scanner and image of which is shown in Figure 5.15.

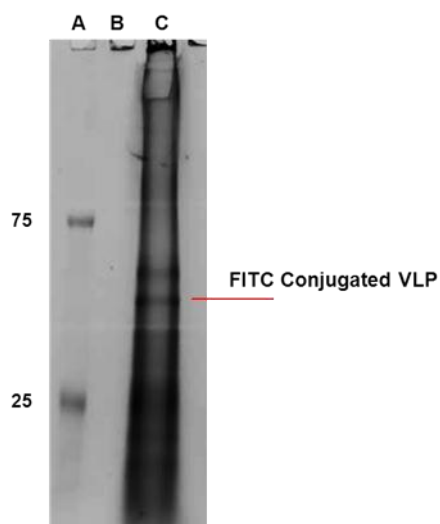


Figure 5.15: Fluorescence image of SDS-PAGE gel of FITC conjugated VLP. Lanes: A) kaleidoscope ladder; B) unmodified D3K6D3 VLP; C) FITC conjugated D3K6D3 VLP.

Despite the high levels of background fluorescence as a result of residual FITC, it is possible to see two distinct bands in the gel above. The band labelled above is proposed to be FITC labelled D3K6D3 VLP, with the second band corresponding to FITC labelled RuBisCo, a major impurity of plant derived proteins. At this stage the SDS-PAGE gel data suggested that the lysine residues present in the insert had been successfully labelled with FITC, but due to low loading and high background the data were inconclusive. As a result of this agarose gels (Figure 5.16) were also run in an attempt to confirm success of the conjugation reaction. Agarose gels were stained using both coomassie and ethidium bromide (EtBr). EtBr staining detects VLPs as the assembly of the VLP *in planta* encapsulates random nucleic acid into the particle, providing an alternative stain to coomassie.

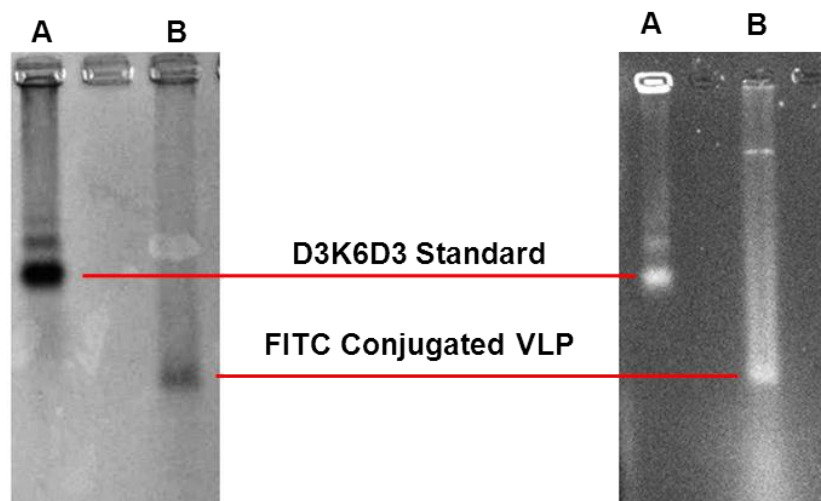


Figure 5.16: Agarose gels of FITC conjugated D3K6D3 VLP. (Left) coomassie stained gel; (Right) ethidium stained gel. Lanes: A) unmodified D3K6D3 VLP; B) FITC conjugated D3K6D3 VLP. Fluorescence imaging of the agarose gel was not possible due to low loading on the agarose gels.

The agarose gels provide further proof that the FITC conjugation of the VLPs was successful. The large band shift between the two samples is indicative of a change in mass and charge of the particles. At pH 8.0 (TBE Buffer) (the charge at the top of the E1) the overall charge of the insert at the top of the E1 loop should theoretically be balanced. Upon conjugation the positive charges of the lysine residues would effectively be neutralised generating an overall negative charge at the top of the E1 loop.

Residue	pKa
Aspartic Acid	3.7
Lysine	10.5
FITC	6.4 ⁴⁶

Table 5.2: Table showing the pKa values for aspartate, lysine and FITC.

This effect would be further enhanced by the presence of the carboxylic acid group in the conjugated FITC. The increase in overall negative charge of the particle will cause the large band shift seen in the agarose gels. Positive staining with ethidium bromide was proof for the presence of nucleic acid indicating that the bands corresponded to VLPs. All the evidence collected at this stage suggested that FITC of the VLPs was successful and that the lysine residues remained chemically accessible upon assembly

5.2.4 Purification of VLPs by size exclusion chromatography

The conjugation of VLPs with FITC raised a number of issues regarding the purity of the plant produced VLPs. The sucrose gradient purification is not sufficient to remove all contaminants such as the RuBisCO and other plant material. In order to improve the purity of the VLPs, a second batch of material was produced in plants. After extraction and purification (in phosphate buffer) using two sucrose gradients, the particles were taken to our collaborators iQur for further purification using size exclusion chromatography. The sample was loaded onto a sepharose CL4B XK 26/40 column and eluted using PBS (Figure 5.17).

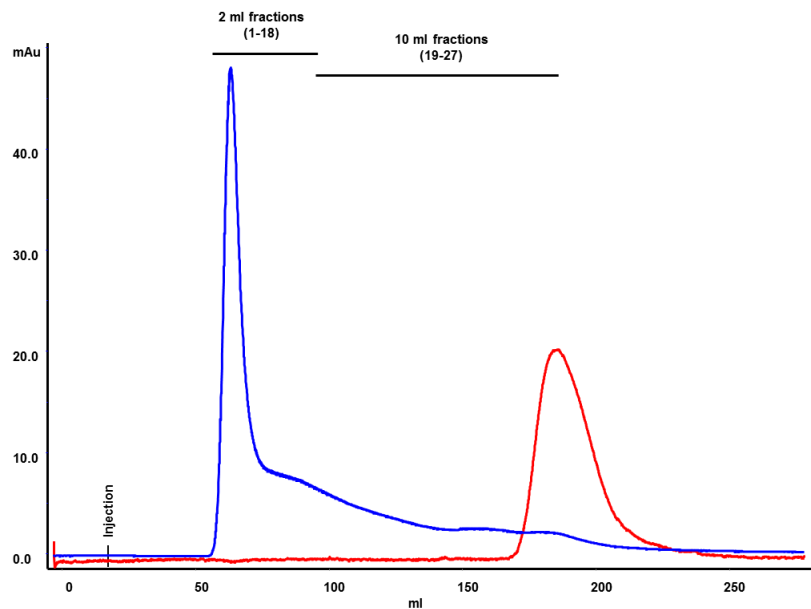


Figure 5.17: Trace from Sepharose CL4B column purification of the D3K6D3 VLPs. Sepharose CL4B XK46/40 column flow rate 2 ml/min; eluent PBS; sample loaded 6 ml of plant prep.; fractions collected (56 ml – 182 ml) volume collected (1-18) 2 ml; (19-27) 10 ml. (Blue) UV trace A₂₈₀; (red) conductivity.

Fractions of interest (1-18) were taken and analysed on a Tris-glycine SDS-PAGE gel (pH 6.8, Bio-Rad). The gel was run under standard conditions (Section 7.1.5) and stained using a silver staining kit as per manufacturer's instructions (Pierce), a western blot of the gel was also taken and imaged using enhanced chemiluminescence detection (Section 7.1.5.6) (Figure 5.18), showing the presence of assembled VLP.

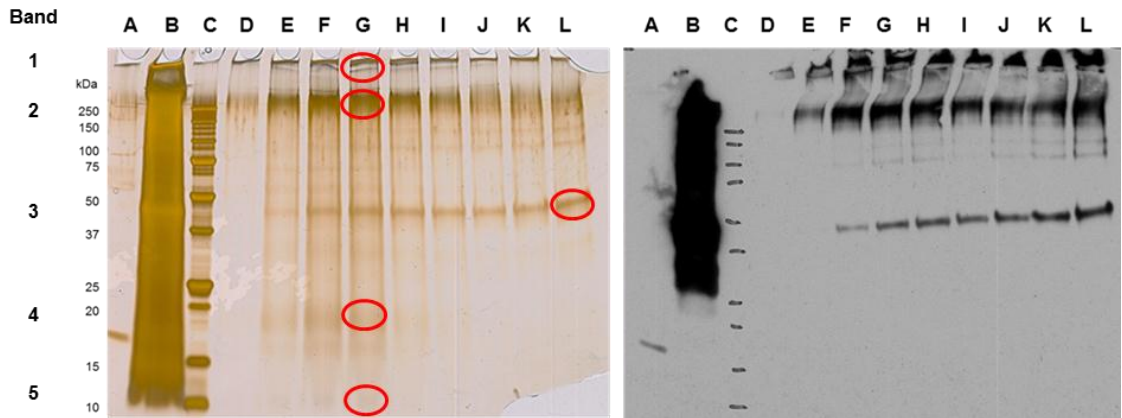


Figure 5.18: (Left) Silver stained tris-glycine gel of D3K6D3 t-HBcAg VLP purification (Sepharose CL4B). (Right) Western blot of tris-glycine gel. Lanes: A) wt-HBcAg (50 ng); B) loaded sample; C) precision plus dual colour ladder; D) fraction 2 E) fraction 3; F) fraction 4 G) fraction 5; H) fraction 6; I) fraction 7; J) fraction 9; K) fraction 11) fraction 15. Primary antibody: mouse anti-Hepatitis B core antigen (10E11 AbCam) (1 in 1000); secondary antibody: goat anti-mouse IgG HRP labelled (1 in 3000); detection method enhanced chemiluminescence.

MS analysis was done on the highlighted bands of the gel in order to confirm the identity of the higher order bands along with the lower molecular weight impurities. The high-order structures were shown to be VLP by MS analysis, confirming the positive response to the monoclonal antibody in the western blot. This indicated that the VLP was not breaking apart under the reducing conditions of the gel demonstrating the robustness of the particles. The lower weight impurity (band 5) was shown to be an unidentified *N. benthamiana* protein. In order to determine whether the protein (bands 1, 2 and 3) in the above gel and blot corresponds to assembled VLP, as opposed to free t-HBcAg D3K6D3 protein, further agarose gels were run. Agarose gels stained for both protein and nucleic acid give a better indication of the presence of VLP (Figure 5.19). Fractions were run without concentration on a 1.2% agarose gel with TBE buffer and stained with SYPRO Ruby (protein) and ethidium bromide (nucleic acid).

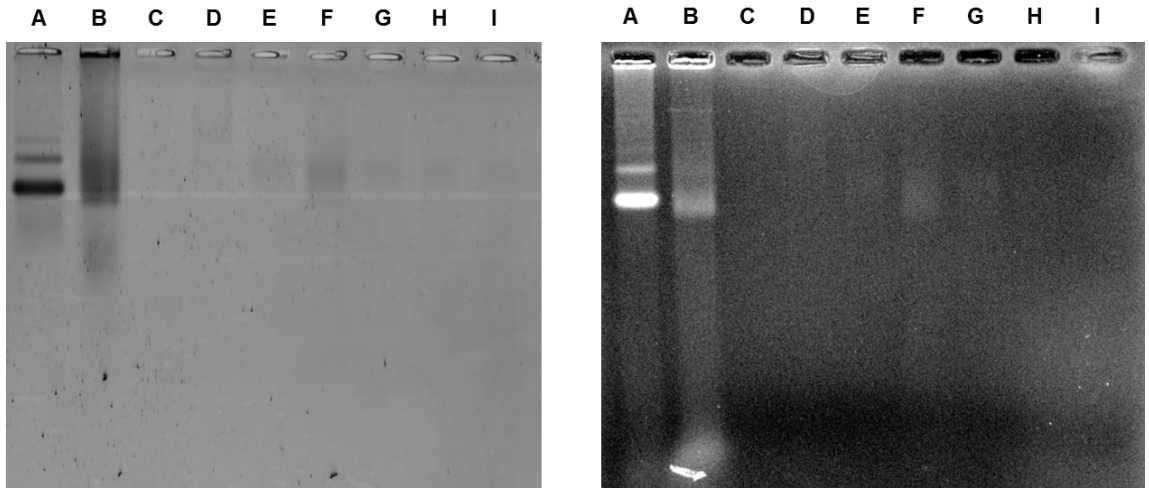


Figure 5.19: Agarose gels (1.2%) of SEC fractions. (Left) SYPRO Ruby stain; (Right) ethidium bromide stain. Lanes: A) Purified D3K6D3 VLP (4.5 μg); B) SEC Input; C) frac 2; D) frac 8; E) frac 15; F) frac 19; G) frac 22; H) frac 23; I) frac 24).

Although the bands are weak the gels give a good indication that the assembled VLP is eluted off the column after the initial void volume as expected. The fractions were concentrated and run again on agarose gel (Figure 5.20) and studied by TEM.

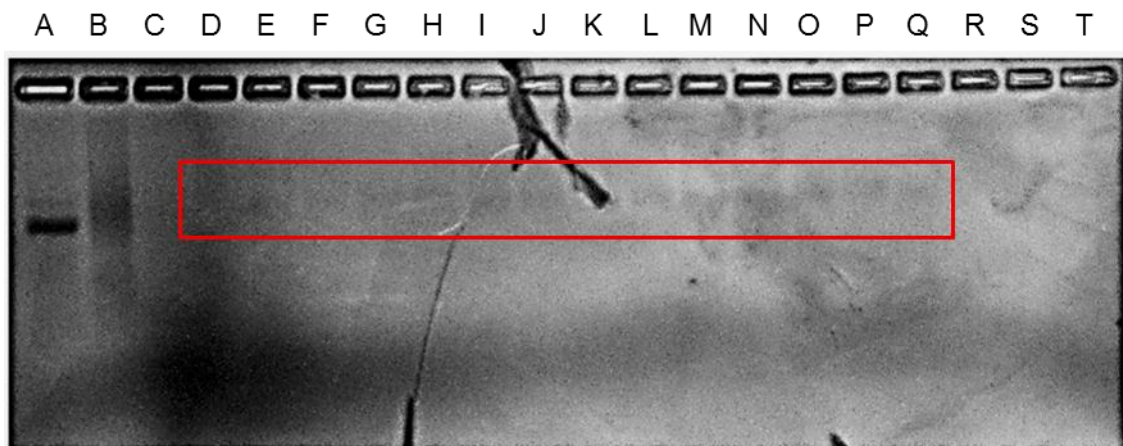
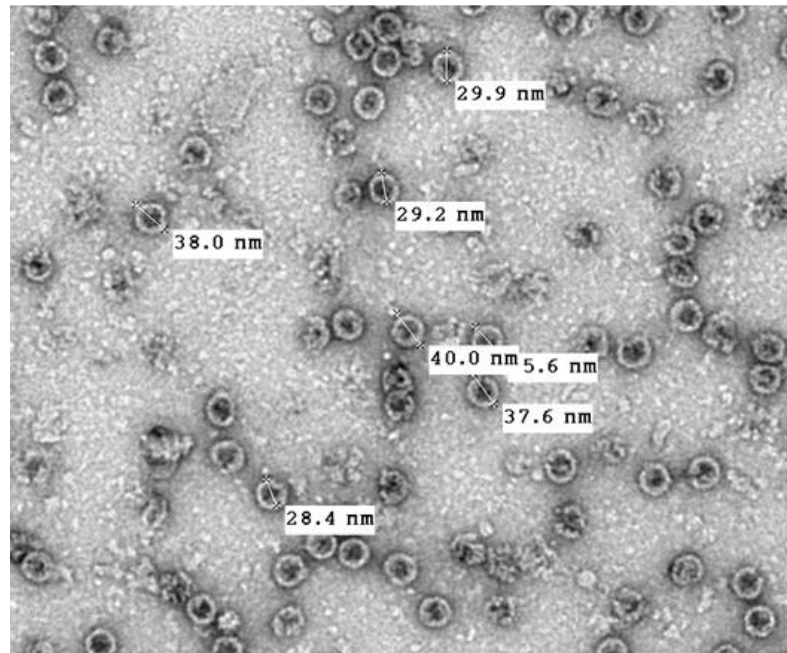


Figure 5.20: Agarose gels (1.2%) of concentrated SEC fractions stained silver nitrate. Lanes: A) Purified D3K6D3 VLP (4.5 μg); B) SEC Input; C – T) fractions 9 – 26.

19,000x



80,000x

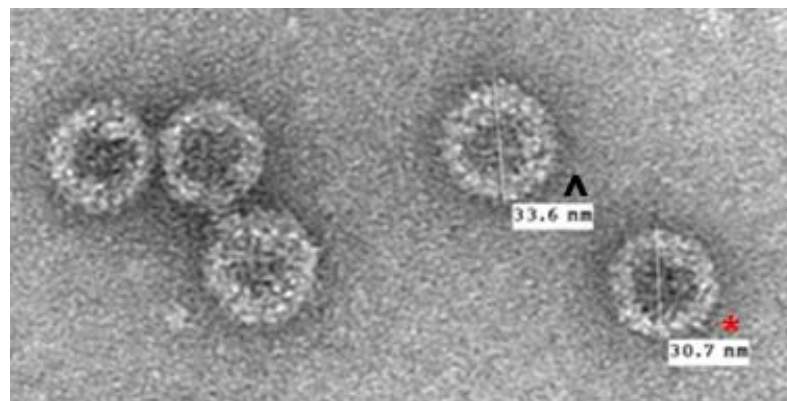


Figure 5.21: Negatively stained TEM of pooled fractions (9 – 23) from size exclusion chromatography of D3K6D3 VLPs. 80,000x magnification shows the presence of T=3 (30 nm) particles denoted * and T=4 (34 nm) particles denoted ^.

The agarose gel (Figure 5.20) showed VLPs in fractions 9-23, which were pooled and further concentrated to a total volume of 2 ml. This was then analysed by TEM (Figure 5.21) to prove the presence of VLPs in the sample. The TEM images indicated the presence of both 30 nm particles (T=3 particles 90 copies of dimer) and 34 nm particles (T=4 120 copies of dimer) particles. The particles were then extensively dialysed (Pierce Float-A-Lyzer, 1000 KD MWCO) into Borax [0.08 mM $\text{Na}_2\text{B}_2\text{O}_7 \cdot 10\text{H}_2\text{O}$, pH = 9.0] buffer. The dialysed VLPs (3 ml) were then conjugated

again to FITC in an attempt to further confirm the availability of the inserted lysines for conjugation. KHCO_3 was added to the VLPs (500 μl) in Borax to give conjugation buffer [0.08 m Borax, 0.35 M KHCO_3 , pH = 9.0] and FITC was added and the conjugation was left at 4 °C overnight. The excess FITC was removed by spin filtration (Sartorius Vivaspin 10,000 MWCO) and the VLPs were isolated by sucrose gradient. The UV visualisation of the FITC-VLP sucrose gradient (Figure 5.22) clearly demonstrates the successful conjugation of FITC to the VLP. Free FITC in solution (from spin filtration wash) demonstrates that due to its small size free FITC does not enter the sucrose gradient and remains in the supernatant layer (Figure 5.22 B). Only FITC which is conjugated to VLP will be able to enter the sucrose gradient. It was shown in Section 5.2.2, during the purification of the VLPs that the particles are purified primarily from the 30-50% sucrose gradient. The fluorescent band (ca. 40 – 50% sucrose) in Figure 5.22 C corresponds to FITC which has been covalently bound to the VLP.

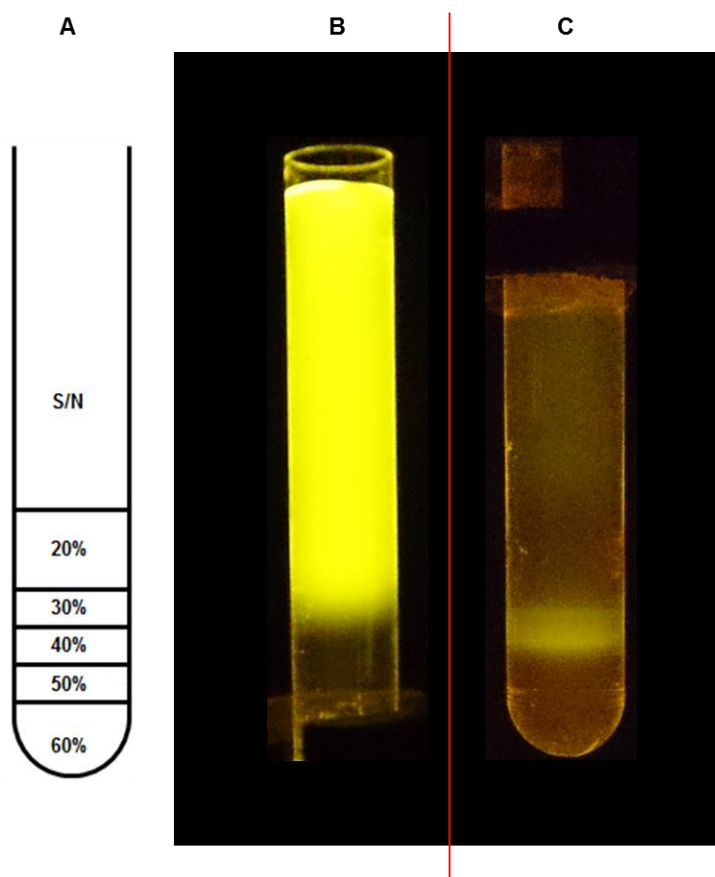


Figure 5.22: UV visualisation of the FITC labelled VLP sucrose gradient. A) schematic representation of the sucrose gradients (not to scale); B) free FITC in the supernatant (S/N); C) FITC-VLP in the S/N.

This result confirms the successful production of, and conjugation of FITC to the t-HBcAg D3K6D3 VLPs. The fluorescent VLPs were collected and analysed by SDS-PAGE and agarose gel electrophoresis for completion (Figure 5.23 & 5.24) and confirm that the conjugated material is FITC-labelled D3K6D3 t-HBc-Ag VLP. The characteristic band shift in the agarose gels (Figure 5.24) further demonstrates the successful conjugation of the D3K6D3 t-HBc-Ag VLPs with FITC.

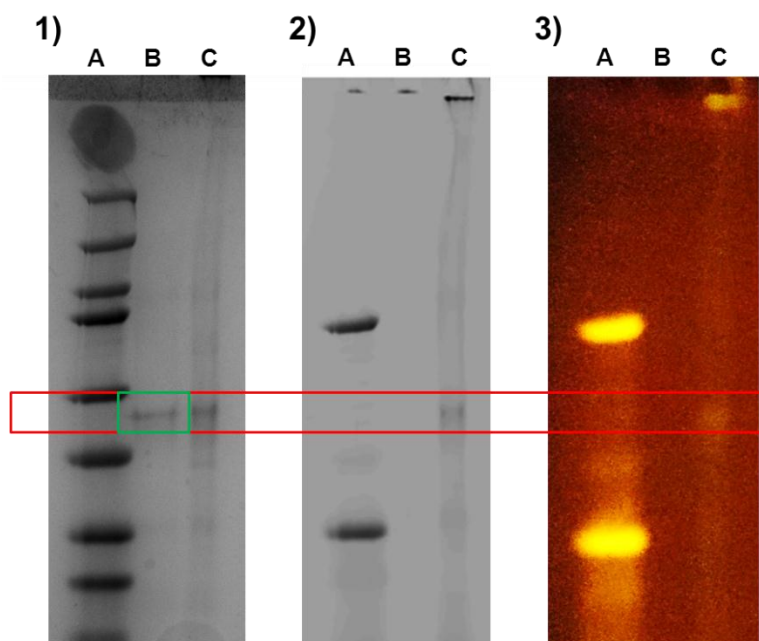


Figure 5.23: SDS-PAGE gel of the isolated sucrose gradient fraction visualised using different techniques: 1) Coomassie stained; 2) fluorescence image (495 nm) and 3) visualised under blue light (470 nm). Lanes: A) Kaleidoscope ladder containing fluorescent proteins at 25 and 75 kDa; B) native D3K6D3 HBc-Ag VLP; c) FITC conjugated D3K6D3 HBc-Ag VLP.

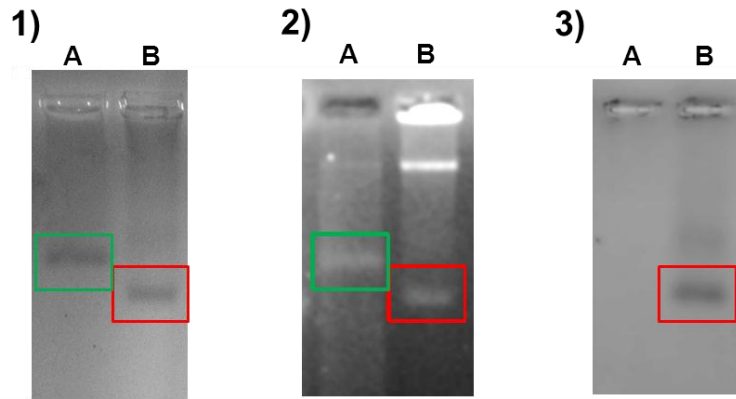


Figure 5.24: Agarose gel of the isolated sucrose gradient fraction visualised using different techniques: 1) Coomassie stained; 2) ethidium-bromide stained and 3) fluorescence image (495 nm). Lanes: A) unmodified D3K6D3 HBc-Ag VLP; B) FITC conjugated D3K6D3 HBc-Ag VLP.

5.3 Conclusions

The initial work described in this chapter demonstrated the development and *in planta* expression of a novel tandem hepatitis B core antigen (t-HBcAg D3K6D3). A peptide consisting of six chemically addressable lysine residues flanked with three aspartate residues on each side was designed. The insert was cloned into both the wild-type and tandem constructs; however, trial expression with the wild-type variant failed but succeeded with the tandem core construct. Tandem particles were initially purified and a trial conjugation with fluorescein isothiocyanate was attempted. Analysis of the conjugate demonstrated the successful conjugation of the VLP material, but also highlighted some issues of purity. More extensive purification methods were developed utilising size exclusion chromatography. In collaboration with iQur Ltd the VLP material was shown to high purity, ca. >90%. The VLPs will be conjugated to existing and future antigens (monosaccharide and CPS) for use in immunisation trials. The generated antibodies will then be used for comparison with the more traditional TetHc glycoconjugates to assess the potential of the t-HBcAg D3K6D3 as a carrier protein; this work is currently on-going in the lab.

5.3.1 Future Directions

The *in planta* production of the D3K6D3 t-HBcAg VLPs described in this chapter has been shown to be an improvement compared to the current alternative expression systems (yeast, *E. coli* and *Baculovirus*) (personal communication, M. Whelan, iQur

Ltd.). However, if the VLPs are shown to be a good carrier protein further work will be needed to establish large scale production of the VLPs as the current method of sucrose gradient purification does not lend itself to scale up. Optimisation of either the purification methodology of the plant derived material, or of a more suitable expression system must be carried out before this material can be developed further. If the production and purification of the D3K6D3 VLPs can be improved, given that the inclusion of antigens is based solely on chemical modification rather than the development of individual constructs, the development of a series of VLP based immunogens is possible.

Owing to the nature of the D3K6D3 tandem core it is possible to utilise the second E1 loop to include a second antigen such as an immunogenic peptide sequence. As discussed in the introduction one of the vaccination strategies for *B. pseudomallei* involves the use of immunogenic peptides (i.e. LoIC). The D3K6D3 tandem core provides the ideal platform for the expression of a peptide containing carrier protein (1st E1 loop) followed by the chemical conjugation of a carbohydrate vaccine to the 2nd E1 loop to give a multi-component vaccine. iQur and DSTL-Porton Down are currently developing *B. pseudomallei* LoIC t-HBcAg constructs which could be used in combination with the D3K6D3 insert to develop a bivalent *B. pseudomallei* vaccine candidate.

5.4 References

1. R. Dagan, J. Poolman and C.-A. Siegrist, *Vaccine*, 2010, **28**, 5513-5523.
2. A. Roldao, M. C. M. Mellado, L. R. Castilho, M. J. T. Carrondo and P. M. Alves, *Exp. Rev. Vaccines*, 2010, **9**, 27.
3. P. Maupas, P. Coursaget, A. Goudeau, J. Drucker and P. Bagros, *The Lancet*, 1976, **307**, 1367-1370.
4. G. J. P. H. J. Krugman S, *JAMA*, 1971, **217**, 41-45.
5. W. Szmuness, C. E. Stevens, E. J. Harley, E. A. Zang, W. R. Oleszko, D. C. William, R. Sadovsky, J. M. Morrison and A. Kellner, *New Engl. J. Med.*, 1980, **303**, 833-841.
6. M. L. Michel and P. Tiollais, *Pathol. Biol.*, 2010, **58**, 288-295.
7. Q. Vos, A. Lees, Z.-Q. Wu, C. M. Snapper and J. J. Mond, *Immunol. Rev.*, 2000, **176**, 154-170.
8. B. Chackerian, P. Lenz, D. R. Lowy and J. T. Schiller, *J. Immunol.*, 2002, **169**, 6120-6126.
9. D. R. Milich, M. Chen, F. Schodel, D. L. Peterson, J. E. Jones and J. L. Hughes, *Proc. Nat. Acad. Sci. U.S.A.*, 1997, **94**, 14648-14653.
10. D. Dhanasooraj, R. A. Kumar and S. Mundayoor, *International Journal of Nanomedicine*, 2013, **8**, 835-843.
11. A. Upasana, T. Poornima, S. Sathyamangalam and K. Navin, *Journal of Nanotechnology*, 2012, **10**, 30.
12. E. H. Nardin, G. A. Oliveira, J. M. Calvo-Calle, K. Wetzel, C. Maier, A. J. Birkett, P. Sarpotdar, M. L. Corado, G. B. Thornton and A. Schmidt, *Infect. Immun.*, 2004, **72**, 6519-6527.
13. K. Roose, *Exp. Rev. Vaccines*, 2013, **12**, 16.
14. S. Zhou and D. N. Strandberg, *Proc. Nat. Acad. Sci. U.S.A.*, 1992, **89**, 10046-10050.
15. Y.-F. Liaw, *Hepatology International*, 2009, **3**, 425-433.
16. S. Locarnini, *Seminars in Liver Disease*, 2004, **24**, 8.
17. D. S. Dane, C. H. Cameron and M. Briggs, *The Lancet*, 1970, **295**, 695-698.
18. J. H. B. S. o. P. Health, *Hepatitis B Virus: The Epidemiology of Hepatitis B and A Infections*,
19. R. P. Beasley, G. Chin-Yun Lee, C.-H. Roan, L.-Y. Hwang, C.-C. Lan, F.-Y. Huang and C.-L. Chen, *The Lancet*, 1983, **322**, 1099-1102.
20. B. E. Clarke, S. E. Newton, A. R. Carroll, M. J. Francis, G. Appleyard, A. D. Syred, P. E. Highfield, D. J. Rowlands and F. Brown, *Nature*, 1987, **330**, 4.

21. A. Gehin, R. Gilbert, D. Stuart, D. Rowlands, *US Pat.*, Hepatitis B core antigen fusion proteins, US 7270821, 2007.
22. A. Birkett, K. Lyons, A. Schmidt, D. Boyd, G. A. Oliveira, A. Siddique, R. Nussenzweig, J. M. Calvo-Calle and E. Nardin, *Infect. Immun.*, 2002, **70**, 6860-6870.
23. S. A. Wynne, R. A. Crowther and A. G. W. Leslie, *Mol. Cell*, 1999, **3**, 771-780.
24. A. Gallina, F. Bonelli, L. Zentilin, G. Rindi, M. Muttini and G. Milanesi, *J. Virol.*, 1989, **63**, 4645-4652.
25. J. Salfeld, E. Pfaff, M. Noah and H. Schaller, *J. Virol.*, 1989, **63**, 798-808.
26. P. Pumpens, G. P. Borisova, R. A. Crowther and E. Grens, *Intervirology*, 1995, **38**, 63-74.
27. F. Fernandes, *Exp. Rev. Vaccines*, 2013, **12**, 12.
28. N. Scotti, *Exp. Rev. Vaccines*, 2013, **12**, 14.
29. S. K. Sharmer, N. Saini and Y. Chwla, *Virology Journal*, 2005, **2**, 82, pp 1-5
30. M. Nassal, C. Skamel, M. Vogel, P. A. Kratz, T. Stehle, R. Wallich and M. M. Simon, *Int. J. Med. Microbiol.*, 2008, **298**, 135-142.
31. A. Jegerlehner, A. Tissot, F. Lechner, P. Sebbel, I. Erdmann, T. Kündig, T. Bächli, T. Storni, G. Jennings, P. Pumpens, W. A. Renner and M. F. Bachmann, *Vaccine*, 2002, **20**, 3104-3112.
32. E. Thuenemann, Thesis: Virus-like Particle Production Using Cowpea Mosaic Virus-based Vectors, University of East Anglia, 2012.
33. T. A. Kost, J. P. Condreay and D. L. Jarvis, *Nat. Biotechnol.*, 2005, **23**, 9.
34. H. C. Levy, V. D. Bowman, L. Govindasamy, R. McKenna, K. Nash, K. Warrington, W. Chen, N. Muzyczka, X. Yan, T. S. Baker and M. Agbandje-McKenna, *J. Struc. Biol.*, 2009, **165**, 146-156.
35. A. Zielonka, A. Gedvilaite, R. Ulrich, D. Lüscho, K. Sasnauskas, H. Müller and R. Johne, *Virus Res.*, 2006, **120**, 128-137.
36. M. Vardakou, F. Sainsbury, N. Rigby, F. Mulholland and G. P. Lomonosoff, *Protein Expression Purif.*, 2012, **81**, 69-74.
37. S. Tsuda, K. Yoshioka, T. Tanaka, A. Iwata, A. Yoshikawa, Y. Watanabe and Y. Okada, *Vox Sang.*, 1998, **74**, 148-155.
38. I. A. Mechtcheriakova, M. A. Eldarov, L. Nicholson, M. Shanks, K. G. Skryabin and G. P. Lomonosoff, *J. Virol. Methods*, 2006, **131**, 10-15.
39. F. Sainsbury and G. P. Lomonosoff, *Plant Physiol.*, 2008, **148**, 1212-1218.
40. F. Sainsbury, E. C. Thuenemann and G. P. Lomonosoff, *Plant Biotechnol. J.*, 2009, **7**, 682-693.

41. H. Peyret and G. Lomonossoff, *Plant Mol. Biol.*, 2013, **83**, 51-58.
42. R. Fischer, C. Vaquero-Martin, M. Sack, J. Drossard, N. Emans and U. Commandeur, *Biotechnol App Biochem*, 1999, **30**, 2.
43. O. Voinnet, S. Rivas, P. Mestre and D. Baulcombe, *The Plant Journal*, 2003, **33**, 949-956.
44. J.-F. Li, E. Park, A. von Arnim and A. Nebenfuhr, *Plant Methods*, 2009, **5**, 6.
45. S. H. J. Turk, R. Lange, T. G. Regensburg-Tuïnk and P. J. Hooykaas, *Plant Mol. Biol.*, 1994, **25**, 899-907.
46. A. Marchetti, E. Lelong and P. Cosson, *BMC Research Notes*, 2009, **2**, 7-15.

6 Conclusions and outlook

Immunisation and lethal challenge studies in mice using the capsular polysaccharide of *B. pseudomallei* (CPS) (**4**) have shown it to be a potential candidate for the development of a carbohydrate vaccine for *B. pseudomallei*^{1,2}. As discussed in the introduction to this thesis, the full chemical synthesis of oligosaccharide fragments of the CPS (**4**) is a challenging endeavour. This thesis has focused on two strategies for the development of carbohydrate antigens of the CPS (**4**). The first involved the synthesis and conjugation of monosaccharide haptens (**64**, **69** & **91**), and the second, the purification and extraction of the polysaccharide from an avirulent strain of *Burkholderia* (Figure 6.1).

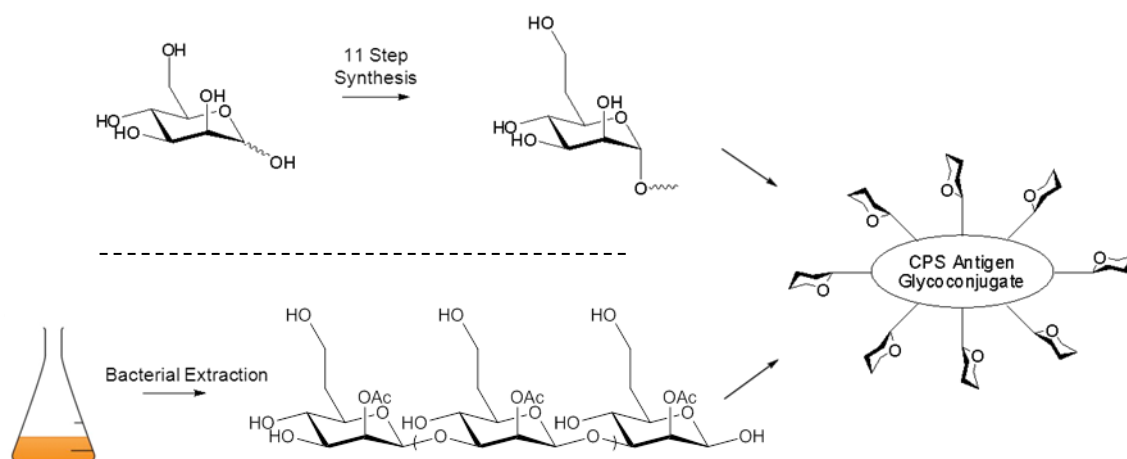


Figure 6.1: Schematic representation of the two methods for the development of CPS antigen glycoconjugates.

This final section will summarise the progress made during this research project, whilst putting the results into the context of the vaccine development program.

6.1 Monosaccharide antigens

In an attempt to explore the potential of multivalent monosaccharide antigens for the purpose of antibody generation two monosaccharide haptens were developed; 8-(methoxycarbonyl)octyl β -D-glucopyranoside (**69**) and 8-(methoxycarbonyl)octyl 6-deoxy-6-fluoro- β -D-glucopyranoside (**111**). The monosaccharide haptens were conjugated to TetHc carrier protein and underwent immunisation trials in sheep. Immunological assessment by ELISA and slot-blot analysis, of the polyclonal sera

demonstrated activity towards the cognate monosaccharide hapten-BSA conjugates. It was shown that the 8-carbon alkyl linker (**58**) had a strong influence on antibody development, resulting in cross-reactivity with the non-cognate monosaccharide haptens, D-mannose (**64**) and 6-deoxy-D-*manno*-heptose (**91**). However, competition experiments using the D-mannose hapten-BSA conjugate (**93**) established that the polyclonal Glc-TetHc sera had a degree of specificity for D-glucose. A second set of short linker haptens using 3-methyl mercaptopropionate were developed and will be used to assess the effect of a shorter linker on antibody development and specificity (Figure 6.2).

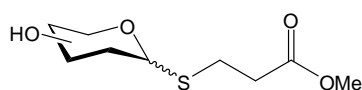


Figure 6.2: General structure of the second generation short-linker haptens. 3-methyl mercaptopropionate was used as the linker in place of 8-methoxycarbonyl octanol (**58**).

The 6-deoxy-6-fluoro-D-glucose antigen (**112**) was developed in order to assess the potential of using fluorine for the development of improved antigens, as seen with other fluorinated carbohydrate antigens³. Preliminary ELISA experiments with the 6-deoxy-6-fluoro-D-glucopyranose hapten derived sera showed activity towards the native D-glucose hapten-BSA conjugate (**97**). Further investigations, including the purification of antibodies using immobilised antigen will be required to assess the potential for the monosaccharide hapten derived antibodies. If purification of these antibodies and further immunological analysis (ELISA and Octet Red 96) are shown to confirm the presence of monosaccharide specific antibodies, then the production of monosaccharide specific monoclonal antibodies should be investigated.

In the context of the development of a vaccine for *B. pseudomallei*, a monosaccharide antigen based on the 6-deoxy-D-*manno*-heptopyranose building block of the *B. pseudomallei* capsular polysaccharide was produced. The monosaccharide hapten, 8-(methoxycarbonyl)octyl 6-deoxy-D-*manno*-heptopyranose (**91**) was again conjugated to TetHc fragment and submitted for immunisation trials in sheep. Preliminary immunological assessment (ELISA and slot-blot) of the polyclonal antibodies demonstrated specificity for the 6-deoxy-heptose monosaccharide. Further investigations with the Octet Red96 biosensor

system suggested activity of the anti-monosaccharide antibodies towards the intact CPS. Purification of the antibodies and further characterisation will be required in order to confirm this activity as outlined in section 4.5. If this activity is confirmed, the use of this monosaccharide antigens will be investigated further. As part of this research project, efforts were made to simplify the synthesis of 6-deoxy-D-manno-heptopyranose using protecting-group free strategies. Continuation of this work in the lab should look at streamlining this process further in order to facilitate further research into synthetic CPS antigens.

Development of the monosaccharide antigens is ongoing, focusing on the use of a synthetic dendrimer for the presentation of the monosaccharide hapten (Figure 6.3).

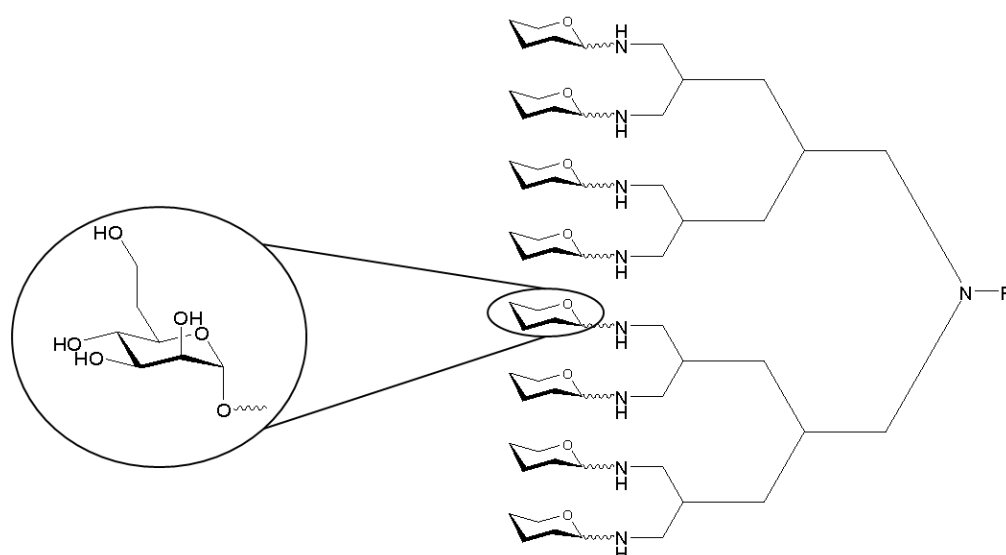


Figure 6.3: Schematic representation of the development of an octameric dendrimer for the multi-valent presentation of the monosaccharide CPS hapten.

The aim of this work is to develop a multivalent scaffold of the monosaccharide which could be conjugated to a carrier protein such as TetHc, or the D3K6D3 t-HBcAg virus-like particle carrier developed in this thesis. Alternatively the dendrimer scaffold could be linked to an immunomodulating peptide or polysaccharide, directing the antigen to antigen-presenting cells resulting in a strong immune response^{4, 5}. The use of an immunomodulating sequence removes the need for reliance on carrier proteins. This work could provide a route for the development of a fully synthetic polysaccharide vaccine for *B. pseudomallei*.

6.2 Natural polysaccharide

The extraction and purification of *B. pseudomallei* CPS in the avirulent *B. thailandensis* E555 $\Delta wbiI$ strain offers a scalable route for the production of CPS. The characterisation of this polysaccharide, confirmed the observation made by Heiss *et al.*⁶ regarding the presence of an α -1,3-mannan polysaccharide (**106**) in *Burkholderia* CPS extracts. It was anticipated, based on the fact that the native *B. thailandensis* E264 strain does not produce the mannan polysaccharide, that the biosynthesis of the α -1,3-mannan (**106**) is associated with the CPS biosynthetic cluster. To date the separation of the two polysaccharides has not been successful and it is not known whether they are two distinct polysaccharides or part of a heteropolysaccharide. Manipulation of the CPS-biosynthetic cluster in the *B. thailandensis* E555 $\Delta wbiI$ may prove to be useful in deciphering the relationship of these two polysaccharides.

The conjugation of isolated Bth-CPS (**104**) to a carrier protein was successful, but led to the formation of a heterogeneous mix of glycoconjugates. Mild acid hydrolysis of the polysaccharide was carried out resulting in a mixed population of 2-O-acetylated and 2-de-O-acetylated oligosaccharide fragments. Method development is required to establish the optimum conditions to provide oligosaccharide fragments for conjugation. Further immunological experiments using the 2-O-acetylated and 2-de-O-acetylated forms of the polysaccharide must also be employed in order to confirm the validity of the assumption regarding the lack of importance of this group on the immune system recognition of the polysaccharide.

Based on ELISA and Octet 96Red analysis of the Ancora hexasaccharide (**54**) (Figure 6.4) and mAb 4IVH12, no binding of the monoclonal antibody to the synthetic oligosaccharide fragment was observed.

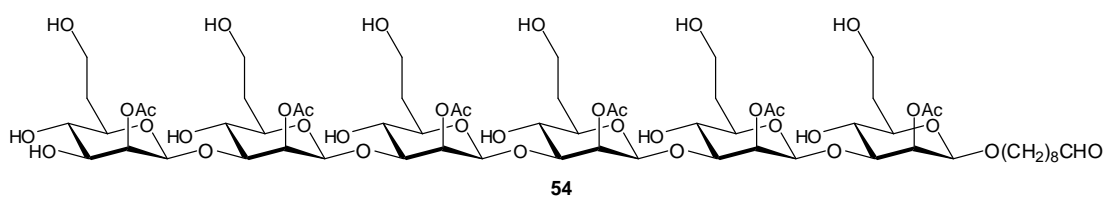


Figure 6.4: Structure of the Ancora Hexasaccharide (**54**) fragment of CPS

It may be the case that mAb 4IVH12 either recognises a conformational epitope of CPS or that it is specific for the α -1,3-mannan polysaccharide (**106**), and as such does not recognise the 6-deoxy-D-*manno*-heptose oligosaccharide fragment. Access to pure α -1,3-mannan (**106**) oligosaccharide would prove helpful in determining which polysaccharide mAb 4IVH12 is specific for. However, SPR experiments using the Biacore T-200 system and immobilised antibody should provide the required sensitivity to finally establish the level of binding of mAb 4IVH12 to the hexasaccharide (**54**). This result, in combination with the further characterisation of the 6dHep-TetHc sera activity to CPS will help to inform the decision regarding the use of monosaccharide/oligosaccharide antigens for vaccination purposes.

6.3 D3K6D3 t-HBcAg virus-like particle

The development of a versatile, chemically conjugatable virus-like particle carrier based on tandem-core technology (iQur) was also conducted as part of this research project. A poly-lysine peptide sequence was inserted into the tip of the major immunodominant region of the tandem hepatitis B core antigen. Initial expression trials demonstrated that wild-type monomeric HBcAg core particles would not assemble with the D3K6D3 insert, highlighting the need for the use of tandem core technology. High purity VLP particles (> 90%) were produced and extracted from *Nicotiana benthamiana* and trial conjugation experiments were carried out using fluorescein isothiocyanate (FITC). Successful conjugation of the VLPs with the FITC fluorophore was achieved and analysed by SDS-PAGE, agarose gel and sucrose gradient. Conjugation of existing monosaccharide haptens to the D3K6D3 VLP, followed by immunisation trials will provide information regarding the potential use of the VLP carrier in the wider vaccine development program. However, further work is needed on development of the extraction and purification techniques from plant material before useful quantities of VLP can be produced. iQur are also investigating different expression systems; yeast, *E. coli* (LPS deficient strain Clearcoli) and *Baculovirus*, however much work is still needed before these methods are viable. Work is currently underway (iQur) to combine the use of synthetic antigens (mono-/oligo-saccharide) with immunogenic *B. pseudomallei* peptides, such as LolC⁷, in an attempt to produce a bi-functional vaccine candidate.

6.4 Summary

There is still a great deal of work required before the components developed as part of this thesis can be combined to produce a viable vaccine candidate. However, the progress made in this work underpins a number of follow-up experiments which will be conducted as part of the ongoing research collaboration between JIC, DSTL-Porton Down, Mologic and iQur. Beyond, the *B. pseudomallei* project, the potential for the development of monosaccharide specific antibodies has broad potential in both therapeutic and diagnostic applications^{8,9,10}. Carbohydrates play an important role in the development and prevention of diseases and much research is still required before the exploitation of these roles can be fully realised.

6.5 References

1. A. E. Scott, T. R. Laws, R. V. D'Elia, M. G. M. Stokes, T. Nandi, E. D. Williamson, P. Tan, J. L. Prior and T. P. Atkins, *Clinical and Vaccine Immunology*, 2013, **20**, 1041-1047.
2. M. Nelson, J. L. Prior, M. S. Lever, H. E. Jones, T. P. Atkins and R. W. Titball, *J. Med. Microbiol.*, 2004, **53**, 1177-1182.
3. T. Oberbillig, C. Mersch, S. Wagner and A. Hoffmann-Roder, *Chem. Commun.*, 2012, **48**, 1487-1489.
4. J. Xie, L. Guo, Y. Ruan, H. Zhu, L. Wang, L. Zhou, X. Yun and J. Gu, *Biochem. Biophys. Res. Commun.*, 2010, **391**, 958-962.
5. G. D. Brown, P. R. Taylor, D. M. Reid, J. A. Willment, D. L. Williams, L. Martinez-Pomares, S. Y. C. Wong and S. Gordon, *J. Exp. Med.*, 2002, **196**, 407-412.
6. C. Heiss, M. N. Burtnick, Z. Wang, P. Azadi and P. J. Brett, *Carbohydr. Res.*, 2012, **349**, 90-94.
7. D. N. Harland, K. Chu, A. Haque, M. Nelson, N. J. Walker, M. Sarkar-Tyson, T. P. Atkins, B. Moore, K. A. Brown, G. Bancroft, R. W. Titball and H. S. Atkins, *Infect. Immun.*, 2007, **75**, 4173-4180.
8. N. F. Reuel, B. Mu, J. Zhang, A. Hinckley and M. S. Strano, *Chem. Soc. Rev.*, 2012, **41**, 5744-5779.
9. H. J. An, S. R. Kronewitter, M. L. de Leoz and C. B. Lebrilla, *Curr. Opin. Chem. Biol.*, 2009, **13**, 601-607.
10. L. S. Kreisman and B. A. Cobb, *Glycobiology*, 2012, **22**, 1019-1030.

7 Experimental

7.1 General Experimental Methods

All reagents were brought from commercial suppliers and were used without further purification (Sigma Aldrich, Toronto Research Chemicals, Pierce, Fisher Scientific Ltd, Carbosynth) unless otherwise stated in the text. Thin-layer chromatography (TLC) was performed using aluminium backed, pre-coated silica plates (Merck, silica gel 60 F₂₅₄). Components were detected by UV light or by immersion in 5% H₂SO₄ in ethanol followed by heating. Flash chromatography was performed on an Isolera 4 (Biotage) flash purification system with pre-packed silica gel columns (10 g, 25 g, 50 g and 100 g; Biotage). Evaporation of solvents was carried out *in vacuo* at 25 – 45°C. NMR spectra were recorded with a Bruker Avance III HD 400 MHz spectrometer at 400 MHz (¹H) or 100.6 MHz (¹³C). Assignments were made with the aid of homonuclear (COSY, NOESY) and heteronuclear (HSQC) two-dimensional correlation spectroscopy. Low-resolution mass spectrometry was performed on a Bruker Daltonics Ultraflex ToF/ToF mass spectrometer using a N₂ laser in 30 shot mode using a ground steel target plate and 2,5-dihydroxybenzoic acid matrix (DHB) in positive mode. A total of 200 shots were collected per sample at 50 – 75% laser power dependant on signal intensity. Mass data were analysed using Bruker Daltonics flexanalysis software. High resolution mass spectrometry was performed by Dr Gerhaard Salbach using a SYNAPT G2-Si spectrometer with electrospray ionisation (ESI) in positive mode. Optical rotations were recorded at 20°C on a Perkin-Elmer 341 polarimeter.

7.1.1 General deacetylation/debenzoylation procedure

A small piece of metallic sodium was added to a solution of protected compound in absolute MeOH, the solution was stirred at room temperature until it was shown to be complete by TLC. The reaction was neutralised with Amberlite IR-120 H⁺ resin, after which the resin was filtered off and the solvent was removed *in vacuo*.

7.1.2 Protein conjugation

A solution of acyl hydrazide, containing 4M HCl in dioxane (5 equiv) and *t*-butyl nitrite (1.8 equiv) in DMF (1 ml) was stirred for 15 minutes at -25°C. After 15

minutes sulfamic acid (1 equiv) in DMF (100 μ l) was added and the reaction mixture was allowed to reach 0°C. The cold acyl azide solution was then added dropwise to a solution of protein (0.01 equiv) in conjugation buffer [0.08M Borax; 0.35M KHCO₃; pH = 9.0]. The solution was stirred overnight at 4°C.

After 16 hours the conjugation reaction was extensively dialysed (4 litres x 5 changes) (Snake Skin; 10 MWCO; Fisher Scientific) against ammonium bicarbonate solution [200 mM, pH 8.0] and lyophilised to afford pure protein conjugate. Protein conjugate were analysed using MALDI-ToF MS **7.1.3** and SDS-PAGE **7.1.4**.

7.1.3 MALDI-ToF MS of protein conjugates^{1 2}

Glycoproteins were solubilised in a saturated solution of sinapinic acid matrix [70% MeCN, 0.1% TFA] at 0.4 mg/ml. A sandwich layer technique was used for the preparation of the sample on to a MALDI-ToF ground steel target plate (Bruker Daltronics). First saturated matrix solution (0.5 μ l) was loaded onto the plate and left to dry on the bench, secondly the freshly prepared matrix and protein solution was added onto the crystallised matrix layer (0.5 μ l). After drying on the bench another layer of saturated matrix solution (0.2 μ l) was layered on top of the spot to form a matrix sandwich.

All protein MS analyses were conducted on a Bruker Daltronics Ultraflex ToF/ToF mass spectrometer using a N₂ laser in 50 shot mode. A total of 200 shots were collected per sample at 50 – 75% laser power dependant on signal intensity. Mass data were analysed using Bruker Daltronics flexanalysis software.

7.1.4 SDS-PAGE analysis of proteins³

Loading buffer (5 μ l) [SDS Running buffer; 10% (v/v) glycerol; 0.1 mg/ml bromophenol blue; 0.1 mg/ml β -mercaptoethanol] was added to protein (25 μ l; 0.4 mg/ml) in MQ-H₂O. After heating at 100°C for 5 min the samples were loaded onto a 4-20% RunBlue precast gel (Expedion) and run in RunBlue running buffer [40 mM Tricine; 60 mM Tris-HCl; 0.1% SDS; 2.5 mM sodium bisulfite; pH 8.2] at 180 V for 53 min. Gels were removed from the case and stained for protein with Instant Blue

protein stain (Expedion). LDS gels for initial VLP work were done using the same protocol with NuPAGE LDS gels (Life Technologies) and LDS buffer.

7.1.5 Western Blot of SDS/LDS-PAGE gel

PVDF blotting membrane cut to size (8 x 11 cm) was pre-wet in MeOH (10 ml), the SDS-PAGE gels were pre-soaked in Towbin blotting buffer [25 mM Tris; 192 mM Glycine; 20% MeOH; pH 8.6] to avoid the gel shrinking during blotting. The gel and membrane were assembled in the blotting apparatus (BioRad) with pre-cooled Towbin buffer. An ice block was placed in the blotting tank to keep the apparatus cool and the blots were run at 100 V for 1.5 hours. Membranes were blocked overnight in 5% BSA in PBS_T and visualised using the appropriate 1^o and 2^o antibodies.

7.1.6 Polysaccharide hydrolysis with strong acid ⁴

A solution of polysaccharide (20 µl of a 3 mg/ml solution in MQ-H₂O) was added to a screw cap reaction vial containing TFA (30 µl in 150 µl of MQ-H₂O). The vial was sealed and heated to 100°C for 4 hours. The reaction was concentrated *in vacuo* using a SpeedVac[®] evaporation centrifuge (Thermo[®]). The polysaccharide was reconstituted in MQ-H₂O (300 µl), vortexed for 30 seconds and centrifuged for 5 mins (14,000 *rcf*). The polysaccharide hydrosylate sample (10 µl, 2 µg) was then injected onto the Dionex[®] ICS-5000[®] HPAEC-PAD for analysis.⁵

7.1.7 Monosaccharide analysis by HPAEC-PAD chromatography

7.1.7.1 Assessment of gradient conditions

A mixture (10 µl) of 6-deoxy-D-mannoheptose, L-fucose, D-galactose, D-glucose, D-mannose and L-rhamnose (each at 10 µM concentration) was injected onto the Dionex[®] HPAEC-PAD system. Isocratic elution with 6, 8, 10 and 12 mM NaOH (Fisher[®] HPLC grade) were run (0.25 ml/min) for 40 minutes followed by a 6 min wash step (100 mM NaOH) and a 15 min re-equilibration step. Detection was achieved using pulsed amperometric detection (PAD).

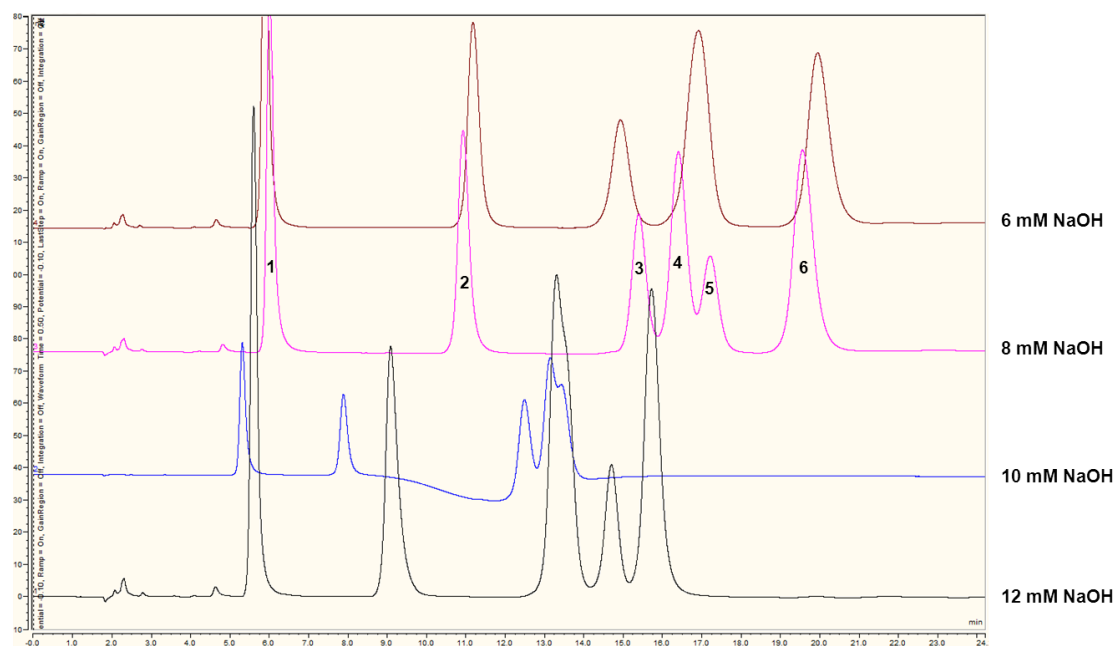


Figure 7.1: Overlay of chromatograms from monosaccharide analysis of a mixed sample 1) L-fucose 2) L-rhamnose 3) 6-deoxy-D-heptose 4) D-galactose 5) D-glucose 6) D-mannose. Dionex PA-100G Column (2 x 50 mm); flow rate 0.25 ml/min; 6, 8, 10 and 12 mM NaOH isocratic elution; 25°C 10 μ l (2 μ g) injection; pulsed amperometric detection (Au electrode).

7.1.7.2 Monosaccharide analysis of polysaccharide hydrosylate

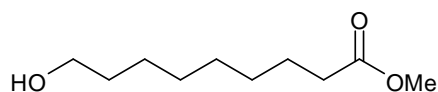
Polysaccharide hydrosylates (10 μ l) were injected onto the system and the monosaccharide analysis was done using an 8 mM NaOH isocratic gradient (see above). Spiking experiments were done on a monosaccharide by monosaccharide basis. This was due to the impact of the addition of a monosaccharide on the retention times of the monosaccharide mixture. The polysaccharide hydrosylate samples were supplemented with monosaccharide standards (10/25 μ M final concentration) and injected onto the column (10 μ l).

7.1.1 Phenol-sulphuric acid assay for carbohydrate⁶

Aliquots (50 μ l) of the analysed solution were added to a 96-well microtitre plate (Nunclon Delta Surface, Thermo Scientific) followed by the addition of concentrated sulphuric acid (150 μ l) and 5% aqueous phenol (30 μ l) to each well. The plate was heated at 90°C for 5 mins in an oven and cooled to room temperature over 5 mins. Absorbance was read at A_{405} using a plate-reader to give relative concentration of carbohydrate.

7.2 Chapter 2 Experimental

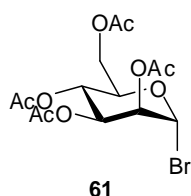
7.2.1 8-Methoxycarbonyl octanol (**58**)^{7, 8}



58

BH₃·THF complex (1 M in THF; 100 ml) was added dropwise to a stirred solution of monomethyl azelate (**57**) (20 g; 99 mmol) in dry THF (50 ml) at -20 °C over a period of 30 min. The reaction mixture was allowed to warm to room temperature and stirring continued for a further 4 hours. After the reaction was shown to be complete (TLC Hex:EtOAc; 1:1) it was quenched using water and K₂CO₃ (20 g; 168 mmol) at 0°C and extracted using Et₂O (3x100 ml). The combined organic layers were washed with brine and dried over MgSO₄, filtered and concentrated *in vacuo*. The resulting oil was purified using flash chromatography [Hex:EtOAc; 1:1] to afford methyl ester (**58**) as a colourless oil, (15.26 g, 82%). ¹H NMR (400 MHz, CDCl₃): 3.65 (3 H, s, OMe), 3.60 (2H, t, *J*_{H7,8} = 6.5 Hz, CH₂OH), 2.31 (2H, t, *J*_{H2,3} = 7.5 Hz, CH₂OOME), 1.90-1.25 (12H); ¹³C NMR (100 MHz, CDCl₃): 176.0, 62.9, 60.0, 34.8, 33.6, 30.7, 30.4, 30.3, 30.1, 26.9, 26.0; MALDI-ToF *m/z* 211.86 [M+Na]⁺, 227.94 [M+K]⁺, calculated for C₁₀H₂₀O₃Na 211.25 and C₁₀H₂₀O₃K 227.36

7.2.2 2,3,4,6-Tetra-O-acetyl- α -D-mannopyranosyl bromide (**61**)⁹



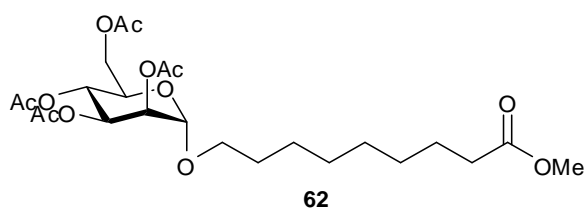
61

Finely ground iodine (90 mg, 0.35 mmol, 2.5 mol %) was dissolved in acetic anhydride (2 ml) and the solution was heated until the exothermic reaction was self-propagating. The hot iodine/acetic anhydride complex was added to a suspension of D-mannose (**59**) (2.5 g, 13.90 mmol) in acetic anhydride (25 ml) and the mixture was vigorously stirred in a 25°C water bath. After 10 min the sugar had completely dissolved and the reaction was shown to be complete by TLC [Hex:EtOAc, 4:1]. The solution was diluted in 50 ml of EtOAc and quenched by the addition of solid NaHCO₃ (5 g), it was then washed with sat. aq. NaHCO₃ solution (50 ml), Na₂SO₃

(50 ml) and H₂O (50 ml), dried over MgSO₄ and solvents were removed *in vacuo*. The residual syrup was used without further purification (5.0 g, 12.80 mmol, 92 %).

Per-O-acetylated D-mannopyranose (**60**) (5.0 g, 12.80 mmol) was dissolved in dry DCM (25 ml) and the solution was cooled to 0°C. HBr (9 ml of 33% w/v solⁿ HBr/AcOH, 38 mmol) was added dropwise and the reaction mixture was left to stir for 3 hours. The solution was washed with H₂O/ice (3 x 30 ml), sat. aq. NaHCO₃ solution (30 ml) and H₂O (30 ml), the organic layer was dried over MgSO₄ and the solvent was removed *in vacuo*, to afford bromide (**61**) as a white foam (4.1 g, 9.85 mmol, 77%). [α]_D = + 110.5 (c 1.0, CHCl₃), Lit⁹ [α]_D + 111.8 (c 1.0, CHCl₃); ¹H NMR (400 MHz, CDCl₃): 6.30 (1H, d, *J*_{1,2} = 1.5 Hz, H-1), 5.72 (1H, dd, *J*_{2,3} = 3.5 Hz, *J*_{3,4} = 10.0 Hz, H-3), 5.45 (1H, dd, *J*_{1,2} = 1.5 Hz, *J*_{2,3} = 3.5 Hz, H-2), 5.37 (1H, t, *J*_{3,4} = *J*_{4,5} = 10.0 Hz, H-4), 4.34 (1H, dd, *J*_{5,6} = 5.0 Hz, *J*_{6a,ab} = 12.5 Hz, H-6_a), 4.24 – 4.20 (1H, m, H-5), 4.17 – 4.13 (1H, m, H-6_b), 2.11 (3H, s, OAc), 2.09 (3H, s, OAc), 2.04 (3H, s, OAc), 2.01 (3H, s, OAc); ¹³C NMR (100 MHz, CDCl₃): 170.6, 170.0, 169.8, 169.5 (C=O), 83.4 (C-1), 73.1 (C-2), 72.6 (C-5), 67.3 (C-3), 66.0 (C-4), 60.9 (C-6), 20.9, 20.8, 20.5 (OAc); MALDI-ToF *m/z* 433.89 [M+Na]⁺, 450.01 [M+K]⁺, calculated for C₁₄H₁₉BrO₉Na 434.19 and C₁₄H₁₉BrO₉K 450.30.

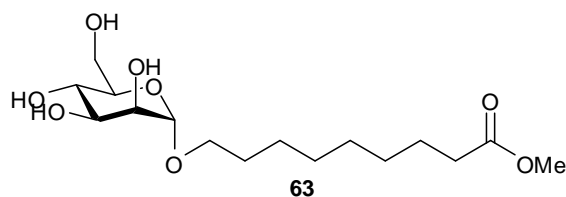
7.2.3 8-(Methoxycarbonyl)octyl 2,3,4,6-O-acetyl- α -D-mannopyranoside (**62**)¹⁰



A solution of mercury bromide (330 mg; 1.30 mmol), mercury cyanide (47 mg; 0.132 mmol), 8-methoxycarbonyl octanol (**58**) (205 mg; 1.10 mmol) and 4Å molecular sieves (250 mg) in dry DCE (4.5 ml) was stirred at room temperature for 30 mins. Bromide (**61**) (300 mg; 0.75 mmol) in dry DCE (0.5 ml) was added dropwise to the stirred solution and the reaction was left at room temperature for 16 hours. After which, the reaction mixture was filtered and the filtrate was washed with KBr (10 ml), H₂O (3 x 10 ml), dried over MgSO₄ and concentrated *in vacuo*. Chromatography [Hex:EtOAc; 5:2] was performed to isolate alkyl mannoside (**62**)

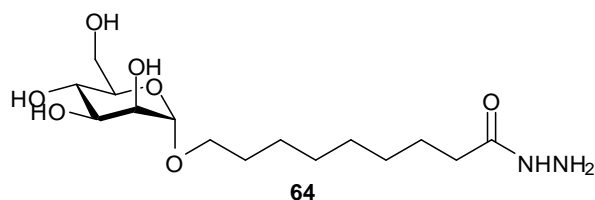
(148 mg, 0.28 mmol, 39%) as a pale yellow oil. $[\alpha]_D = +45.3$ (c 1.0, CHCl_3), Lit¹⁰ $[\alpha]_D + 40.0$ (c 1.02, CHCl_3); ¹H NMR (400 MHz, CDCl_3): 5.35 (1H, dd, $J_{2,3} = 3.0$ Hz, $J_{3,4} = 10.0$ Hz, H-3), 5.30 (1H, t, $J_{3,4} = J_{4,5} = 10.0$ Hz, H-4), 5.26 (1H, dd, $J_{1,2} = 1.5$ Hz, $J_{2,3} = 3.0$ Hz), 4.78 (1H, d, $J_{1,2} = 1.5$ Hz), 4.30 (1H, dd, $J_{5,6} = 5.0$ Hz, $J_{6a,6b} = 12.0$ Hz, H-6_a), 4.07 (1H, dd, $J_{5,6} = 5.0$ Hz, $J_{6a,6b} = 12.0$ Hz, H-6_b), 4.01 (1H, m, H-5), 3.65 (3H, s, OMe), 3.62-3.54 (2H, m, OCH_2 -spacer), 2.30 (2H, t, $J = 7.0$ Hz, CH_2COOMe), 2.10 (3H, s, OAc), 2.07 (3H, s, OAc), 2.05 (3H, s, OAc), 2.03 (3H, s, OAc), 1.59 - 1.47 (4H, m, 2 x CH_2), 1.36 - 1.17 (8H, m, 4 x CH_2); ¹³C NMR (100 MHz, CDCl_3): 177.9 (COOMe), 169.9, 169.7, 169.6 (C=O), 98.6 (C-1), 72.7 (C-5), 70.6 (C-2), 70.1 (C-3), 67.9 (CH_2O), 66.7 (C-4), 60.7 (C-6), 52.0 (OMe), 33.7 (CH_2COOMe), 28.4-24.2 (4 x OAc; 6 x CH_2); MALDI-ToF m/z 541.71 $[\text{M}+\text{Na}]^+$, 557.81 $[\text{M}+\text{K}]^+$, calculated for $\text{C}_{24}\text{H}_{38}\text{O}_{12}\text{Na}$ 541.54 and $\text{C}_{24}\text{H}_{38}\text{O}_{12}\text{K}$ 557.65.

7.2.4 8-(Methoxycarbonyl)octyl- α -D-mannopyranoside (**63**)^{10, 11}



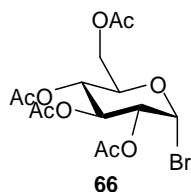
8-Methoxycarbonyloctyl 2,3,4,6-acetyl- α -D-mannopyranoside (**62**) (100 mg; 1.92 mmol) was deprotected using general deacetylation procedure **7.1.1**. The solvents were evaporated *in vacuo* to afford alkyl mannoside (**63**) as a white amorphous solid (56.7mg, 0.16 mmol, 84%). $[\alpha]_D = + 49.4$ (c 0.6, MeOH), Lit¹¹ $[\alpha]_D = + 51.5$ (c 1.0, MeOH), Lit¹⁰ $[\alpha]_D = 43.4$ (c 0.4, MeOH); ¹H NMR (400 MHz, D_2O): 4.80 (1H, dd, $J_{1,2} = 1.5$ Hz, H-1), 3.90 (1H, dd, $J_{1,2} = 1.5$ Hz, $J_{2,3} = 4.0$ Hz, H-2), 3.83-3.78 (2H, m, H-6_{a,b}), 3.75 (1H, dd, $J_{2,3} = 4.0$ Hz, $J_{3,4} = 9.0$ Hz, H-3), 3.73 - 3.70 (2H, m, H-4, CH_2O), 3.66 (3H, s, OMe), 3.58 - 3.62 (1H, m, H-5), 3.49 - 3.46 (1H, m, CH_2O), 2.33 (2H, t, CH_2COOMe), 1.60 - 1.49 (4H, m, 2 x CH_2), 1.36 - 1.19 (8H, m, 4 x CH_2); ¹³C NMR (100 MHz, D_2O): 177.8 (COOMe), 99.5 (C-1, $^1J_{\text{C}1,\text{H}1} = 171$ Hz), 72.9 (C-5), 72.0 (C-3), 68.9 (CH_2O), 67.5 (C-4), 62.1 (C-6), 53.1 (OMe), 35.1 (CH_2COOMe), 29.4 - 25.1 (6 x CH_2), MALDI-ToF m/z 373.89 $[\text{M}+\text{Na}]^+$, 390.01 $[\text{M}+\text{K}]^+$, calculated for $\text{C}_{16}\text{H}_{30}\text{O}_8\text{Na}$ 373.39 and $\text{C}_{16}\text{H}_{30}\text{O}_8\text{K}$ 389.54.

7.2.5 8-(Hydrazinocarbonyl)octyl- α -D-mannopyranoside (**64**)



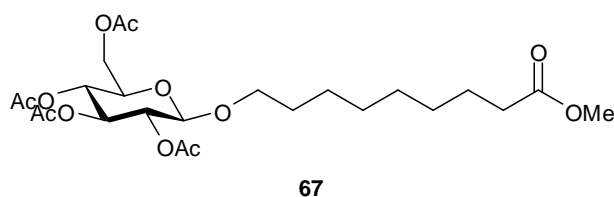
Treatment of alkyl mannoside (**63**) (10 mg, 0.03 mmol) with hydrazine monohydrate (1 ml) in EtOH (2.5 ml) at 55°C for 6 hours afforded the hydrazide hapten (**64**) in quantitative yield. The product (**64**) was cleaned up by co-evaporation of excess reagent with toluene (3 x 10 ml) and NMR analysis confirmed complete conversion by loss of the singlet at δ 3.66 ppm (OMe) in the ^1H NMR spectra.

7.2.6 2,3,4,6- Tetra-*O*-acetyl- α -D-glucopyranosyl bromide (**66**)¹²



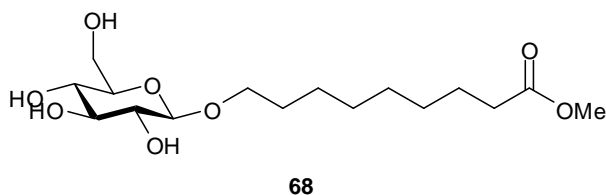
Per-*O*-acetylated glucose (**65**) (10.0 g, 25.50 mmol) was dissolved in dry DCM (50 ml) and cooled to 0°C. HBr (18 ml of 33% w/v solⁿ HBr/AcOH, 76.6 mmol) was added drop-wise and the reaction mixture was left to stir for 3 hours. The solution was washed with H₂O/ice (3 x 50 ml), sat. aq. NaHCO₃ solution (50 ml) and H₂O (50 ml), the organic layer was dried over MgSO₄ and the solvent was removed *in vacuo*, the product was recrystallized from Et₂O to afford bromide (**66**) (8.4 g, 20.2 mmol, 79%). $[\alpha]_{\text{D}} = +180.8$ ($c = 1.0$, CHCl₃), Lit¹³ = +190.9 ($c = 1.0$, CHCl₃); ^1H NMR (400 MHz, CDCl₃): 6.61 (1H, d, $J_{1,2} = 4.0$ Hz), 5.56 (1H, t, $J_{2,3} = J_{3,4} = 9.5$ Hz, H-3), 5.17 (1H, t, $J_{3,4} = J_{4,5} = 9.5$ Hz, H-4), 4.84 (1H, dd, $J_{1,2} = 4.0$ Hz, $J_{2,3} = 10.0$ Hz, H-2), 4.37 – 4.27 (2H, m, H-5, H-6_a), 4.13 (1H, m, H-6_b), 2.11 (3H, s, OAc), 2.10 (3H, s, OAc), 2.06 (3H, s, OAc), 2.04 (3H, s, OAc); ^{13}C NMR (100 MHz, CDCl₃): 170.5, 169.9, 169.8, 169.5 (C=O), 86.6 (C-1), 72.1 (C-5), 70.6 (C-2), 70.1 (C-3), 67.1 (C-4), 60.9 (C-6), 20.7, 20.6 (4 x OAc); MALDI-ToF m/z 434.07 [M+Na]⁺, 450.21 [M+K]⁺, calculated for C₁₄H₁₉BrO₉Na 434.19 and C₁₄H₁₉BrO₉K 450.30.

7.2.7 8-(Methoxycarbonyl)octyl-2,3,4,6-O-acetyl- β -D-glucopyranoside (**67**)¹⁴



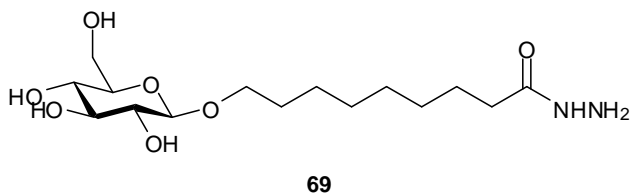
A solution of mercury bromide (115 mg; 0.32 mmol), mercury cyanide (830 mg; 3.28 mmol), 8-methoxycarbonyl octanol (**58**) (310 mg; 1.64 mmol) and 4Å molecular sieves (500 mg) in dry DCE (9.5 ml) was stirred at room temperature for 30 mins. Bromide (**66**) (750 mg; 1.83 mmol) in dry DCE (0.5 ml) was added dropwise to the stirred solution and the reaction mixture was left at room temperature for 16 hours. After which, the solution was filtered and the filtrate was washed with KBr (10 ml), H₂O (3 x 20 ml), dried over MgSO₄ and concentrated *in vacuo*. Chromatography [Hex:EtOAc; 5:2] was performed to isolate alkyl glucoside (**67**) (148 mg, 0.285 mmol, 68%) as a pale yellow oil. $[\alpha]_D = -12.6$ (c 1.0, CHCl₃), Lit ¹⁴ $[\alpha]_D = -14.0$ (c 1.0, CHCl₃); ¹H NMR (400 MHz, CDCl₃): 5.21 (1H, t, $J_{2,3} = J_{3,4} = 9.5$ Hz, H-3), 5.09 (1H, t, $J_{3,4} = J_{4,5} = 9.5$ Hz, H-4), 4.27 (1H, dd, $J_{1,2} = 7.5$ Hz, $J_{2,3} = 9.5$ Hz, H-2), 4.50 (1H, d, $J_{1,2} = 7.5$ Hz, H-1), 4.27 (1H, dd, $J_{5,6a} = 5.0$ Hz, $J_{6a,6b} = 12.5$ Hz, H-6_a), 4.14 (1H, dd, $J_{5,6b} = 2.5$ Hz, $J_{6a,6b} = 12.5$ Hz, H-6_b), 3.86 (1H, m, CH₂O), 3.7 (1H, m, H-5), 3.67 (3H, s, OMe), 3.47 (1H, m, CH₂O), 2.30 (2H, t, $J = 7.5$ Hz, CH₂COOMe), 2.09 (3H, s, OAc), 2.04 (3H, s, OAc), 2.03 (3H, s, OAc), 2.01 (3H, s, OAc), 1.63 – 1.49 (4H, m, 2 x CH₂), 1.32 – 1.21 (8H, m, 4 x CH₂); ¹³C NMR (100 MHz, CDCl₃): 172.5, 170.3, 169.9, 169.3 (C=O), 100.8 (C-1), 72.9 (C-3), 71.7 (C-4), 71.3 (C-5), 70.2 (CH₂O), 68.5 (C-2), 62.0 (C-6), 51.4 (OMe), 34.0 (CH₂COOMe), 29.3, 29.1, 29.0, 25.7, 24.8 (6 x CH₂), 20.7, 20.6 (4 x OAc); MALDI-ToF m/z 541.25 [M+Na]⁺, 557.24 [M+K]⁺, calculated for C₂₄H₃₈O₁₂Na 541.54 and C₂₄H₃₈O₁₂K 557.65.

7.2.8 8-(Methoxycarbonyloctyl)- β -D-glucopyranoside (**68**)¹⁴



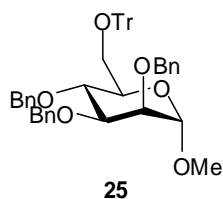
8-Methoxycarbonyloctyl 2,3,4,6-*O*-acetyl- β -D-glucopyranoside (**67**) (145 mg; 0.28 mmol) was deprotected using the standard deprotection method (Section 7.1.1). The solvents were evaporated *in vacuo* to afford alkyl glucoside (**68**) as a colourless oil (91 mg, 0.26 mmol; 89%). $[\alpha]_D = -28.3$ (*c* 1, MeOH), Lit¹⁴ $[\alpha]_D = -24.1$ (*c* 1.14, MeOH); ¹H NMR (400 MHz, CD₃OD): 4.15 (1H, d, $J_{1,2} = 8.0$ Hz, H-1), 3.83 – 3.74 (2H, m, CH₂O, H-6_a), 3.59 – 3.54 (1H, m, H-6_b), 3.57 (3H, s, OMe), 3.47 – 3.40 (1H, m, CH₂O), 3.27 – 3.14 (3H, m, H-3, H-4, H-5), 3.06 (1H, t, $J_{1,2} = J_{2,3} = 8.0$ Hz, H-2), 2.21 (2H, t, $J = 7.5$ Hz, CH₂COOMe), 1.54 – 1.45 (4H, m, 2 x CH₂), 1.34 – 1.19 (8H, m, 4 x CH₂); ¹³C NMR (100 MHz, CD₃OD): 176.2 (COOMe), 104.4 (C-1), 78.2 (C-3), 77.9 (C-2), 75.1 (C-5), 71.7 (C-4), 70.9 (CH₂O), 62.8 (C-6), 52.0 (OMe), 34.8 (CH₂COOMe), 30.8 – 26.0 (6 x CH₂); MALDI-ToF *m/z* 373.02 [M+Na]⁺, 389.01 [M+K]⁺, calculated for C₁₆H₃₀O₈Na 373.39 and C₁₆H₃₀O₈K 389.54.

7.2.9 8-(Hydrazinocarbonyloctyl)- β -D-glucopyranoside (**69**)



Alkyl glucoside (**68**) (10 mg, 0.03 mmol) was treated with hydrazine monohydrate (1 ml) in EtOH (2.5 ml) at 55°C for 6 hours afforded the hydrazide hapten (**69**) in quantitative yield. The product (**69**) was cleaned up by co-evaporation of excess reagent with toluene (3 x 10 ml) and NMR analysis confirmed complete conversion by loss of the singlet at δ 3.57 ppm (OMe) in the ¹H NMR spectra.

7.2.10 Methyl 2,3,4-tri-*O*-benzyl-6-*O*-triphenylmethyl- α -D-mannopyranoside (25)¹⁵



7.2.10.1 Tritylation method A

Triphenylmethyl chloride (8.64 g, 31.0 mmol) and DMAP (100 mg) were added to a solution of methyl α -D-mannopyranoside (**35**) (5 g, 25.8 mmol) in pyridine (50 ml). The reaction was stirred at 40°C overnight. Upon completion of the reaction [CHCl₃:MeOH; 9:1], the solvent was removed *in vacuo* and the resulting residue was dissolved in EtOAc (150 ml). After washing with H₂O (2 x 50 ml), the extracted organic layer was dried over MgSO₄, filtered and concentrated *in vacuo*. The resulting syrup was used without further purification, (7.71 g, 68%, crude).

7.2.10.2 Tritylation method B

Methyl α -D-mannopyranoside (**35**) (5 g, 25.8 mmol) and triphenylmethyl chloride (8.64 g, 31.0 mmol) were dissolved in a mixture of DMF (50 ml) and triethylamine (10 ml, 64.5 mmol) and stirred at room temperature for 16 hours. The reaction was monitored by TLC [CHCl₃:MeOH; 9:1] and upon completion of the reaction, the product was isolated as above and used in the subsequent reaction without further purification, (8.05 g, 72%, crude).

7.2.10.3 Benzylation of monotrityl ether

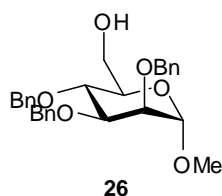
Trityl ether (**24**) (5 g, 11.45 mmol) was dissolved in anhydrous DMF (50 ml) and the solution was cooled to 0°C. Sodium hydride (2.75 g of a 60% mineral oil suspension, 68.7 mmol) was added slowly and the mixture was stirred vigorously for 30 minutes. Benzyl bromide (6.81 ml, 57.3 mmol) was added dropwise at 0°C and the reaction was stirred overnight at rt. After 16 hours the reaction was shown to be complete by TLC [Hex:EtOAc; 4:1].* Upon completion, the reaction was quenched using MeOH (5 ml) and the solvent was removed *in vacuo*. The resulting residue was redissolved in DCM (30 ml), washed with H₂O (3 x 30 ml) and dried using MgSO₄, then filtered and concentrated. The resulting syrup was purified using flash

chromatography [Hex:EtOAc, 4:1] to afford benzylated trityl ether (**25**) as a white foam (5.34 g, 7.56 mmol, 68%).

* If reaction is carried out on large scale (>5 grams) then compound **24** is dissolved in anhydrous DMF (10 mol% solution) and benzyl bromide (5 equivs.). The reaction mixture is cooled to 0°C and sodium hydride 60% in mineral oil is added in 500 mg portions.

$[\alpha]_D = +20.4$ (c 1.0, CHCl₃), Lit.¹⁵ $[\alpha]_D = +23.0$ (c 4.0, CHCl₃); ¹H NMR (400 MHz, CDCl₃): 7.53-7.14 (30H, m, ArH), 4.82 (1H, d, $J_{1,2} = 2.0$ Hz, H-1), 4.31-4.82 (6H, m, CH₂Ph), 4.04 (1H, t, $J_{3,4} = J_{4,5} = 10.0$ Hz, H-4), 3.88 (1H, dd, $J_{2,3} = 3.5$, $J_{3,4} = 10.0$ Hz, H-3), 3.82 (1H, dd, $J_{1,2} = 2.0$, $J_{2,3} = 3.5$ Hz, H-2), 3.80-3.76 (1H, m, H-5), 3.52 (1H, dd, $J_{5,6} = 2.0$, $J_{6a,6b} = 11.5$ Hz, H-6_a), 3.37 (3H, s, OMe), 3.28 (1H, dd, $J_{5,6} = 2.0$, $J_{6a,6b} = 11.5$ Hz, H-6_b); ¹³C NMR (100 MHz, CDCl₃): 144.4, 138.8, 138.5, 129.6, 128.5, 128.3, 127.9-126.9 (ArC), 98.9 (C-1), 86.4 (OCPh₃), 80.4 (C-3), 75.6 (C-2), 75.2 (C-4), 75.1 (CH₂Ph), 72.9 (CH₂Ph), 72.4 (CH₂Ph), 71.9 (C-5), 63.3 (C-6), 54.7 (OMe); MALDI-ToF m/z 729.49 [M+Na]⁺, 745.53 [M+K]⁺, calculated for C₄₇H₄₆O₆Na 729.85 and C₄₇H₄₆O₆K 745.96.

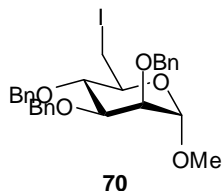
7.2.11 Methyl 2,3,4-Tri-O-benzyl- α -D-mannopyranoside (**26**)¹⁶



90% Aqueous TFA (2 ml) was added dropwise to a solution of benzyl ether (**25**) (5g, 7.10 mmol) in DCM (25 ml) and the solution as stirred at room temperature for 20 minutes. The reaction was neutralized using NaHCO₃ (decolourisation and effervescence). The resulting solution was further washed with cold aqueous 10% NaHCO₃ solution (25 ml) and H₂O (25 ml), the resulting organic layer was dried and concentrated. The resulting syrup was purified using flash chromatography [Hex:EtOAc; 3:1] to afford product (**26**), (2.86 g, 6.16 mmol, 87%). $[\alpha]_D = +28.4$ (c 1, CHCl₃), Lit¹⁶ $[\alpha]_D = +34.8$ (c 0.3, CHCl₃); ¹H NMR (400 MHz, CDCl₃): 7.46-7.29 (15H, m, ArH), 4.96-4.82 (6H, m, CH₂Ph), 4.70 (1H, d, $J_{1,2} = 2.0$ Hz, H-1), 3.96 (1H, t, $J_{3,4} = J_{4,5} = 9.0$ Hz, H-4), 3.90 (1H, dd, $J_{2,3} = 3.5$, $J_{3,4} = 9.0$ Hz, H-3), 3.84 (1H, m, H-2), 3.80-3.74 (3H, m, H-2, H-6_{a,b}), 3.64-3.59 (1H, m, H-5), 3.29 (3H, s, OMe), 2.1 (1H, bs, OH); ¹³C NMR (100 MHz, CDCl₃): 128.3, 127.9, 12.7, 127.6 (ArC), 99.5 (C-

1), 80.2 (C-3), 75.2 (CH₂Ph), 74.9 (C-4), 74.8 (C-2), 73.0 (CH₂Ph), 72.3 (CH₂Ph), 72.1 (C-5), 62.5 (C-6), 54.1 (OMe); MALDI-ToF m/z 487.12 [M+Na]⁺, 503.29 [M+K]⁺, calculated for C₂₈H₃₂O₆Na 487.54 and C₂₈H₃₂O₆K 503.65.

7.2.12 Methyl 2,3,4-Tri-O-benzyl-6-deoxy-6-iodo- α -D-mannopyranoside (**70**)¹⁷



7.2.12.1 Method 1

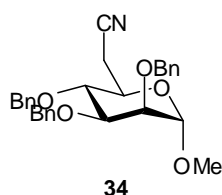
To a solution of benzyl ether (**26**) (3 g, 6.5 mmol) in anhydrous toluene (30 ml) were added; finely ground triphenylphosphine (2.4 g, 9.1 mmol), imidazole (883 mg, 13.0 mmol) and iodine (6.6 g; 26.0 mmol). The reaction mixture was heated under reflux conditions for 4 hours and the reaction progress was monitored by TLC [Tol:EtOAc; 4:1]. The cooled reaction mixture was transferred to a separating funnel and washed with 10% Na₂S₂O₃ solution (50 ml); Sat. aq. NaHCO₃ solution (50 ml) and H₂O (50 ml) successively and dried over MgSO₄. The volatiles were removed *in vacuo* and the resulting syrup was purified using two rounds of flash chromatography [Hex:EtOAc; 3:1] to afford iodide (**70**) as a pale orange oil (2.72 g, 4.75 mmol, 73%). [α]_D = +28.4 (c 1.0, CHCl₃), Lit¹⁷ [α]_D = +26.0 (c 1.39, CHCl₃); ¹H NMR (400 MHz, CDCl₃): 7.37-7.28 (15H, m, ArH), 4.79 (1H, d, *J*_{1,2} = 1.5 Hz, H-1), 4.98-4.58 (6H, m, 3 x CH₂Ph), 3.93 (1H, dd, *J*_{2,3} = 3.0, *J*_{3,4} = 9.5 Hz, H-3), 3.81-3.84 (2H, m, H-2, H-4), 3.55 (1H, m, H-5), 3.61 (1H, m, H-6_a), 3.41 (3H, s, OMe), 3.37 (1H, m, H-6_b); ¹³C NMR (100 MHz CDCl₃): 139.1, 139.0, 128.8, 128.6, 128.3, 128.2 (ArC), 98.71 (C-1), 76.2 (CH₂Ph), 74.3 (CH₂Ph), 71.9 (CH₂Ph), 71.6 (C-3), 71.4 (C-2, C-4), 70.9 (C-5), 54.1 (OMe), 6.8 (C-6); MALDI-ToF m/z 597.57 [M+Na]⁺, 613.42 [M+K]⁺, calculated for C₂₈H₃₁IO₅Na 597.44 and C₂₈H₃₁IO₅K 613.54.

7.2.12.2 Method 2 – Iodination using Sp-PPh₃

To a solution of benzyl ether (**26**) (100 mg, 0.22 mmol) in anhydrous toluene (5 ml) were added; Sp-PPh₃ (230 mg, 0.48 mmol, 2.0 mmol/g loading), imidazole (33 mg, 0.48 mmol) and iodine (156 mg, 0.62 mmol). The reaction mixture was heated under reflux for 4 hours and monitored by TLC [Tol:EtOAc; 4:1]. Upon completion of the reaction, the Sp-PPh₃ was filtered off and the solvents removed *in vacuo*.

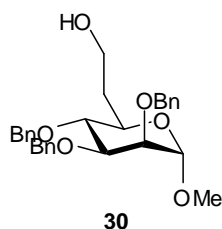
The residual syrup was washed with 10% Na₂S₂O₃ (20 ml), Sat. aq. NaHCO₃ solution (20 ml) and H₂O (20 ml) successively and dried over MgSO₄ and concentrated *in vacuo*. The resulting syrup was purified using flash chromatography [Hex:EtOAc; 3:1] to afford iodide (**70**) as a pale orange oil (123 mg, 0.21 mmol, 97%). All characterisation data was in accordance with the literature and results obtained for compound (**70**) as synthesised by method **7.2.12.1**.¹⁷

7.2.13 Methyl 2,3,4-tri-*O*-benzyl-6-deoxy- α -D-mannoheptopyranosylurononitrile (**34**)¹⁸



Iodide (**70**) (250 mg, 0.44 mmol) was dissolved in anhydrous DMF (0.5 ml) in a microwave reaction vial (Biotage 0.5 – 2 ml). Sodium cyanide (55 mg, 1.1 mmol), was added to the reaction mixture and the vial was sealed using a rubber septum and cap. The vial was placed in the microwave reactor (Biotage Initiator) and was heated at 70°C for two 1.5 hour time periods, at which point the reaction was complete, TLC [Hex: EtOAc, 3:1]. Upon completion of the reaction, the solvent was removed *in vacuo* and the resulting syrup was dissolved in DCM (10 ml) and washed successively with H₂O (20 ml), 1 M HCl (10 ml), sat. aq. NaHCO₃ solution (10 ml) and H₂O (10 ml), the organic phase was dried over MgSO₄ and concentrated *in vacuo*. The resulting oil was passed through a 5 cm bed of silica gel [Hex:EtOAc, 3:1] to remove impurities and the solvent was removed *in vacuo* to afford nitrile (**34**) (185 mg, 0.39 mmol, 89%). [α]_D = + 47.7 (*c* 1, CHCl₃), Lit¹⁸ [α]_D = +47.0 (*c* 1.35, CHCl₃); ν_{\max} (thin film): 2278 cm⁻¹; ¹H NMR (400 MHz, CDCl₃): 7.38-7.24 (15H, m, ArH), 4.71 (1H, d, *J*_{1,2} = 1.5 Hz, H-1), 4.84-4.74 (2H, m, CH₂Ph), 4.68 (2H, d, *J* = 10.5 Hz, CH₂Ph), 4.61 (2H, m, CH₂Ph), 3.81 (1H, dd, *J*_{2,3} = 3.0, *J*_{3,4} = 9.0 Hz, H-3), 3.80 (1H, dd, *J*_{1,2} = 1.5, *J*_{2,3} = 3.0 Hz, H-2), 3.77-3.74 (2H, m, H-4, H-5), 3.34 (3H, s, OMe), 2.73 (1H, dd, *J*_{5,6} = 3.0, *J*_{6a,6b} = 15.0 Hz, H-6_a), 2.49 (1H, m, H-6_b); ¹³C NMR (100 MHz, CDCl₃): 139.9, 138.7, 128.9, 128.7, 128.2 (ArC), 99.3 (C-1), 75.1 (CH₂Ph), 73.3 (CH₂Ph), 72.5 (CH₂Ph), 71.6 (CH₂Ph), 71.4 (C-3), 70.8 (C-2), 70.4 (C-4), 68.0 (C-5), 53.5 (OMe), 20.2 (C-6); MALDI-ToF *m/z* 496.47 [M+Na]⁺, 512.32 [M+K]⁺, calculated for C₂₉H₃₁NO₅Na 496.55 and C₂₉H₃₁NO₅K 512.66.

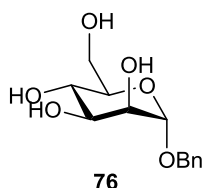
7.2.14 Methyl 2,3,4-tri-O-benzyl-6-deoxy- α -D-manno-heptopyranoside (**30**)¹⁸



7.2.14.1 Reduction of (**34**) with DIBAL-H

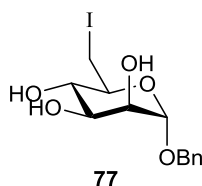
DIBAL-H (1 M in hexane, 0.91 ml, 0.91 mmol) was added dropwise to a solution of nitrile (**34**) (361 mg, 0.83 mmol) at -15°C ; after 30 minutes further DIBAL-H (0.26 ml, 0.26 mmol) was added and the reaction was terminated after 15 min by the addition of MeOH (0.75 ml) followed by aqueous 2 M HCl (0.75 ml). The mixture was stirred for 45 minutes and filtered and extracted with diethyl ether (5 ml). The organic layers were washed with 2M HCl (5 ml), sat. aq. NaHCO_3 solution (5 ml) and H_2O (5 ml), dried and concentrated *in vacuo*. Sodium borohydride (15 mg) was added to the resulting syrup dissolved in MeOH (5 ml) and the mixture was stirred for 30 min. Upon completion, TLC [Hex:EtOAc; 3:1], the reaction was quenched by the addition of acetone (5 ml) and concentrated *in vacuo*, the residual syrup was concentrated again (x3) with hot MeOH (5 ml) to remove borate impurities. The residue was dissolved in EtOAc (5 ml) and washed with 2 M HCl (5 ml); sat. aq. NaHCO_3 solution (5ml) and H_2O (5ml), dried over MgSO_4 and concentrated *in vacuo* to a syrup that was purified using flash chromatography [Hex:EtOAc; 2:1] to afford alcohol (**30**) as an oil, (220 mg, 0.46 mmol, 56%). $[\alpha]_{\text{D}} = +30.3$ (*c* 1.0 CHCl_3), Lit¹⁸ $[\alpha]_{\text{D}}$, + 31.0 (*c* 1.8, CHCl_3); ν_{max} (thinfilm) 3468 cm^{-1} (broad); $^1\text{H NMR}$ (400 MHz, CDCl_3): 7.47–7.23 (15H, m, ArH), 4.99–4.59 (6H, m, 3 x CH_2Ph), 4.66 (d, $J_{1,2} = 2.0$ Hz, H-1), 3.89 (1H, dd, $J_{2,3} = 3.5$, $J_{3,4} = 8.5$ Hz, H-3), 3.79 (1H, dd, $J_{1,2} = 2.0$, $J_{2,3} = 3.5$ Hz, H-2), 3.75–3.70 (4H, m, H-4, H-5, H-7_{a,b}), 3.31 (3H, s, OMe), 2.15–2.06 (1H, m, H-6_a), 1.89–1.80 (1H, m, H-6_b); $^{13}\text{C NMR}$ (100 MHz, CDCl_3): 138.7, 138.1, 128.4, 128.0, 127.8, 127.7 (ArC) 99.1, (C-1), 80.1 (C-3), 78.3 & 71.4 (C-4 & C-5), 75.3 (CH_2Ph), 74.6 (C-2), 72.1 (CH_2Ph), 61.2 (C-7), 54.8 (OMe), 33.8 (C-6); MALDI-ToF *m/z* 501.87 $[\text{M}+\text{Na}]^+$, 517.89 $[\text{M}+\text{K}]^+$; calculated for $\text{C}_{29}\text{H}_{34}\text{O}_6\text{Na}$ 501.56 and $\text{C}_{29}\text{H}_{34}\text{O}_6\text{K}$ 517.67.

7.2.15 Benzyl α -D-mannopyranoside (**76**)^{19, 20}



Acetyl chloride (20 ml, 0.28 mmol) was added drop-wise to a solution of D-mannose (**59**) (20 g, 110 mmol) in benzyl alcohol (100 ml) at 50°C under inert atmosphere. The solution was heated at 50°C for 1.5 hours and then stirred at room temperature for a further 15 hours. The product mixture was poured into ice/H₂O (500 ml) and extracted (3x) with EtOAc (100 ml), the organic layer was washed (3x) with H₂O (100 ml), dried and concentrated *in vacuo*. The resulting oil was recrystallized from Hex-EtOAc to afford benzyl- α -D-mannopyranoside (**76**) as a white solid (28.5 g, 96%): $[\alpha]_D = +84.3$ (*c* 1, MeOH), Lit = 85.1 (*c* 1, MeOH); ¹H (400 MHz, D₂O): 7.40-7.28 (5H, m, ArH), 4.85 (1H, d, $J_{1,2} = 2.0$ Hz, H-1), 4.67 (2H, AB_q, $J_{Ha,Hb} = 12.0$ Hz, CH₂Ph), 3.87 (1H, dd, $J_{5,6} = 2.0$ Hz, $J_{6a,6b} = 12.0$ Hz, H-6_a), 3.84 (1H, dd, $J_{1,2} = 2.0$ Hz, $J_{2,3} = 4.0$ Hz, H-2), 3.77-3.71 (2H, m, H-3, H-6_b), 3.65 (1H, t, $J_{3,4} = J_{4,5} = 9.0$ Hz, H-4), 3.62 (1H, m, H-5); ¹³C NMR (100 MHz, D₂O): 129.4, 129.2, 128.8 (ArC), 100.7 (C-1), 74.9 (C-4), 72.7 (C-3), 72.2 (C-2), 69.9 (CH₂Ph), 68.7 (C-5), 63.0 (C-6); MALDI-ToF *m/z* 293.13 [M+Na]⁺, 309.11 [M+K]⁺, calculated for C₁₃H₁₈O₆Na 293.27 and C₁₃H₁₈O₆K 309.38.

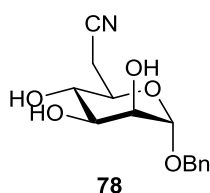
7.2.16 Benzyl 6-deoxy-6-iodo- α -D-mannopyranoside (**77**)¹⁹



To a solution of benzyl α -D-mannopyranoside (**76**) (2.0 g, 7.5 mmol) in dry THF (20 ml) was added triphenylphosphine (2.9 g, 11.3 mmol), imidazole (1.0 g, 15 mmol) and iodine (2.8 g, 11.3 mmol). The reaction was stirred under reflux conditions for 4 hours before the solvent was removed *in vacuo*. The resulting syrup was diluted with EtOAc (20 ml) and washed with 10% Na₂SO₃ solution (20 ml) and H₂O (20 ml), dried over MgSO₄ and concentrated. The resulting oil was purified using flash

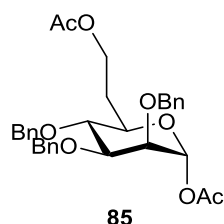
chromatography [DCM:MeOH; 10:1] to yield (**77**) as a white foam (2.4 g, 6.45 mmol, 86%). $\alpha_D = +63.6$ (*c* 1.0, CHCl₃); ¹H NMR (400 MHz, CDCl₃): 7.35-7.27 (5H, m, ArH), 4.93 (1H, d, $J_{1,2} = 1.5$ Hz, H-1), 4.67 (2H, AB_q, $J_{Ha,Hb} = 11.5$ Hz, CH₂Ph), 3.59-3.50 (4H, m, H-2, H-3, H-4, H-6_a), 3.84-3.80 (1H, m, H-6_b), 3.32 (1H, dd, $J_{4,5} = 10.0$ Hz, $J_{5,6} = 7.0$ Hz, H-5); ¹³C NMR (100 MHz, CDCl₃): 128.6, 128.4, 128.2 (ArC), 99.7 (C-1), 71.9, 71.6, 71.4 (C-2, C-3, C-4), 70.9 (C-5), 69.3 (CH₂Ph), 6.9 (C-6); MALDI-ToF *m/z* 402.97 [M+Na]⁺, 419.01 [M+K]⁺, calculated for C₁₃H₁₇IO₅Na 403.16 and C₁₃H₁₇IO₅K 419.27.

7.2.17 Benzyl 6-dexoy- α -D-manno-heptopyranosylurononitrile (**78**)



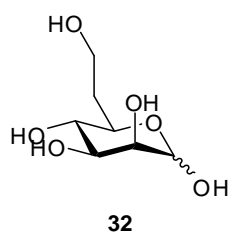
To a stirred solution of iodide (**77**) (100 mg, 0.26 mmol) in 50:50 MeCN:H₂O (5 ml) was added KCN (50 mg, 0.78 mmol). The reaction mixture was left to stir for 16 hours at room temperature. The solvent was removed *in vacuo* and the aqueous solution was washed with EtOAc (3 x 10 ml); the combined organic layers were then washed with 1M HCl (10 ml) and H₂O (10 ml), dried over MgSO₄ and concentrated. Nitrile (**78**) (70 mg) was afforded in quantitative yield after being passed through a 3 cm bed of silica gel [DCM:MeOH; 10:1]. $\alpha_D = +79.5$ (*c* 0.5, CHCl₃); ¹H NMR (400 MHz, CDCl₃): 7.35 – 7.26 (5H, m, ArH), 4.86 (1H, d, $J_{1,2} = 1.5$ Hz, H-1), 4.60 CH₂Ph (2H, AB_q, $J_{Ha,Hb} = 12.0$ Hz, CH₂Ph) 3.94, (1H, dd, $J_{1,2} = 1.5$ Hz, $J_{2,3} = 3.0$ Hz, H-2), 3.80 (1H, dd, $J_{2,3} = 3.0$ Hz, $J_{3,4} = 9.0$ Hz, H-3), 3.75 (1H, m, H-5), 3.64 (1H, t, $J_{3,4} = J_{4,5} = 9.0$ Hz, H-4), 2.75 – 2.65 (2H, m, H_{6a,b}); ¹³C NMR (100 MHz, CDCl₃): 128.6, 128.2, 128.1 (ArC), 99.3 (C-1), 71.5 (C-3), 70.8 (C-2), 70.0 (C-4), 69.7 (CH₂Ph), 97.6 (C-5), 20.7 (C-6); MALDI-ToF *m/z* 302.16 [M+Na]⁺, 318.17 [M+K]⁺, calculated for C₁₄H₁₇NO₅Na 302.28 and C₁₄H₁₇NO₅K 318.39.

7.2.18 1,7-Di-O-acetyl-2,3,4-tri-O-benzyl-6-deoxy- α -D-manno-heptopyranoside¹⁸ (85**)**



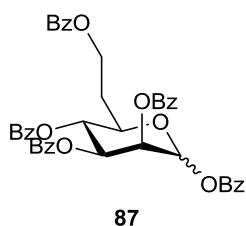
Benzylated 6-deoxy-heptose (**30**) (200 mg, 0.42 mmol) was dissolved in Ac₂O:AcOH (1:1, 10 mL) at 0°C and catalytic H₂SO₄ was added dropwise, eliciting a colour change. The reaction was stirred for 30 minutes and then neutralised using solid NaHCO₃, the resulting suspension was added to a conical flask containing H₂O and ice (25 mL) and left stirring overnight. The product was extracted using DCM (15 mL) and washed with 1 M HCl (10 mL), sat. aq. NaHCO₃ solution (10 mL) and H₂O (10 mL), dried and concentrated *in vacuo*. The resulting syrup was purified using flash chromatography [Hex:EtOAc; 2:1] to afford protected di-acetate (**85**) (115 mg, 0.21 mmol, 65%). $[\alpha]_D = 37.4$ (c 1.0, CHCl₃); ¹H NMR (400 MHz, CDCl₃) 7.42-7.37 (15H, m, ArH), 6.11 (1H, d, $J_{1,2} = 2.0$ Hz, H-1), 4.79-4.63 (4H, m, 2 x CH₂Ph), 4.58 (2H, s, CH₂Ph), 4.18-4.09 (1H, m, H-7_a), 4.108-4.09 (1H, m, H-7_b), 3.82 (1H, dd, $J_{2,3} = 3.0$, $J_{3,4} = 9.0$ Hz, H-3), 3.77-3.75 (3H, m, H-2, H-4 & H-5), 2.23-2.15 (1H, m, H-6_a), 2.02 (3H, s, OAc), 2.00 (3H, s, OAc), 1.91-1.83 (1H, m, H-6_b); ¹³C NMR (100 MHz, CDCl₃): 170.8 (C=O), 168.7 (C=O), 138.1, 138.0, 128.5, 128.4, 128.2 (ArC), 91.7 (C-1), 79.4 (C-3), 77.8, 72.2 & 70.9 (C-2, C-4, C-5), 75.5 (CH₂PH), 73.5 (CH₂Ph), 72.6 (CH₂Ph), 60.9 (C-7), 30.7 (C-6), 21.1 (2 x OAc); MALDI-ToF m/z 572.05 [M+Na]⁺, 588.10 [M+K]⁺, calculated for C₃₂H₃₆O₈Na 571.61 and C₃₂H₃₆O₈K 587.72.

7.2.19 6-deoxy-D-manno-heptopyranose (**32**)^{21, 22}



Protected 6-deoxy-heptose (**85**) (354 mg, 0.65 mmol) was dissolved in EtOAc:EtOH [3:2, 5 ml] at room temperature and catalytic 10% Pd/C was added. The solution was degassed under vacuum and H₂ was added using a gas bladder, this was repeated 3 times to ensure saturation with H₂. The reaction was heated to 40°C and left stirring overnight. The catalyst was removed via filtration and the solvents were removed *in vacuo*. The product (157 mg, 0.56 mmol, 87%) was used without further purification. The crude triol (**86**) (157 mg, 0.56 mmol) was deacetylated using the standard deprotection **7.1.1** to afford 6-deoxy-manno-heptose (**32**) as a white amorphous solid as an anomeric mixture in the α : β ratio 2.5:1 (101 mg, 0.52 mmol, 87%). ¹H NMR (400 MHz, CD₃OD): 5.00 (1H, d, $J_{1,2} = 2.0$ Hz, H-1 _{α}), 4.71 (1H, d, $J_{1,2} = 1.0$ Hz, H-1 _{β}), 3.89-3.66 (5H, m, H-2, H-3, H-5, H-7_{a+b}), 3.45 (1H, t, $J_{3,4} = J_{4,5} = 9.5$ Hz, H-4), 2.18-2.04 (1H, m, H-6_a), 1.74-1.66 (1H, m, H-6_b); ¹³C NMR (100 MHz, CD₃OD) 95.9 (C-1), 73.2 (C-2), 72.8 (C-4), 72.2 (C-3), 70.6 (C-5), 59.8 (C-7), 35.8 (C-6); HR ESI-MS m/z 217.0688 [M+Na]⁺, calculated for C₇H₁₄O₆Na 217.0692

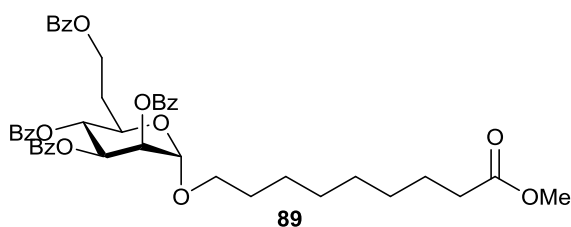
7.2.20 1,2,3,4,7-Penta-O-benzoyl-6-deoxy-D-manno-heptopyranoside (**87**)



To a stirred solution of 6-deoxy-heptose (**32**) (100 mg, 0.52 mmol) in anhydrous pyridine (2 ml) benzoyl chloride (0.315 ml, 3.64 mmol) was added dropwise at 0°C and the reaction mixture was allowed to reach room temperature and left stirring overnight. After careful addition of H₂O (1 ml), the solvent was removed *in vacuo* and the residue was dissolved in DCM (5 ml), washed with 1M HCl (5 ml), NaHCO₃ aq. sat. solution (5 ml) and H₂O (5 ml), dried over MgSO₄ and concentrated *in vacuo*. The product was purified using flash chromatography [Hex:EtOAc; 5:2] to

afford protected 6-deoxy-heptose (**87**) as a colourless oil (315 mg, 0.44 mmol, 84%, α/β ratio 2:1). ^1H NMR (400 MHz, CDCl_3): 8.13-7.28 (25H, m, ArH), 6.57 (d, $J_{1,2} = 2.0$ Hz, H-1 $_{\alpha}$), 6.36 (d, $J_{1,2} = 1.5$ Hz, H-1 $_{\beta}$), 6.01 (1H, dd, $J_{1,2} = 2.5$, $J_{2,3} = 10.0$ Hz, H-2), 5.90-5.85 (2H, m, H-3 & H-4), 4.54-4.48 (2H, m, H-5 & H-7 $_{\text{a}}$), 4.22-4.19 (1H, m, H-7 $_{\text{b}}$), 2.21-2.16 (2H, m, H-6 $_{\text{a+b}}$); ^{13}C NMR (100 MHz, CDCl_3): 168.1, 167.8 (C=O), 134.2, 130.4, 129.7, 128.0, 127.8 (ArC), 91.2 (C-1), 69.8 (C-3), 69.7 (C-4), 69.4 (C-2, C-5), 60.2 (C-7) 30.7 (C-6); HR ESI-MS $[\text{M}+\text{Na}]^+$ 737.1944, calculated for $\text{C}_{45}\text{H}_{48}\text{O}_{12}\text{Na}$ 737.1999.

7.2.21 8-(methoxycarbonyl)octyl 2,3,4,7-tetra-O-benzoyl- α -D-mannoheptopyranoside (**89**)

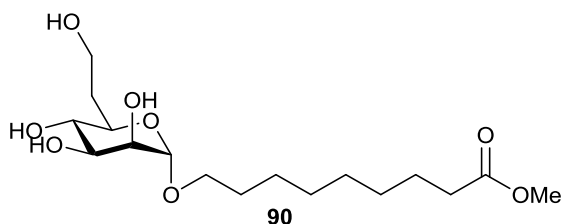


To a solution of benzoylated 6-deoxy-heptose (**87**) (200 mg, 0.30 mmol) in absolute DCM (4 ml) was added HBr/AcOH (4 ml of a 33% w/v solⁿ in AcOH, 1.64 mmol HBr) and the reaction mixture was stirred at 0°C for 3 hours. Upon completion of the reaction TLC [Hex:EtOAc; 5:1] the mixture was poured into ice water (10 ml) and extracted twice with DCM (2 x 10 ml). The crude bromide (**88**) (147 mg, 73%) was used without further purification. MALDI-ToF m/z $[\text{M}+\text{Na}]^+$ 673.04, $[\text{M}+\text{K}]^+$ 689.09 calculated for $\text{C}_{33}\text{H}_{29}\text{BrO}_9\text{Na}$ 672.47, $\text{C}_{33}\text{H}_{29}\text{BrO}_9\text{K}$ 688.58

A solution of mercury bromide (10 mg, 0.03 mmol), mercury cyanide (70 mg, 0.26 mmol), 8-methoxycarbonyl octanol (**58**) (45 mg, 0.24 mmol) and 4Å molecular sieves (75 mg) in dry DCE (2.5 ml) was stirred at room temperature for 30 minutes. Bromide (**88**) (150 mg, 0.22 mmol) in dry DCE (0.5 ml) was added dropwise and the reaction was left at room temperature and monitored by TLC [Hex:EtOAc, 5:3]. After 48 hours, the reaction was shown to be complete, the solution was filtered and solvent was removed *in vacuo*. The resulting syrup was diluted with EtOAc (5 ml) and washed with KBr (5 ml), H_2O (3 x 5 ml) and dried over MgSO_4 . Flash chromatography [Hex:EtOAc; 5:2] afforded the protected alkyl 6-deoxy-manno-

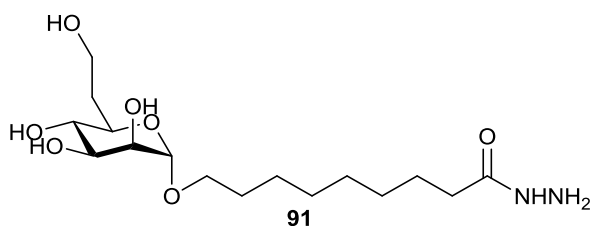
heptopyranoside (**89**) (160 mg, 0.20 mmol, 59%) as a colourless oil. $[\alpha]_D = +21.9$ (c 1, CHCl_3); $^1\text{H NMR}$ (400 MHz, CDCl_3): 8.11-7.33 (20H, m, ArH), 5.89 (1H, dd, $J_{2,3} = 3.5$, $J_{3,4} = 10.0$ Hz, H-3), 5.76 (1H, at, $J_{3,4} = J_{4,5} = 10.0$ Hz, H-4), 5.66 (1H, dd, $J_{1,2} = 2.0$, $J_{2,3} = 3.5$ Hz, H-2), 5.02 (1H, d, $J_{1,2} = 2.0$ Hz, H-1), 4.55-4.49 (2H, m, H-7_{ab}), 4.34-4.28 (1H, m, H-5), 3.75-3.69 (1H, m, Spacer- CH_2O), 3.67 (3H, s, OMe), 3.50-3.43 (1H, m, Spacer- CH_2O), 2.35 (2H, t, $J = 7.7$ Hz, CH_2COOMe), 2.25-2.18, (1H, m, H-6_a), 2.17-2.09 (1H, m, H-6_b), 1.67-1.52 (4H, m, 2 x CH_2), 1.35-1.19 (8H, m, 4 x CH_2); $^{13}\text{C NMR}$ (100 MHz, CDCl_3): 168.3 (CH_2COOMe), 167.9 (C=O), 133.3, 132.8, 130.0, 129.8, 128.4, 128.1 (ArC), 97.4 (C-1, $^1J_{\text{C}_1, \text{H}_1} = 172.6$ Hz), 70.7 (C-2), 70.5 (C-4), 69.5 (C-3), 68.3 (Spacer- CH_2O), 66.9 (C-5), 60.7 (C-7), 51.4 (OMe), 34.3 (CH_2COOMe), 30.7 (C-6), 29.4, 26.4, 25.0 (CH_2); HR ESI-MS m/z 803.3028 $[\text{M}+\text{H}]^+$, calculated for $\text{C}_{45}\text{H}_{48}\text{O}_{12}$ 803.3043.

7.2.22 8-(Methoxycarbonyl)octyl- α -D-6-deoxy-manno-heptopyranoside (**90**)



Protected alkyl mannoside (**89**) (100 mg, 0.13 mmol) was debenzoylated using the standard deprotection procedure outlined in general methods 7.1.1. The resulting oil was passed through a bed of silica gel [CHCl_3 :MeOH, 9:1] to afford alkyl 6-deoxy-mannoheptoside (**90**) as an amorphous white solid (36 mg, 0.10 mmol, 77%). $[\alpha]_D = +2.2$ ($c = 1.0$, MeOH); $^1\text{H NMR}$ (400 MHz, CD_3OD): 4.57 (1H, d, $J = 1.5$ Hz, H-1), 3.70-3.59 (5H, m, H-2, H-3, H-7_a, Spacer- CH_2O), 3.55 (3H, s, OMe), 3.49 (1H, at, $J_{3,4} = J_{4,5} = 8.5$ Hz, H-4), 3.36-3.26 (2H, m, H-5, H-7_b), 2.22 (2H, t, $J = 7.5$ Hz, CH_2OOMe), 2.04-1.97 (1H, m, H-6_a), 1.61-1.57 (1H, m, H-6_b), 1.52-1.45 (4H, m, 2x CH_2), 1.27-1.20 (8H, m, 4x CH_2); $^{13}\text{C NMR}$ (100 MHz, CD_3OD): 101.5 (C-1), 72.7 (C-3), 72.4 (C-5), 72.3 (C-2), 70.9 (C-4), 68.5 (Spacer- CH_2O), 60.1 (C-7), 52.03 (OMe), 35.6 (C-6), 34.8 (CH_2COOMe), 30.6, 30.4, 30.3, 30.1, 27.3, 26.0 (6x CH_2); HR ESI-MS m/z 387.1987 $[\text{M}+\text{Na}]^+$, calculated for $\text{C}_{17}\text{H}_{32}\text{O}_8\text{Na}$ 387.1995.

7.2.23 8-(Hydrazinocarbonyl)octyl- α -D-6-deoxy-manno-heptopyranoside (**91**)



Alkyl mannoside (**90**) (20 mg, 0.05 mmol) was treated with hydrazine monohydrate (1 ml) in EtOH (2.5 ml) at 55°C for 6 hours to afford the hydrazide hapten (**92**) in quantitative yield. The product (**91**) was cleaned up by co-evaporation of excess reagent with toluene (3 x 10 ml) and ^1H NMR analysis confirmed complete conversion by loss of the singlet at δ 3.55 ppm (OMe) in the ^1H NMR spectra.

7.2.24 Expression of Tet-Hc Fragment in *E. coli*

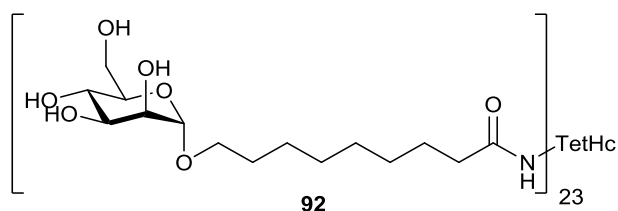
4 x 1 litre of Luria-Bertani (LB) broth containing kanamycin (50 $\mu\text{g ml}^{-1}$) were inoculated with 1 ml of an overnight culture of *E. Coli* BL21 cells transformed with pSK1-Tet-Hc. At an $\text{OD}_{650} = 0.8$ (approx.), expression of CRM mutant Tet-Hc protein was induced by the addition of IPTG to a final concentration of 1 mM. The cells were transferred to a 16°C incubator; after 16 h the cells were harvested by centrifugation (7,500 *rcf*) for 7 min; and frozen at -80 °C until required. To purify the His-tagged proteins, cell pellets were thawed and resuspended in lysis buffer [50 ml of 20 mM HEPES, 150 mM NaCl, pH 7.5, 1 x complete protease inhibitor tablet (Roche), 0.1 mg/ml lysosyme, 0.02 mg/mL DNase]. Cells were lysed using a cell disrupter (Constant Systems, UK, one shot mode, 25 kpsi) and the cell debris was removed by centrifugation (30,000 *rcf*) for 20 min.

The protein was purified using an ÄKTA Xpress FPLC system (GE Healthcare); the supernatant was passed through a HiTrap Ni-IMAC column [5 ml, GE Healthcare), washed with wash buffer (50 mM Tris-HCl pH 8.0, 0.5M NaCl, 30 mM imidazole (BioUltra)] until UV absorption was stable with 5 mAU over 3 mins, then eluted using elution buffer [50 mM Tris-HCl pH 8.0, 0.5 M NaCl, 0.5 M imidazole]. The protein was further purified by GPC on a Superdex S75 XK26/60 column using elution buffer [50 mM HEPES, 100 mM NaC, pH 7.5] at a flow rate of 3.2 ml/min. The peak over 100 mAU with a slope steeper than 100 mAU/min was collected automatically. Further purification was achieved using a Superdex 200 (GE Healthcare) gel

filtration column; using GF buffer [20 mM HEPES, 150 mM NaCl, pH 7.5] at a flow rate of 3.2 ml/min. The protein containing peak was collected automatically and the resulting solution was dialysed (Snake Skin; 10 MWCO; Fisher Scientific) into ammonium bicarbonate buffer [100 mM pH 8.0] and lyophilized to give TetHc at a concentration of 55 mg/ml of cell culture.

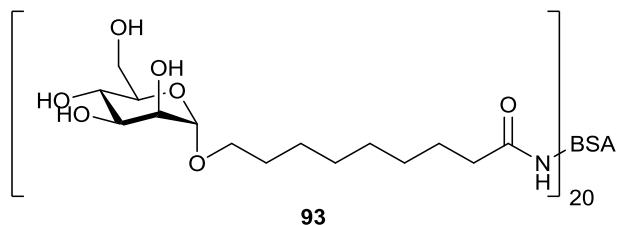
The quality of the protein was analysed on coomassie stained (Instant Blue Expedeon) SDS-PAGE (Section 2.3.1, Figure 2.4) (RunBlue 4-20% SDS Gel, Expedeon) and MALDI-TOF (Section 2.3.1, Figure 2.5) MS 53.8 kDa, calculated 51.7 kDa for TetHc fragment.

7.2.25 Mannose (TetHc) Conjugate (92)



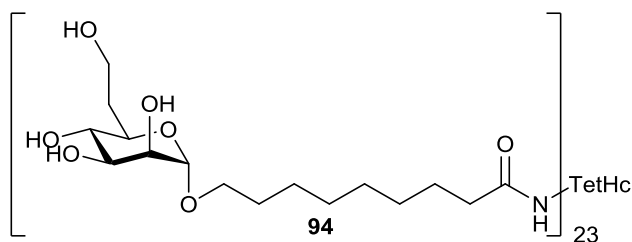
Hydrazide (**64**) (5 mg) was conjugated to Tet-Hc carrier protein (8 mg) according to general method **7.1.2**. The prepared antigen (**92**) (9 mg) was analysed using MALDI-TOF (61.3 kDa) and SDS-PAGE gel which gave an estimate of 23 D-mannose hapten molecules per protein. $[(61.3 \text{ kDa} - 53.6 \text{ kDa})/334 = 23]$ Western blot analysis of the glycoprotein was done according to standard procedure **7.1.3**, the blot membrane was visualised using Alexa 633 labelled Con A (1 in 5,000) and imaged using a FLA7000 phosphoimager (Fuji).

7.2.26 Mannose (BSA) Conjugate (93)



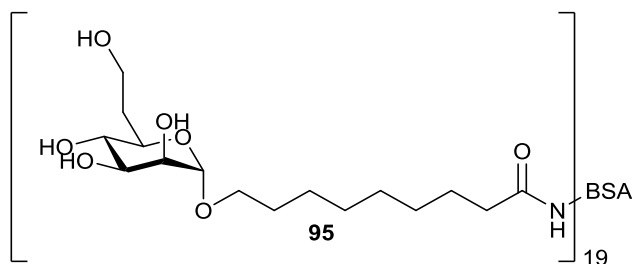
Hydrazide (**64**) (6 mg) was conjugated to BSA carrier protein (10 mg) according to general method **7.1.3**. The prepared antigen (**93**) (9 mg) was analysed using MALDI-TOF (73.4 kDa) and SDS-PAGE gel analysis which gave an estimate of 20 hapten molecules per protein. $[(73.4 \text{ kDa} - 66.5 \text{ kDa})/334 = 20]$

7.2.27 Mannoheptose (TetHc) Conjugate (94)



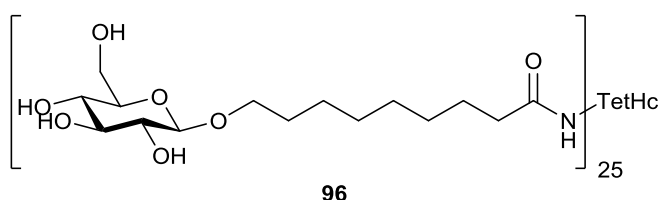
Hydrazide (**91**) (5 mg) was conjugated to TetHc carrier protein (9 mg) according to general method **7.1.3**. The prepared antigen (**94**) (8 mg) was analysed using MALDI-TOF [61.1 kD]; SDS-PAGE gel analysis, which gave an estimate of 22 hapten molecules per protein. $[(61.5 - 53.6)/348 = 23]$

7.2.28 Mannoheptose (BSA) Conjugate (95)



Hydrazide (**91**) (5 mg) was conjugated to BSA carrier protein (9 mg) according to general method **7.1.3**. The prepared antigen (**95**) (11 mg) was analysed using MALDI-TOF [73.2 kD]; SDS-PAGE gel analysis, which gave an estimate of 18 hapten molecules per protein. $[(73.2 \text{ kDa} - 66.5 \text{ kDa})/348 = 19]$

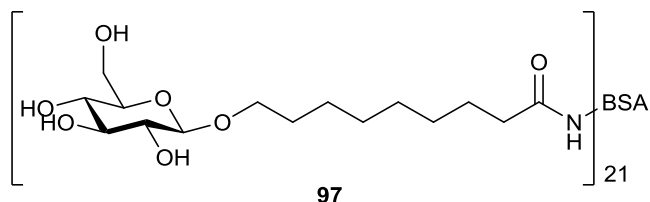
7.2.29 Glucose (TetHc) Conjugate (96)



Hydrazide (**69**) (13 mg) was conjugated to TetHc carrier protein (20 mg) according to general method **7.1.3**. The prepared antigen (**96**) (19 mg) was analysed using

MALDI-TOF [ca. 61.8 kDa]; SDS-PAGE gel analysis, which gave an estimate of 24 hapten molecules per protein. $[(62.2 \text{ kDa} - 53.6 \text{ kDa})/334 = 25]$

7.2.30 Glucose-BSA Glycoconjugate (97)



Hydrazide (**69**) (8 mg) was conjugated to BSA carrier protein (15 mg) according to general method **7.1.3**. The prepared antigen (**77**) (13 mg) was analysed using MALDI-TOF [ca. 73.4 kDa]; SDS-PAGE gel analysis, which gave an estimate of 20 hapten molecules per protein. $[(73.4 \text{ kDa} - 66.5 \text{ kDa})/334 = 21]$

7.3 Chapter 3 Experimental

7.3.1 *B. thailandensis* E555 $\Delta wbiI$ capsular polysaccharide (104) extraction and purification

A 10 ml starter culture of *Burkholderia thailandensis* E555 (*wbiI* pKNOCK KmR mutant) was incubated overnight at 37°C in LB-Lennox (LB-L; 1 litre containing 10 g tryptone, 5g yeast extract and 5g NaCl in 1 litre). LB-L media (4 x 1 litre) in 2 litre baffled flasks was inoculated with the starter culture and the flasks were placed in a shaking incubator for 16 hours at 37°C. The cells were pelleted (10 minutes at 7,500 *rcf*) and resuspended in MQ-H₂O (100 ml). The cell suspension was added to 90% aqueous phenol (100 ml) and heated to 80°C with gentle stirring. After 30 minutes the slurry was allowed to cool and extensively dialysed against MQ-H₂O (Spectra/Por[®] 6-8K MWCO dialysis tubing, flat width 100mm). After 8 changes of MQ-H₂O (5 litre) the insoluble material was collected by centrifugation (10 minutes at 7,5000 *rcf*) and the supernatant was lyophilised. The crude preparation (780 mg) was solubilised in 10 mM Tris-HCl [1 mM MgCl₂; 1 mM CaCl₂; pH 7.5] to an approximate concentration of 30 mg/ml. Both RNase and DNase (50 µg/ml) were added and the solution was incubated at 37°C for 3 hours with gentle shaking. After which, Proteinase K (50 µg/ml) was added and the mixture was incubated overnight in a heating block at 60°C. Centrifugation of the mixture (10 minutes @ 8,000 *rcf*) afforded three layers, insoluble material which was discarded, the supernatant and a white waxy substance. Both the supernatant and the white layer were combined and underwent ultracentrifugation (3 x 2 hrs at 100,00 *rcf*), with the supernatant being replaced with MQ-H₂O each time. After ultracentrifugation, the white sediment was collected and lyophilised to afford a white powder (635 mg). ¹H NMR (400 MHz, D₂O) diagnostic peaks only: 2.03 (1H, m, H-6_a), 1.99 (3H, s, OAc), 1.59 (1H, m, H-6_b).

7.3.1.1 Removal of lipid contaminants

The crude CPS preparation was solubilised in aqueous acetic acid (2% AcOH) at an approximate concentration of 5 mg/ml and heated at 100°C for 4 hours in a sealed glass reaction vial. After cooling the mixture was clarified using centrifugation (40 min, @ 8,000 *rcf*) and the supernatant was lyophilised to afford a white powder (365 mg).

The hydrosylate (30 mg) was solubilised in MQ-H₂O (2 ml) and loaded onto a Sephadex G-50 gel permeation chromatography column (GPC) (XK26/40 Phenomenex) and eluted using MQ-H₂O (0.25 ml/min). Fractions (4 ml) were collected and assayed using a high-throughput phenol-sulphuric acid method as described in Section 7.1.8. The carbohydrate containing fractions were pooled and lyophilised to afford Bth-CPS (5 mg). ¹H NMR (400 MHz, D₂O): 5.17 (H-2), 4.80 (H-1), 3.86 (H-3), 3.63 (H-7_{a,b}), 3.65 (H-4, H-5), 2.03 (H-6_a), 2.00 (OAc), 1.58 (H-6_b); ¹³C NMR (100 MHz, D₂O): 173.4 (C=O), 96.0 (C-1), 78.7 (C-3), 72.5 (C-5), 69.3 (C-2), 68.8 (C-4), 57.7 (C-7), 33.4 (C-6) 20.1 (OAc).

7.3.2 Partial acid hydrolysis of Bth-CPS⁴

A solution of Bth-CPS (**104**) (1 mg) in 0.75 M H₂SO₄ (2 ml) was heated at 85°C for 1 h in a sealed screw cap glass reaction vial. After cooling the reaction was neutralised by the addition BaCO₃ (30 mg) in MQ-H₂O (2 ml). The insoluble BaSO₄ was removed by centrifugation (5 min at 14,000 *rcf*) and the solution was clarified using a 0.45 µm filter and lyophilised.

7.3.3 APTS labelling of oligosaccharides²³

The partially hydrolysed oligosaccharide fragments of CPS isolated from *B. thailandensis* E555 $\Delta wbiI$ were labelled with APTS (**105**) for analysis by capillary electrophoresis. The crude oligosaccharide preparation (1 mg) was dissolved in AcOH (5 µl, 30%), NaBH₃CN (0.5 mg, 8 µmol) and APTS (0.5 mg, 1 µmol) were added to the reaction, which was incubated at 37°C for 18 hours. The sample was loaded onto a 30% mono:bis (38:2) acrylamide Tris-borate [100 mM, pH 8.2] gel and labelled oligosaccharides were separated by electrophoresis (400 V, Tris-borate 100 mM, pH 8.2), (**Figure 7.2**).

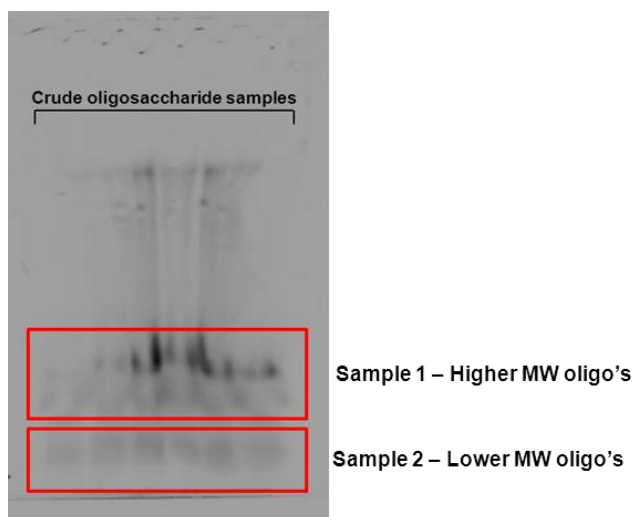


Figure 7.2: Fluorescence image of Tris-borate gel of APTS labelled oligosaccharides of CPS

The bands highlighted by the two red boxes were excised from the gel and the APTS labelled oligosaccharides extracted into MQ-H₂O (1 ml) by means of a bead mill (Thermo[®], Fast Prep FP 120). The gel impurities were removed by centrifugation (10 min at 14,000 rcf) and residual borate buffer was removed through co-evaporation with methanol (x3) at elevated temperature to afford APTS labelled oligosaccharides.

7.3.4 Capillary electrophoresis²³

APTS labelled oligosaccharides were injected (0.5 psi, 20 s) onto an N-CHO capillary (Beckman Coulter) in a PA800 Proteome Lab[®] System (Beckman Coulter[®]). Separation in running buffer [25 mM LiOAc, 0.4% polyethylene oxide, pH 4.75] was achieved at 30 kV for 20 min. Laser-induced fluorescence (LIF) (excitation 488 nm, detection 520 nm) was used for the detection of the APTS labelled oligosaccharides.

7.3.5 Deacylation of APTS labelled oligosaccharides²⁴

The partially acetylated APTS labelled oligosaccharides (above) were fully deacylated by means of hydrazine monohydrate, the protocol was adapted from Takasu *et al.*²⁴ To the crude oligosaccharide preparation (100 µl) was added hydrazine monohydrate (100 µl) in methanol (500 µl). The reaction mixture was heated to 40°C for 3 hours, after cooling the hydrazine was quenched by addition of

acetone (500 μ l) and the solvents were removed (x3) by SpeedVac[®] evaporative centrifugation (Thermo[®]). The samples were then re-submitted for CE analysis using protocol **7.3.4**.

7.4 Chapter 4 Experimental

7.4.1 Antibody Generation

Each Tet-Hc antigen sample (2.5 mg) was submitted to Ig-innovations for antibody generation in sheep. Initial immunisations were done with an emulsion comprised of antigen (0.5 mg), Freund's Complete Adjuvant and saline. Each animal was injected at 6 sites. Re-immunisations with an emulsion of antigen (0.25 mg), Freund's Incomplete Adjuvant and saline were administered at weeks 4, 8, 12, 16, 20, 24 & 28. Blood samples were taken at weeks 0, 6, 10, 14, 18.

Coagulation of the blood samples was induced and the blood was incubated at 37°C for 40 minutes. At which point the clot was collected by centrifugation and the isolated sera was stored at -20°C for use in immunological assessments.

7.4.2 ELISA protocols

All reagents including anti-sheep IgG (whole molecule)-alkaline phosphatase and anti-mouse IgG (whole molecule)-alkaline phosphatase secondary antibodies were ordered from Sigma Chemical. Costar high binding polystyrene 96 well plates were used for all ELISAs with BSA glycoconjugate antigens. (Pierce) Thermo Scientific streptavidin coated 96-well plates coated with SuperBlock were used for all ELISAs with biotin-CPS (124). Absorbance readings were done on a FLUOstar Omega (BMG labtech) plate reader in absorbance mode at a wavelength of 405_{nm}. All dilutions were made in PBS_T unless otherwise stated. Each sample was run in triplicate, with the average result and standard error used for data analysis. For details of the individual ELISAs please refer to the appropriate section in the results and discussion Section 4.2. Controls with no 1^o or 2^o secondary antibody and analyte were performed for each experiment and were within the experimental error for each ELISA experiment

7.4.2.1 Standard ELISA general protocol

- The plate was coated with target antigen(s) at 50 µg/ml (100 µl each well) and incubated for 2 h at room temperature.
- The plate was washed 3 times with PBS_T (PBS with 0.1% Tween 20).

- The plate was blocked with 5% w/v BSA in PBS_T (200 µl each well) and incubated for 1 h at room temperature
- Serial dilutions of combined sample serum* (1 in 100, 1 in 200, 1 in 400, 1 in 800, 1 in 1600, 1 in 3200, 1 in 6400, 1 in 12800 & 1 in 25600) were prepared in PBS_T.
- The plate was washed 3 times with PBS_T
- Serum serial dilutions were loaded onto the plate (100 µl each well) in triplicate and incubated at 37°C for 1 h.
- The plate was washed 3 times with PBS_T
- Secondary antibody (anti-sheep IgG-alkaline phosphatase) in PBS_T at 1 in 30,000 dilution was loaded (100 µl each well) and incubated at 37°C for 1 h.
- The plate was washed 3 times with PBS_T
- Phosphatase substrate (5 mg/ml) in alkaline phosphatase buffer [100 mM Tris-HCl, 100 mM NaCl, 50 mM MgCl₂, 1% Tween 20] was loaded (100 µl each well) into each well and incubated at 37°C for 25 min.
- Plates were read on plate reader (405_{nm})

* An ELISA was run on individual sheep sera samples and was shown to be analogous to that of the combined sera results (Appendix 8.5) and as such all ELISAs were run on the combined sera.

7.4.2.2 Competition ELISA general protocol

- The plate was coated with target antigen(s) at 50 µg/ml (100 µl each well) and incubated for 2 h at room temperature.
- The plate was washed 3 times with PBS_T
- The plate was blocked with 5% w/v BSA in PBS_T (200 µl each well) and incubated for 1 h at room temperature.
- Serial dilutions of the target analyte in PBS_T were prepared, mixed 50:50 with 1 in 800 dilution of target serum in PBS_T and incubated at 37°C for 30 min.
- The plate was washed 3 times with PBS_T
- Serum:analyte mix was loaded onto plate (100 µl each well) and incubated at 37°C for 1 h
- The plate was washed 3 times with PBS_T
- Secondary antibody (anti-sheep IgG-alkaline phosphatase) in PBS_T at 1 in 30,000 dilution was loaded (100 µl each well) and incubated at 37°C for 1 h.
- The plate was washed 3 times with PBS_T

- Phosphatase substrate (5 mg/ml) in alkaline phosphatase buffer [100 mM Tris-HCl, 100 mM NaCl, 50 mM MgCl₂, 1% Tween 20] was loaded (100 µl each well) into each well and incubated at 37°C for 25 min.
- Plates were read on plate reader (405_{nm})

7.4.2.3 Biotin CPS ELISA on streptavidin plate general protocol

- Streptavidin 96 well plates (Pierce) were coated with biotin labelled CPS (**124**) at 2 µg/ml in PBS_T (100 µl) and incubated at room temperature for 30 min.
- Serial dilutions of antibody in PBS_T were loaded onto the plate (100 µl) and incubated at 37°C for 1 h. **For competition ELISAs the analyte:mAb dilutions were pre-incubated as previously described.**
- The plate was washed 3 times with PBS_T
- Secondary antibody (anti-sheep IgG-alkaline phosphatase) in PBS_T at 1 in 30,000 dilution was loaded (100 µl each well) and incubated at 37°C for 1 h.
- The plate was washed 3 times with PBS_T
- Phosphatase substrate (5 mg/ml) in alkaline phosphatase buffer [100 mM Tris-HCl, 100 mM NaCl, 50 mM MgCl₂, 1% Tween 20] was loaded (100 µl each well) into each well and incubated at 37°C for 25 min.
- Plates were read on plate reader (405_{nm})

7.4.3 Slot-blot analysis of polyclonal sera

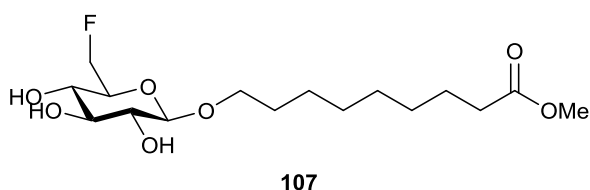
Slot-blot analysis was conducted using a Hoefer PR600 24-slot-blot apparatus with PVDF blotting membrane cut to 3.8 x 11 cm (Immobilon, Millipore). A biometra mini vacuum pump was used as the vacuum source.

- The blotting membrane was soaked in MeOH for 1 min, then transferred to blotting buffer (PBS_T) for 2 min.
- The blot apparatus was assembled with the pre-wet membrane and the target antigen (50µg/ml) was loaded into the slots (150 µl).
- Vacuum (350 mBar) was applied for two minutes to load the antigen onto the membrane.
- After the samples were loaded the vacuum was released and 1 ml of PBS_T was loaded into each slot.
- Vacuum was reapplied (750 mBar) and a further 1 ml of PBS_T was added to wash the membrane.
- The blot was removed and blocked in 5% BSA for 2 h at room temperature.

- The blot was washed in PBS_T 3 x 5 min
- The blots were incubated with respective sample serum (Glc-TetHc & Glc-BSA; 1 in 1600 dilution) for 1 h at 37°C.
- The blot was washed in PBS_T 3 x 5 min
- Incubation with the anti-sheep IgG-alkaline phosphatase secondary antibody was done at 37°C for 1 h.
- The blot was washed in PBS_T 3 x 5 min
- Visualisation of the blot was achieved using the insoluble BCIP/NBT substrate reagent system (Promega) for 45 min at 37°C. An image of the blot was taken and the picture was analysed using ImageJ gel analysis software²⁵.

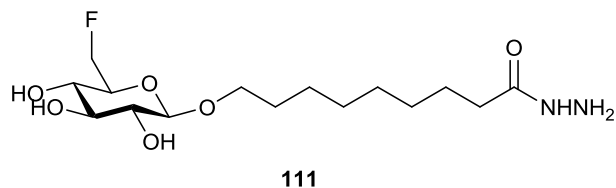
7.4.4 Synthesis of 6-deoxy-6-fluoro glucose hapten

7.4.4.1 8-(Methoxycarbonyl)octyl-6-deoxy-6-fluoro-β-D-glucopyranoside (107)



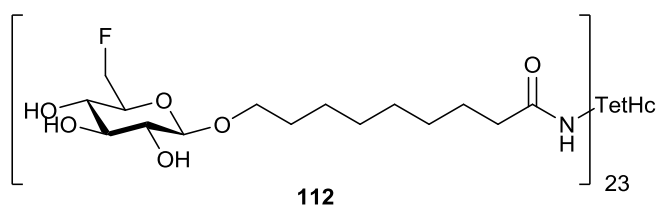
8-(Methoxycarbonyl)octyl-β-D-glucopyranoside (**68**) (36 mg; 0.11 mmol) was suspended in anhydrous DCM (2.5 mL) and cooled to -40°C. DAST (84 μl, 0.66 mmol) was added drop-wise and the reaction mixture was allowed to warm to room temperature and left stirring for 1 hour. Upon completion, TLC [DCM:MeOH, 9:1], the solution was cooled to -10°C and the reaction was quenched with MeOH (5 mL) and then the solvents were removed *in vacuo*. 6-Deoxy-6-fluoro glycoside (**107**) was isolated using flash chromatography [DCM:MeOH, 13:1] (rf 0.45) (14 mg, 0.04 mmol, 36%). $[\alpha]_D = -1.81$ (*c* 1, MeOH); ¹⁹F NMR (CD₃OD): ϕ -235.4 (s); ¹H NMR (400 MHz, CD₃OD): 4.74-4.67 (1H, m, H-6_a), 4.62-4.55 (1H, m, H-6_b), 4.28 (1H, d, $J_{1,2} = 8.0$ Hz, H-1), 3.96-3.86 (1H, m, CH_{2a}), 3.67 (3H, s, OMe), 3.57-3.34 (5H, m, H-2, H-3, H-4, H-5 & CH_{2b}), 2.30 (2H, t, $J = 7.5$ Hz, CH₂COOMe), 1.68-1.55 (4H, m, 2 x CH₂), 1.38 – 1.24 (8H, m, 4 x CH₂); ¹³C NMR (100MHz, CD₃OD): 176.9 (C=O), 102.5 (C-1), 82.2 (d, $J_{6,F} = 170$ Hz, C-6), 76.4 (C-3), 74.5 (d, $J_{5,F} = 16$ Hz, C-5), 73.5 (C-2), 70.3 (CH₂O), 69.1 (d, $J_{4,F} = 7.6$ Hz, C-4), 51.5 (OMe), 34.1 (CH₂COOMe), 29.5 – 24.9 (6 x CH₂); MALDI-ToF *m/z* 374.31 [M+Na]⁺, 390.32 [M+K]⁺, calculated for C₁₆H₂₉FO₇Na 375.18 and C₁₆H₂₉FO₇K 391.15

7.4.4.2 8-(Hydrazinocarbonyl)octyl-6-deoxy-6-fluoro- β -D-glucopyranoside (111)



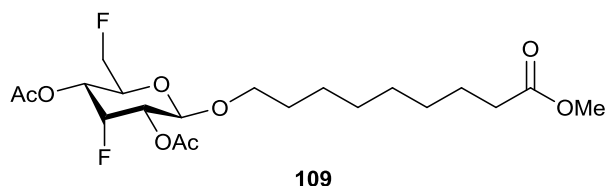
6-Deoxy-6-fluoro glucoside (**107**) (5 mg, 0.015 mmol) was treated with hydrazine monohydrate (0.5 ml) in EtOH (1 ml) at 55°C for 6 hours to afford 6-deoxy-6-fluoro hydrazide hapten (**111**) in quantitative yield. The product was cleaned up by co-evaporation with toluene (3 x 5 ml) and NMR analysis showed successful conversion to the hydrazide by loss of the singlet at δ 3.67 ppm (OMe) in the ^1H NMR spectrum.

7.4.4.3 6-Deoxy-6-fluoro Conjugate (6D6FGlc-TetHc) (112)



Hydrazide (**111**) (5 mg) was conjugated to TetHc carrier protein (8 mg) according to general method **7.1.2**. The prepared antigen (**112**) (5 mg) was analysed using MALDI-ToF MS 61.5 kDa and SDS-PAGE gel electrophoresis to give an estimate of 23 hapten molecules per protein. $[(61.5 - 53.9)/336 = 23]$

7.4.4.4 8-(methoxycarbonyloctyl) 2,4-di-O-acetyl-3,6-di-deoxy-3,6-di-fluoro-β-D-allopyranoside (109)

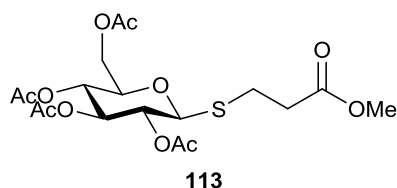


8-Methoxycarbonyloctyl-β-D-glucopyranoside (**107**) (36 mg; 0.11 mmol) was suspended in anhydrous DCM (2.5 mL) and cooled to -40°C. DAST (84 μl, 0.66 mmol) was added drop-wise and the reaction was allowed to warm to room temperature and left stirring for 1 hour. Upon completion, TLC [DCM:MeOH, 9:1], the solution was cooled to -10°C and quenched using MeOH (5 mL) and then the solvents were removed *in vacuo*. 3,6-di-deoxy-3,6-di-fluoro glycoside (**108**) was isolated using flash chromatography [DCM:MeOH, 13:1] (rf 0.4).

The difluoride was acetylated with Ac₂O (1 mL) and catalytic DMAP in anhydrous pyridine (5 mL). The reaction was left stirring overnight (ca. 16 h) and the solvents were removed *in vacuo*. The resulting residue was diluted in DCM (5 mL) and washed with 1M HCl (5 mL), sat. aq. NaHCO₃ solution (5 mL) and H₂O (5 mL), dried and concentrated *in vacuo*. Flash chromatography was performed [Hex:EtOAc, 5:3] to afford acetylated difluoride (**109**) as a pale yellow oil (11 mg, 0.03 mmol, 21%). ¹H decoupled ¹⁹F NMR φ -215.6 (F-3), -235.4 (s, F-6); ¹H NMR (400 MHz, CDCl₃): 5.13 (1H, dt, $J_{2,3} = J_{3,4} = 3.5$ Hz, $J_{3,3F} = 55.5$ Hz, H-3), 4.89 (1H, ddd, $J_{3,4} = 3.5$ Hz, $J_{4,5} = 10.0$ Hz, $J_{4,3F} = 27.0$ Hz, H-4), 4.81 (1H, d, $J_{1,2} = 7.5$ Hz, H-1), 4.84-4.74 (1H, m, H-2), 4.59 (1H, ddd, $J_{5-6a} = 3.0$ Hz, $J_{6a,6b} = 10.0$ Hz, $J_{6a,6F} = 22.0$ Hz, H-6_a), 4.48 (1H, ddd, $J_{5-6b} = 3.0$ Hz, $J_{6a,6b} = 10.0$ Hz, $J_{6b,6F} = 22.0$ Hz, H-6_b), 4.14-4.02 (1H, ddq, $J_{5,6a/b} = 3.0$ Hz, $J_{4,5} = 10.0$ Hz, $J_{5,6F} = 24.0$ Hz, H-5), 3.93-3.86 (1H, m, CH₂O), 3.67 (3H, s, OMe), 3.54-3.47 (1H, m, CH₂O), 2.30 (1H, t, $J = 7.5$ Hz, CH₂COOMe), 2.13 (6H, s, 2 x OAc), 1.67-1.55 (4H, m, 2 x CH₂), 1.33-1.26 (8H, m, 4 x CH₂); ¹³C NMR (100 MHz, CDCl₃): 176.3 (C=O), 98.3 (C-1), 88.1 ($J_{3,3F} = 181.5$, C-3), 81.6 (d, $J_{6,6F} = 179.0$ Hz, C-6), 70.4 (d, $J_{5,6F} = 4.0$ Hz, C-5), 70.2 (CH₂O), 70.0 (d, $J_{2,3F} = 17.0$ Hz, C-2), 67.7 (dd, $J_{4,6F} = 8.0$ Hz, $J_{3F,4} = 17.0$ Hz, C-4), 51.5 (OMe), 34.1 (CH₂COOMe), 29.7 – 24.9 (6 x CH₂), 20.7 (2 x OAc); MALDI-ToF m/z 442.05 [M+Na]⁺, calculated for C₂₀H₃₂FO₈Na 442.20.

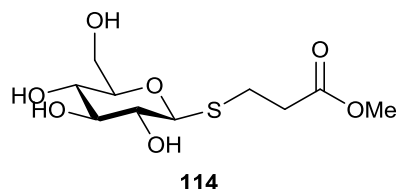
7.4.5 Synthesis of Short Linker Haptens

7.4.5.1 Methyl 3-(2,3,4,6-tetra-O-acetyl- β -D-glucopyranosylthio)propanoate (113)²⁶



Per-O-acetylated D-glucose (**65**) (1.0 g, 2.56 mmol) was dissolved in dry DCM (20 ml), methyl 3-mercapto propanoate (1.2 ml, 10.3 mmol) and $\text{BF}_3 \cdot \text{OEt}_2$ (475 μL , 3.9 mmol) were added at 0°C. The reaction mixture was allowed to warm to room temperature and left stirring overnight until the reaction was shown to be complete, TLC [Hex:EtOAc, 2:1]. The solution was washed with sat. aq. NaCHO_3 solution (3 x 20ml) and H_2O (20 ml) and then dried over MgSO_4 and concentrated *in vacuo*. The resulting syrup was isolated by flash chromatography [Hex: EtOAc, 3:1], the fractions were collated and solvents removed *in vacuo* to afford thioglycoside (**113**) as a white foam (450 mg, 1.00 mmol, 39%). $[\alpha]_{\text{D}} = -53.1$ (*c* 1.0, CHCl_3), Lit²⁶ $[\alpha]_{\text{D}} = -32.0$ (*c* 0.26, CHCl_3); $^1\text{H NMR}$ (400 MHz, CDCl_3): 5.24 (1H, m, H-2), 5.13-5.01 (2H, m, H-3, H-4), 4.56 (1H, d, $J_{1,2} = 10.0$ Hz, H-1), 4.25-4.22 (1H, m, H-6_a), 4.20-4.10 (1H, m, H-6_b), 3.78 -3.69 (4H, m, H-5, OMe), 2.99 (1H, dt, $J = 4.0$ Hz, $J = 11.5$ Hz, CH_{2a}), 2.89 (1H, dt, $J = 2.0$, $J = 12.0$ Hz, CH_{2b}), 2.69 (2H, t, $J = 7.0$ Hz, SCH_2), 2.09 (3H, s, OAc), 2.06 (3H, s, OAc), 2.03 (3H, s, OAc), 2.01 (3H, s, OAc); $^{13}\text{C NMR}$ (100 MHz, CDCl_3): 172.0, 170.5, 170.0, 169.3 (C=O), 83.8 (C-1), 75.8 (C-5), 73.7 (C-2), 69.7, 69.4 (C-3 & C-4), 61.9 (C-6), 51.7 (OMe), 35.3 (SCH_2), 25.3 (CH_2), 20.6, 20.5 (4 x OAc); MALDI-ToF m/z 472.95 $[\text{M}+\text{Na}]^+$, 488.99 $[\text{M}+\text{K}]^+$, calculated for $\text{C}_{18}\text{H}_{26}\text{O}_{11}\text{SNa}$ 473.12 and $\text{C}_{18}\text{H}_{26}\text{O}_{11}\text{SK}$ 489.08.

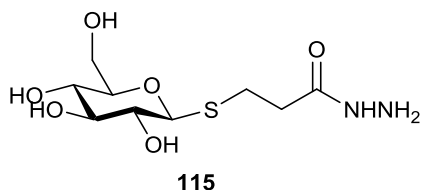
7.4.5.2 Methyl 3-(β -D-glucopyranosylthio)propanoate (114)²⁶



Protected thioglycoside (**113**) (450 mg, 1.00 mmol) underwent Zemplén deacetylation as described in general procedure **7.1.1** to afford deprotected thioglycoside (**114**) as

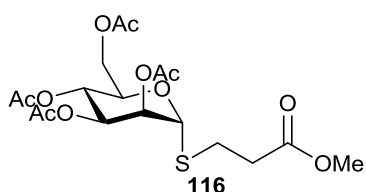
colourless oil (240 mg, 0.85 mmol, 92%). $[\alpha]_D = -52.3$ (c 1.0, MeOH), Lit²⁶ $[\alpha]_D = -74.0$ (c 0.19, H₂O); ¹H NMR (400 MHz, CD₃OD): 4.42 (1H, d, $J_{1,2} = 10.0$ Hz, H-1), 3.87 (1H, dd, $J_{5,6} = 2.5$ Hz, $J_{6a,6b} = 11.5$ Hz, H-6_a), 3.70 (3H, s, OMe), 3.69-3.65 (1H, m, H-6_b), 3.44-3.31 (3H, m, H-3, H-4 & H-5), 3.21 (1H, pt, $J_{1,2} = J_{2,3} = 10.0$ Hz), 3.05-2.97 (1H, quintet, CH_{2a}), 2.95 – 2.87 (1H, m, CH_{2b}), 2.74 (2H, t, $J = 7.0$ Hz, SCH₂); ¹³C NMR (100MHz, CD₃OD): 173.7 (C=O), 87.8 (C-1), 82.0, 79.5, 79.2, (C-3, C-4 & C-5), 71.5 (C-2), 63.0 (C-6), 52.3 (OMe), 36.3 (SCH₂), 29.1 (CH₂); MALDI-ToF m/z 305.37 [M+Na]⁺, 321.22 [M+K]⁺, calculated for C₁₀H₁₈O₇SNa 305.07 and C₁₀H₁₈O₇SK 321.04

7.4.5.3 β -D-(Glucopyranosylthio)propanoic acid hydrazide (**115**)



(**114**) (10 mg, 0.03 mmol) was treated with hydrazine monohydrate (1 ml) in EtOH (2.5 ml) at 55°C for 6 hours afforded the hydrazide (**115**) in quantitative yield. The product was cleaned up by co-evaporation with toluene (3 x 10 ml) and NMR analysis showed successful conversion by loss of the singlet at δ 3.70 ppm (OMe) in the ¹H NMR spectra.

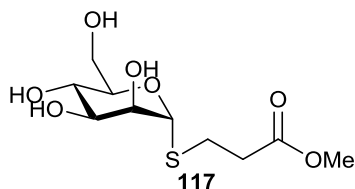
7.4.5.4 Methyl 3-(2,3,4,6-tetra-O-acetyl- α -D-mannopyranosylthio)propanoate (**116**)



Peracetylated D-mannose (**60**) (670 mg, 1.71 mmol) was dissolved in dry DCM (20 ml), methyl 3-mercapto propanoate (840 μ l, 6.93 mmol) and BF₃.OEt₂ (270 μ L, 2.57 mmol) were added at 0°C. The reaction was allowed to warm to room temperature

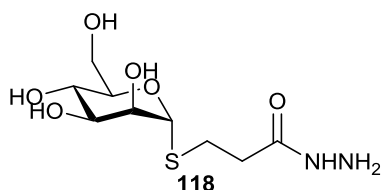
and left stirring overnight (ca. 16h) until the reaction was shown to be complete, TLC [Hex:EtOAc, 2:1]. The solution was washed with sat. aq. NaCHO₃ solution (3 x 20ml) and H₂O (20 ml) and then dried over MgSO₄ and concentrated *in vacuo*. The resulting syrup was isolated by flash chromatography [Hex: EtOAc, 3:1], the fractions were collated and solvents removed *in vacuo* to afford thiomannoside (**116**) as a colourless oil (350 mg, 0.77 mmol, 51%). $[\alpha]_D = +48.4$ (c 1.0, CHCl₃); ¹H NMR (400 MHz, CDCl₃): 5.33 (1H, d, $J_{1,2} = 1.5$ Hz, H-1), 5.31 (1H, dd, $J_{1,2} = 1.5$ Hz, $J_{2,3} = 3.0$ Hz, H-2), 5.29 (1H, t, $J_{3,4} = J_{4,5} = 9.5$ Hz), 5.21 (1H, dd, $J_{2,3} = 3.0$ Hz, $J_{3,4} = 9.5$ Hz, H-3), 4.40-4.36 (1H, m, H-5), 4.30 (1H, dd, $J_{5,6a} = 6.0$ Hz, $J_{6a,6b} = 12.0$ Hz, H-6_a), 4.13 (1H, dd, $J_{5,6b} = 2.0$ Hz, $J_{6a,6b} = 12.0$ Hz, H-6_b), 3.71 (3H, s, OMe), 2.94-2.86 (2H, m, CH₂), 2.71 (2H, t, $J = 7.0$, SCH₂), 2.17 (3H, s, OAc), 2.11 (3H, s, OAc), 2.06 (3H, s, OAc), 1.99 (3H, s, OAc); ¹³C NMR (100 MHz, CDCl₃): 172.4, 170.5, 169.3 (C=O), 82.8 (C-1), 70.7 (C-2), 69.3 (C-5), 69.8 (C-3), 68.6 (C-4), 62.2 (C-6), 51.6 (OMe), 34.6 (SCH₂), 26.4 (CH₂), 20.6, 20.4, 20.3 (4 x OAc); MALDI-ToF m/z 473.58 [M+Na]⁺, 489.51 [M+K]⁺, calculated for C₁₈H₂₆O₁₁SNa 473.12 and C₁₈H₂₆O₁₁SK 489.08.

7.4.5.5 Methyl 3-(α -D-mannopyranosylthio)propanoate (**117**)



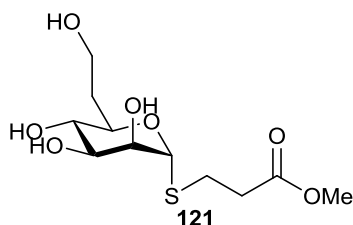
Protected thiomannoside (**116**) (350 mg, 0.77 mmol) underwent Zemplén deacylation as described in general procedure **7.4.1** to afford deprotected thiomannoside (**117**) as colourless oil (1.95 mg, 0.96mmol, 96%). $[\alpha]_D = +61.3$ (c 0.8, MeOH); ¹H NMR (400 MHz, CD₃OD): 5.30 (1H, d, $J_{1,2} = 1.5$ Hz, H-1), 3.91-3.89 (2H, m, H-2, H-3), 3.85 (1H, dd, $J_{5,6a} = 3.0$ Hz, $J_{6a,6b} = 12.0$ Hz, H-6_a), 3.75-3.72 (2H, m, H-6_b), 3.70 (3H, s, OMe), 3.66-3.62 (2H, m, H-4, H-5), 2.95-2.83 (2H, m, CH₂), 2.73 (2H, t, $J = 7.0$ Hz, SCH₂); ¹³C NMR (100MHz, CD₃OD): 172.8 (C=O), 86.7 (C-1), 75.0 (C-2), 73.6 (C-4), 73.2 (C-3), 73.1 (C-5), 63.1 (C-6), 52.3 (OMe), 35.6 (SCH₂), 27.2 (CH₂); MALDI-ToF m/z 305.75 [M+Na]⁺, 321.72 [M+K]⁺, calculated for C₁₀H₁₈O₇SNa 305.07 and C₁₀H₁₈O₇SK 321.04

7.4.5.6 α -D-(Mannopyranosylthio)propanoic acid hydrazide (**118**)



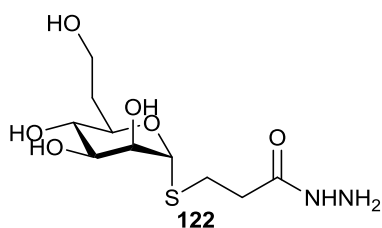
117 (10 mg, 0.03 mmol) was treated with hydrazine monohydrate (1 ml) in EtOH (2.5 ml) at 55°C for 6 hours afforded the hydrazide (**118**) in quantitative yield. The product was cleaned up by co-evaporation with toluene (3 x 10 ml) and NMR analysis showed successful conversion by loss of the singlet at δ 3.70 ppm (OMe) in the ^1H NMR spectra.

7.4.5.7 Methyl 3-(α -D-mannoheptopyranosylthio)propanoate (**121**)



Protected thiomannoheptoside (**120**) was provided by G. Pergolizzi (Field Lab) (450 mg, 0.97 mmol) underwent Zemplén deacylation as described in general procedure **7.1.1** to afford deprotected thiomannoside (**121**) as colourless oil (260 mg, 0.89, 92%). $[\alpha]_{\text{D}} = +170.0$ (c 1.0, CHCl_3); ^1H NMR (400MHz, CD_3OD): 5.19 (1H, d, $J_{1,2} = 1.5$ Hz, H-1), 3.96 (1H, dd, $J_{1,2} = 1.5$ Hz, $J_{2,3} = 3.0$ Hz, H-2), 3.91 (1H, td, $J_{5,6} = 3.0$ Hz, $J_{4,5} = 10.0$ Hz, H-5), 3.72-3.64 (3H, m, H-3, H-7_{ab}), 3.65 (3H, s, OMe), 3.46 (1H, t, $J_{3,4} = J_{4,5} = 10.0$ Hz, H-4), 2.86-2.82 (2H, m, CH_2), 2.69 (2H, t, $J = 7.0$ Hz, SCH_2), 2.04-2.01 (1H, m, H-6_a), 1.66-1.63 (1H, m, H-6_b); ^{13}C NMR (100MHz, MeOD): 175.1 (C=O), 84.70 (C-1, $J_{\text{H1-C1}} = 170.32$ Hz), 71.99 (C-2), 71.6 (C-3), 70.7 (C-4), 69.9 (C-5), 58.2 (C-7), 52.3 (OMe), 34.8 (SCH_2), 33.2 (C-6), 25.6 (CH_2); MALDI-ToF m/z 296.38 $[\text{M}+\text{Na}]^+$, 315.81 $[\text{M}+\text{K}]^+$, calculated for $\text{C}_{11}\text{H}_{20}\text{O}_7\text{SNa}$ 316.08 and $\text{C}_{11}\text{H}_{20}\text{O}_7\text{SK}$ 335.06

7.4.5.8 α -D-Mannoheptopyranosylthio)propanoic acid hydrazide (**122**)



(**121**) (10 mg, 0.03 mmol) was treated with hydrazine monohydrate (1 ml) in EtOH (2.5 ml) at 55°C for 6 hours afforded the hydrazide (**122**) in quantitative yield. The product was cleaned up by co-evaporation with toluene (3 x 10 ml) and NMR analysis showed successful conversion by loss of the singlet at δ 3.65 ppm (OMe) in the ^1H NMR spectra.

7.4.6 Conjugation CPS to cBSA²⁷

Sodium *meta*-periodate (6 mg, 0.3 mmol) and CPS (5 mg) was dissolved in PBS (1 ml) and the reaction mixture was left at room temperature for 1 hour. Excess sodium *meta*-periodate was removed using a PD-10 desalting column (GE Healthcare), equilibrated with PBS. The oxidised CPS was added to a solution of cBSA (Pierce) at 5mg/ml (1 ml) in PBS. 20 μl of NaBH_3CN [1 M in 10 mM NaOH] was added to the solution and it was left for four days at room temperature in the dark. 20 μl of NaBH_4 [1 M NaBH_4 in 10 mM NaOH] was added, after agitation the reaction was left for 40 min. The solution was diluted in MQ- H_2O and extensively dialysed (Snakeskin 10,000 MWCO, Pierce) against MQ- H_2O (x 5) and lyophilised to afford crude conjugate (9 mg).

The crude preparation was run on an SDS-PAGE gel according to general protocol **7.1.4**. Following SDS-PAGE analysis the CPS-cBSA conjugate was purified on an AKTA Xpress FPLC purification system. The conjugate solution (500 μl at 12 mg/ml) was injected onto a Superdex S200 HR (GE Healthcare) XK 26/60 column (Phenomenex) and eluted using elution buffer [50 mM HEPES, 150 mM NaCl, pH 7.5] at 1ml/min. All fractions (1 ml) were collected and analysed for carbohydrate using the phenol:sulphuric acid assay (**7.3.5**). A selection of carbohydrate active fractions (A4, A8, A12, A15, B12, B8, B4 & C7) were analysed by SDS-PAGE gel (**7.1.4**) and western blot (**7.1.5**).

7.4.7 The biotinylation of Bth-CPS

Bth-CPS (**104**) (2 mg) was dissolved in coupling buffer (1 ml) [0.1 M sodium acetate, pH 5.5] and cooled to 0°C, sodium *meta*-periodate solution (1 ml) [20 mM in coupling buffer] was added and the solution was left in the dark at 4°C. After 30 min glycerol, to a final concentration of 15 mM and the reaction mixture was left for 10 min at 4°C to quench the NaIO₄. A PD-10 column pre-equilibrated with coupling buffer was used to remove the impurities. The oxidised Bth-CPS (**104**) was collected and treated with EZ-link Hydrazide-PEG₄-Biotin (Pierce, Thermo Fisher), in DMSO, to a final solution of 5 mM and was left stirring at room temperature for 2 hours. Again the impurities were removed through the use of a PD-10 desalting column. The resulting solution was lyophilized to afford a white solid (**124**) (ca. 2 mg).

Biotinylated Bth-CPS (**124**) (2 mg) was dissolved in MQ-H₂O (20 mL of PBS_T) and spotted (3x10 µl) onto a streptavidin labelled microscope slide (Xenopore[®]) and left for 10 mins. The excess liquid was pipetted off and the slide was washed with PBS_T (x3), after which the slide was soaked in primary anti-CPS-antibody (1 in 3200 dilution in PBS_T) for 1 hour at 37°C. After extensive washing with PBS_T (x3) the slide was then soaked in the secondary antibody (Alexa 566 labelled anti-mouse antibody, Invitrogen, 1 in 30,000 dilution in PBS_T) for another hour at 37°C. The slide was washed thoroughly with PBS (x5) before it was imaged on a fluorescence scanner (FLA-7000, Fuji).

7.4.8 Octet analysis

All Octet analysis was conducted using an Octet Red (ForteBio) system using Dip and Read Streptavidin coated Biosensors (ForteBio; 18-5019). The Biosensors were first dipped into 1 x Kinetics buffer (ForteBio) in PBS for 5 min prior to the experiment. An equilibration step of 60 seconds was run (baseline), after which the streptavidin biosensors were dipped into 200 µl of biotinylated CPS at 10 µg/ml (loading step) for 400 seconds. A second baseline stabilisation step was done in fresh Kinetics buffer (60 seconds) before the biosensors were dipped into the target antibody solution (mAb 4IVH12 and Hep-TetHc sera 0 & 18W) at decreasing nM concentrations (see Section 4.5.1 and 4.5.2). The association step was carried out for 900 seconds before the biosensors were moved to Kinetics buffer for 1200 seconds to allow dissociation of the antibody to occur (Figure 7.3). Analysis of the

binding curves was carried out using Octet analysis software (ForteBio) using a 1:1 binding mode.

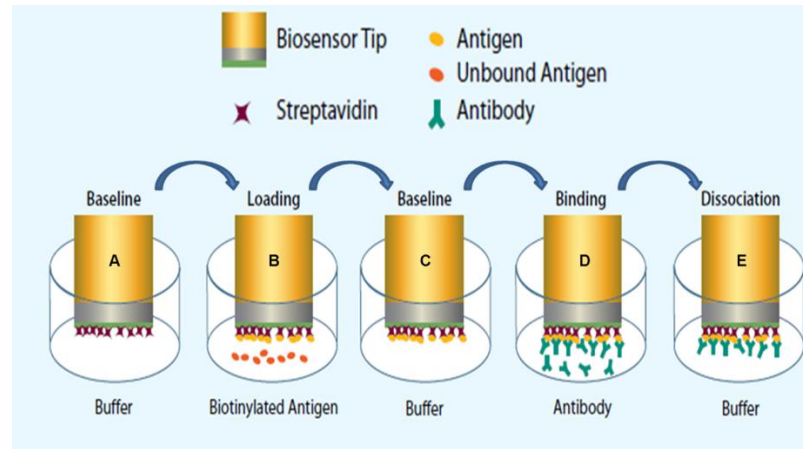


Figure 7.3; Schematic representation of the octet experiment for mAb 4IVH12. Workflow: A) Initial baseline for biosensor stabilisation (60 seconds); B) loading of biotinylated CPS (400 Seconds); C) baseline stabilisation (60 seconds); D) binding of antibodies to immobilised CPS (900 Seconds); E) dissociation of antibodies (1200 seconds). Image adapted from ForteBio Octet Brochure²⁸

7.5 Chapter 5 Experimental

7.5.1 General methods

7.5.1.1 Nucleic Acid Agarose Gels

0.8% agarose solution in TBE buffer [100 mM Tris-HCl; 90 mM boric acid; 10 mM EDTA] was poured into gel mould supplemented with 50 µl of ethidium bromide and left to set at 4°C. Samples (5 µl) were loaded in DNA loading buffer (5 µl; New England Biolabs) and gels were run at 90 V for 60 mins.

7.5.1.2 VLP Agarose Gels

1.2 % agarose solution in TBE buffer [100 mM Tris-HCl; 90 mM boric acid; 10 mM EDTA] was poured into gel mould and left to set at 4°C. Samples (20 µl) were loaded in DNA loading buffer (5 µl; New England Biolabs) and gels were run at 60 V for 120 mins.

7.5.1.3 Coomassie staining of agarose gels

Agarose gels were transferred to coomassie staining solution [1 g Coomassie R250; 100 ml AcOH; 400 ml MeOH; 500 ml MQ-H₂O] and incubated overnight. The stain solution was poured off and the gel was rinsed (x2) with MQ-H₂O. The excess stain was removed using de-stain solution [20% MeOH; 10% AcOH; 70% MQ-H₂O] (5 x 2 hours washes) and finally with MQ-H₂O (2 x 1 hour washes).

7.5.1.4 Silver staining of agarose gels

Silver staining of agarose gels was done according to the method described by Prieto and co-workers in 1997.²⁹ After electrophoresis the gels was immersed 10% AcOH solution for 10 minutes at room temperature. The gels were washed with MQ-H₂O (x2) to remove excess fix solution and the gel was stained using 20 mM AgNO₃ at 40°C for 20 minutes. The gel was extensively washed with MQ-H₂O (x 10) and developing solution [3% NaOH, 1 ml/l of 37% formaldehyde] until bands were visible.

7.5.1.5 Ethidium bromide staining of agarose gels

Gels were submerged in ethidium bromide stain (10 mg/ml) for 30 minutes and then washed with MQ-H₂O (x1) and visualised with a Syngene G:Box transilluminator.

7.5.1.6 Enhanced chemiluminescence of western blot

Enhanced chemiluminescence was carried out using ECL-Plus Western Blotting Detection Kit as per manufacturer's instructions. Blots were visualised using an ImageQuant LAS 500 scanner (GE Healthcare) or by UV film detection with the assistance of Aadil El-Turabi (iQur)

7.5.1.7 Transmission Electron Microscopy

All TEM was performed with the assistance of H. Peyret (Lomonossoff Lab, JIC) on a FEI Tecnai20 microscope, at 200 kV and imaged with an AMT digital camera. VLP particles were deposited onto TEM grids (Pd/Cu with plastic/carbon coating) and stained with 2% uranyl acetate³⁰ and imaged using TEM

7.5.2 Cloning of t-HBcAg D3K6D3 and wt-HBcAg D3K6D3

7.5.2.1 Restriction Digest

The optimised pEAQ-HT-t-HBcAg-EL and pEAQ-HT-t-HBcAg plasmids were kindly donated by the Lomonossoff group (JIC). Restriction digests of the plasmids were carried out using Sall and AseI (New England Biolabs) as per the manufacturer's instructions.

Reaction (37°C for 60 mins):

- 9µl MQ-H₂O
- 4 µl of buffer (NEB buffer 3) [100 mM NaCl; 50 mM Tris-HCl; 10 mM MgCl₂; 1 mM DTT; pH 7.9
- 0.2 µl BSA (x 100)
- 1 µl Ase I
- 1 µl Sal I
- 5 µl of plasmid (1 µg) in elution buffer (Qiagen Mini-prep kit) [10 mM Tris-HCl; pH 8.5]

- X μ l of insert (0.23 μ l for pEAQ-HT-t-HBcAg or 0.49 μ l of pEAQ-HT-wt-HBcAg)
- 2 μ l of 10 x T4 DNA ligase reaction buffer (NEB) [50 mM Tris-HCl; 10 mM MgCl₂; 1 mM ATP; 10 mM DTT; pH 7.5°C]
- 1 μ l of T4 DNA polymerase enzyme
- 9 – X μ l of MQ-H₂O

A control reaction was carried out with no insert in order to assess the levels of self-ligation.

7.5.2.3 Transformation of plasmids into *E. coli*

The ligation reactions were transformed into chemically competent *E. coli* cells (One shot Top10 *E. coli* cells; Invitrogen) by heat shock.

Reaction

- 1 μ l of ligated plasmid
- 25 μ l of SOC media

The samples were cooled on ice for 30 mins and then subjected to heat shock treatment 42°C for 30 seconds before recovery on ice (10 mins). 200 μ l of LB was added to the cells which were immediately plated out onto agar for Kanamycin resistance and incubated at 37°C overnight. Individual colonies were grown up in LB (10 ml) with kanamycin and single successful cultures were stored at -80°C in 40% (v/v) glycerol for long term storage.

7.5.2.4 Colony PCR of plasmids

Successful single colonies (7 from each plasmid) were picked and subjected to colony PCR and reactions (5 μ l) were run on a 0.8% agarose gel to demonstrate successful cloning of the D3K6D3 encoding plasmids (Figure 7.6)

Reactions

- 10 µl of GoTaq green
- 0.5 µl of C¹ primer (specific for the CPMV UTR region of the pEAQ cassette)
- 0.5 µl of C³ primer (specific for the CPMV UTR region of the pEAQ cassette)
- 9 µl of nuclease free H₂O
- Colony prick

PCR Cycle

- 95°C 2 mins (denature)
- [95°C 30 seconds (denature); 63°C 45 seconds (anneal); 72° 130 seconds (extension)] x 29
- 72° 300 seconds (final extension)
- 4°C rest

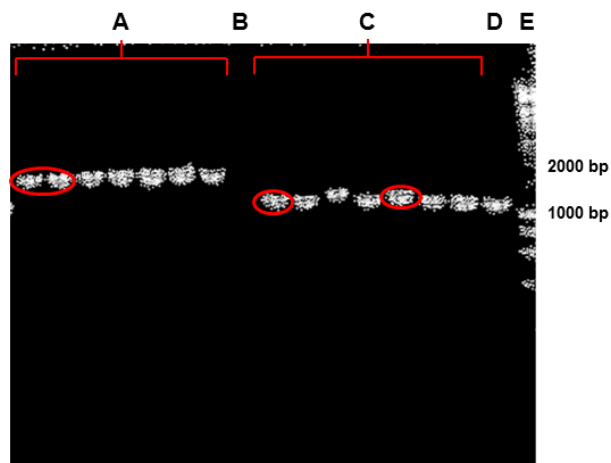


Figure 7.6: Agarose gel (0.8%) of colony PCR reactions. Lanes: A) pEAQ-HT-t-HBcAg D3K6D3 samples; B) -ve control; C) pEAQ-HT-wt-HBc-Ag D3K6D3 samples; D) re-ligation control pEAQ-HT-wt-HBcAg; E) Ladder (Hyperladder 1; Bioline. The pEAQ-HT-t-HBcAg D3K6D3 samples gave rise to bands around 2000 bp corresponding to 1835 bp and the pEAQ-Ht-wt-HBcAg D3K6D3 plasmid gave rise to bands around 1000 bp corresponding to 1288 bp, indicating successful cloning of the D3K6D3 constructs.

Selected colonies (highlighted with red circles) were grown up in LB media (10 mL) overnight at 37°C to select for kanamycin resistance. The plasmids were extracted with a Miniprep kit (Qiagen) and sent to Genome Enterprise Limited for sequencing.

7.5.3 Transformation of D3K6D3 plasmids into *Agrobacterium tumifaciens*

Agrobacterium tumifaciens LBA4404 cells (50 µl, OD₆₀₀ = 0.6) were transformed the plasmid pEAQ-HT-wt-HBcAg D3K6D3 and pEAQ-HT-t-HBcAg D3K6D3 (50 µg) by electroporation (2.5 kV, 1 second). The cells were transferred into SOC media (200 µl) to recover for 2.5 hours at 28°C. Cells (150 µl) were then plated on agarose containing 50 µl/ml kanamycin and rifampicin and incubated at 27°C for 3 days. Colony PCR was performed as before (section 7.5.1.4) (3 samples for each construct) and reactions (5 µl) were run on at 0.8% agarose gel (Figure 7.7).

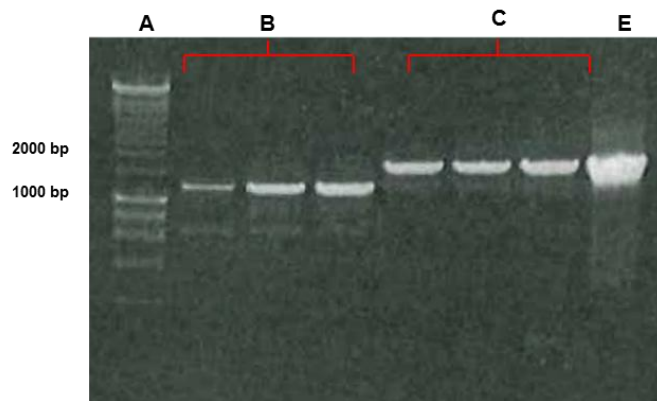


Figure 7.7: Agarose gel of colony PCR of *A. tumifaciens* transformation. Lanes: A) Ladder (Hyperladder 1; Bioline; B) pEAQ-HT-wt-HBcAg D3K6D3; C) pEAQ-HT-t-HBcAg D3K6D3. The pEAQ-HT-t-HBcAg D3K6D3 samples gave rise to bands around 2000 bp corresponding to 1835 bp and the pEAQ-Ht-wt-HBcAg D3K6D3 plasmid gave rise to bands around 1000 bp corresponding to 1288 bp, indicating successful cloning of the D3K6D3 constructs.

7.5.4 Trial expression of wt/t-HBcAg D3K6D3 constructs *in planta*

Each sample colony were grown in LB media (10 ml; 50 µg/ml kanamycin/rifampicin) at 27°C over the weekend. The cell cultures were diluted with fresh LB media to achieve an OD₆₀₀ = 0.4 and centrifuged for 5 mins @ 4,000 *rcf*. The cells were re-suspended in the appropriate volume of MMA buffer [10 mM MES pH 5.6; 1 mM MgCl₂; 10 µM acetosyringone] to make an OD₆₀₀ of 0.4. Each culture was used to infiltrate the leaves of two plants (3 weeks old). The leaves were nicked with a sterile needle and the infiltration solution is injected into the intracellular space. Plants were grown in glasshouses maintained at 25°C with supplemental lighting to provide 16 hours of daylight and were watered daily. The leaves were harvested 6 days post infiltration.

7.5.5 Large scale expression of t-HBcAg D3K6D3 *in planta*

Cultures of the pEAQ-HT-t-HBcAg D3K6D3 *Agrobacterium* strains were grown in LB media (100 ml; 50 µg/ml kanamycin/rifampicin) at 27°C over the weekend. The cell cultures were diluted with fresh LB media to achieve an OD₆₀₀ = 0.4 and centrifuged for 5 mins @ 4,000 *rcf*. The cells were re-suspended in the appropriate volume of MMA buffer [10 mM MES pH 5.6; 1 mM MgCl₂; 10 µM acetosyringone] to make an OD₆₀₀ of 0.4. The surface of young plant leaves (3 weeks old) were nicked with a sterile needle and the infiltration solution is injected into the intracellular space. Plants were grown in glasshouses maintained at 25°C with supplemental lighting to provide 16 hours of daylight and were watered daily. The leaves were harvested 6 days post infiltration.

7.5.6 Purification of VLPs from plants

The fresh plant material was weighed and added to extraction buffer (3 ml per gram of plant material) and homogenised in a blender. During the initial plant expression two extraction buffers were assessed for the extraction of the D3K6D3 VLPs. It was shown that the phosphate buffer gave rise to better virus like particles and was used exclusively for subsequent expressions.

HBex Buffer [10 mM Tris-HCl; 120 mM NaCl; 1 mM EDTA; 0.75 M sodium deoxycholate; 1 mM DTT; Roche cOmplete protease inhibitor tablet (EDTA free) as per manufacturer's instructions]

Phosphate Buffer [100 mM sodium phosphate; Roche cOmplete protease inhibitor tablet (EDTA free) as per manufacturer's instructions]

The homogenised cells were filtered through Miracloth (Merck Millipore) to remove plant debris before centrifugation at 9,000 *rcf* for 10 mins at 4°C before being decanted and centrifuged at 3,000 *rcf* for 5 mins at 4°C. The supernatant was then purified using a sucrose gradient*, solutions of 20, 30, 40 50 and 60% sucrose (w/v) were made up using the appropriate buffer. Gradients were made by underlying solutions of increasing density in ultracentrifuge tubes (Thinwall, Ultra-Clear, 38.5 ml, Beckmann Coulter) before loading the supernatant on top. The gradients were centrifuged in a SureSpin 630i swing arm rotor (28,000 rpm, *ca.* 240,000 *rcf*) for 2.5 hours at 4°C. The sucrose layers were collected and dialysed (Snake Skin, 10,000

MWCO, Thermo Scientific) against PBS and analysed by western blot (section 7.1.5).

- * For large scale preps (20+ plants) an initial sucrose cushion was carried out (25% and 70% (w/v) sucrose). The 70-25% sucrose interface and 25% layer were shown to contain VLP by Western blot and were subsequently dialysed (Snake Skin, 10 MWCO, Thermo Scientific) against PBS before further purification by sucrose gradient.

The VLP active fractions were combined and extensively dialysed (5 x 1L) against ammonium bicarbonate buffer [20 mM, pH 7.4] and concentrated to 10% original volume using Speed-Vac (Thermo Scientific) and analysed using TEM.

7.5.7 Conjugation of t-HBcAg D3K6D3 VLP to FITC

t-HBcAg D3K6D3 (ca. 500 µg) in AmBic buffer (1.2 ml of 0.4 mg/ml solution) was extensively dialysed (Snake Skin, 10 MWCO, Thermo Scientific) against Borax conjugation buffer [0.08 M, pH 9.0]. After dialysis potassium hydrogen carbonate (70 mg) was added to the solution (2 ml) give a final concentration of 350 mM. FITC (100 µg) was added and the conjugation reaction was allowed to stir at 4°C overnight. The conjugate was extensively dialysed against AmBic [20 mM; pH 7.4] (Snake Skin, 10,000 MWCO, Thermo Scientific) before being concentrated on Speed-Vac (Thermo Scientific). The VLP sample was analysed by SDS-PAGE, western blot, agarose gel.

7.5.8 SEC purification of VLPs

VLPs were purified using an AKTA prime system at room temperature. The VLP solution (6 ml) was clarified with a 0.2 µm filter before being loaded onto Sepharose CL4B XK 26/40 column and eluted with PBS at a flow rate of 2 ml/min. Fractions (1 – 18, 2 ml; 19 – 27, 10 ml) were collected and analysed by SDS-PAGE, western blot, agarose gels (1.2%) and TEM.

7.5.9 Second conjugation of t-HBcAg D3K6D3 VLP with FITC

Conjugation of FITC to the t-HBcAg D3K6D3 VLPs was achieved as previously stated, section 7.5.6. Free FITC was removed from the conjugated VLP using spin

filtration (x5) (Sartorius VivaSpin; 10,000 MWCO) with PBS as the eluent. FITC-labelled VLPs were suspended in PBS (5 ml) and added to a sucrose gradient (20, 30, 40, 50 & 60%) (section 7.5.5) (Thinwall, Ultra-Clear, 13 ml, Beckmann Coulter) and centrifuged in a T684 swing arm rotor (40,000 rpm; ca. 270,000 *rcf*) for 2.5 hours at 4°C. After centrifugation the sucrose gradient was visualised with blue light excitation (470 nm, Safe Imager) and the UV active layer was collected and dialysed (Pierce Float-A-Lyzer; 1000 KD MWCO) into AmBic [20 mM. pH 7.4]. The sample was then analysed by SDS-PAGE and agarose gel (1.2%).

7.6 References

1. M. H. J. Selman, M. Hoffmann, G. Zauner, L. A. McDonnell, C. I. A. Balog, E. Rapp, A. M. Deelder and M. Wuhrer, *Proteomics*, 2012, **12**, 1337-1348.
2. E. Giménez, F. Benavente, J. Barbosa and V. Sanz-Nebot, *Anal. Bioanal. Chem.*, 2010, **398**, 357-365.
3. U. K. Laemmli, *Nature*, 1970, **227**, 6.
4. X. Di, K. K. C. Chan, H. W. Leung and C. W. Huie, *J. Chromatogr. A*, 2003, **1018**, 85-95.
5. T. Scientific, in *Thermo Scientific Technical Note*, Editon edn., 2011, pp. 1-10.
6. T. Masuko, A. Minami, N. Iwasaki, T. Majima, S.-I. Nishimura and Y. C. Lee, *Anal. Biochem.*, 2005, **339**, 69-72.
7. M. J. Gorczynski, J. Huang and S. B. King, *Org. Lett.*, 2006, **8**, 2305-2308.
8. K. Kai, J. Takeuchi, T. Kataoka, M. Yokoyama and N. Watanabe, *Tetrahedron*, 2008, **64**, 6760-6769.
9. N. Floyd, B. Vijaykrishnan, J. R. Koeppe and B. G. Davis, *Angew. Chem. Int. Ed.*, 2009, **48**, 7798-7802.
10. K. Wada, T. Chiba, Y. Takei, H. Ishihara, H. Hayashi and K. Onozaki, *Journal of Carbohydrate Chemistry*, 1994, **13**, 941-965.
11. B. Becker, R. H. Furneaux, F. Reck and O. A. Zubkov, *Carbohydr. Res.*, 1999, **315**, 148-158.
12. S. Pearson, W. Scarano and M. H. Stenzel, *Chem. Commun.*, 2012, **48**, 4695-4697.
13. C. Wang, P.-F. Ren, X.-J. Huang, J. Wu and Z.-K. Xu, *Chem. Comm.*, 2011, **47**, 3930-3932.
14. J. Kerékgyártó, Z. Nagy and Z. Szirmai, *Carbohydr. Res.*, 1997, **297**, 107-115.
15. X. Ding, W. Wang and F. Kong, *Carbohydr. Res.*, 1997, **303**, 445-448.

16. Z.-J. Li, H. Li and M.-S. Cai, *Carbohydr. Res.*, 1999, **320**, 1-7.
17. S. E. Kurhade, T. Mengawade, D. Bhuniya, V. P. Palle and D. S. Reddy, *Organic & Biomolecular Chemistry*, 2011, **9**, 744-747.
18. G. O. Aspinall, A. G. McDonald and R. K. Sood, *Can. J. Chem.*, 1994, **72**, 247-251.
19. M. Zunk and M. J. Kiefel, *Tetrahedron Lett.*, 2011, **52**, 1296-1299.
20. T. Klein, D. Abgottspon, M. Wittwer, S. Rabbani, J. herold, H. Jiang, J. Xiao, S. Kleeb, C. Luethi, M. Scharenberg, J. Bezencon, E. Gubler, L. Pang, M. Smiesko, B. Cutting, O. Schwardt and B. Ernst, *J. Med. Chem.*, 2010, **53**, 8672 - 8641.
21. S. Vidal, A. Morère and J.-L. Montero, *Heteroat. Chem*, 2003, **14**, 241-246.
22. Y. A. Knirel, N. A. Paramonov, A. S. Shashkov, N. K. Kochetkov, R. G. Yarullin, S. M. Farber and V. I. Efremenko, *Carbohydr. Res.*, 1992, **233**, 185-193.
23. F. Goubet, P. Jackson, M. J. Deery and P. Dupree, *Anal. Biochem.*, 2002, **300**, 53-68.
24. A. Takasu, S. Horikoshi and T. Hirabayashi, *Biomacromolecules*, 2005, **6**, 2334-2342.
25. C. A. Schneider, W. S. Rasband and K. W. Eliceiri, *Nat. Methods*, 2012, **9**, 671-675.
26. K. Czifrák and L. Somsák, *Carbohydr. Res.*, 2009, **344**, 269-277.
27. M. N. Burtnick, C. Heiss, R. A. Roberts, H. P. Schweizer, P. Azadi and P. J. Brett, *Frontiers in cellular and infection microbiology*, 2012, **2**.
28. ForteBio, ed. ForteBio, Editon edn., 2008.
29. C. C. Prieto, R. I. Leonardelli and F. E. Zalazar, *Analytical Biochemistry*, 1997, **252**, 15-18.
30. M. Nakakoshi, H. Nishioka and E. Katayama, *Journal of Electron Microscopy*, 2011, **60**, 401-407.

8 Appendix

8.1 Glycoconjugate MALDIs

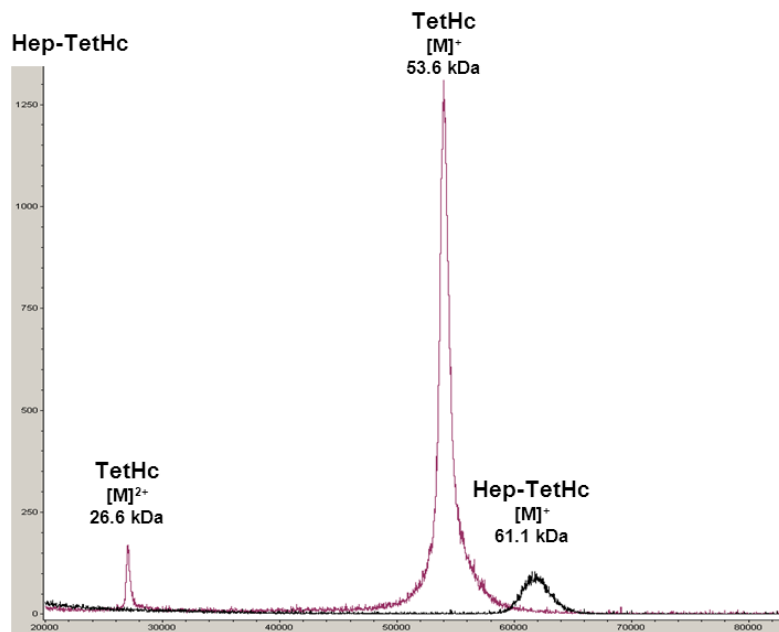


Figure 8.1: Overlay of MALDI-ToF spectra for native TetHc and Hep-TetHc (94) glycoconjugates

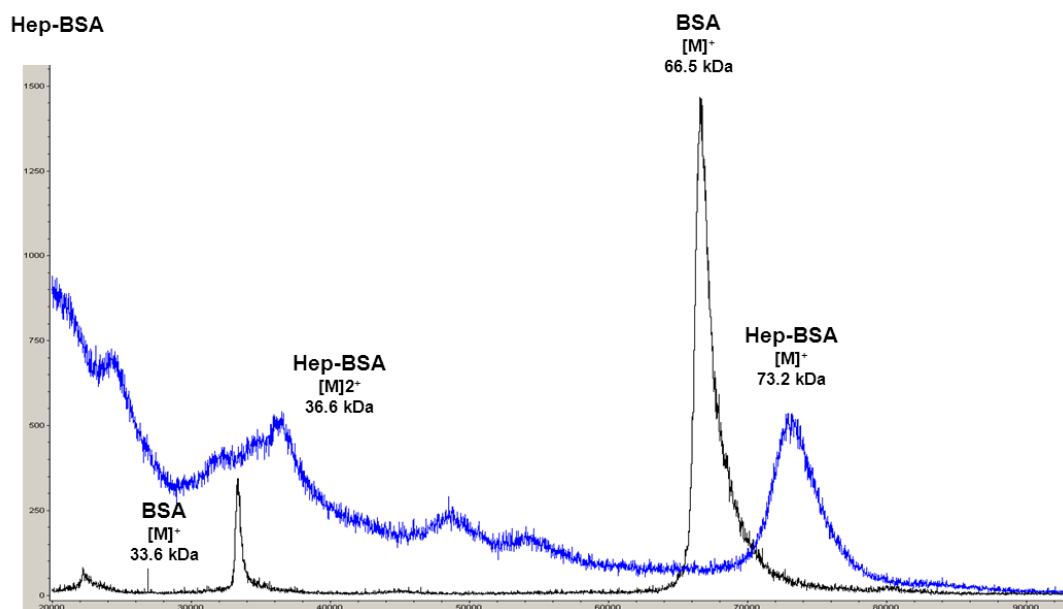


Figure 8.2: Overlay of MALDI-ToF spectra for native BSA and Hep-BSA (95) glycoconjugates

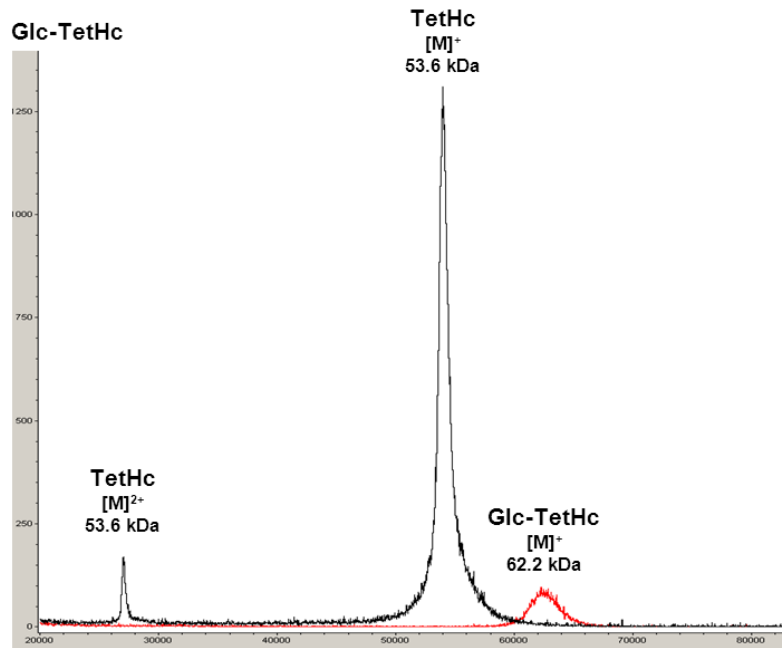


Figure 8.3: Overlay of MALDI-ToF spectra for native TetHc and Glc-TetHc (96) glycoconjugates

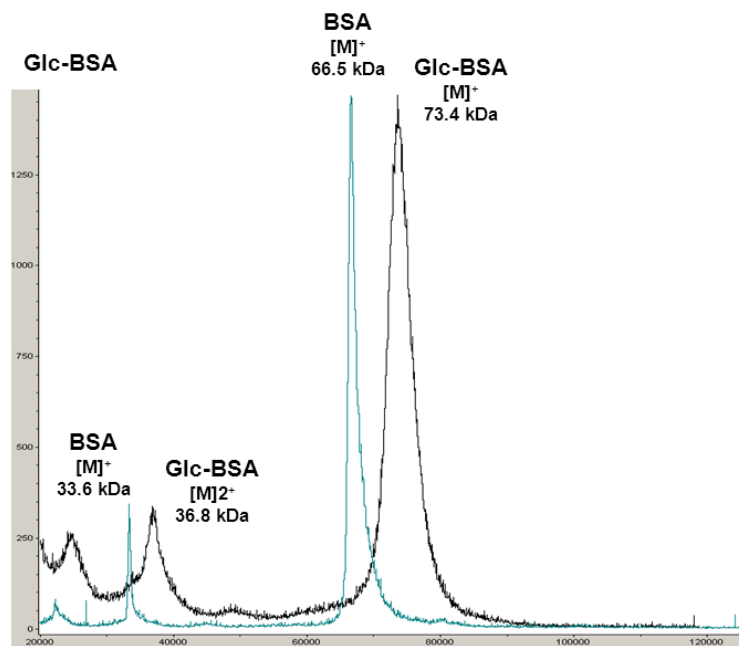


Figure 8.4: Overlay of MALDI-ToF spectra for native BSA and Glc-BSA (97) glycoconjugates

8.2 NMR overlay of crude *B. thailandensis* CPS prep and authentic *B. pseudomallei* sample

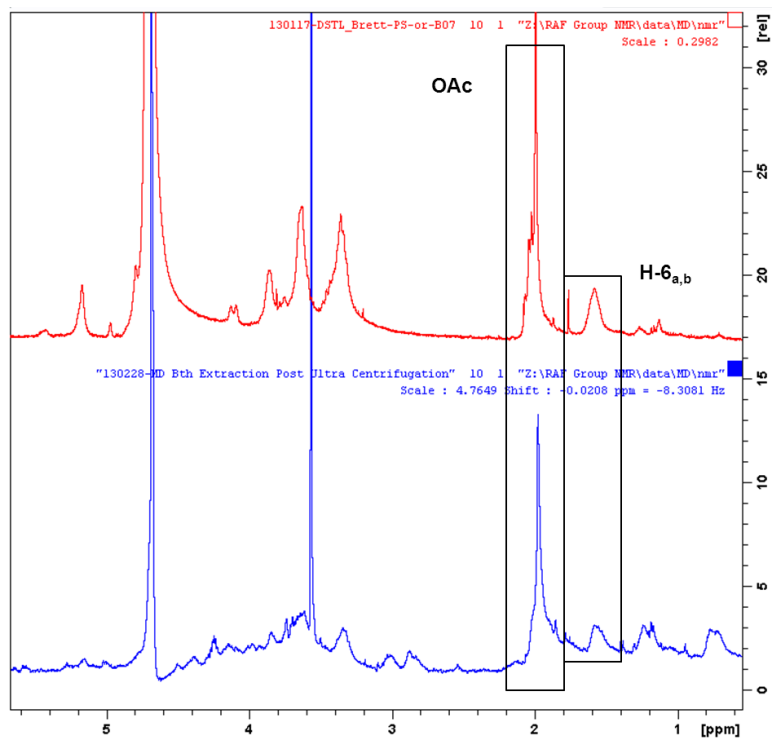


Figure 8.5: Crude *B. thailandensis* CPS prep and authentic *B. pseudomallei* sample

8.3 ^{13}C NMR of *B. thailandensis* CPS prep

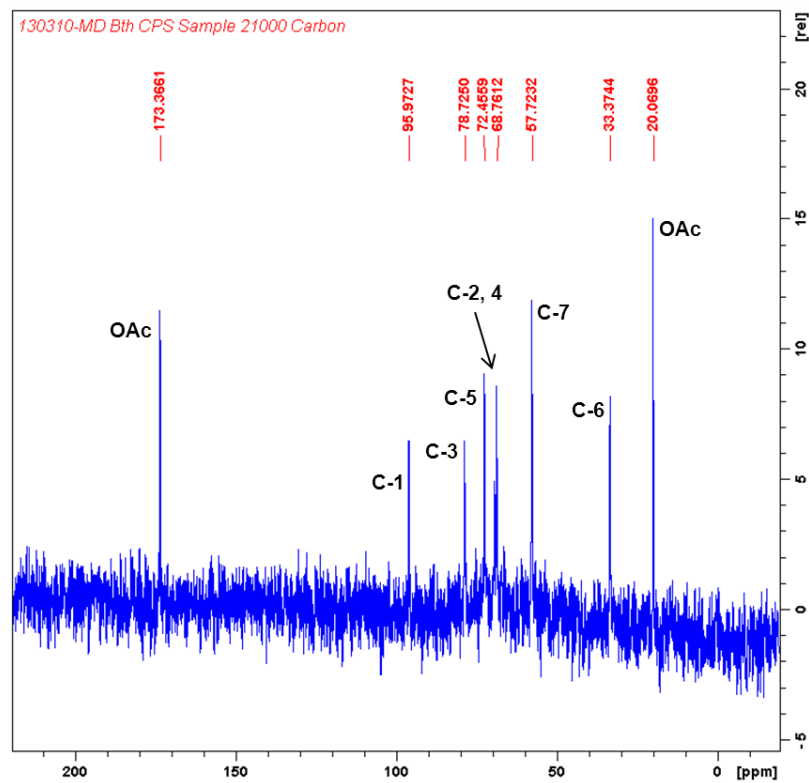


Figure 8.6: *B. thailandensis* CPS prep ^{13}C NMR (21,000 scans)

8.4 NMR integration of H-1 and H-2 of CPS preparations from *B. pseudomallei* and *B. thailandensis*

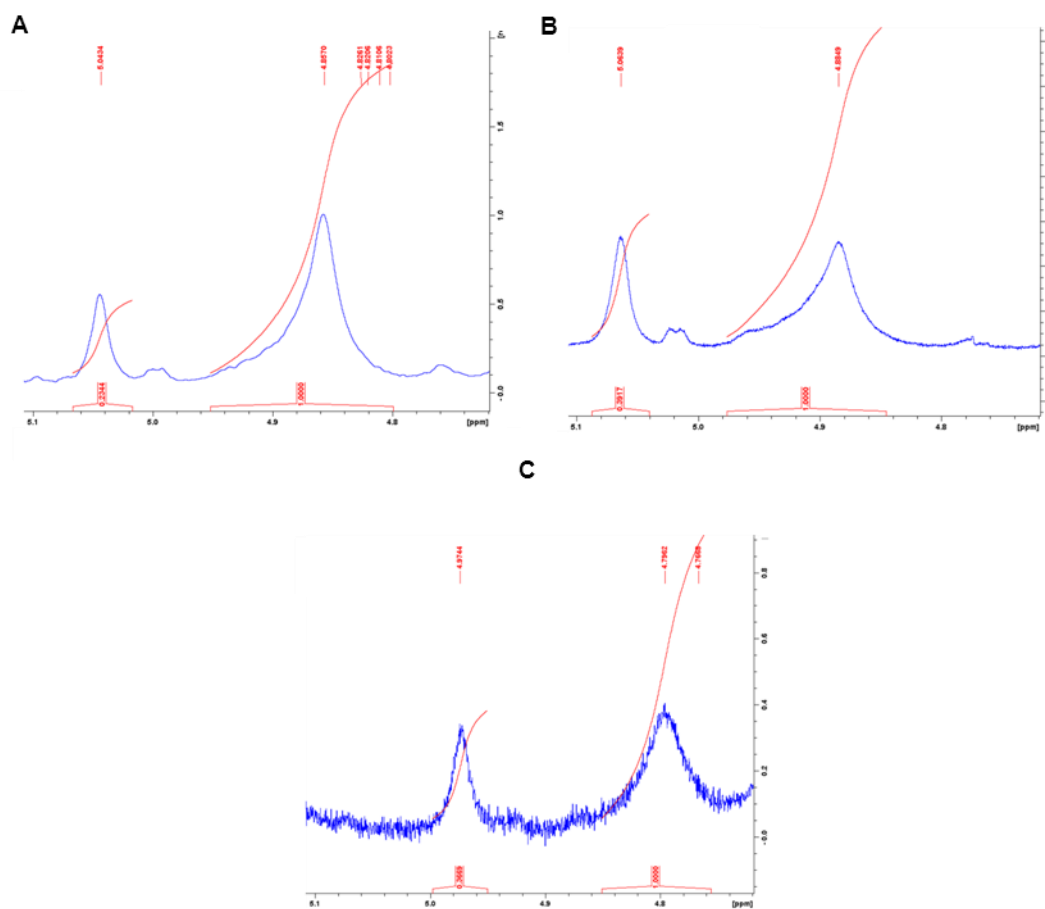


Figure 8.7: NMR Integration of H-1 protons of CPS and mannan polysaccharides for A) *B. pseudomallei* extract 1: CPS (82%) and mannan (18%), B) *B. pseudomallei* extract 2: CPA (72%) and manna (28%) and C) *B. thailandensis* extract: CPS (73%) and mannan (27%)

8.5 ELISA of separate sera samples CF1497 and CF1498

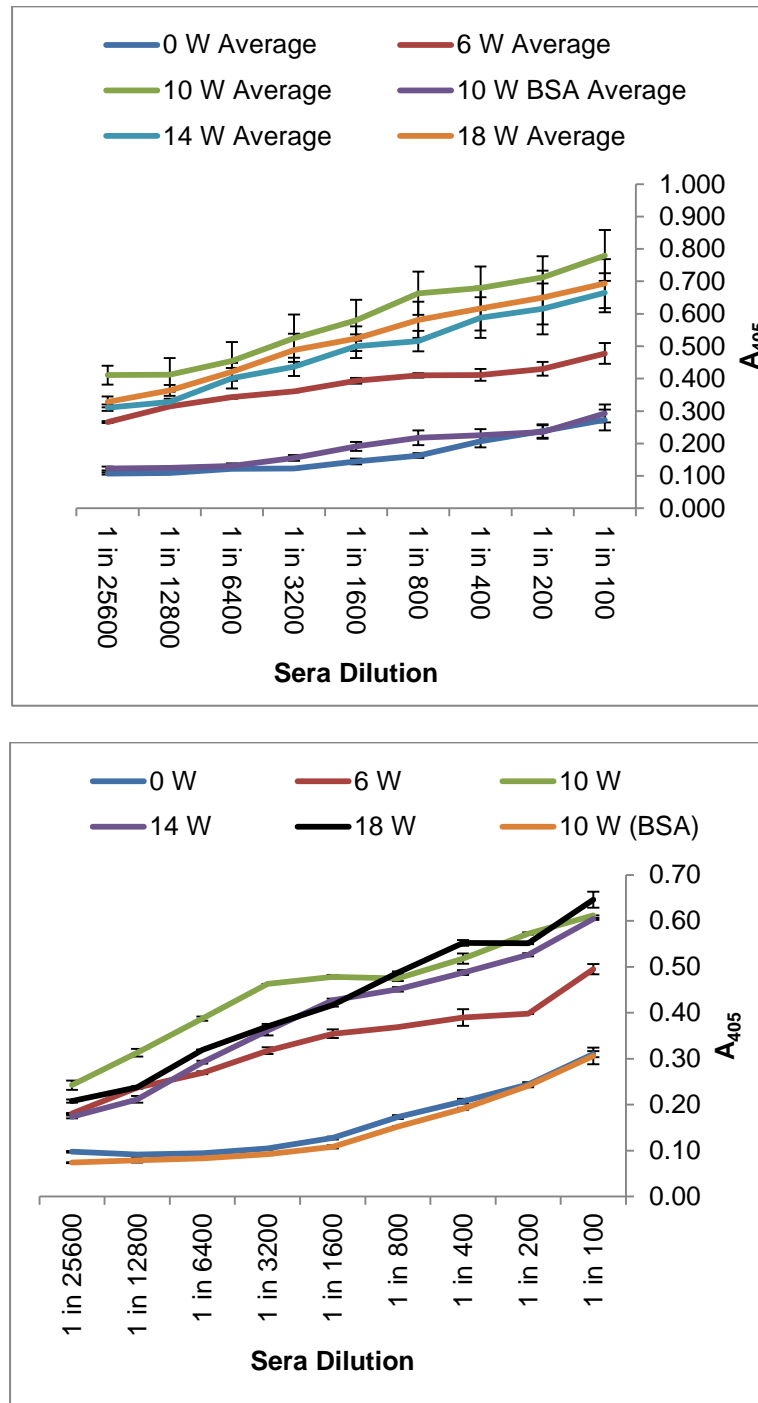


Figure 8.8: (Top) Average of ELISA data for separate sera samples from single sheep bleeds (CF1497 & CF1498); (Bottom) Data from combined sheep sera as used throughout the thesis. The data for the separate sera has larger error as a result of reduced activity in CF1498. Based on this result the data from the combined sheep sera was shown to be suitable

8.6 MALDI-ToF of 6D6FGlc-TetHc glycoconjugate (112)

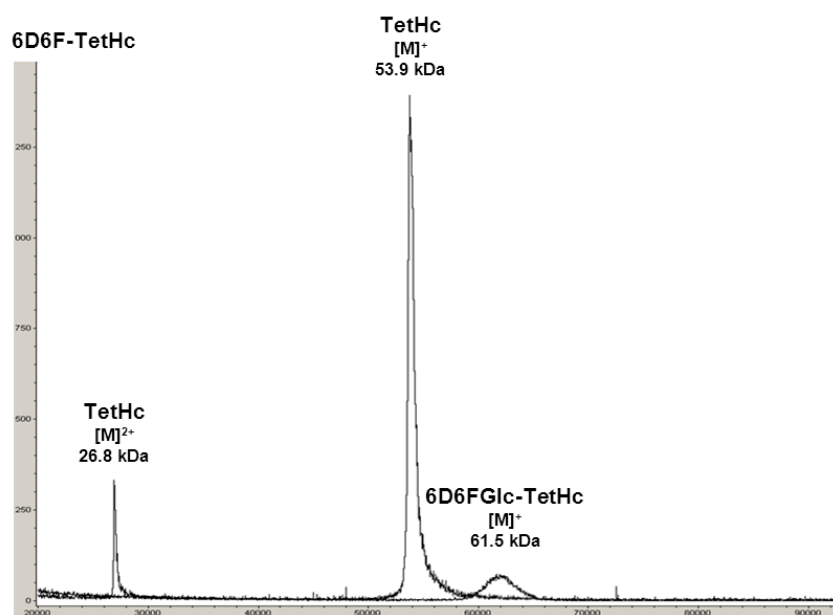


Figure 8.9: Overlay of MALDI-ToF spectra for native TetHc and 6D6FGlc-TetHc (112) glycoconjugates

8.7 ^{13}C NMR data for 8-(methoxycarbonyl)octyl 6-deoxy-6-fluoro- β -D-glucopyranose (107) and 8-(methoxycarbonyl)octyl 2,4-di-O-acetyl- β -D-allopyranoside (109)

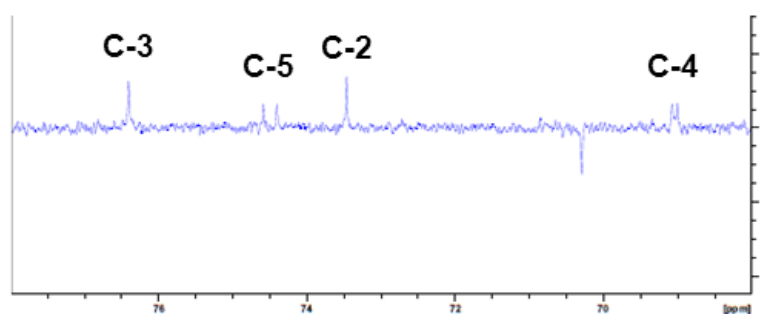
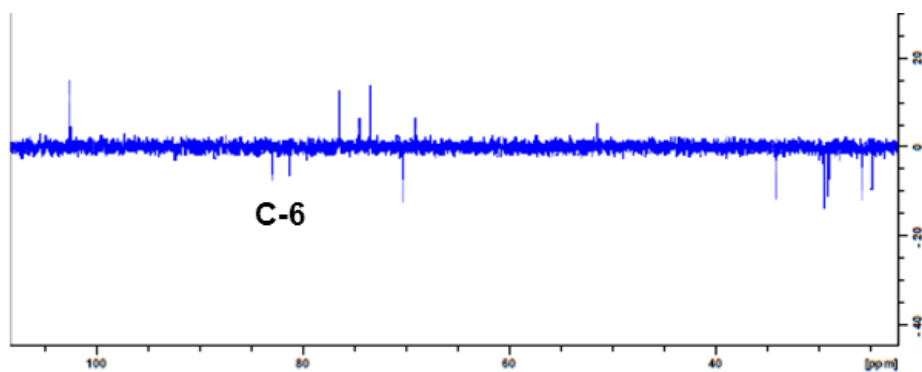


Figure 8.10: ^{13}C NMR data for 6-deoxy-6-fluoro-D-glucoside (107), with zoomed in region for δ 68-78 ppm. Diagnostic carbon peaks labelled indicating the carbon-fluorine coupling of the C-4, C-5 and C-6 carbons.

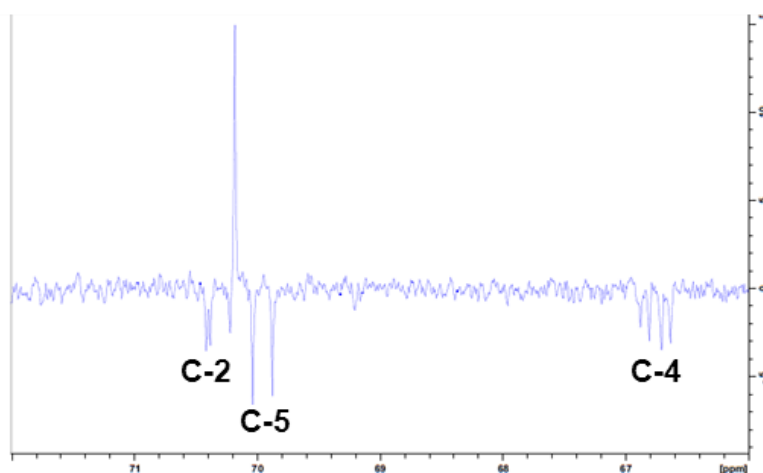
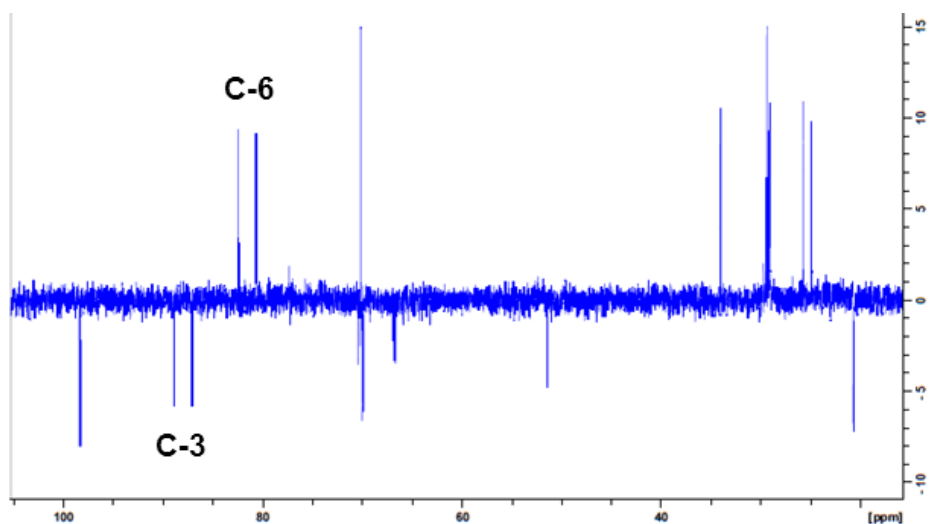


Figure 8.11: ¹³C NMR data for 3,6-dideoxy—3,6-difluoro-D-alloside (109), with zoomed in region for δ 66-72 ppm. Diagnostic carbon peaks labelled indicating the carbon-fluorine coupling of the C-2, C-3, C-4, C-5 and C-6 carbons.

The coupling patterns of the two NMR spectra above help to confirm the location of the fluorine groups on the carbohydrate ring. The double spiting pattern of C-4 indicates and single coupling of C-2 to fluorine place the two fluorine atoms at the 3-OH and 6-OH positions.

8.8 pEAQ-HT wtHBcAg Plasmid

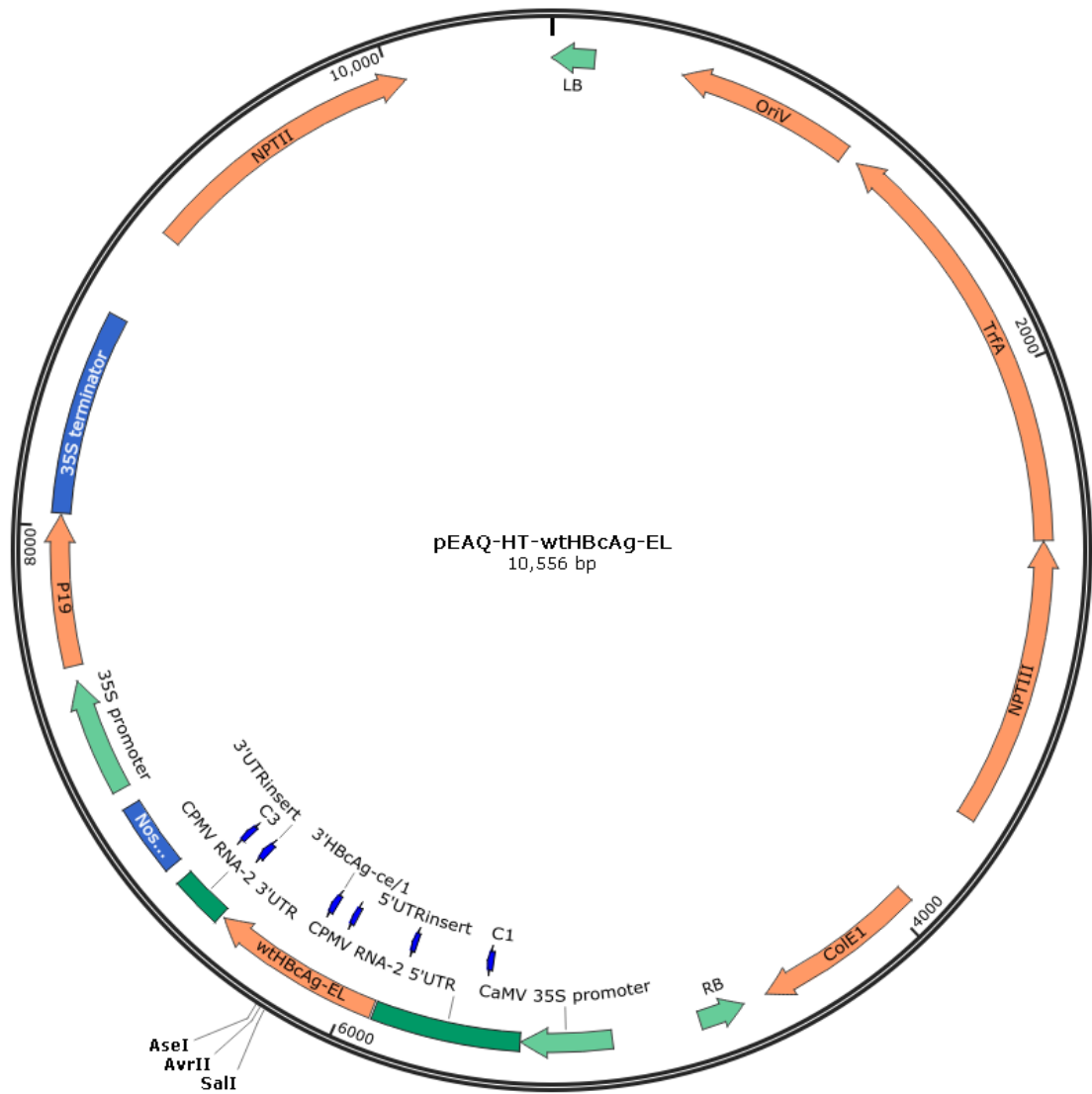


Figure 8.12: Plasmid map of the pEAQ-HT-t-HBcAg-EL expression system with the specific restriction sites (Sall and AseI) highlighted. (Plasmid is the same for wt-HBcAg-El apart from protein sequence)

Region	Use
CaMV 35S promoter	Strong promoter region enhancing transcription. It is widely used in plant transformations. ^{1,2}
5'-UTR	Modified 5'-UTR from CPMV RNA-2, used to promote gene expression. ³
tHBcAg-EL	Sequence for the desired protein, in this case the tandem core HBc VLP.
3'-UTR	3'-UTR form CPMV RNA-2, used to promote gene expression
NOS terminator	Signals end of transcription region. ²
P19	Supressor of RNA silencing from Carnation Italian ringspot virus. ^{4,5}
NPT(II)	Neomycin phosphotransferase (II) encodes for kanamycin resistance. ⁶⁻⁸
LB/RB	Borders for genomic data
ORiV and TfrA	Control plasmid replication in bacteria ⁹

Table 8.1: Table identifying the regions of the pEAQ-HT plasmid

8.9 References

1. R. T. Fraley, R. B. Horsch, S. G. Rogers, *US Pat.*, Chimeric genes for transforming plant cells using viral promoters US 5352605, 1994.
2. M. Hardegger, P. Brodmann and A. Herrmann, *Eur. Food Res. Technol.*, 1999, **209**, 83-87.
3. F. Sainsbury, E. C. Thuenemann and G. P. Lomonosoff, *Plant Biotechnol. J.*, 2009, **7**, 682-693.
4. D. Silhavy, A. Molnar, A. Luciola, G. Szittyá, C. Hornyik, M. Tavazza and J. Burgyan, *The EMBO Journal*, 2002, **21**, 3070.
5. O. Voinnet, S. Rivas, P. Mestre and D. Baulcombe, *The Plant Journal*, 2003, **33**, 949-956.
6. J. de Vries and W. Wackernagel, *Molecular and General Genetics MGG*, 1998, **257**, 606-613.
7. R. L. Yenofsky, M. Fine and J. W. Pellow, *Proc. Nat. Acad. Sci. U.S.A.*, 1990, **87**, 3435-3439.
8. M. Brzezinska and J. Davies, *Antimicrob. Agents Chemother.*, 1973, **3**, 266-269.
9. J. Mei, S. Benashski and W. Firshein, *J. Bacteriol.*, 1995, **177**, 6766-6772.